UNIVERSITÉ DE STRASBOURG

ÉCOLE DOCTORALE Sciences de la Vie et de la Santé

Institut de Génétique et de Biologie Moléculaire et Cellulaire
UMR 7104 – U964 – Université de Strasbourg

THÈSE présentée par :

Jinxiang TAN

soutenue le : **21 septembre 2012**

pour obtenir le grade de : **Docteur de l'université de Strasbourg**

Discipline/ Spécialité : Sciences du Vivant

Aspects Moléculaires et Cellulaires de la Biologie

Etude de la fonction de la métalloprotéase matricielle 11 dans l'interaction/dialogue adipocyte-cellule épithéliale dans la glande mammaire

THÈSE dirigée par :

Marie-Christine RIO	DR1 INSERM, IGBMC, Strasbourg

RAPPORTEURS :

Agnès NOEL	Professeur, Université de Liège
Philippe BIREMBAUT	Professeur, Université de Reims

AUTRE MEMBRE DU JURY :

Patrick ANGLARD	DR2 INSERM, Centre de Neurochimie, Strasbourg

There is no end to learning……

学无止境……

Acknowledgements

I would give my greatest thanks to my supervisor Dr. Marie-Christine RIO for offering me the opportunity to study in this laboratory. She not only provided encouragement and guidance in my research, but also offered care and help in my life.

My special thanks go to Dr. Catherine-Laure TOMASETTO for her constant support and patience that carried me on through all times. Her encouragement and constructive criticisms were very helpful towards my progress.

I am grateful to Dr. Fabien ALPY for his good suggestions and technical support in my research.

I would like to acknowledge my Chinese supervisor prof. Guosheng REN and China Scholarship Council for provide me the funding for the PhD study.

I would thank Elisabeth DAGUENET for her technical help in my research and language help in my life. She is a good French teacher, I have shown a lot of French letters to her, let her help me to translate into English. Please translate into Chinese in the next time.

My thanks go to members in the Marie-Christine RIO/Catherine-Laure TOMASETTO laboratory, Isabelle STOLL, Corinne WENDLING, Emilie BUACHE, Stéphanie DELPOUS, Adrien ROUSSEAU, David SIMOES, Anne Laure BAILLY and Nassim Dali YOUCEF. We have spent a fantastic time together during this four years!

I appreciate the technical support from Martine MUCKENSTURM (HUS Hautepierre), Olivia WENDLING (ICS), the staff in microscopy platform and animal facility (IGBMC and ICS).

I would like to thank my Chinese friends, Qi CAI, Hua JIANG, Yadong LI, Pan LI, Jiagui LI, Guoqiang HUA, Yi LUO, etc. Your friendship and encouragement have helped me through some difficulties during my PhD study.

The greatest credit for my success goes to my parents, my sisters, my brothers, my wife and my son for their constant support and encouragement to pursue my PhD.

Last but not least, my thanks to all those help me in many ways throughout my PhD study, whose names I have not mentioned, but they are indeed in my thoughts.

THANK YOU ALL　　MERCI　　谢谢！

Table of Contents

List of Figures and Tables

List of Abbreviations

AKT/PKB	Protein Kinase B
α1-CT	alfa1-ChymoTrypsin
α1-PI	alfa1-Proteinase Inhibitor
α2-AP	alpha2-AntiPlasmin
α-SMA	alfa-Smooth Muscle Actin
α2-M	alfa2-Macroglobulin
aP2/FABP4	Adipocyte Protein 2/Fatty Acid Binding Protein 4
bFGF	basic Fibroblastic Growth Factor
Cav-1	Caveolin-1
CAAs	Cancer-Associated-Adipocytes
CCL	Chemokine (C-C motif) Ligand
Cox-2	Cyclooxygenase-2
CXCL	Chemokine (C-X-C motif) Ligand
CXCR	CXC chemokine Receptor
DCIS	Ductal Carcinoma In Situ
E10	Embryonic day 10
ECM	Extra-Cellular Matrix
EMT	Epithelial to Mesenchymal Transition
EGF	Epidermal Growth Factor
EGFR	Epidermal Growth Factor Receptor
ER	Estrogen Receptor
EZH2	Enhancer of Zeste Homolog 2
FGF	Fibroblast Growth Factor
FGFR	Fibroblast Growth Factor Receptor
GH	Growth Hormone
H&E	Hematoxylin-Eosin
HGF	Hepatocyte Growth Factor

HGFR	Hepatocyte Growth Factor Receptor
HIF	Hypoxia Inducible Factor
IDC	Invasive Ductal Carcinomas
IGF	Insulin-like Growth Factor
IGFBP	Insulin-like Growth Factor Binding Protein
IGFIR	Insulin-like Growth Factor 1 (IGF-1) Receptor
IL	InterLeukin
ITS	Insulin-Transferrin-Selenium
MAP	Mitogen-Activated Protein
MAPK	Mitogen-Activated Protein Kinase
MCP	Monocyte Chemoattractant Protein
MEFs	Mouse Embryonic Fibroblasts
MMP	Matrix MetalloProteinase
MMP-11-/-	MMP-11-deficient, MMP-11-knockout
MMP-11 Tg	MMP-11 Transgene
MT-MMP	Membrane-Type MMP
NET	Neutrophil Extracellular Trap
NF-κB	Nuclear Factor kappa-light-chain-enhancer of activated B cells
NK	Natural Killer
PAR	Proteinase-Activated Receptor
PCR	Polymerase Chain Reaction
PDGF	Platelet-Derived Growth Factor
PI3K	PhosphoInositide 3-Kinase/Phosphatidylinositol 3-Kinase
PPARγ	Peroxisome Proliferator-Activated Receptor gamma
PR	Progesterone Receptor
RANKL	Receptor Activator for Nuclear factor κB Ligand
RARE	Retinoic-Acid-Responsive-Element
ROS	Reactive Oxygen Species
RT-PCR	Reverse Transcription-Polymerase Chain Reaction

ST3	STromelysin-3
STAT	Signal Transducer and Activator of Transcription
Tam	Tamoxifen
TEB	Terminal End Bud
TGF	Transforming Growth Factor
3D	Three-Dimensional
TIMP	Tissue Inhibitor of MetalloProteinase
TNF	Tumor Necrosis Factor
TRAP	Tartrate-Resistant Acid Phosphatase
TRE	Thyroid hormone Responsive Element
UTR	UnTranslated Regions
VEGF	Vascular Endothelial Growth Factor
VEGFR	Vascular Endothelial Growth Factor Receptor
WT	Wild-Type

Chapter 1 Introduction and Literature Review

The adult female mammary gland structure affords for the growth, development and immune protection of the new borns through its production of milk. The dynamic development of the mammary gland in response to physiological stimulation allows its programmed branching morphogenesis at puberty, cyclical turnover during the reproductive cycle, differentiation into a secretory organ during pregnancy/parturition, involution after lactation, and ultimately, regression with age. Extracellular matrix metalloproteinases (MMPs) are essential for these programs that remodel the tissue microenvironment at the interface of the epithelium and the stroma, coupling form with function. Moreover, MMPs have been shown to play a role in mammary gland tumor development and progression.

1.1 The MMP family

MMPs are a family of zinc-dependent endopeptidases. MMPs mediate a number of physiological and pathological processes, such as matrix degradation, tissue remodeling, inflammation, tumor progression (Rouyer et al., 1994-1995; Shim et al., 2007). Currently, 25 MMP family members have been identified (Lohi et al., 2001; Egeblad and Werb, 2002). They are often grouped according to their modular domain structure. There are eight distinct structural classes of MMPs (Figure 1.1).

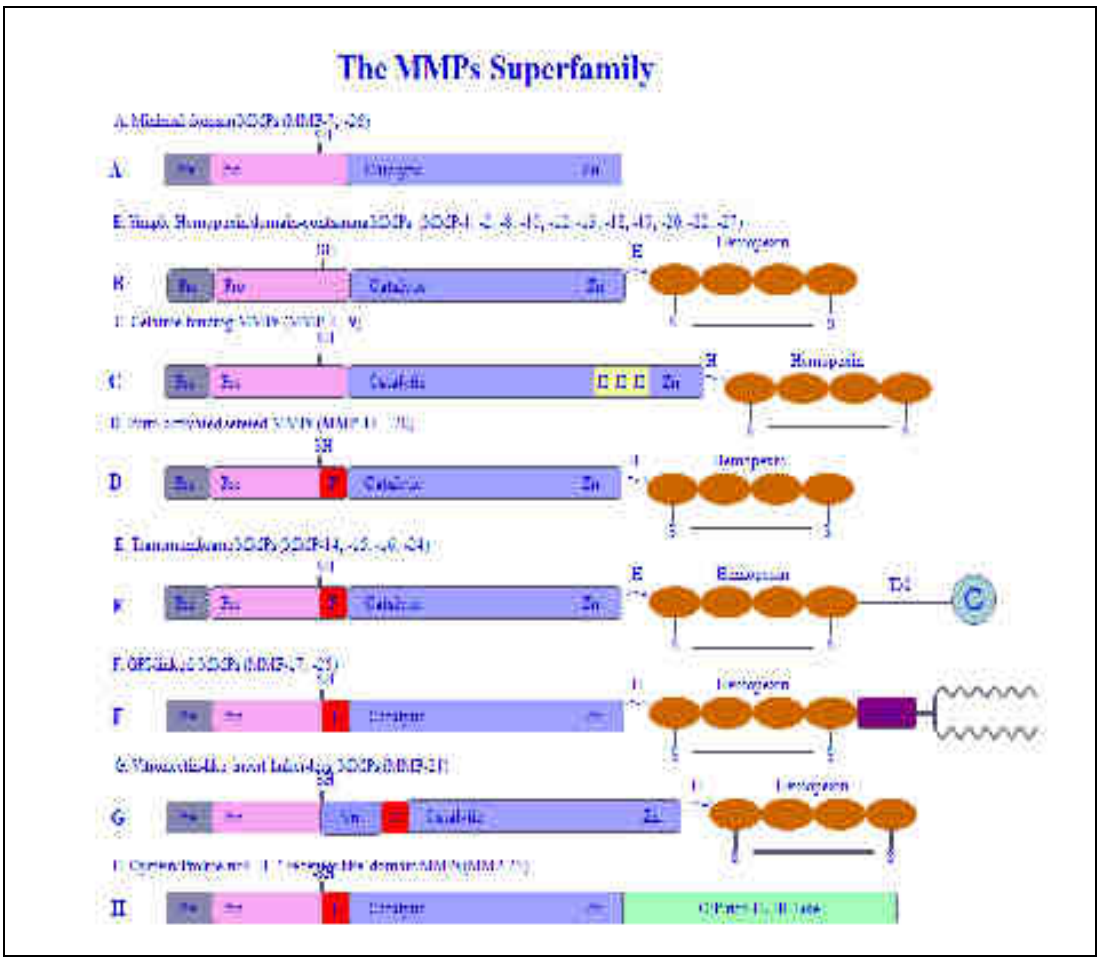

Figure 1.1 Domain structure of MMPs. The various domain organizations of human MMPs are illustrated; **Pre:** signal peptide sequence; **Pro:** pro-peptide with a free zinc-ligating thiol (SH) group; **F:** furin-susceptible site; **Zn:** zinc ion; **II:** collagen binding fibronectin type II insert; **H:** hinge region; **TM:** transmembrane domain; **C:** cytoplasmic domain; **GPI:** glycophosphatidyl inositol membrane anchoring domain; **C/P:** cysteine/proline array; **IL-1R:** interleukin-1 receptor; **Vn:** vitronectin-like domain; **Hemopexin:** hemopexin domain. The flexible, variable length of linker or hinge region is depicted as a wavy black ribbon. Modified from Egeblad and Werb, 2002; Radisky and Radisky, 2010.

Most of the MMPs are able to cleave one or more major components of the extra-cellular matrix (ECM) (Liu et al., 2001; Egeblad and Werb, 2002; Motrescu et al., 2008; Kessenbrock et al., 2010). According to their substrates, the MMPs can be divided into 5 general subgroups: stromelysins, collagenases, gelatinases, membrane-type MMPs (MT-MMPs) and elastases (Liu et al., 2001), and the common names of the MMPs reflect this classification (Table 1.1). However, as the list of MMPs has grown, a sequential numbering system for the MMPs has been adopted.

Designation	Structural class	Common name(s)
MMP-1	Simple hemopexin domain	Collagenase-1, interstitial collagenase, fibroblast collagenase, tissue collagenase
MMP-2	Gelatin-binding	Gelatinase A, 72-kDa gelatinase, 72-kDa type IV collagenase, neutrophil gelatinase
MMP-3	Simple hemopexin domain	Stromelysin-1, transin-1, proteoglycanase, pro-collagenase-activating protein
MMP-7	Minimal domain	Matrilysin, matrin, PUMP1, small uterine metalloproteinase
MMP-8	Simple hemopexin domain	Collagenase-2, neutrophil collagenase, PMN collagenase, granulocyte collagenase
MMP-9	Gelatin-binding	Gelatinase B, 92-kDa gelatinase, 92-kDa type IV collagenase
MMP-10	Simple hemopexin domain	Stromelysin-2, transin-2
MMP-11	Furin-activated and secreted	Stromelysin-3
MMP-12	Simple hemopexin domain	Metalloelastase, macrophage elastase, macrophage metalloelastase
MMP-13	Simple hemopexin domain	Collagenase-3
MMP-14	Transmembrane	MT1-MMP, MT-MMP1
MMP-15	Transmembrane	MT2-MMP, MT-MMP2
MMP-16	Transmembrane	MT3-MMP, MT-MMP3
MMP-17	GPI-linked	MT4-MMP, MT-MMP4
MMP-18	Simple hemopexin domain	Collagenase-4 (*Xenopus;* no human homologue known)
MMP-19	Simple hemopexin domain	RASI-1
MMP-20	Simple hemopexin domain	Enamelysin
MMP-21	Vitronectin-like insert	Homologue of *Xenopus* XMMP
MMP-22	Simple hemopexin domain	CMMP (chicken; no human homologue known)
MMP-23	Type II transmembrane	Cysteine array MMP (CA-MMP), femalysin, MIFR
MMP-24	Transmembrane	MT5-MMP, MT-MMP5
MMP-25	GPI-linked	MT6-MMP, MT-MMP6, leukolysin
MMP-26	Minimal domain	Endometase, matrilysin-2
MMP-27	Simple hemopexin domain	MMP-27
MMP-28	Furin-activated and secreted	Epilysin

Table 1.1 The matrix metalloproteinase family. Adapted from Egeblad and Werb, 2002; Kessenbrock et al., 2010.

Most of the extracellular signalling pathways that regulate cell behaviors occur at or near the cell membrane and are regulated by pericellular proteolysis (Werb, 1997). The cell-membrane-associated MMPs are either covalently linked to the cell

membrane or possess a trans-membrane domain, which is the most obvious way of restricting MMP activity to the cell membrane. However, the secreted MMPs can also localize to the cell surface by binding to integrins (Brooks et al., 1996) or to CD44 (Yu and Stamenkovic, 1999; Yu et al., 2002), or through interactions with cell-surface-associated heparan sulphate proteoglycans, collagen type IV, and/or the extracellular matrix metalloproteinase inducer (EMMPRIN) (Sternlicht and Werb, 2001).

1.1.1 Regulation of MMP activity

1.1.1.1 Regulation of MMP activity independent on TIMPs

MMP activity has been particularly studied in the context of carcinomas. The complexity of the tumor microenvironment allows for a variety of regulatory cascades that determine the functions of the various MMPs expressed. Proteolytic activity of MMPs can be regulated at different levels: gene expression, compartmentalization, transformation from inactive zymogen form to active enzyme, and at finally, by the presence of specific inhibitors. Indeed, when judging the pathophysiological relevance of increased expression of proteinases in tumors, the particular context is important, that is whether endogenous inhibitors or activating enzymes are present in the microenvironment (Kessenbrock et al., 2010).

The critical step of regulating MMP activity is to transform a zymogen status into an active proteolytic enzyme. Several proteinases can mediate this MMP activation, such as furin, plasmin, or active MMPs (Sternlicht and Werb, 2001). When activated, MMP-2, MMP-3, MMP-7, MMP-9 and MMP-12 may emit some negative feedback signals, for example, by degrading plasminogen and thus interfering with plasminogen conversion to active plasmin. This complex regulation of MMP activity is necessary, since unhampered proteinase activity may lead to tissue damage and the perpetuation of the inflammatory response in chronic inflammatory diseases and cancer (Parks et al., 2004). An example of how MMP activity is controlled is shown by the observation that MMPs also degrade plasmin-suppressing serpin proteinase inhibitors, and therefore promote the conversion of pro-MMPs. For example, MMP-3

is a potent inactivator of alpha2-antiplasmin (α2-AP) (Lijnen et al., 2001), and several MMPs inactivate other serpins such as alfa1-proteinase inhibitor (α1-PI) and alfa1-chymotrypsin (α1-CT) and thus prolong the catalytic activity of extracellular proteinases that are normally inhibited by these molecules. A crucial interplay of MMP-9, α1-PI, and neutrophil elastase occurs in skin blister formation, in which MMP-9 efficiently degrades α1-PI, a physiological serpin inhibitor of neutrophil elastase and other serine proteinases. This promotes elastase mediated matrix degradation that manifests in dermal-epidermal separation and blister formation in vivo (Liu et al., 2000). This study well illustrates the interaction between extracellular proteinases and their endogenous inhibitors as may occur in normal physiological situations and in the course of disease (Kessenbrock et al., 2010).

The MMP function can also be affected by reactive oxygen species (ROS). The inflammatory response at the tumor site produces a large amounts of ROS that are generated by activated neutrophils and macrophages. These oxidants initially activate MMPs through oxidation of the pro-domain cysteine (Weiss et al., 1985). However, eventually, in combination with the enzyme myeloperoxidase contributed by inflammatory cells, they inactivate MMPs by modification of amino acids of the catalytic domain by hypochlorous acid (Fu et al., 2003).

The localization of MMPs often indicates their biological function. Several MMPs interact with surface receptors such as integrins and/or localize to specific ECM, which up-regulates MMP activity by increasing their local concentration, and also may interfere with adjacent endogenous inhibitors (Nagase et al., 2006). The binding of MMP-2 to integrin αvβ3 through its hemopexin domain is crucial for mesenchymal cell invasive activity (Rupp et al., 2008). Similarly, high local concentrations of active MMP-14 on the cell membrane of metastatic cancer cells play important roles in cell migration (Friedl and Wolf, 2008; Sabeh et al., 2004, 2009; Wolf et al., 2007). However, there may also be additional mechanisms to concentrate extracellular proteinases in some specific sites of the microenvironment. One example relates to neutrophilic granulocytes that upon cellular activation, overflow their nuclear chromatin to form so-called neutrophil extracellular traps (NETs), a structure

with highly concentrated proteinases such as MMP-9 and leukocyte elastase with chromatin together form an extracellular structure that amplifies the effectiveness of its antimicrobial substances (Brinkmann et al., 2004). These NETs act primarily to fight off bacterial infections, but they also contribute to the pathogenesis of autoimmune diseases (Kessenbrock et al., 2009). It remains to be determined whether NETs exist in the tumor microenvironment, and whether these structures play a role in malignant diseases by localizing proteinase activity to certain sites in the tumor.

It has been found that MMP-2 formed a reduction-sensitive homodimer in a controlled manner and that Ca^{2+} ion is essential for homodimerization of MMP-2. Homodimerization is not associated with protein kinase C-mediated phosphorylation of MMP-2. MMP-2 formed a homodimer through an intermolecular disulfide bond between Cys102 and neighboring Cys102. Homodimerization of MMP-2 enhanced thrombin-mediated activation of pro-MMP-2. Moreover, MMP-2 homodimer could cleave a small peptide substrate without removal of the propeptide (Koo et al., 2012). The peroxynitrites are able to nitrate and activate MMP-2 and MMP-9 in the placenta (Capobianco et al., 2012). It is also suggested that caveolin-1 (cav-1) plays important roles in negative regulation of MMP-2 and MMP-9 activity (Gu et al., 2012), and that it also negatively regulates MMP-1 gene expression via inhibition of Erk1/2/Ets1 signaling (Haines et al., 2011). It has been revealed that electrophilic fatty acid derivatives can serve as effectors during inflammation, first by activating pro-MMP proteolytic activity via alkylation of the cysteine switch domain, and then by transcriptionally inhibiting MMP expression, thereby limiting the further progression of inflammatory processes (Bonacci et al., 2011).

1.1.1.2 Regulation of MMP activity dependent on TIMPs

There are four tissue inhibitor of metalloproteinase (TIMP) family members, TIMP-1, TIMP-2, TIMP-3 and TIMP-4. TIMPs are 21 to 30 kDa proteins that share substantial sequence homology and structural identity (Croker et al., 2004). Their basic properties are summarized in Table 1.2.

Characteristics	TIMP-1	TIMP-2	TIMP-3	TIMP-4
Chromosomal location (gene)	Xp11.23-11.4	17q23-25	22q12.1-13.2	3p25
mRNA (kb)	0.9	1.0-3.5	5.0 (2.6-2.4)	1.4
Molecular mass (kDa) Unglycosylated/glycosylated	20.5/28.5	26	21/27	23/29
Protein localization	Secreted	Secreted	Membranous	Secreted
MMPs poorly inhibited	MT-MMPs	None reported	None reported	None reported

Table 1.2 Molecular characteristics of TIMPs. Modified from Croker et al., 2004; Moore et al., 2011.

The TIMPs possess 12 conserved cysteine residues forming six disulfide bonds that fold the protein into two domains each containing three loops, an MMP-inhibiting N-terminal domain (loops 1–3), and a C-terminal domain (loops 4–6) (Tuuttila et al., 1998). Crystallographic structures are available for TIMP-1 and TIMP-2 whereby accurate assignment of these disulfide bonds has been determined, while hypothetical structures have been proposed for TIMP-3 and TIMP-4 (Moore et al., 2011). Computational scheme of the loop structures and disulfide bond arrangement for human TIMPs are shown in Figure 1.2.

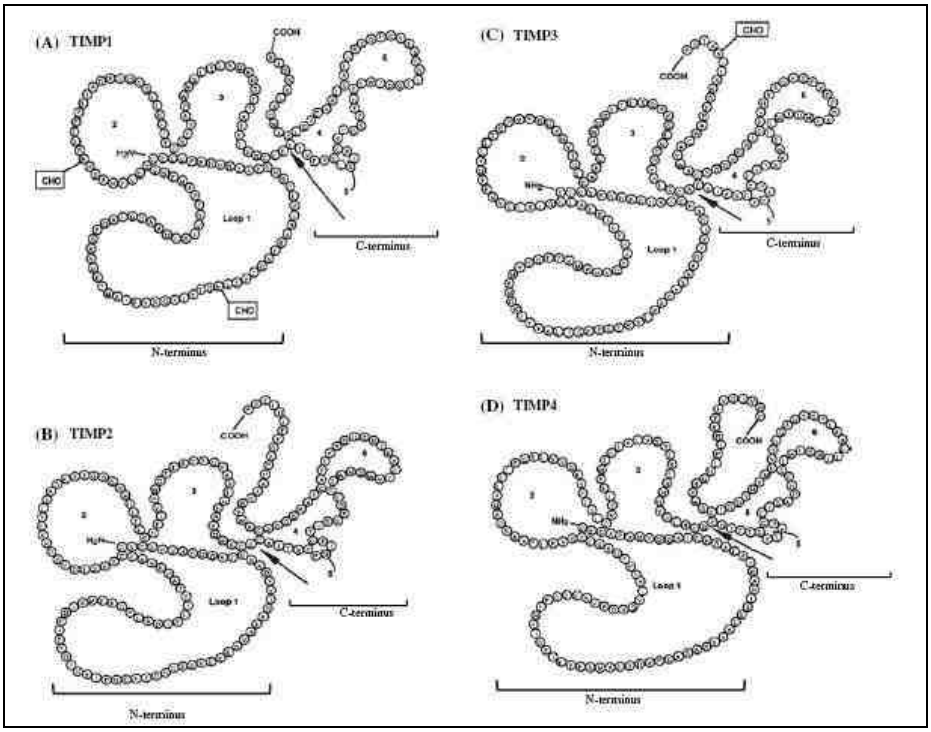

Figure 1.2 Computational structure of human TIMPs. Scheme of TIMP-1, TIMP-2, TIMP-3 and TIMP-4 loop structures and disulfide bond arrangement. The boxed CHO indicates glycosylation sites for TIMP-1 and TIMP-3. The arrows separate the three N-terminal loops from the three C-terminal loops. Adapted from Moore et al., 2011.

TIMPs are produced in glycosylated and unglycosylated forms (Apte et al., 1995). Glycosylation results in an increase in the molecular weight of TIMPs, but has not been shown to alter their MMP-inhibitory function (Langton et al., 1998; Caterina et al., 1998). TIMP-1 has two N-linked glycosylation sites that are important in the correct folding and enhanced stability of TIMP-1, but do not impact its MMP-inhibitory function (Caterina et al., 1998). TIMP-3 has also been shown to be N-glycosylated (Apte et al., 1995); however, this glycosylation is not required for MMP inhibition or ECM binding of this TIMP (Langton et al., 1998). Glycosylation of TIMP-4 occurs by O-linked glycosylation (Dennis et al., 1999). Changes in unglycosylated to glycosylated TIMP-4 have been suggested to represent changes in the rates of TIMP-4 turnover, but no report has been made on the effect of glycosylation on the inhibitory capacity of TIMP-4 (Stroud et al., 2005). There is no TIMP-2 glycosylation has been reported.

TIMPs reversibly inhibit the proteolytic activity of activated MMPs by forming non-covalent 1:1 stoichiometric complexes that are resistant to heat denaturation and proteolytic degradation (Gomez et al., 1997). The N-terminal region of TIMPs binds to the MMP catalytic domain and inhibits MMP activity, whereas, the C-terminal region interacts with the pro-forms of MMP-2 and MMP-9 C-terminal hemopexin domain to stabilize the pro-enzyme-inhibitor complex. TIMP-2 is the only TIMP member that specifically interacts on the cell surface with both MMP-14 and pro-MMP-2 in order to facilitate the activation of pro-MMP-2 (Strongin et al., 1995; Hernandez-Barrantes et al., 2000). Thus TIMP-2 is unique in that it functions both as an MMP inhibitor and activator.

TIMPs can inhibit all active MMPs, however, not with the same efficacy. TIMP-1 preferentially inhibits MMP-7, MMP-9, MMP-1 and MMP-3, but is a poor inhibitor of the MT-MMPs and MMP-19. TIMP-2 is also a more effective inhibitor of MMP-2. TIMP-3 can inhibit MMP-2 and MMP-9. TIMP-4 inhibits MMP-14 and MMP-2 (Croker et al., 2004; Bourboulia and Stetler-Stevenson, 2010; Moore et al., 2011).

TIMPs are usually described solely as MMP inhibitors and, therefore,

mechanistic studies explain TIMP effects, in both physiological and pathological conditions, on the restrained MMP activities and mediated functions. Studies have revealed that TIMPs are involved in several biological activities including cell differentiation, growth, migration, invasion, angiogenesis and apoptosis (Brew and Nagase, 2010; Bourboulia and Stetler-Stevenson, 2010; Moore et al., 2011; Moore and Crocker, 2012). Moreover, the transcriptional repression of the TIMP genes by EZH2 (polycomb group protein enhancer of zeste homolog 2) may be a major mechanism to shift the MMPs/TIMPs balance in favor of MMP activity and thus to promote ECM degradation and subsequent invasion of prostate cancer cells (Shin and Kim, 2012).

1.1.2 MMP substrates

The MMPs were thought to principally degrade structural components of the ECM (Egeblad and Werb, 2002; Kessenbrock et al., 2010) (Table 1.3), therefore, facilitating cell migration. However, because cells have receptors for structural ECM components (for example: integrins, cell-adhesion molecules), cleavage of ECM proteins by MMPs also affects cellular signalling and functions (Streuli, 1999). Cleavage of ECM components by MMPs can also generate fragments with new functions, for example, cleavage of laminin and several collagen type results in exposure of cryptic sites that promote migration (Giannelli et al., 1997; Xu et al., 2001; Robichaud, et al., 2011).

MMPs	Substrates	Docking mechanisms
MMP-1	Collagens (types I, II, III, VII, VIII, X, XI), gelatins, aggrecan, brevican, entactin/nidogen, fibronectin, IGFBP, laminin, link protein, myelin basic protein, tenascin, vitronectin, α1-antichymotrypsin, α2-macroglobulin, α1-proteinase inhibitor, C1q, casein, CXCL12, fibrin, fibrinogen, IL-1β, L-selectin, pro-MMP-2 , pro-MMP-9, pro-TNF-α.	EMMPRIN, α2β1 integrin
MMP-2	Collagens (types I, III, IV, V, VII, X, XI), gelatins, aggrecan, brevican, decorin, elastin, entactin/nidogen , fibrillin, fibronectin, fibulins, IGFBP, laminin, link protein, myelin basic protein, osteonectin, tenascin, vitronectin,	MT-MMPs/TIMP-2, αvβ3 integrin

	α1-antichymotrypsin,α1-proteinase inhibitor, ADAMTS-1, C1q2, CCL7, CXCL12, endothelin, FGFR, fibrin, fibrinogen, galectin-3, IL-1β, pro-MMP-9 and MMP-13, plasminogen, substance P, latent TGFβ, pro-TNFα.	
MMP-3	Collagens (type III, IV, V, VII, IX, X, XI), gelatins, aggrecan, brevican, decorin, elastin, entactin/nidogen, fibrillin, fibronectin, IGFBP, laminin, link protein, myelin basic protein, osteonectin, osteopontin, perlecan, tenascin, vitronectin, α1-antichymotrypsin, α2-macroglobulin, α1-proteinase inhibitor, C1q, casein, CXCL12, E-cadherin, fibrin, fibrinogen, pro-HB-EGF, IL-1β, L-selectin, pro-MMP-1, pro-MMP-7, pro-MMP-8, pro-MMP-9, pro-MMP-13, NC1 fragment of collagen XVIII, PAI-1, plasminogen, substance P, T kininogen, pro-TNF-α, uPA.	
MMP-7	Collagens (types I, IV), gelatins, aggrecan, brevican, decorin, elastin, entactin/nidogen, fibronectin, fibulins, laminin, link protein, myelinbasic protein, osteonectin, osteopontin, tenascin, vitronectin,α1-proteinase inhibitor, casein, E-cadherin, FAS ligand, fibrinogen, pro-HB-EGF, β4 integrin, pro-MMP-1, pro-MMP -2, pro-MMP-9, plasminogen, pro-TNF-α.	Heparan-sulphate proteoglycans, CD44
MMP-8	Collagens (types I, II, III), aggrecan, brevican, α2-macroglobulin, α1-proteinase inhibitor, ADAMTS-1, C1q, fibrinogen, substance P.	
MMP-9	Collagens (types IV, V, XI, XIV), gelatins, aggrecan, decorin, elastin, fibrillin, IGFBP3, laminin, link protein, myelin basic protein, osteonectin, vitronectin, α2-macroglobulin, α1-proteinase inhibitor, casein, C1q, CXCL1, CXCL4, CXCL7-precursor, CXCL12, endothelin, fibrin, fibrinogen, galectin-3, IL-1β, IL-8/CXCL8, IL-2Rα, c-kit ligand, pro-MMP-2, NC1 fragment of collagen XVIII, plasminogen, substance P, latent TGF-β, pro-TNF-α.	CD44, collagen IV
MMP-10	Collagens (types III, IV, V), gelatins, aggrecan, brevican, elastin, fibronectin, link protein, casein, fibrinogen, pro-MMP-1, pro-MMP-7, pro-MMP-8, pro-MMP-9.	
MMP-11	Collagen type VI , IGFBP1, α2-macroglobulin,	

	α2-antiplasmin, α1-proteinase inhibitor, laminin receptor.	
MMP-12	Collagens (types I, IV), gelatins, aggrecan, elastin, entactin/nidogen, fibrillin, fibronectin, laminin, myelin basic protein, vitronectin, α2-macroglobulin, α1-proteinase inhibitor, factor XII, fibrinogen, IgG, NC1 fragment of collagen XVIII, plasminogen, pro-TNF-α.	
MMP-13	Collagens (types I, II, III, IV, VI, IX, X, XIV), gelatins, aggrecan, brevican, fibrillin, fibronectin, osteonectin, tenascin, α2-macroglobulin, C1q, casein, CXCL12, factor XII, fibrinogen, pro-MMP-9, NC1 fragment of collagen XVIII.	
MMP-14	Collagens (types I, II1, III), gelatins, aggrecan, entactin/nidogen, fibrillin, fibronectin, perlecan, vitronectin, α2-macroglobulin, α1-proteinase inhibitor, CD44, CXCL12, factor XII, fibrin, fibrinogen, αv integrin, pro-MMP-2, pro-MMP-13, tenascin, tissue transglutaminase, pro-TNF-α.	Transmembrane domain
MMP-15	Aggrecan, entactin/nidogen, fibronectin, laminin, perlecan, tenascin, tissue transglutaminase, ADAMTS-1, pro-MMP-2.	Transmembrane domain
MMP-16	Collagen III, gelatin, casein, fibronectin, tissue transglutaminase, pro-MMP-2.	Transmembrane domain
MMP-17	Gelatin, fibrin, fibrinogen, pro-MMP-2, pro-TNF-α.	GPI-anchor
MMP-18 (*Xenopus*)	Collagen, gelatins.	
MMP-19	Collagen (types I, IV), gelatins, aggrecan, cartilage oligomeric matrix protein, entactin/nidogen, fibronectin, laminin, tenascin, casein.	
MMP-20	Aggrecan, amelogenin, cartilage oligomeric matrix protein, NC1 fragment of collagen XVIII.	
MMP-21	No substrates reported	
MMP-22 *(chicken)*	Casein, gelatin.	
MMP-23	No substrates reported	Type II (N-terminal) transmembrane domain
MMP-24	Gelatin, fibronectin, pro-MMP-2.	Transmembrane Domain
MMP-25	Collagen type IV, gelatin, fibronectin, fibrinogen, fibrin, pro-MMP-2.	GPI-anchor
MMP-26	Collagen type IV, gelatin, fibrinogen, fibronectin, vitronectin, α1-proteinase inhibitor, casein,	

	pro-MMP-9.	
MMP-27	No substrates reported	
MMP-28	Casein.	

Table 1.3 MMPs and their substrates. Adapted from Liu et al., 2001; Egeblad and Werb, 2002; Motrescu et al., 2008; Kessenbrock et al., 2010.

In addition to cleaving ECM components, MMPs participate in the release of cell-membrane-bound precursor forms of many growth factors, including transforming growth factor-α (TGF-α) (Peschon et al., 1998). Bioavailability of TGF-β is regulated differently: it is released by MMP-2 and MMP-9 from an inactive extracellular complex (Yu and Stamenkovic, 2000). Moreover, cleavage of insulin-like growth-factor-binding protein (IGFBP) and perlecan releases IGFs and fibroblast growth factors (FGFs), respectively (Manes et al., 1997, 1999; Whitelock et al., 1996; Miyamoto, et al., 2004). Apolipoprotein A-IV (apoA-IV) has been identified as a novel substrate for MMP-14 and MMP-7, based on the fact that apoA-IV plays important roles in lipid metabolism and possesses anti-oxidant activity, suggesting that cleavage of lipid-free apoA-IV has pathological implications in the development of hyperlipidemia and atherosclerosis (Park et al., 2011 and 2012).

Growth-factor receptors are also MMP substrates. FGF receptor-1 (FGFR-1) is cleaved by MMP-2 (Levi et al., 1996), whereas two members of the epidermal growth factor receptor (EGFR) family: HER2/ERBB2 and HER4/ERBB4, and the hepatocyte growth factor receptor (HGFR) c-MET, are substrates for unidentified MMPs (Codony-Servat et al., 1999; Vecchi et al., 1998; Nath et al., 2001). In all cases, the extracellular domains of the receptors are released, and these might function as ligands for receptors.

Cell-adhesion molecules are also MMP substrates. Cleavage of E-cadherin and CD44 results in the release of fragments of the extracellular domains and increase invasive behaviour (Noe et al., 2001; Kajita et al., 2001), and cleavage of the αv integrin subunit precursor by MMP-14 enhances cancer-cell migration (Deryugina et al., 2001). Finally, the MMPs might cleave and activate their zymogen forms, and/or their inhibitors (see 1.1.1).

1.1.3 The roles of MMPs in cancer

1.1.3.1 MMPs regulate cell growth

Incontrollable proliferation is a common feature of cancer cells. There are two principal ways in which the tumor achieves this characteristic condition: one is acquire self-sufficiency in growth-promoting signals, the other is get insensitive to antigrowth signals. The MMPs may be critically involved in disrupting the balance between growth and antigrowth signals in tumor microenvironment, as they potently influence the bioavailability and/or functionality of multiple important factors that regulate growth.

One fundamental signaling pathway with essential roles in tissue homeostasis is the TGF-β pathway. TGF-β normally exerts tumor suppressive effects by enforcing cytostasis and differentiation. However, as the tumor advances in malignant progression, the genome often accumulates mutations in the TGF-β receptor system that afford the cancer cells irresponsive to TGF-β. Moreover, it also effects on non-malignant stromal cells, for example, to escape immune surveillance, which can be exploited by the tumor, and therefore turn TGF-β into a tumor promoting factor that leads to increased invasion and metastasis (Massague, 2008). Active TGF-β form is derived from an inactive pro-form by proteolytic conversion by furin or other proteinases, such as MMP-9, which is localized to the cell surface by docking to the surface receptor CD44 (Yu and Stamenkovic, 2000). Similarly, MMP-14 proteolytically activates TGF-β1 (Mu et al., 2002). On the other hand, MMP-2, MMP-9 and MMP-14 indirectly modulate TGF-β bioactivity by cleaving the ECM latent component TGF-β-binding-protein-1 (LTBP-1), thereby solubilizing ECM-bound TGF-β (Dallas et al., 2002; Tatti et al., 2008). Since tumor cells often acquire non-responsiveness to TGF-β, this suggests that proteolytic activation of TGF-β by MMPs has tumor promoting effects by selectively driving stroma mediated invasion and metastasis of the tumor.

The ligands of the EGFR are potent drivers of cell proliferation and important regulators of tissue homeostasis. Malfunction or genetic mutations of the molecules

involved is frequently observed in breast cancer and other malignant diseases (Hynes and Lane, 2005). It has been indicated that MMP-2 promotes colorectal cancer cell growth and invasion via up-regulating VEGF (vascular endothelial growth factor) and MMP-14 expression (Dong et al., 2011). The possible role of MMP-2/α5β1 integrin interaction in the regulation of α5β1 integrin-mediated IL-6/Stat3 signaling activation might enhance the proliferative, invasive and metastatic potential in cancer (Kesanakurti et al., 2012).

Activation of EGFR results in the upregulation of MMP-9, which in turn degrades E-cadherin (a potent control element of many cellular functions including cell-cell adhesion and differentiation). These association between EGFR, MMP-9 and E-cadherin may play an important role in ovarian cancer and metastasis, as activated EGFR and MMP-9 in these specimens colocalize with a region of reduced E-cadherin (Cowden Dahl et al., 2008). Moreover, the cleavage of E-cadherin by MMPs impacts on cancer cell proliferation.

These studies provide mechanistic insight into proteolytic acceleration of cell growth, and suggest that specific inhibition of MMPs may be utilized to interfere with unregulated cell growth and proliferation in several tumors.

1.1.3.2 MMPs regulate apoptosis

Avoiding programmed cell death and/or apoptosis is another strategy that increases the cell number and size of tumors. Apoptosis is normally initiated through extracellular receptors, such as the Fas receptors, which activate a proteolytic cascade of intracellular caspases once they encounter Fas ligand, ultimately leading to the selective degradation of subcellular compartments and nuclear DNA. MMPs interfere with the induction of apoptosis in malignant cells, which may involve the cleavage of ligands or receptors that transduce pro-apoptotic signals. For example, MMP-7 cleaves Fas ligand from the surface of doxorubicin-treated cancer cells (Mitsiades et al., 2001), lowering the impact of chemotherapy on the tumor by abolishing apoptosis. Indeed, MMP-7 expression may also serve as a predictive marker for the resistance to chemotherapy in patients with non-small cell lung cancer (Kessenbrock et al., 2010).

The interaction between MMP-7 and Fas ligand also may play a role in pancreatic ductal adenocarcinoma, as MMP-7 is expressed in human pancreatic cancer specimens and mice deficient in MMP-7 or carrying a nonfunctional Fas ligand mutation, show greatly reduced metaplasia during pancreatic duct ligation (Crawford et al., 2002). The MMP-14 protects breast carcinoma cells against type I collagen-induced apoptosis (Maquoi, et al., 2012). It remains unclear whether MMPs can interact with natural killer (NK) cell mediated tumor killing. However, use of MMP inhibitors in combination with interleukin-15 (IL-15) succeeded in overcoming the resistance of small-cell lung cancer cells to NK cell killing (Le Maux Chansac et al., 2008).

Thus, these examples suggest a tumor-promoting role of these MMPs by blocking receptor-transmitted or lymphocyte-mediated apoptosis.

1.1.3.3 MMPs regulate angiogenesis

The tumor vasculature is derived from sprouting of local blood vessels (named as angiogenesis) and circulating vasculogenic progenitor cells derived from the bone marrow (named as vasculogenesis) (Kessenbrock et al., 2010). The new vessels are often irregular and leaky due to lack of the pericyte cover, with the result that tumor cells can penetrate more easily. As compared with blood capillaries, lymphatic endothelial cells have even less developed junctions with frequently large inter-endothelial gaps and impaired basement membranes. The invasive margin is a critical area for stimulation of angiogenesis and lymphangiogenesis in tumors, which contributes to tumor invasion and metastasis (Padera et al., 2002). The major MMPs involved in tumor angiogenesis are MMP-2, MMP-9, and MMP-14, and to a lesser extent MMP-1 and MMP-7. Given that several MMPs are expressed in all tumors, it is now evident that several MMPs can contribute to distinct vascular events in most tumors (Littlepage et al., 2010, Dao Thi et al., 2012).

MMP-9 has a distinct role in tumor angiogenesis, mainly by regulating the bioavailability of VEGF (the most potent inducer of tumor angiogenesis and a major therapeutic target). MMP-9 is expressed by inflammatory cells and enables an

angiogenic switch by making sequestered VEGF bioavailable for its receptor VEGFR2 in pancreatic islet tumors (Bergers et al., 2000). Angiogenic switching by MMP-9 involves a complex interplay of interconnected factors. In a mouse model of glioblastoma, the hypoxia inducible factor-1α (HIF-1α) induces recruitment of CD45-positive bone marrow derived cells, as well as endothelial and pericyte progenitor cells, to promote neovascularization. MMP-9 activity provided by these CD45-positive myeloid cells is essential and sufficient for the angiogenic switch by increasing VEGF bioavailability. This process induces angiogenesis and regulates tumor cell invasiveness. Interestingly, VEGF prevents tumor cell migration along blood vessels, but it promotes perivascular tumor cell infiltration into the brain parenchyma (Du et al., 2008). This action of VEGF as a brake on perivascular tumor cell migration is surprising. In addition, the direct cleavage of matrix-bound VEGF by MMP-3, MMP-7, MMP-9, or MMP-16 results in modified VEGF molecules with altered bioavailability, which changes the vascular patterning of tumors in vivo (Lee et al., 2005).

In addition to its role in regulating angiogenesis, MMP-9 is also implicated in vasculogenesis. Tumors transplanted into tissue irradiated to prevent angiogenesis are unable to grow in MMP-9 knockout mice. However, tumor growth is restored by transplanting CD11b-positive myeloid cells from the bone marrow of wild-type mice, suggesting that MMP-9 is required for tumor vasculogenesis (Ahn and Brown, 2008). Therefore, MMP-9 could be an important target for therapy to enhance the response of tumors to radiotherapy.

A special role is attributed to MMP-9 delivered by neutrophilic granulocytes. In contrast to other cell types, neutrophil derived pro-MMP-9 is not complexed with TIMP-1 and therefore is more readily activated to drive tumor angiogenesis (Ardi et al., 2007). The angiogenic function of neutrophil MMP-9 requires both its active site and hemopexin domain, and activates the basic FGF-2/FGFR-2 pathway (Ardi et al., 2009). This highlights the important effects of proteinase inhibitors on the function of MMPs, and shows that MMPs produced by different cell types may function in different ways. The release of TIMP-1-free MMP-9 may be an important aspect in the

pro-angiogenic effects triggered by tumor infiltrating neutrophils. Indeed, elevated numbers of neutrophils present in patients with myxofibrosarcoma correlate with microvessel density in the tumor (Mentzel et al., 2001), and depleting neutrophils in a mouse model of pancreatic cancer markedly reduces angiogenic switching in dysplasias (Nozawa et al., 2006). These findings support an important role of infiltrating neutrophils in the induction of tumor angiogenesis.

The degradation of ECM components and other extracellular molecules may also generate fragments with new bioactivities that inhibit angiogenesis (Ribatti, 2009). For example, biologically active endostatin is generated through cleavage of type XVIII collagen by MMP-3, MMP-7, MMP-9, MMP-13, and MMP-20 (Heljasvaara et al., 2005). Moreover, the degradation of collagen IV-α3 by MMP-9 results in the generation of the monomeric NC1 domain (called tumstatin), a potent suppressor of angiogenesis, which induces pathological vascularization and increases tumor growth in MMP-9-knockout mice (Hamano et al., 2003). The degradation of plasminogen by MMP-2, MMP-9 and MMP-12, produces angiostatin, a cleavage product with antiangiogenic function (Cornelius et al., 1998; Patterson and Sang, 1997). Angiostatin production by MMP-12 may explain the suppressive effects of this MMP on outgrowth of lung metastases (Houghton et al., 2006a). Taken together, MMPs can generate both angiogenesis-inhibiting as well as -promoting signals, depending on the time frame of MMP expression and the availability of substrates.

MMPs also regulate vascular stability and permeability. For example, MMP-14 appears to mediate the vascular response to tissue injury and tumor progression though activation of TGF-β (Sounni et al., 2010). Antagonists of MMP-14 and TGF-β signaling could be therapeutically exploited to improve the delivery of therapeutics or molecular contrast agents into tissues where chronic damage or neoplastic disease limits their efficient delivery. It has been indicated that microRNA-9 suppresses MMP-14 expression via the binding site in the 3’-untranslated regions (3'-UTR), thus inhibiting the invasion, metastasis and angiogenesis of neuroblastoma (Zhang, et al., 2012).

1.1.3.4 MMPs regulate lymphangiogenesis

Lymphangiogenesis plays an important role in tumor biology, because it is directly linked with the formation of lymphatic metastases. MMPs certainly have a general impact on lymphangiogenesis as supported with broad-spectrum MMP inhibitors (Nakamura et al., 2004). However, only a few reports directly link MMPs to the formation of new lymphatic vessels. The modulation of VEGF bioavailability by MMPs, especially by MMP-9, may also affect lymphangiogenesis and, in turn, promotes lymph node metastases. The most direct proof for MMP involvement in lymphangiogenesis has come from experiments modeling lymphangiogenesis in a three-dimensional culture system using mouse thoracic duct fragments embedded in a collagen gel in which lumen containing lymphatic capillaries form (Bruyere et al., 2008). Increased expression of MMP-1, MMP-2 (Langenskiold et al., 2005; Detry, et al., 2012) and MMP-3 (Islekel et al., 2007) is linked with lymphatic vessel formation and lymph node metastases. Inhibition of MMP-2, MMP-9 and MMP-14 decreases both angiogenesis and lymphangiogenesis and reduces lymph node metastasis (Nakamura et al., 2004; Yoo, et al., 2011). The lymphatic vasculature, but not aortic vasculature, is impaired by targeted deletion of MMP-2 (Bruyere et al., 2008). MMP-2-driven collagenolytic pathway is involved in lymphatic vessel formation and morphogenesis (Detry et al., 2012).

1.1.3.5 MMPs regulate cell adhesion, migration and epithelial to mesenchymal transition

Cell movement is highly related with the proteolytic activity of MMPs regulating the dynamic ECM-cell and cell-cell interactions during cell migration. Initially, the generation and activation of latent peptides through degradation of ECM molecules, such as collagen type IV and laminin-5, promotes the migration of cancer cells (Xu et al., 2001; Koshikawa et al., 2000). Several integrins play an active role in regulation of cell migration because they can serve as substrates for MMPs (Baciu et al., 2003). It has been demonstrated that cell adhesion, force generation, and force sensing are vital for the regulation of MMP-14 for efficient cleavage of collagen-I (Kirmse et al.,

2012). Besides, cross-talk between MMP-14 and CD44 results in phosphorylation of EGF receptor and downstream activation of the MAPK and PI3K signaling pathways involved in cell migration (Zarrabi et al., 2011).

Epithelial to mesenchymal transition (EMT) is a highly conserved and fundamental process of morphological transition (Egeblad and Werb, 2002). In particular, during this event, epithelial cells actively down-regulate cell–cell adhesion systems, lose their polarity, and acquire a mesenchymal phenotype with reduced intercellular interactions and increased migratory capacity (Figure 1.3) (Polyak and Weinberg, 2009; Radisky and Radisky, 2010). Over-expression of several MMPs (MMP-2, MMP-3, MMP-9, MMP-13, MMP-14) has been associated with EMT. MMP-1 and MMP-7 appear to contribute to this morphological transition by cleaving E-cadherin (Noe et al., 2001). Recent studies indicate the implication of MMP-28 in the proteolytic activation of TGF-β, thus leading to EMT (Illman et al., 2006; Heldin et al., 2009). It has been shown that TGF-α, cyclooxygenase-2 (Cox-2), MMP-7, MMP-9 and CXCR-4 are involved in EMT, which are associated with poor overall survival of gastric cancer patients (Fanelli et al., 2012), and MMP-9 can cooperate with transcription factor Snail to induce EMT (Lin et al., 2011). Moreover, over-expression of MMP-3 in mammary epithelium triggers a cascade of events including the cleavage of E-cadherin resulting in EMT (Lochter et al., 1997; Radisky et al., 2005).

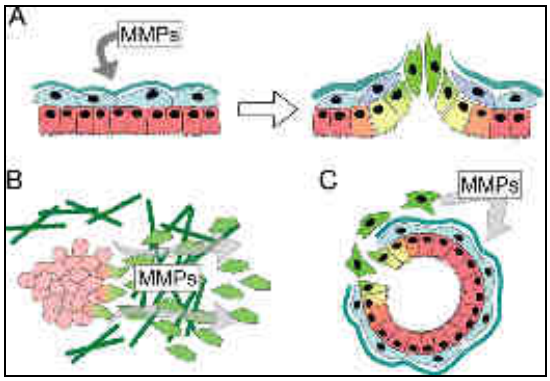

Figure 1.3 MMPs facilitate EMT-associated tumor progression. A: Exposure of epithelial cells to MMPs can directly induce EMT. **B:** Increased expression of MMPs in cells which have undergone EMT facilitates cancer cell invasion. **C:** EMT can produce nonmalignant stromal cells which drive tumor initiation and progression through production of MMPs. Adapted from Radisky and Radisky, 2010.

1.1.3.6 MMPs regulate cancer cell invasion and metastasis

The lethal outcome of cancers is due to the dissemination of metastatic tumor cells and the outgrowth of secondary tumors at distant sites. The initiation of metastasis involves the invasion of tumor cells into the peripheral tissue, leading to intravasation of cancer cells into blood or lymphatic vessels from where they can disseminate into secondary organs through extravasation. Invasion and metastasis require the crossing of several physical barriers, such as the endothelial basement membrane.

An interesting mechanism of MMP-mediated signal transduction linked with increased metastasis is observed in the presence of MMP-1. The proteinase-activated receptors (PARs), a set of G protein-coupled receptors with distinct functions in thrombosis and inflammation, could affect tumor invasion by inducing cancer cell migration upon proteolytic cleavage of the receptor. PAR-1 expression is increased in several cancers, including breast, colon and lung. A study using a xenograft model of breast carcinoma cells, demonstrates a critical role for MMP-1 derived from tumor-infiltrating fibroblasts in the cleavage of PAR-1, which appears to drive cancer cell migration and invasive behavior of the tumor (Boire et al., 2005; Kessenbrock et al., 2010). This indicates an important role of stroma-derived proteinases in tumor progression, carried out by specific signal transduction on cancer cells.

Bone is one of the most common sites for metastasis. MMPs expressed at the interface between tumor and stromal cells play an important role in osteolysis and dissemination into bone tissue. Thus, MMP-7 expressed by osteoclasts triggers osteolysis and subsequent bone metastasis in a rodent model of prostate cancer (Lynch et al., 2005). The target of MMP-7 is the TNF family member RANKL (Receptor Activator for Nuclear Factor κB Ligand). Normally, RANKL is expressed on activated osteoblasts, so that the close contact between osteoclasts and osteoblasts enables binding of RANKL to its receptor RANK on osteoclast progenitors leading to osteoclast differentiation. Cleavage by MMP-7 releases an active form of RANKL that promotes osteoclast activation without osteoblasts in the close proximity. A

similar effect has recently been elucidated for MMP-1 by knocking-down this protease in a highly bone metastatic clone of the human breast cancer cell line MDA-MB-231 (Lu et al., 2009). The MMP-13 activates pre-MMP-9 and promotes the cleavage of galectin-3 (a suppressor of osteoclastogenesis), thus contributing to pre-osteoclast differentiation. Accordingly, MMP-13 abrogation in tumor cells injected into the femurs of nude mice reduced the differentiation of TRAP (Tartrate-Resistant Acid Phosphatase) positive cells in bone marrow and within the tumor mass as well as bone erosion (Pivetta et al., 2011). Further analyses reveal that MMP-1 proteolytically engage EGF-like ligands, resulting in activation of the RANKL pathway, which in turn promotes osteolysis and metastasis to the bone. This finding support the identification of MMP-1 gene as part of the multigenic program that mediates bone metastasis of breast cancer cells (Kang et al., 2003). Taken together, these MMPs could serve as therapeutic target to prevent metastasis to the bone in breast or prostate cancer.

Although there is a wide range of biological functions of MMPs in cancer, a central role is the degradation and remodeling of the ECM, and promotion of the peripheral tissue for invasion and metastasis. Recent studies using high-resolution multimodal microscopy have further corroborated the importance of ECM remodeling by MMP-14 driven pericellular proteolysis, which potently patterns the tissue to facilitate single-cell and finally collective-cell migration and invasion (Wolf et al., 2007). A number of ECM degrading proteolytic enzymes, such as MMP-1, MMP-2, MMP-13 and MMP-14 have been also implicated in this process; however MMP-14 may be critical and rate limiting in collagen turnover (Sabeh et al., 2004; Friedl and Wolf, 2008). A striking observation is that metastatic cancer cells can switch from a protease-dependent to a protease-independent invasion program by utilizing an amoeboid migration mode (Wolf et al., 2007). It remains a subject of ongoing debate whether the amoeboid migration mode is only relevant under in vitro conditions when the surrounding collagen network is devoid of covalent crosslinks (Sabeh et al., 2009).

Several evidences from in vivo analyses support the view that motility of

metastatic cancer cells and their outflow into the circulation occur in close cooperation with tumor associated macrophages (Wyckoff et al., 2004). Proteolytic degradation of the endothelial basement membrane and other matrix components has long been associated with immune cell extravasation during inflammatory conditions and may be crucial for intravasation of tumor cells into the circulation. Indeed, macrophage-derived MMP-2 and MMP-9 are important mediators of immune cell migration into the brain in a mouse model for auto-immune encephalitis, which involves degradation of the ECM component dystroglycan (Agrawal et al., 2006). These studies suggest that MMPs delivered by tumor-associated macrophages might contribute to intravasation of cancer cells into the blood stream.

1.1.3.7 MMPs regulate inflammatory reaction

There is increasing evidences implicating MMPs as major regulators of innate and acquired immunity. The process of inflammation and production of cytokines by immune cells are in many ways linked to cancer progression (Lin and Karin, 2007). There is potent evidence from studies in knockout mice that MMPs play an important role in acute as well as chronic inflammation (Parks et al., 2004). One of the most important pro-inflammatory cytokines is TNF-α, which is expressed as a membrane bound precursor (pro-TNF-α) on a variety of cells, including macrophages and T cells. Conversion of pro-TNF-α into the soluble form requires proteolytic cleavage by several MMPs including MMP-1, MMP-2, MMP-3, MMP-9, MMP-12, MMP-14, MMP-15 and MMP-17 (Manicone and McGuire, 2008; Khan et al., 2012). MMPs may be important TNF-α converting mediators in specific physiological or pathological circumstances, such as MMP-7 in the regulation of inflammation during resorption of herniated discs (Haro et al., 2000). Many tumor cells produce abundant TNF-α, and it promotes cancer cell growth in an NF-κB dependent manner (Luo et al., 2004), suggesting that the conversion of TNF-α by MMPs might be a crucial step in this tumor promoting cascade. It has been reported that MMP-14 modulates inflammatory responses in a protease-independent fashion in tandem with MMP-14 trafficking to the nuclear compartment, where it triggers the expression and activation

of a phosphoinositide 3-kinase δ (PI3Kδ)/Akt/GSK3β signaling cascade. In turn, MMP-14-dependent PI3Kδ activation regulates the immunoregulatory Mi-2/NuRD nucleosome remodeling complex that is responsible for controlling macrophage immune response (Shimizu-Hirota et al., 2012).

A number of studies have shown the proteolytic alteration of chemokines by MMPs. Several members of the CCL/monocyte chemoattractant protein (MCP) family of chemokines are cleaved by MMPs, which specifically renders them into non-activating receptor antagonists with inflammation dampening effects (McQuibban et al., 2002). For example, CCL-8/MCP-2 is processed by MMP-1 and MMP-3. The proteolytic cleavage of CCL-8 can counteract the antitumor capacity of this chemokine in a melanoma model (Struyf et al., 2009). This study shows that proteolytic cleavage of a chemokine have great impact in a clinically relevant setting of tumor development. MMP-8, MMP-9, and MMP-12 also modulate the bioactivity of CXCL-11/I-TAC, a potent Th1 lymphocyte-attracting chemokine (Cox et al., 2008). Although MMP-mediated N-terminal truncation of CXCL-11 leads to inactivation of the chemokine and creates a potent receptor antagonist, further C-terminal cleavage abolishes the antagonist function and removes heparin-binding capacity of CXCL-11, thereby solubilizing the chemokine from the ECM. These findings implicate myeloid cell-derived MMPs in the regulation of T cell responses, which may have important consequences on the adaptive antitumor immune response. CXCR-7, the chemokine receptor for CXCL-11, is also expressed on many tumor cells and can transmit growth- and survival promoting signals (Burns et al., 2006). Modulation of CXCL-11 by MMPs might therefore reduce the antitumor immune response and thus have direct consequences on tumor growth.

The classical function of MMPs, the degradation of ECM, may have secondary effects on the immune system. Some of the proteolytic fragments of MMP-processed ECM components exert chemotactic properties. Thus, macrophage elastase MMP-12 produces neutrophil attracting peptides by degrading elastin (Houghton et al., 2006b). Moreover, ECM breakdown during airway inflammation generates the fragment N-acetyl Pro-Gly-Pro (PGP), a tripeptide with chemotactic activity through activation

of CXC chemokine receptors on neutrophilic granulocytes (Weathington et al., 2006). MMP-8 is involved in the generation of chemotactic PGP and thus regulates neutrophil recruitment to the sites of inflammation (Rocks et al., 2008), which may cause a delay in the wound healing response and increase inflammation over time, as observed previously in MMP-8-deficient mice (Gutierrez-Fernandez et al., 2007). MMP-8 contributed by neutrophils also has a tumor suppressing role in a mouse model of carcinogen induced skin cancer (Balbin et al., 2003). The defect in the resolution of inflammation and the tendency to develop chronic inflammation in the absence of MMP-8 in mice, explain how loss of MMP-8 function contributes mechanistically to increase susceptibility of skin adenocarcinoma and melanoma formation in humans (Palavalli et al., 2009). However, expression of MMP-8 in tumor cells also tightens their adhesion to the ECM and thereby may directly suppress metastatic behavior (Gutierrez-Fernandez et al., 2008). Thus, interference with the tumor suppressing function of MMP-8 should be regarded as one of the unwanted effects of broad-spectrum MMP inhibitors.

The infiltration of neutrophils in the tumor microenvironment often correlates with poor prognosis (de Visser et al., 2006). Like other inflammatory cells, neutrophils sense the concentration gradient of chemokines, such as CXCL-1/KC, a mouse homolog of CXCL-8, which forms complexes with the heparan sulfate proteoglycan syndecan-1 on interstitial cell surfaces. MMP-7 indirectly modulates the bioactivity of CXCL-1 by cleaving syndecan-1 from cell surfaces and thereby releasing chemotactic complexes of syndecan-1 and CXCL-1 (Li et al., 2002). This efficiently leads to the generation of a concentration gradient of soluble chemotactic CXCL-1-syndecan-1 complexes. In a comparable manner, N-terminal processing of neutrophil-attracting CXCL-8/IL-8 by MMP-9 leads to nearly 10-fold increased chemotactic activity on neutrophils compared to full-length CXCL-8 (Van den Steen et al., 2000). The IL-17A could promote hepatocellular carcinoma metastasis by the upregulation of MMP-2 and MMP-9 expression via activating NF-κB signaling pathway (Li et al., 2011). Therefore, MMPs orchestrate the recruitment of leukocytes as an essential component of tumor-associated inflammation.

1.1.3.8 Non-proteolytic functions of MMPs

An emerging interesting field is the noncatalytic function of MMPs. The hemopexin domain of MMPs plays an important role in the non-proteolytic function of MMPs. The first in vivo hint for a crucial hemopexin mediated function of MMPs was established with the observation that TIMP-1 and TIMP-2 bind to several MMPs through their hemopexin domains. Indeed, activation of MMP-2 requires TIMP-2 that is bound to one molecule of MMP-14 via its catalytic domain and to pro-MMP-2 via its hemopexin domain. A second molecule of MMP-14 then catalytically activates MMP-2 (Strongin et al., 1995).

Several members of the MMP family trigger cancer cell migration. However, recent evidence suggests that they mediate chemotaxis without using their proteolytic domain. For example, precursor forms of MMP-2 and MMP-9 enhance cell migration in a transwell chamber assay. The hemopexin domain of MMP-9, but not its proteolytic activity, is necessary for MMP-9 mediated epithelial cell migration in this assay (Dufour et al., 2008). Activation of the MAP kinase and PI3 kinase pathways appear to be involved in this nonproteolytic function of MMP-9. The distinct molecular pathway as well as the in vivo role of this function yet remain elusive. Moreover, the cytoplasmic tail of MMP-14 carries out a migration promoting function on macrophages, as genetic depletion of the cytoplasmic tail, but not of the extracellular hemopexin or catalytic domain impairs the migration of macrophages during in vitro migration through Matrigel (Sakamoto and Seiki, 2009). Moreover, the inhibition of MMP-9 and MMP-14 hemopexin domain using either deletion or appropriate antibodies could repress tumor growth (Dufour et al., 2011; Remacle et al., 2012).

Some evidences for the physiological relevance of hemopexin domains of MMPs have come more recently using genetic modification of one of the two MMP genes of drosophila melanogaster (Glasheen et al., 2009). These investigations reveal that the hemopexin domain is specifically implicated in tissue invasion during metamorphosis.

Moreover, the hemopexin domain of MMP-12 plays an essential role in the

recently described anti-microbial function of this enzyme. Deleting MMP-12 genetically in mice results in impaired bacterial clearance and increased mortality when infected with gram-negative and gram-positive bacteria. The anti-microbial properties of MMP-12 map to a unique four amino acid sequence within the hemopexin-like C-terminal domain and do not require catalytic activity of the enzyme (Houghton et al., 2009). It remains to be determined whether similar non-proteolytic motifs are present in other MMPs and whether these non-proteolytic modes of action are also implicated in cancer-related functions of these enzymes.

Several MMPs may interact with other extracellular molecules without inducing proteolytic cleavage. MMP-14 interacts with the C1q component of the complement system in a non-proteolytic receptor ligand manner, without inducing C1qr and C1qs proteinase activity, suggesting that this binding may inhibit activation of the complement proteinase cascade (Rozanov et al., 2004). MMPs also bind to members of the integrin family of cell surface receptors. A study has linked the non-proteolytic interaction of pro-MMP-1 with α2β1 integrin on neurons and induced neuronal cell death in cell culture (Conant et al., 2004). Reduced de-phosphorylation of AKT after MMP-1 incubation, which is inhibited by blocking α2 integrin antibody, but not by administration of batimastat (an inhibitor of MMP activity), suggests that integrin binding, rather than proteinase activity, is relevant for MMP-1 transmitted cytotoxicity. In chronic lymphocytic leukemia, MMP-9 promotes B cell survival in a non-proteolytic fashion through its hemopexin domain by docking to the surface receptors α4β1 and CD44v, which induce intracellular signaling involving Lyn activation and STAT3 phosphorylation that prevents B cell apoptosis (Redondo-Munoz et al., 2010).

Taken together, these data indicated that the complexity of the mode of action of MMPs has expanded considerably from proteinases that simply degrade the ECM to various biological functions, such as specific modulators of angiogenesis, fine-tuners of cell signaling pathways or inflammatory response (Figure 1.4).

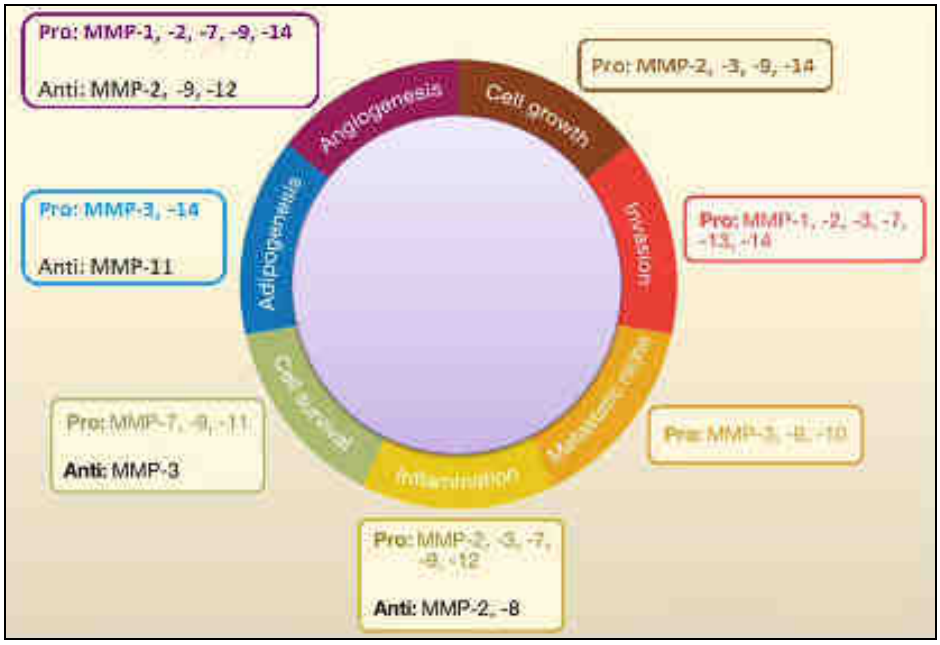

Figure 1.4 Modulation of the tumor microenvironment by MMPs. Summary of the various processes that are modulated by MMPs in the tumor microenvironment. Selected examples of MMPs that promote (pro) or suppress (anti) these processes. This image illustrates the complexity of the tumor microenvironment, which is largely influenced by MMPs. Modified from Kessenbrock, et al., 2010.

1.2 MMPs and mammary gland development

1.2.1 Mammary gland dynamic development

1.2.1.1 Morphogenesis of the embryonic mammary gland

The development of the mammary gland begins with the formation of the mammary lines at the ventral aspect of the Wolfian ridge on embryonic day 10 (E10) (Sakakura, 1987). These are bilateral ectodermal ridges that stretch in a rostral–caudal orientation between the fore and hind limb buds. In mice, this line has been noted by expression of several molecular markers of the Wnt signaling pathway. Wnt signaling promotes placode development and is required for initiation of mammary gland morphogenesis (Chu et al., 2004; Veltmaat et al., 2004; Veltmaat et al., 2006). The ectoderm of the mammary line is organized as a pseudostratified epithelium connecting the developing mammary placodes at around E11.5, whereas all other surface ectoderm is single-layered (Sakakura, 1987; Veltmaat et al., 2004).

Within 24-36 h of its formation, the mammary line resolves into five pairs of

placodes (three thoracic and two inguinal) in characteristic locations along the ventral–lateral border of the embryo (Figure 1.5). Each pair of placodes develops symmetrically, but the different molecular requirement of each placode also suggests that different molecular mechanisms may underlie the formation of such identical structures (Veltmaat et al., 2003; Veltmaat et al., 2004). Individual placodes form in a characteristic sequence: the first to become visible are placodes 3, followed by pairs 4, 1 and 5, and finally by pair 2. The placodes are lens-shaped thickenings of the surface ectoderm, which consist of several layers of cells that are larger and more columnar in appearance than are those in the surrounding epidermis. The orientation of the placodal cells is not uniform, which may represent that mammary placodes may form by the migration and accumulation of motile cells at defined locations along the mammary lines (Propper, 1978; Hens and Wysolmerski, 2005; Robinson, 2007).

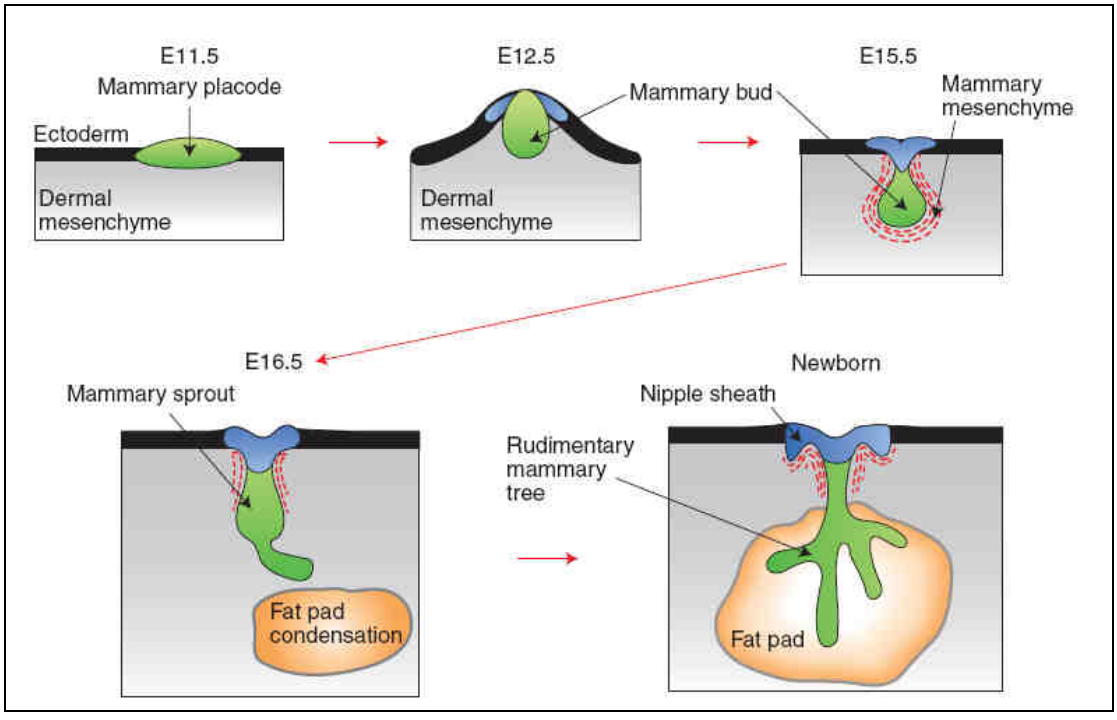

Figure 1.5 Overview of embryonic mammary development. Adapted from Cowin and Wysolmerski, 2010.

The placodal epithelial cells invaginate and invade the mesenchyme to form bud, a process that is essentially completed by E14 (Sakakura, 1987; Watson and Khaled, 2008). As the cells from the placode begin to invaginate, they pile up at the surface and begin to array themselves in a concentric orientation so that the early bud is

elevated above the plane of the surrounding epidermis. As a result, the developing buds are visible as prominent knobs on the ventral surface of the embryo at E12, which then submerge beneath the plane of the skin (Chu et al., 2004; Veltmaat et al., 2004). The formation of the epithelial bud is also accompanied by dramatic changes in the underlying mesenchyme (Sakakura, 1987; Dunbar et al., 1999; Foley et al., 2001). Cells surrounding the epithelium elongate, condense, and orient their long axis in a radial fashion around the developing epithelial cells. At the end of this process, the mature bud consists of a sphere of concentrically arrayed epithelial cells connected to the skin surface by a stalk of epidermal-like cells. Both ball and stalk are, in turn, surrounded by three to five layers of condensed mesenchyme, referred to as the primary mammary mesenchyme. In female mice, the mammary buds remain relatively quiescent from E14 to E16, then ductal morphogenesis commences. However, in male mice, the mesenchyme around the stalk enlarges and condenses further, eventually severing the connection to the skin (Heuberger et al., 1982; Dunbar et al., 1999; Veltmaat et al., 2003), which is followed by apoptosis of the mammary mesenchyme and many cells within the epithelial bud as well (Dunbar et al., 1999). Therefore, male mice have either no mammary epithelial ducts or only very rudimentary ones.

The next phase of development involves the onset of ductal branching morphogenesis. A solid cord of epithelial cells emerges from the mammary bud and primary mammary mesenchyme into a second stromal compartment, namely the mammary fat pad (Sakakura, 1987; Hens and Wysolmerski, 2005). The embryonic fat pad consists of a loose collection of pre-adipocytes that originate from a mesenchymal condensation formed on E14 (Sakakura et al., 1982). Once the primary cord or mammary sprout reaches the adipocytes of the fat pad, it begins to branch in a characteristic dichotomous fashion to form the initial ductal tree. This initial round of branching growth extends from E16 to the perinatal period to give one primary duct with about 10-15 initial branches (Watson and Khaled, 2008). At the conclusion of embryonic development, the mammary gland consists of a short primary duct ending in a small, branched ductal tree that is embedded in larger mammary fat pad. This

rudimentary duct system forms the scaffold on which further development during puberty and pregnancy will eventually produce the mature milk-producing glands found during lactation (Cowin and Wysolmerski, 2010).

1.2.1.2 Mammary gland dynamic stages during postnatal development

The most remarkable and dynamic morphological changes of the mammary gland occur from puberty to menopause. The discrete stages of the mammary gland are shown in Figure 1.6.

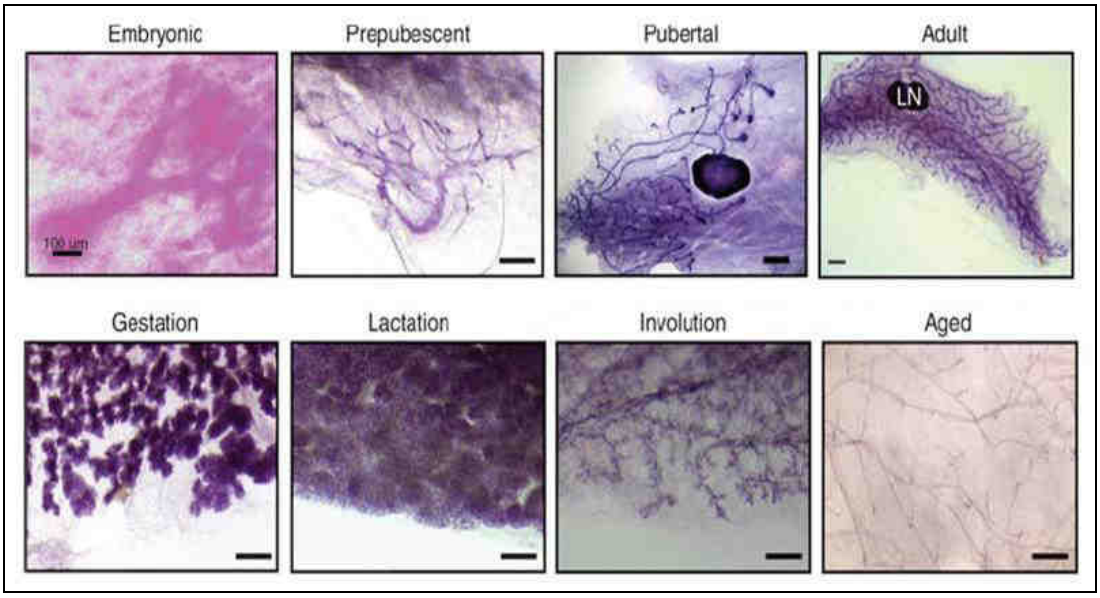

Figure 1.6 Distinct stages of mammary gland remodeling. A series of murine mammary whole mounts illustrating distinct mammary morphology during the indicated stages of development from embryonic through to adult: the prenatal rudimentary ductal tree (E18.5), postnatal prepubescent mammary gland (2 weeks of age); rapidly elongating pubertal mammary gland with bulbous TEBs (5 weeks of age); and the fully developed adult gland (10 weeks of age) that has reached the limits of the fat pad. The major reproductive phases that involve extensive remodeling are gestation (day 18.5 gestation), which shows extensive lobuloalveolar differentiation; lactation, which highlights a functionally differentiated gland; postlactational involution (day 8 postlactation), which shows the loss of secretory epithelium; and finally, 20-month-old mice, which have ceased the reproductive cycle show a dormant ductal tree. Modified from Khokha and Werb, 2011.

At puberty, branching morphogenesis is triggered by mammotrophic signals provided by the hypothalamic-pituitary-ovarian axis (Sternlicht et al., 2006). Following the rules common to many organs that display branched tubular structures

(Affolter et al., 2003), the mammary ductal trees elongate as epithelial cells grow and invade the fat pad led by terminal end buds (TEBs), which are highly motile structures located at the forefront of ducts (Hinck and Silberstein, 2005). Stimulation by growth hormone (GH) induces stromal IGF-1, whereas ovarian estrogen stimulates release of epithelial amphiregulin to mediate stromal-epithelial crosstalk during pubertal mammary development (Sternlicht, 2006; Sternlicht et al., 2006). The bulbous TEBs undergo repeated dichotomous branching to form adequately spaced primary ducts with lumens, whereas concomitant secondary and tertiary side branching occurs by ductal lateral bud sprouting (Wiseman and Werb, 2002; Lu et al., 2006; Lu and Werb, 2008). The ductal tree structure ceases forward growth when it approaches the distal limits of the fat pad, commanded in part by TGF-β signaling (Sternlicht, 2006).

The branched structure of the mammary gland is well suited for maximizing its cellular surface area, as it structurally and functionally adapts to the assigned physiological demand. In the adult female, the mammary gland undergoes repeated cyclical turnover during each reproductive cycle, systematically displaying lobuloalveologenesis during the murine diestrus phase (Robinson et al., 1995; Fata et al., 2001), which parallels the luteal phase in humans. Increased mammographic density has been reported during this phase of the reproductive cycle in women (Ursin et al., 2001). In mice, this changing morphology is accompanied by rounds of cell proliferation as well as cell death that peak at diestrus.

Progesterone secretion rises in response to the post-coitum maintenance of the corpus luteum, and this function is taken over by the placenta as pregnancy establishes. Progesterone, together with pituitary-derived prolactin, provides key signals for orchestrating mammary epithelial differentiation during pregnancy (Brisken et al., 1999; Oakes et al., 2008). Extensive mammary epithelial proliferation ensues, resulting in about 100-fold increase in the cell number, accompanied by cellular differentiation, polarization and development of secretory epithelium during a relatively short period of about 19-21 days of gestation in the mouse. The ratio of adipocytes to epithelia decreases to facilitate parenchymal expansion during this

phase. A complex milieu of hormones marked by a drop in progesterone activates epithelial changes leading to lactation, which is typically maintained by the suckling response of the newborn (Neville et al., 2002; Pang and Hartmann, 2007). Post-lactation mammary involution involves rapid regression of the differentiated gland and depends on programmed cell death pathways that eliminate up to 50-80% of the secretory epithelium within 1 week of weaning (Walker et al., 1989). Two phases of involution have been described, the first is a potentially reversible period initiated by mechanical triggers associated with milk stasis, and the second is a irreversible programmed deconstruction of the lobuloalveolar acini and the supporting structural ECM (Lund et al., 1996; Alexander et al., 2001;Watson, 2006). The latter phase is dominated by the involvement of extracellular proteins with concomitant reconstitution of the adipocyte compartment. The secretory alveoli collapse, forming epithelial cords, eventually returning the glandular structure to a pre-gestation phenotype that resembles the virgin mammary gland. Along with the classical apoptosis pathways (Watson, 2006), phagocytosis by cells of the monocyte lineage (O'Brien and Schedin, 2009), as well as the more recently discovered epithelial cell autophagy (Atabai et al., 2007; Monks et al., 2008; Zarzynska and Motyl, 2008), contribute to involution. Distinct from post-lactation involution is the irreversible process of lobular involution that is associated with age-related, gradual loss of breast epithelial tissue (Radisky and Hartmann, 2009). In humans, this regression begins at variable ages, early or during perimenopause, and leads to decreased size and complexity of the mammary ductal tree.

The substantial plasticity of the ductal network is thus evident throughout the female lifespan. Plasticity of the mammary gland is not merely biologically intriguing, it is intimately tied to breast cancer as documented by epidemiology literature. Briefly, a higher number of menstrual cycles, because of early menarche or late menopause correlate with an increased risk of developing breast cancer (Kelsey et al., 1993; Veronesi et al., 2005). Conversely, pregnancies and breast feeding are considered preventative against breast cancer when compared with nulliparous women or those who never breastfed (Akbari et al., 2010). Mammary gland regression after pregnancy

has been suggested to be implicated in tumor promotion because poorer prognosis is seen in a subset of patients diagnosed within 5 years postpartum (O'Brien and Schedin, 2009; Lyons et al., 2011). More recent literatures suggest that premenopausal women displaying partial or complete lobular involution have a reduced breast cancer risk (Radisky and Hartmann, 2009). Distinct from the above examples is the well established fact that women with higher mammographic density, which is attributable to a greater cellularity and ECM content, have a significantly higher lifetime risk of developing breast cancer (Boyd et al., 2009). Overall, the complexity of ductal cellular structures where breast cancer originates, as well as continuing cycles of turnover, impact women's susceptibility to develop breast cancer.

1.2.2 MMP involvement in mammary gland dynamic development

Mammary stroma remodels concurrently with the epithelial ductal structure. A large part of the stroma is the structural ECM, which is also believed to be an important component of the mammary stem cell niche (Wiseman and Werb, 2002; Chepko and Dickson, 2003; Brisken and Duss, 2007). The collective activity of MMPs is sufficient to degrade almost all proteins of the ECM network (see chapter 1, 1.1.2). MMPs and TIMPs show specific spatiotemporal expression patterns in female reproductive tissues at discrete mammary stages. Their mRNA and/or protease activity are evident during branching morphogenesis and involution (Talhouk et al., 1991; Witty et al., 1995; Fata et al., 1999, 2000a; Green and Lund, 2005). Some are produced by periductal fibroblasts (MMP-2, MMP-3), others are expressed by both epithelial and stromal cells (MMP-14, TIMP-1, TIMP-3, TIMP-4), whereas some members are only present in epithelial cells (MMP-7, TIMP-2) or predominant in the local immune cells (MMP-9). MMP-14 is concentrated in the TEBs and has been found in myoepithelial cells, which also express TIMP-3 (Wiseman et al., 2003; Fata et al., 2004; Mori et al., 2009).

TEB bifurcation mainly involves stromal matrix deposition, and side branching requires extension through the layer of myoepithelial cells, degradation of the basement membrane that surrounds mature epithelial ducts followed by invasion of

the periductal layer of fibrous stromal tissue. Therefore, the two processes may differentially need MMP activity (Wiseman and Werb, 2002). For all MMPs and TIMPs, only a few have been investigated in various aspects of the remodeling mammary gland. Their specific contributions to the processes of TEB growth and bifurcation, ductal tree elongation, secondary or tertiary branching, and mammary involution have been demonstrated using transgenic mice (Page-McCaw et al., 2007). Notable is the finding that MMP-2-knockout mice have deficient TEB invasion but excessive lateral branching during mid-puberty, whereas mice lacking MMP-3 show defective secondary and tertiary lateral branching of ducts during mid-puberty and early pregnancy. On the other hand, mice over-expressing MMP-3 or MMP-14 have excessive side branching, precocious alveologenesis, and eventually develop mammary tumors (Witty et al., 1995; Sternlicht et al., 1999; Ha et al., 2001; Wiseman et al., 2003). It has been indicated that high levels of S100 calcium binding protein S100A4 promotes invasion into the fat pad during branching via activating MMP-3 (Andersen et al., 2011). However, The mammary branching morphogenesis was reduced by inhibition of MMP-9 (Lee et al., 2000). When slow-release pellets were used to compare the local effects of individual TIMPs on pubertal mammary morphogenesis, TIMP-1, TIMP-3, and TIMP-4 inhibited ductal elongation, whereas TIMP-2 promoted this process (Fata et al., 1999; Hojilla et al., 2007). This may in part be due to up-regulation of MMP-2 activity in TIMP-2 enriched glands, related to the adaptor function of TIMP-2 in the MMP-14/TIMP-2/MMP-2 trimolecular complex, which is essential for the cell surface activation of MMP-2 (Ellerbroek and Stack, 1999; English et al., 2006). Up to now, the effects of ovarian hormones on the expression of individual MMPs or their inhibitors are not very well defined, although a few (MMP-9, MMP-13, TIMP-3 and TIMP-4) are altered at the diestrus phase of the murine reproductive cycle. Indeed, the link between hormonal response, proliferation, modulation of MMP activity and maintenance of basement membrane integrity depend on a balance in the expression levels of progesterone receptor-A (PR-A) and PR-B isoforms (Simian et al., 2009).

From above data, the relations of MMPs and TIMPs with mammary gland

development are summarized in Table 1.4.

Mouse genotype	Mammary gland phenotype
MMP-2-/-	↓ TEB invasion ↑ Lateral branching
MMP-3-/-	↓ Lateral branching
MMP-3 over-expression	↑ Lateral branching ↑ Duct elongation ↑ Precocious alveogenesis
MMP-9 suppression	↓ Branching morphogenesis
MMP-14 over-expression	↑ Lateral branching ↑ Precocious alveogenesis
TIMP-1 over-expression	↓ Duct elongation
TIMP-2 over-expression	↑ Duct elongation
TIMP-3 over-expression	↓ Duct elongation
TIMP-4 over-expression	↓ Duct elongation

Table 1.4 MMPs and TIMPs in mammary gland development. ↑ means promote; ↓ means inhibit.

1.2.3 MMP involvement in mammary gland remodeling after weaning

The extracellular proteinases are abundant during mammary involution as this involves plentiful restructuring of the mammary gland, whereas their expression is repressed during lactation (Sorrell et al., 2005). Microarray expression profiling has shown that MMP-3 and MMP-14 are markedly increased during pregnancy and involution and, MMP-7 and MMP-12 at involution, with MMP-3 showing the most profound up-regulation. Implantation of TIMP-1 pellets during post-lactational involution hinders this process (Talhouk et al., 1992), whereas TIMP-3 deficiency accelerates mammary involution (Fata et al., 2001b).

1.2.4 MMPs regulate signaling pathways during mammary gland postnatal development and regression

A recurrent theme during mammary remodeling is paracrine signaling, which necessitates the delivery of growth factors, and/or cytokines from the stromal to epithelial compartments, luminal epithelial cells to myoepithelial cells, or vice versa.

Several MMPs (MMP-1, MMP-2, MMP-3, MMP-9 and MMP-11) can potentially release IGFs from their binding proteins present in the circulation or the interstitium before the interaction of IGFs with their tyrosine kinase receptor IGFIR (Hojilla et al., 2003). Further, ECM bound ligands (such as TGFβ and HGF) exist in latent form and require proteolytic processing for their maturation and subsequent signal transduction (Mohammed and Khokha, 2005; Jenkins, 2008).

Although multiple mitogens or inhibitors direct mammary remodeling processes, some apparently play more prominent functions. For example, TGFβ plays a central role in a number of developmental and pathological processes, TGFβ exerts a wide-ranging control over mammary epithelial cell proliferation and morphology. It regulates ECM remodeling, as it allows ECM deposition while inhibiting ECM degrading proteases in the immediate vicinity of the TEBs and branching ducts. In turn this facilitates the generation of an ECM obstacle for tubular morphology. Additionally, TGFβ transcriptionally regulates several MMPs and TIMP genes during tissue remodeling (Wilkins-Port and Higgins, 2007; Kassiri et al., 2009). However, activation of TGFβ is the key biological checkpoint controlling TGFβ bioavailability. The MMPs play an important role in TGFβ activation, such as MMP-2 can directly cleave latent TGFβ, whereas MMP-14 interact with integrin mediated TGFβ activation pathways (Jenkins, 2008). Thus, although MMPs can enhance TGFβ bioavailability, TGFβ in turn controls the expression of these proteases. Such a mechanism of positive feedback uniquely authorizes these enzymes as useful regulators during remodeling programs. With regard to Wnt activity, TIMP-3 deficiency leads to increased β-catenin signaling in primary mammary epithelial cells and expression of epithelial specific MMP-7, which is a key transcriptional target of Lef/Tcfs downstream of canonical Wnt signaling (Hojilla et al., 2007). Although Wnt signaling is important for multiple aspects of the mammary gland including the mammary stem cells (Brisken and Duss, 2007), little is currently known of the mechanisms by which secreted Wnt ligands are sequestered extracellularly and made available to their receptors. Interestingly, syndecan-1 (a cell surface heparan sulfate proteoglycan) knockout can inhibit mammary development (Dontu et al., 2003) and

profoundly affected Wnt-induced mammary tumorigenesis in mice (Alexander et al., 2000). Moreover, ectodomain shedding of syndecan-1 and syndecan-4 occurs by TIMP-3-sensitive MMPs (Alexander et al., 2000; Fitzgerald et al., 2000).

Compared to the remodeling of the epithelial ductal network, restructuring of the vascular network during mammary remodeling is not well understood. It has been demonstrated that mammary epithelium-derived VEGF is a critical factor in angiogenesis, however, its bioavailability depends on MMPs regulation (Rossiter et al., 2007; Bergers et al., 2000).

Another mode by which MMPs facilitates the mammary gland remodeling is by ectodomain cleavage of cell adhesion proteins, such as E-cadherin, which must be intact to provide a strong survival signal for mammary epithelial cells. For example, MMP-7 and MMP-3 can cleave E-cadherin at the cell surface and release soluble E-cadherin fragments (sE-CAD) into the medium. The sE-CAD inhibits E-cadherin functions in a paracrine way by induction of invasion into collagen type I and inhibition of E-cadherin-dependent cell aggregation (Noe et al., 2001). Indeed, excessive E-cadherin cleavage occurs during the accelerated loss of the epithelial compartment and gain of adipocyte reconstitution at post-lactational mammary involution in TIMP-3 knockout mice. Thus, TIMP-3 is a critical epithelial survival factor during mammary gland involution (Fata et al., 2001b).

Overall, the typical localization of MMPs and their inhibitors at the stromal-epithelial interface, where ligand-receptor interactions occur, engages multiple and diverse signal transduction pathways (Figure. 1.7). It must be recognized, however, that the same ligand or signal can produce vastly different biological outcomes because of context-dependent effects (Egeblad and Werb, 2002; Kessenbrock et al., 2010).

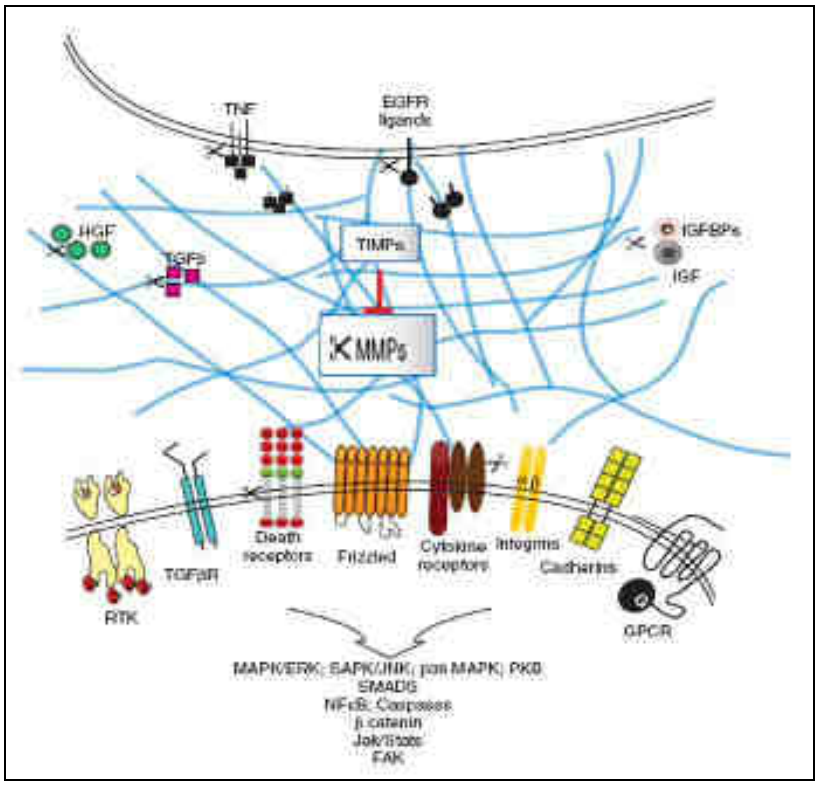

Figure 1.7 Lateral integration of critical signal transduction pathways by MMP activity. TIMPs together with MMPs operate at the stromal-epithelial interface to affect growth factor bioavailability by regulating the release of ECM bound factors, shedding of cell surface ligands and cytokines or their receptors, as well as alter the release of factors complexed with their binding proteins. EGFR, epidermal growth factor receptor; GPCR, G-protein coupled receptor; HGF, hepatocyte growth factor; IGF, insulin-like growth factor; IGFBPs, IGF binding proteins; MMP, matrix metalloproteinase; RTK, receptor tyrosine kinase; TGFb, transforming growth factor beta; TIMP, tissue inhibitor of metalloproteinase; TNF, tumor necrosis factor. Modified from Khokha and Werb, 2011.

1.3 MMP-11

1.3.1 MMP-11 discovery and name

MMP-11 cDNA was first cloned by differential screening between malignant and benign human breast tumor samples. MMP-11 was initially recognized as the third member of the stromelysin subfamily within the MMP family on the basis of its similarity with the stromelysin-1 (ST1) and stromelysin-2 (ST2), so the product of this gene was named as stromelysin-3 (ST3) (Basset et al., 1990). Despite the original designation as ST3, its sequence is quite divergent from the ST1 and ST2, and it has distinct mechanism of activation and proteolytic activity (Murphy et al., 1993; Pei et

al., 1994; Pei and Weiss, 1995). Thus, the name ST3 does not reflect any functional similarities with other stromelysins. A more generic designation based on the sequence of MMP discovery has assigned ST3 the serial number 11, *i.e.* matrix metalloproteinase-11. It is expressed specifically in stromal cells surrounding invasive breast carcinomas (Basset et al., 1990). As the other MMPs, MMP-11 is involved during ECM remodeling events, such as development, tissue involution, wound healing, tumor invasion and metastasis (Anderson et al., 1995; Lefebvre at al., 1992; Rodgers et al., 1992; Lefebvre et al., 1995). However, from literatures, MMP-11 appears to be an unique member of the MMP family exhibiting peculiar features and function (Rio, 2002).

1.3.2 MMP-11 protein structure

1.3.2.1 Primary and secondary structures

The MMP-11 gene encodes a pre-pro-protein containing from its N-terminal end to its C-terminal end, a signal peptide, a pro-domain, a furin recognition site, a catalytic domain and an hemopexin-like domain (Figure 1.8).

Figure 1.8 MMP-11 schematic organization. pre: signal peptide; pro: pro-peptide; F: furin-susceptible site; SH: thiol group; Zn^{++}: zinc ion. Modified from Basset et al., 1990.

Pro-MMP-11, unlike other MMPs, cannot be activated by organomercurials or detected by standard zymographic techniques in vitro. This unusual behavior has been attributed to structural characteristics peculiar to both its pro- and catalytic domains (Basset et al., 1990; Pei and Weiss, 1995; Santavicca et al., 1996). Furthermore, while numerous MMPs are normally synthesized and secreted as inactive zymogens, MMP-11 is secreted as an active enzyme (Pei and Weiss, 1995; Santavicca et al., 1996). Initially synthesized as a ~54-56 kDa precursor, MMP-11 is then modified in the trans-Golgi network to a ~62-65 kDa form, presumably following the glycosylation of serine/threonine residues in the pro-domain (Pei and Weiss, 1995;

Santavicca et al., 1996). Subsequently, the ~45-47 kDa mature species is generated intracellularly by furin, a trans-Golgi network-associated proprotein convertase, which cleaves pro-MMP-11 at the C-terminal end of a unique RXRXKR motif (Figure 1.9). In the absence of MMP inhibitors, the 45 kDa form is unstable and undergoes autocatalytic processing (Pei and Weiss, 1995).

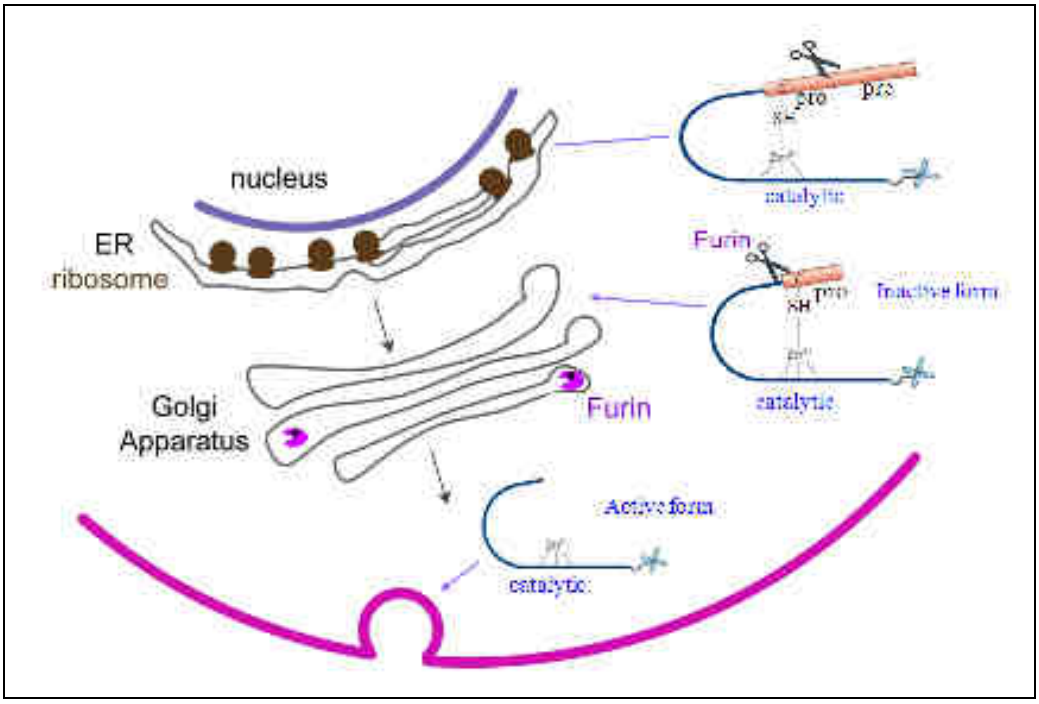

Figure 1.9 Domain structure of MMP-11 and activation processes. MMP-11 is synthesized as inactive zymogen form in endoplasmic reticulum, then transfered into Golgi apparatus for modification by furin. The MMP-11 active form is secreted. Thus, MMP-11 activation is not dependent on extracellular processing. Pre: N-terminal signal sequence; Pro: pro-domain; SH: thiol-group; Catalytic: catalytic domain; Zn: zinc ion. Modified from Pei and Weiss, 1995; Santavicca et al., 1996.

1.3.2.2 MMP-11 crystal structure

The 3D-structure of the mouse MMP-11 catalytic domain has been solved with the RXPO3 phosphinic inhibitor mimicking a (D, L) peptide (Vassiliou et al., 1999; Gall et al., 2001) (Figure 1.10). As observed for the already known structures of MMPs, the catalytic domain of MMP-11 is made up of 5-stranded β-sheets and 3 α-helices, and is a charged negative globular protein containing several pockets. The topology of MMPs is remarkably well conserved, making the design of highly specific inhibitors difficult. The crystal structure clearly demonstrates that its S1'

pocket looks like a tunnel running through the enzyme. This open channel is filled by the inhibitor P1' group which adopte a constrained conformation to fit this pocket, together with two water molecules interacting with the MMP-11-specific residue Gln215, which plays a pivotal role in determing the PI' selectivity as determined by site-directed mutagenesis (Holtz et al., 1999). These observations provide clues for the design of more specific inhibitors and show how MMP-11 can accommodate a phosphinic inhibitor mimicking a (D, L) peptide. The presence of a water molecule interacting with one oxygen atom of the inhibitor phosphinyl group and the proline residue of the Met-turn, suggests how the intermediate form during proteolysis may be stabilized. Furthermore, the hydrogen bond distance observed between the methyl of the phosphinic group and the carbonyl group of Ala182 mimics the interaction between this carbonyl group and the amide group of the cleaved peptidic bond. Thus, this characteristic of the MMP-11 protein structure allows to design synthetic inhibitors exhibiting a longer chain in their P1' position leading to a higher specificity against MMP-11 than other MMPs, MMP-11 therefore represents an appropriate target for specific inhibitor(s) in future cytostatic therapeutic approaches directed against the stromal compartment of human carcinoma (Rio, 2002).

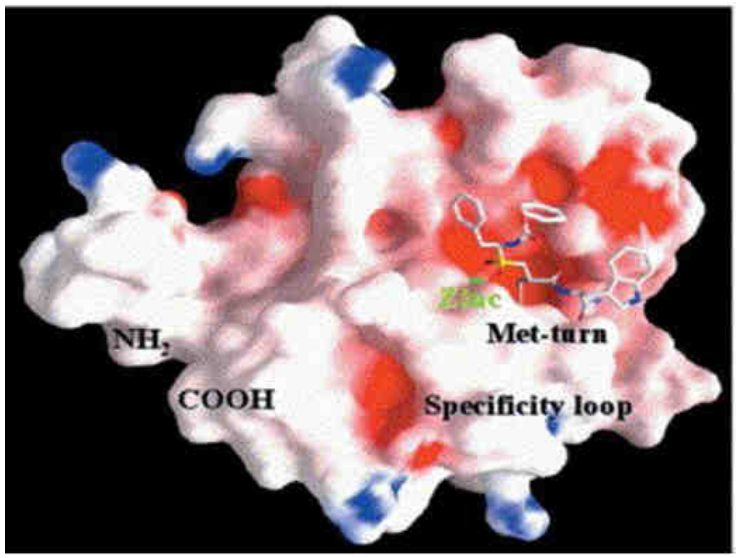

Figure 1.10 Crystal structure of the MMP-11 catalytic domain. The molecular surface of the MMP-11 catalytic domain is colored according to its potential (red: negatively charged residues; blue, positively charged residues). The catalytic zinc atom (green) lies on the surface of the active site. Adapted from Gall et al., 2001.

1.3.3 MMP-11 substrates

MMP-11 has rather restricted substrate specificity compared to other MMPs. MMP-11 can cleave the serine proteinase inhibitor (serpin), α1-proteinase inhibitor (α1PI). Proteolysis occurred at Ala350-Met351 site within the reactive-site loop of the inhibitor, which results in a complete loss of anti-proteolytic activity (Pei et al., 1994). It also cleaves α2-antiplasmin, plasminogen activator inhibitor 2 and α2-macroglobulin (α2-M) (Pei et al., 1994). Moreover, a 28 kDa C-terminally truncated form of MMP-11 exhibits weak matrix-degrading activity against laminin as well as type IV collagen in mouse (Murphy et al., 1993), but not in human (Noel et al., 1995). This functional difference is probably due to an unusual Ala 'substitution' of the Pro235 in human MMP-11, a residue conserved in all MMPs (Noel et al., 1995). MMP-11 cleaves the laminin receptor in mammals and *Xenopus* (Fiorentino et al., 2009). Recently, we have found both in mouse and human that MMP-11 cleaves the native α3 chain of collagen VI, but not the α1 and α2 chains (Motrescu et al., 2008). Collagen VI is an adipocyte-related ECM component, but the precise site of cleavage remains to be determined. IGFBP-1 is also cleaved by MMP-11 in human. The cleavage site is between His140-Val141 within in the mid-region of IGFBP-1 (Manes et al., 1997). Since IGFBP-1 inhibits the function of IGF-I, cleavage of IGFBP-1 releases IGF-1 for cell survival and proliferation (Manes et al., 1997). Given the fact that IGFs play a prominent role in the development of cancer, MMP-11 may contribute to tumorigenesis by releasing IGF-1 from IGFBPs.

The proteolytic properties of MMP-11 have been analyzed using synthetic substrates. Recombinant MMP-11 cleaves the fluorogenic substrate Dansyl-Pro-Leu-Ala-Leu-Trp-Ala-Arg-NH_2 (Holtz et al., 1999). It has been indicated that MMP-11 prefers substrates with P1' positions containing unusually long side chains (Mucha et al., 1998).

1.3.4 Natural MMP-11 forms

Using western blot analysis, the pro- and the mature forms of human MMP-11 are usually observed at about 56 and 47 kDa, respectively (Santavicca et al., 1996).

However, several other MMP-11 forms are observed. In an in vitro stroma/epithelial cell co-culture model, a 35 kDa protein lacking enzymatic activity is produced by normal pulmonary fibroblasts (Mari et al., 1998). Two forms of 35 and 28 kDa are also observed in human atherosclerotic tissues (Schonbeck et al., 1999). Moreover, a 28 kDa form was also seen after furin cleavage of recombinant human MMP-11 (Santavicca et al., 1996). The diversity of the observed forms of MMP-11 raises the question of the existence of possible various post-translational maturations of the MMP-11 protein.

1.3.5 Recombinant MMP-11

Since the in vivo sources are not practical for large-scale purification of the enzyme, recombinant MMP-11 has been produced in mammalian cell lines (Pei et al., 1994; Murphy et al., 1993; Santavicca et al., 1996), prokaryotes (Kannan et al., 1999), or insect cells (del Mar Barbacid et al., 1998). In the presence of the reversible hydroxamate MMP inhibitor BB94, a ~47 kDa active species can be purified in large scale by a combination of dye-affinity, heparin-affinity and gel-filtration chromatographies (Pei et al., 1994). In the absence of BB94, a ~28 kDa C-terminally truncated species has been obtained (Murphy et al., 1993). The mammalian expression system produces a recombinant MMP-11 close to its native state, but not as efficiently as the bacteria- or baculovirus-based system. The latter ones are utilized successfully to produce large MMP-11 quantity in the laboratory (Kannan et al., 1999; del Mar Barbacid et al., 1998).

1.3.6 MMP-11 genomic structure

MMP-11 is localized on human chromosome 22q11.2 (Levy et al., 1992) and to the C band of mouse chromosome 10 (Cole et al., 1998) showing a syntenic conservation during evolution. The human and mouse MMP-11 gene span 11.5 kb and 9.2 kb respectively, and contain eight exons and seven introns. The genomic organization of MMP-11 gene exons is well conserved compared with other members of the MMP family, except for the 3 last exons corresponding to the hemopexin-like domain and to a long 3'UTR (Anglard et al., 1995). The first four exons match those

of other classic MMPs while the remaining four exons are organized differently: (1) the hinge region in MMP-11 is an extension of exon 5 which encodes a portion of the catalytic domain; (2) the first Cys residue for the conserved disulfide bond in the hemopexin domain is not part of the exon encoding the hinge region as in other MMPs, but part of the first exon of the hemopexin-like domain; and (3) a conserved intron located between the second and third exons of the hemopexin domains present in other MMPs is absent in MMP-11. These differences place MMP-11 outside of the main MMP cluster between the mammalian MMPs and the bacterial metalloproteinases (Murphy et al., 1991). The Xenopus MMP-11 gene also has a structure distinct from other MMP genes, with its hemopexin domain encoded by four instead of six exons.

1.3.7 MMP-11 promoter region

Analysis of the 5' region upstream of the TATA box shows several functional regulatory elements common to the human, mouse and/or Xenopus MMP-11 genes. A proximal cis-acting retinoic-acid-responsive-element (RARE) of the DR1 type (direct repeat of the core motif PuGGTCA separated by 1 bp), and two distal RAREs of the DR2 type are present in the human and mouse MMP-11 genes. The Xenopus MMP-11 promoter is devoid of RARE element. The proximal DR1 is sufficient for MMP-11 promoter activity in vitro. This RARE may be responsible, at least partially, for the in vivo expression of MMP-11 since retinoic acid receptor beta and gamma (RARβ and RARγ)-deficient mice exhibit lower levels of MMP-11 (Guerin et al., 1997; Dupe et al., 1999). Additional distal elements have been reported (Luo et al., 1999; Ludwig et al., 2000). An AP1-like responsive element is responsible for the basal human MMP-11 promoter activity. This element is not present in the mouse promoter. One (human) and two (mouse) CCAAT/enhancer-binding-protein (C/EBP)-binding sites that efficiently bind the C/EBPβ transcription factor, are involved in the TPA-regulated induction of MMP-11 gene expression. The MMP-11 promoter also contains one (human and mouse) or two (Xenopus) GAGA factor binding sites. Moreover, a thyroid hormone responsive element (TRE), shared by

human, mouse and Xenopus, is present in the distal region of the MMP-11 promoter. This TRE has been shown to be functional in frog, and MMP-11 is a direct immediate-early thyroid hormone (T3) responsive gene (Patterton et al., 1995; Shi et al., 2007). In contrast to the other MMPs, no proximal AP1-binding site was identified in the MMP-11 promoter in all the species studied (Luo et al., 1999; Ludwig et al., 2000). Finally, in Xenopus, two transcription start sites (+1, -94) and a second TATA box (-87, -82) were reported, suggesting a possible second MMP-11 messenger RNA (Li et al., 1998). Similar organization leading to two types of messenger RNAs also exists in the human MMP-11 gene (Luo et al., 2002). Recently, it has been indicated that Sp1 is able to bind to the GC-boxes within the MMP-11 proximal promoter region and regulate MMP-11 expression. This regulation requires the formation of Sp1/Smad2 heterocomplexes, which are stimulated by an increase in the acetylation status of Smad. Besides, ERK1/2-mitogen-activated protein kinase (MAPK) is also involved in the regulation of MMP-11 (Barrasa et al., 2012).

These results suggest that the MMP-11 gene evolved prior to most other metalloproteinase genes and uses distinct regulation pathways to achieve similar expression profiles and serve similar functions in mammals and amphibians (Li et al., 1998). Indeed, in mammals and Xenopus, MMP-11 is expressed during limb bud development, a phenomenon dependent on retinoic acid in mammals (Dupe et al., 1999), but on thyroid hormone in Xenopus (Li et al., 1998).

1.3.8 MMP-11 as a paracrine factor

In both normal and pathological events, cells expressing MMP-11 are usually of mesenchymal origin. Moreover, MMP-11 expression is restricted to a cell sub-population located at the vicinity of ‘stressed’ or malignant epithelial cells, notably when the integrity of the basement membrane, which separates epithelial and stromal compartments is altered and allows cell-cell crosstalk/interaction. This highly precise MMP-11 location, strongly supports a drastic regulation of the MMP-11 gene in vivo, and a spatially restricted MMP-11 function. Accordingly, diffusible factors from neighboring cells can induce MMP-11 expression by mesenchymal cells.

In vitro, epidermal growth factor (EGF), basic fibroblastic growth factor (bFGF) and platelet-derived growth factor (PDGF) induce MMP-11 expression in normal human fetal and adult pulmonary fibroblasts (Anderson et al., 1995; Ahmad et al., 1997). In primary cultures of human endometrial fibroblasts, MMP-11 is selectively induced by IGF, EGF, PDGF, TNFα and IL1α (Singer et al., 1999). Finally, the CD40 ligand, an inflammatory mediator, induces MMP-11 expression in endothelial cells, smooth muscle cells and macrophages (Schonbeck et al., 1999). MMP-11 can also be induced in osteoblasts by FGF2 (Delany and Canalis, 1998), which is consistent with its detection in osteoarthritis tissue.

Using epithelial cancer cell/stroma cell co-culture models both soluble factors and cell/cell contact allow for the expression of MMP-11. Thus, breast cancer cells up-regulate reporter genes under the transcriptional control of a 3.4 kb human 5' flanking sequence of MMP-11 (Ahmad et al., 1997). Non-small cell lung cancer epithelial cells stimulate normal pulmonary fibroblasts to express and secrete MMP-11 (Mari et al., 1998). Using in vitro co-culture model, murine and human cancer cells induce adipocytes to express MMP-11 (Tan et al., 2011). These data are consistent with what is observed in vivo in tumors where invasive cancer cells induce MMP-11 expression by adjacent stromal cells (Andarawewa et al., 2005; Motrescu and Rio, 2008; Tan et al., 2011).

1.3.9 Normal MMP-11 physiological function

1.3.9.1 MMP-11 and embryonic development

MMP-11 is expressed during developmental processes. In mouse, MMP-11 is detected as early as 7.5-8.5 days in trophoblastic cells at the site of embryonic implantation (Lefebvre et al., 1995; Alexander et al., 1996). It also participates in several developing tissues such as the limb, tail and snout, and to the bone and spinal cord morphogenesis (Lefebvre et al., 1995). MMP-11 positive fibroblasts constitute a thin layer of cells located just beneath the basement membrane lining the extending epithelium (Figure 1.11). The skeletal muscle of the tongue in mouse also expresses MMP-11 (Chin and Werb, 1997). Functionally, MMP-11 is detected in mesenchymal

cells, which line the basement membrane at the junction of primitive dermis and epidermis, where epithelial cells proliferation and/or die (Lefebvre et al., 1995). MMP-11 is implicated in Xenopus development (Berry et al., 1998; Ishizuya-Oka et al., 1996; Shi, 1995; Puzianowska-Kuznicka et al., 1997) and metamorphosis (Patterton et al., 1995). It is involved in apoptotic tissue remodeling or resorption (Damjanovski et al., 1999; Ishizuya-Oka et al., 2000). During human placentation, extravillous trophoblasts invading the maternal deciduas produce MMP-11, and later, MMP-11 is restricted to the syncytiotrophoblasts that line the intervillous vascular spaces (Maquoi et al., 1997).

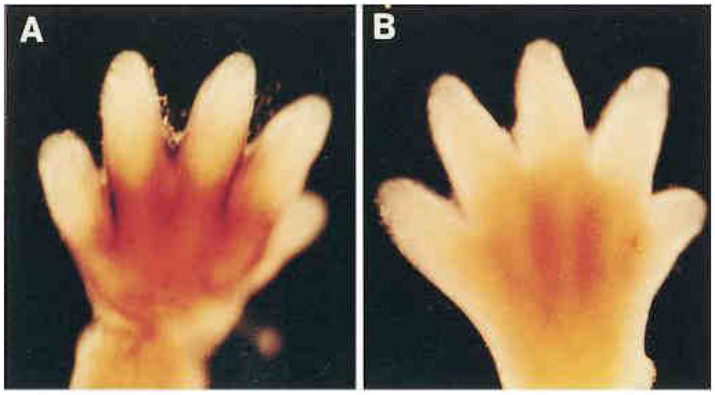

Figure 1.11 Whole mount RNA *in situ* hybridization of limb buds of wild-type and MMP-11-/- mouse embryos. MMP-11 mRNA was observed in the interdigital parts of the limb of wild-type (A) but not in that of MMP-11-/- (B) embryos. No obvious morphological differences were observed between limb buds from wild-type and MMP-11-/- mice. Adapted from Masson et al., 1998.

1.3.9.2 MMP-11 and tissue remodeling

MMP-11 participates to various tissue remodeling processes (i.e. post-weaning mammary gland involution, uterus post-partum involution, ovulation, endometrial menstrual breakdown) (Lefebvre et al., 1992). MMP-11 is expressed in human rheumatoid arthritis and in traumatic synovial membrane, suggesting that MMP-11 may participate in physiological synovial remodeling (Konttinen et al., 1999). Epithelium homeostasis requires equilibrium between epithelial cells, stromal cells (fibroblasts, adipocytes, endothelial cells, inflammatory and immune cells) and the ECM. Tissue remodeling leads to basement membrane alteration and subsequently to

transient epithelial/stromal communication or contacts. MMP-11 is specifically expressed during these biological processes, whereas the gene is silent in resting tissues (Rio et al., 1996). Although a correlation can be drawn between MMP-11 expression and intense apoptosis during normal tissue remodeling processes, in contrast to other MMPs that rather exhibit pro-apoptotic effects, MMP-11 exhibits an anti-apoptotic function and help epithelial cells to circumvent apoptotic mechanisms (e.g. anoikis) and survive in an unusual and hostile environment (Boulay et al., 2001).

Thus, MMP-11 transiently preserve the viability of regenerating cells during intense apoptotic processes, and participate in the regulation of homeostasis of epithelial cell compartment. Thus, during malignant invasive processes, epithelial cells may use this anti-apoptotic MMP-11 function to circumvent tissue homeostasis and anarchically proliferate.

1.3.9.3 MMP-11 and adipogenesis

MMP-11 negatively regulates adipogenesis in an autocrine manner. MMP-11-/- mice were developed in the laboratory (Masson et al., 1998). They have a significantly higher mean body weight than wild-type littermates in normal fat diet (Andarawewa et al., 2005) and in high fat diet condition (Lijnen et al., 2002) (Figure 1.12).

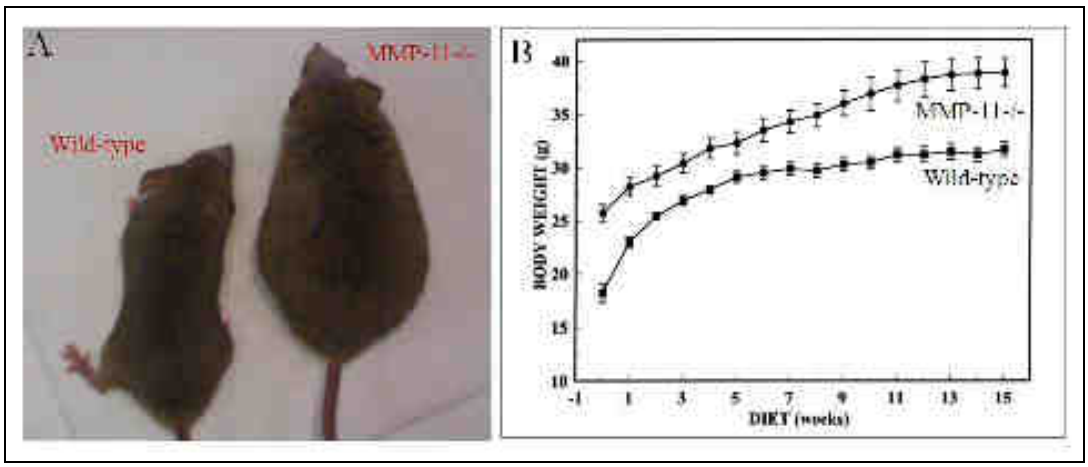

Figure 1.12 Body weight comparison of MMP-11-/- and wild-type mice. A: under normal fat diet; B: under high fat diet. Adapted from Andarawewa et al., 2005; Lijnen et al., 2002.

The MMP-11-/- mouse embryonic fibroblasts (MEFs) differentiate better into adipocytes compared to wild-type MEFs. Moreover, treatment of adipocytes-

differentiated MMP-11-/- MEFs with recombinant MMP-11 leads to lipid depletion and reversal of the adipocyte phenotype. Thus, MMP-11 controls fat mass homeostasis by limiting pre-adipocyte differentiation and/or reversing mature adipocyte differentiation (Andarawewa et al., 2005; Motrescu et al., 2008) (Figure 1.13).

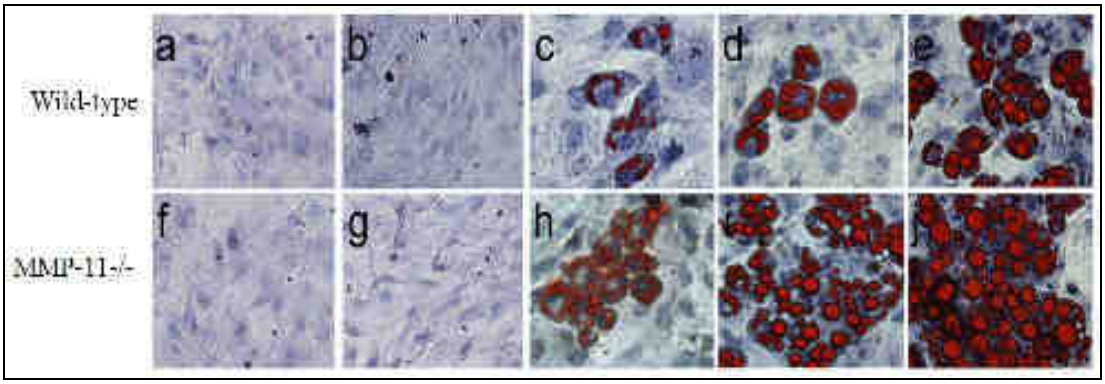

Figure 1.13 Oil Red O staining analysis of MEF adipocyte differentiation. Oil Red O staining of confluent wild-type and MMP-11-/- MEFs (a and f , respectively). Increased number and size of lipid droplets were observed in MMP-11-/- MEFs compared to wild-type MEFs at 2 (b and g), 4 (c and h), 6 (d and i), 8 (e and j) days of adipocyte differentiation. Adapted from Andarawewa et al., 2005.

1.3.10 MMP-11 and diseases

1.3.10.1 MMP-11 and tumor progression

Only rare sarcomas present MMP-11 positivity, whereas almost all carcinomas express MMP-11. MMP-11 is not expressed by the cancer cells themselves, but by stromal cells (Basset et al., 1997), most notably fibroblast-like and/or adipocytes surrounding malignant epithelial tumor cells (Basset et al., 1990; Andarawewa et al., 2005) (Figure 1.14). MMP-11 is observed in almost all types of carcinomas, including breast, lung, ovary, prostate, small intestine, stomach, uterus, colon, larynx, esophagus, pancreas, bladder, skin, and head and neck carcinomas. But it is rarely observed in liver, kidney and lung small cell carcinomas. Moreover, MMP-11 is more frequent in primary tumors (50-100%), than in secondary tumors (30-70%) (Rio et al., 1996).

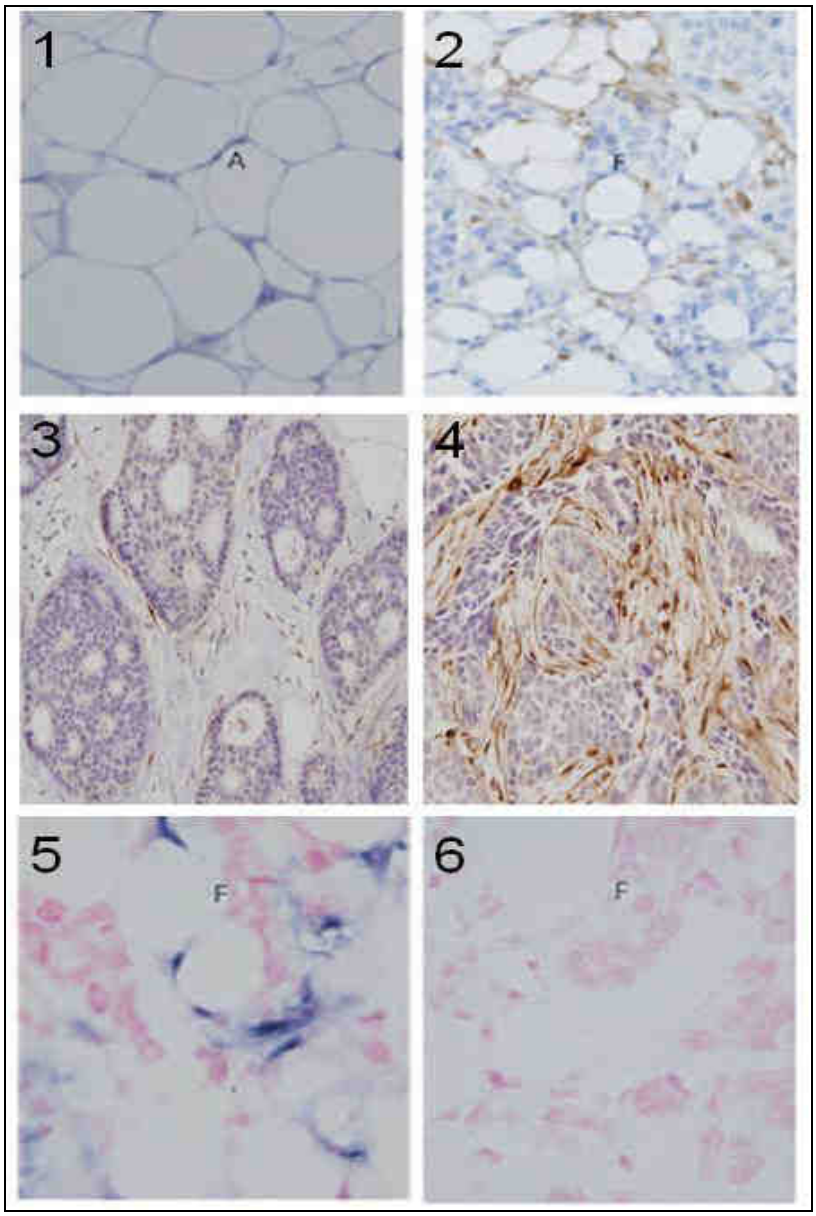

Figure 1.14 Histology and MMP-11 expression of normal human breast tissue and breast carcinomas. 1, 2, 3 and 4: MMP-11 immunohistochemistry of normal (1), peritumoral (2) adipose tissues, ductal carcinoma in situ (3) and invasive ducal carcinoma (4). 5 and 6: MMP-11 in situ hybridization of tumor invasive front using antisense (5) and sense (6) probes. MMP-11 protein (brown) was visualized in adipocytes (lipids in white) and fibroblasts adjacent to invading cancer cells but not in normal tissue. 6, sense control probe gave a negative result. Cell nuclei are stained in blue(1-4) or pink (5,6). Abbreviations: A, adipocyte; F, tumor invasive front. Adapted from Andarawewa et al., 2005.

In human carcinomas, almost all studies provide evidence that MMP-11 expression by non-malignant peritumoral mesenchymal cells is a bad prognostic factor (Basset et al., 1997). Thus, clinical trials showed that high levels of MMP-11 expression correlate with poor prognosis in patients with breast cancer (Engel et al.,

1994; Chenard et al., 1996) (Figure 1.15). MMP-11 is one of the factors often found in association with tumor invasion using high-throughput approaches (Peruzzi et al., 2009; Ma et al., 2009). Consistently, MMP-11 is part of a gene expression signature that distinguishes invasive ductal breast carcinomas (IDC) from ductal carcinoma in situ (DCIS) (Hannemann et al., 2006).

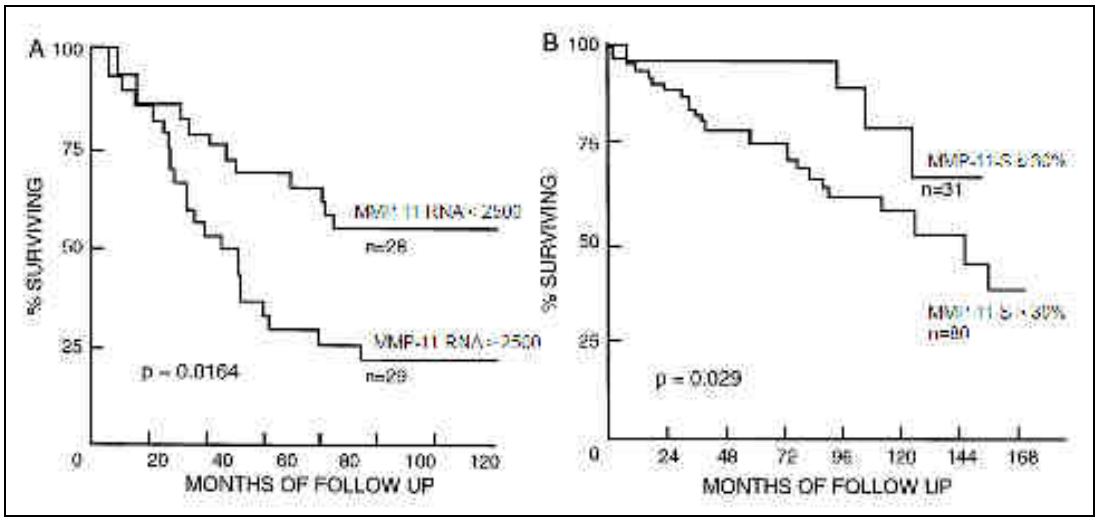

Figure 1.15 Relationship between MMP-11 expression levels in tumor tissue and overall survival in patients with invasive human breast cancer. (A) RNA expression. Tumors were stratified for low (< 2500 units) or high (> 2500 units) MMP-11 transcript levels evaluated by quantitative in situ hybridization. (B) Protein expression. Tumors were stratified for low (MMP-11-S ≤ 30%) or high (MMP-11-S > 30%) MMP-11 protein levels evaluated by semiquantitative immunohistochemistry using monoclonal antibody 5ST-4A9 directed against the MMP-11 hemopexin domain. S means tumor stromal cell. Adapted from Engel et al., 1994; Chenard et al., 1996.

However, the role of MMP-11 in tumor progression has been shown to be more complicated than originally thought at least in experimental animals. Thus, MMP-11 increased tumorigenesis does not result from increasing cancer cell proliferation but from decreasing cancer cell death through apoptosis and necrosis (Figure 1.16). These data indicated that host MMP-11 is a key player during local invasion, favoring cancer cell survival and implantation in connective tissues through an anti-apoptotic function (Boulay et al., 2001; Wu et al., 2001).

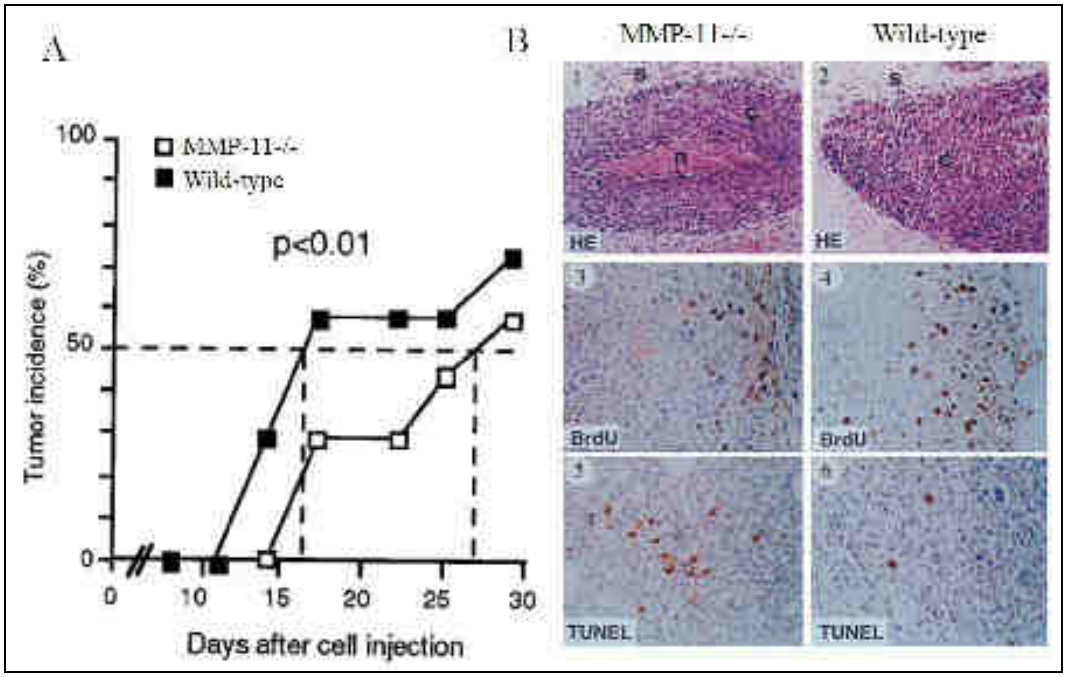

Figure 1.16 MMP-11 increases tumorigenesis via decreasing cancer cell apoptosis and necrosis. A: Analysis of C26 colon cancer cell tumorigenicity in syngeneic wild-type and MMP-11-/- mice. The delay required for palpable tumor development at 50% injection sites was improved in the absence of MMP-11. B: Histological (H&E) and immunohistological features of nonpalpable microcarcinomas found in wild-type and MMP-11-/- mice; BrdU and TUNEL stained in brown proliferating and apoptotic cells, respectively. The lack of MMP-11 led to increased cancer cell death through necrosis (1, 2) and apoptosis (5, 6), but did not modify cancer cell proliferation (3, 4). s, stroma; c, carcinoma; n, necrosis. Adapted from Boulay et al., 2001.

Moreover, in addition to reduce number of primary tumors, MMP-11 deficiency leads to unexpected higher number of metastases, suggesting that the cancer cells developing in MMP-11-/- stroma have an increased potential for hematogenous dissemination (Rio, 2005). Real-time imaging of developing lung metastases in living mice using X-ray computed tomography system (micro CT) shows that metastases occur earlier and grow faster in wild-type mice, but in lower numbers compared with MMP-11-/- mice. Thus, there is significant spatio-temporal variability of host MMP-11 function, favoring the local invasion and the onset and growth of metastases, but limiting cancer cell dissemination and metastasis focus number (Brasse et al., 2010).

MMP-11 is actually a paracrine key player during tissue remodeling processes occurring under malignant conditions. The ECM adaptation via the desmoplastic

response (Mueller and Fusenig, 2002) is associated with modification in the nature, and relative ratio of the stromal cells, notably adipocytes disappear and fibroblast-like cells accumulate. In this context, MMP-11, which negatively regulates adipogenesis by limiting pre-adipocyte differentiation and/or reversing mature adipocyte differentiation, participates in this process and to the accumulation/maintenance of peritumoral fibroblast-like cells at the center of the growing tumors. Indeed, invasive cancer cells induce the expression of MMP-11 in neighboring cancer-associated-adipocytes (CAAs) (Andarawewa et al., 2005) (Figure 1.17). CAAs become smaller than those observed at a distance and the number of peritumoral fibroblast-like cells increases (Rio, 2011). Thus, MMP-11 and CAAs participate in a highly complex vicious tumor progression cycle orchestrated by the invasive cancer cells to support tumor progression (Motrescu and Rio, 2008)

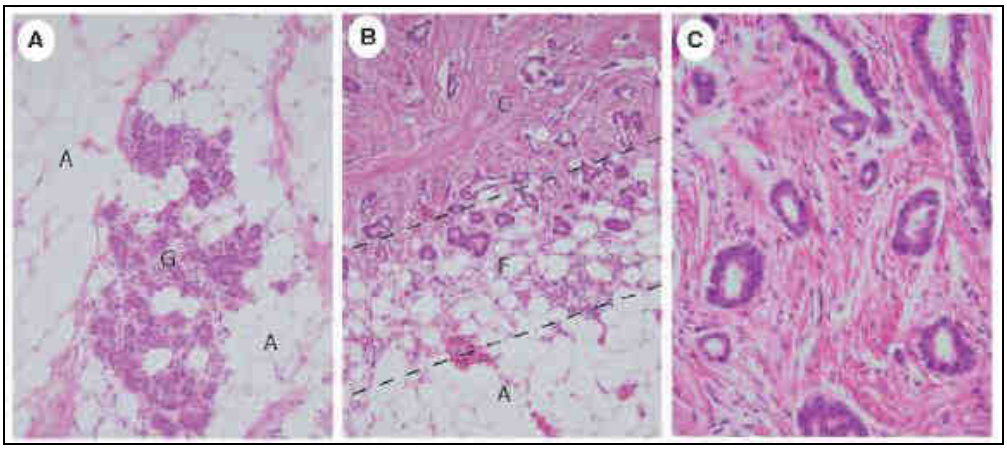

Figure 1.17 H&E examination of human normal breast tissue and invasive breast tumor. Compared with normal adipose tissue (A), the number and the size of adipocytes are greatly reduced at the invasive front of the tumor (B), and adipocytes have totally disappeared in the tumor center, whereas numerous peritumoral fibroblasts are seen (C). These adipocytes were named cancer-associated-adipocytes (CAAs). Abbreviations: A, adipose tissue; C, tumor center; F, tumor invasive front; G, normal mammary gland. Adapted from Andarawewa et al., 2005.

1.3.10.2 MMP-11 and cardiovascular diseases

MMP-11 expression is detected in diseased plaques mostly in endothelial cells, smooth muscle cells and macrophages. MMP-11 appears to be induced by the T-cell CD40 ligand which acts on the CD40 receptor in recipient cells (Schonbeck et al., 1999). Interestingly, MMP-11 cleaves and inactivates α1-PI, a serpin known to

regulate cellular functions related to atherosclerosis (Schonbeck et al., 1999). MMP-11-/- mice developed significantly more neointima than their wild-type counterparts following vascular injury, suggesting that MMP-11 plays a positive role in suppressing the formation of neointima (Lijnen et al., 1999), perhaps by promoting the degradation of elastin through MMP-11-mediated inactivation of α1-PI, a potent elastase inhibitor (Pei et al., 1994). Finally, MMP-11 polymorphism is associated with Kawasaki disease in the Korean population (Ban et al., 2010).

1.3.10.3 MMP-11 and skin diseases

MMP-11 is observed during repair processes such as skin wound-healing in man (Wolf et al., 1992). In a rat model of skin repair, MMP-11 is highly expressed from day 5 to 10 after cutaneous incision. MMP-11 RNAs are detected, similar to the human system, in stromal cells of the scar tissue, below the thickened epithelial cell layer (Okada et al., 1997). In general, very few cases of benign tumors have been shown to express MMP-11. However, surprisingly, almost all dermatofibromas, which correspond to benign fibrous nodules are MMP-11 positive, although MMP-11 is not expressed in malignant dermatofibrosarcomas (Unden et al., 1996; Thewes et al., 1999; Kim et al., 2007; Cribier et al., 2002). These data corroborate the anti-apoptotic function of MMP-11 since dermatofibromas are frequently accompanied by epithelial huperplasia and annexogenesis (Unden et al., 1996; Thewes et al., 1999).

1.3.11 Conclusion

Although numerous questions remain to be addressed, several conclusions can actually be drawn in the field of MMP-11 (Table 1.5): (1) MMP-11 acts at epithelial/stroma interfaces during tissue remodeling; (2) MMP-11 is involved in epithelium homeostasis; (3) Malignant cancer cells induce MMP-11 expression by adjacent fibroblasts and/or adipocytes; (4) MMP-11 is a negative regulator of adipogenesis; (5) Malignant cancer cells subvert MMP-11 function in order to circumvent homeostasis processes and survive in connective host tissues; (6) MMP-11 exerts anti-apoptotic function; (7) During cancer progression, MMP-11 can exert a dual effect, depending on the invasive steps; and (8) although the development

of MMP inhibitors for cancer treatment is more challenging than originally thought, MMP-11 remains an interesting target for potential therapeutics.

Time of MMP-11 expression	Cells/Tissues	Biological processes
Development	Invading trophoblasts	Embryonic implantation
	Syncytiotrophoblasts	Placentation
	Limb bud mesenchyme	Interdigitation
	Invading osteoblasts	Osteogenesis
	Neuroepithelial cells	Spinal cord morphogenesis
	Snout, tail mesenchyme	Epithelium growth
	Tongue	Not known
Metamorphosis	Tail	Larval tissue resorption
	Intestine	Morphogenesis
Adult tissues	Endometrium	Menstrual breakdown
	Uterus	Post-partum involution
	Ovary	Ovulation
	Mammary gland	Post-partum involution
	Adipose tissue	Adipogenesis
Non-malignant diseases	Atherosclerosis	Inflammation, repair
	Skin	Wound healing
	Arthritis	Inflammation
	Dermatofibroma	Benign tumor proliferation
Malignant tumors (Carcinomas)	Fibroblast-like cells, adipocytes	Tumor progression

Table 1.5 MMP-11 in physiopathological tissue remodeling processes. Adapted from Rio, 2012.

1.4 Adipocyte involvement in mammary gland morphogenesis

The mammary gland consists of various microenvironments that contribute and crosstalk to maintain ductal epithelial cell homeostasis (McCave et al., 2010). The relevance of stromal contributions towards the growth of ductal epithelium in the

mammary gland is thought to be important for the development of the mammary architecture both during embryogenesis and in the postnatal phase. Thus, the embryonic mammary epithelium can form salivary gland-like structures if it is combined with salivary gland mesenchyme, indicating that the stroma play an important role in mammary gland development (Sakakura et al., 1976). Stromal-derived factors have a profound impact on ductal morphogenesis and elongation, regulation of TEBs growth and branching, as well as β-casein accumulation within the epithelium (Howlett and Bissell, 1993; Wiseman and Werb, 2002; Hinck and Silberstein, 2005; Ching, et al., 2011).

The stromal environment in the mammary gland is rather complex, which is made up of various cells, mainly including adipocytes, pre-adipocytes, fibroblasts, as well as endothelial cells and several cells of the immune system (Figure 1.18) (Neville et al., 1998; Wiseman and Werb, 2002). Insights into the individual contributions of these cells are rather limited. For instance, the localization of macrophages around the TEBs of the mammary gland is critical for the formation of elongated ducts, branching, orientation of the ducts and mammary gland involution (Gouon-Evans et al., 2000; Van Nguyen and Pollard, 2002; O'Brien et al., 2012).

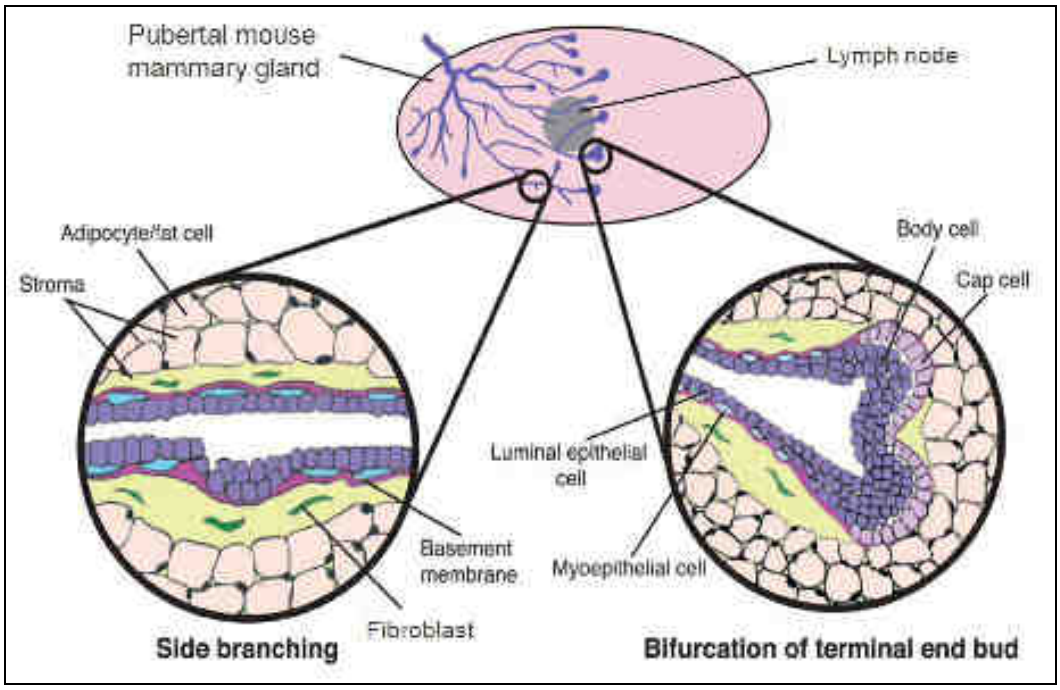

Figure 1.18 The duct, TEB and stromal architectures of pubertal mouse mammary gland. The mature mammary gland duct features an outer layer of myoepithelial cells surrounding an inner layer of luminal epithelial cells. The developing mouse mammary gland invades through the empty fat pad led by the terminal end buds, the outer layer of cap cells leads invasion and eventually give rise to myoepithelial cells. Many of the inner body cells undergo apoptosis, with some of the progeny of inner body cells forming the luminal epithelial cells that line the ducts of the gland. The stromal environment is made up of various components, including adipocytes, fibroblasts, endothelial cells and several cells of the immune system. The adipocytes are the main stromal cells of mammary gland surrounding the ducts and TEBs. Modified from Wiseman and Werb, 2002.

Adipocytes are the main stromal cells of the mammary gland. These mammary-associated-adipocytes undergo massive remodeling during lactation and involution, including lipid depletion and appearance as long projections during the former and regaining of the lipid stores and their morphogenic state in the latter. It is also postulated that during involution, part of adipocytes might dedifferentiate into pre-adipocytes, fibroblast-like cells or actually undergo apoptosis (Neville et al., 1998). Interestingly, MMP-11 have been shown to be highly expressed during post-weaning involution (Lefebvre et al., 1992). In addition to their function as a lipid source, adipocytes are a rich source of endocrine factors (Halberg et al., 2008). Adipocyte-derived factors (generally called as “adipokines”), include leptin, adiponectin, HGF, collagen VI, IL-6 and TNFα (Trujillo and Scherer, 2006). Altered

circulating levels of some of these factors are seen not only with obesity and related metabolic disorders, but are also associated with increased breast cancer risk (Trujillo and Scherer, 2006; Vona-Davis and Rose, 2007; Tan et al., 2011; Carter et al., 2012). Soluble secretory products from adipocytes impact on breast cancer cell proliferative, anti-apoptotic, migratory, invasive and pro-angiogenic behaviors both in vitro and in vivo (Iyengar et al., 2003; Iyengar et al., 2005; Landskroner-Eiger et al., 2009; Tan et al., 2011; Nieman et al., 2011; Carter and Church, 2012).

In vitro studies demonstrated that mammary adipocytes enhance morphological and functional differentiation of mammary epithelial organoids via undefined secreted soluble factors (Howlett and Bissell, 1993; Zangani et al., 1999; Couldrey et al., 2002; Pavlovich et al., 2010). Co-transplantion experiments of embryonic mammary epithelium with either embryonic fibroblastic mesenchyme or embryonic fat pads, identified that it was the fatty stroma that was necessary for the mammary epithelium to undergo its characteristic morphogenesis (Sakakura et al., 1982). In a separate set of observations, the lack of functional leptin or leptin receptor leads to failure of ductal epithelium development (Hu et al., 2002; Li et al., 2010). Interestingly, A-ZIP/F-1 transgenic mice never develop white adipose tissue and are therefore considered to be lipoatrophic mice (Moitra et al., 1998; Couldrey et al., 2002). They are severely diabetic, have an enlarged fatty liver and die prematurely (Moitra et al., 1998). Female mice have reduced fertility with rudimentary mammary anlagen and severely distended mammary ducts, and almost no pups survive beyond weaning (Couldrey et al., 2002).

In FAT-ATTAC mouse model (fat apoptosis through triggered activation of caspase-8), apoptosis of adipocytes can be induced at any developmental stage by administration of a FK1012 synthetic analog (AP20187). It binds with ~1,000-fold greater affinity to FKBPv (Phe36-Val mutant FKBP) than to endogenous FKBP, thus leading to the forced dimerization of a membrane-bound FKBP-caspase-8 fusion protein uniquely expressed in adipose tissue. Adipocyte ablation occurred systemically and allowed for the elimination of almost all fat pads, even in an ob/ob (obese) background, a strain suffering from a very high degree of adiposity due to a

mutation in the leptin gene (Pajvani et al., 2005). Loss of adipose tissue AP20187-initiated 2 weeks after birth triggers fewer duct branching and TEBs, and also triggers changes in proliferation and apoptosis in the epithelium associated with the TEBs. The reduced developmental progress that adipocyte-ablated glands undergo is reversible, as the emergence of new local adipocytes, upon cessation of treatment, enables the ductal epithelium to resume growth. Conversely, loss of local adipocytes initiated at 7 weeks of age resulted in excessive lobulation, indicating that adipocytes are critically involved in maintaining proper architecture and functionality of the mammary epithelium, suggesting that adipocytes are required for proper development during puberty and for the maintenance of the ductal architecture in the adult mammary gland (Landskroner-Eiger et al., 2010).

It has been demonstrated that local mammary-associated adipocytes play an important role, thus supporting the view that adipocytes are potent mediators in the proper development and maintenance of ductal morphogenesis (Couldrey et al., 2002; Pavlovich et al., 2010; Landskroner-Eiger et al., 2010; Ching et al., 2011).

1.5 Aim of study

Recently, it has been shown in the laboratory that the invasive cancer cells induce MMP-11 expression by proximal adipocytes and pre-adipocytes. Moreover, MMP-11 is a negative regulator of adipogenesis, able to reduce and even to revert mature adipocyte differentiation in vitro. In turn, MMP-11 leads to the accumulation of non-malignant peritumoral fibroblast-like cells, which favor cancer cells survival and tumor progression (Figure 1.19).

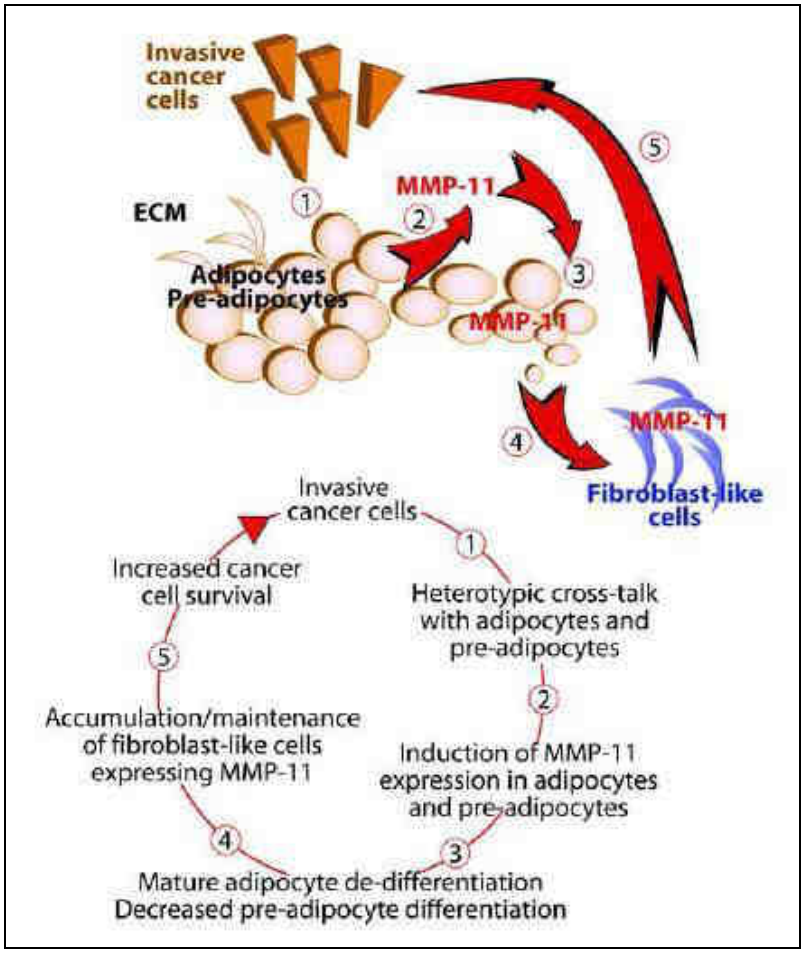

Figure 1.19 Schematic representation of the vicious tumor progression cycle involving invasive cancer cells, adipocytes and MMP-11. Adipocytes/pre-adipocytes and MMP-11 participate in a highly complex vicious cycle to support tumor progression, and this process is orchestrated by cancer cells. The scenario in five acts might be the following. At the beginning, both the invasive cancer cells and the resting adipocytes/pre-adipocytes do not express MMP-11. When a cancer cell meets an adipocyte/pre-adipocyte, their cross-talk/interaction induces the expression/ secretion of MMP-11 by the adipocyte/pre-adipocyte. MMP-11 negatively regulates adipogenesis, leading to a decrease in adipocyte differentiation and an accumulation/maintenance of MMP-11-expressing fibroblast-like cells. These latter cells then act on the adjacent invasive cancer cells to favor their survival and potentiate this vicious cycle. Adapted from Motrescu and Rio, 2008.

Many questions remain to be addressed to understand the adipocyte-related MMP-11 function in pathophysiology. Adipocyte is one of the more frequent stromal cell in the breast, and it has been demonstrated that local mammary-associated adipocytes play an important role, thus supporting the view that adipocytes are potent mediators in the proper development and maintenance of ductal morphogenesis. Since MMP-11 was shown to play a role in adipocyte homeostasis, it might be hypothetized that MMP-11 expressed by adipocytes plays an important function in normally

occuring postnatal development of the mammary gland, and that this function could be aberrantly restored during carcinogenesis. So, in order to further study biological and cellular function(s) of adipocyte-related MMP-11, I have created numerous tolls and initiated several experiments to investigate:

1) The impact of MMP-11 on adipogenesis;
2) The impact of MMP-11 on postnatal mammary gland development;
3) The impact of MMP-11 over-expression restricted to adipocytes on mammary gland development and tumorigenesis.

Chapter 2 Results

Part I The impact of MMP-11 on adipogenesis

MMP-11-knockout (MMP-11-/-) mice with 129/Svj D3 genetic background have been previously generated (Masson et al. 1998), and it has been shown that the potential of MMP-11-/- MEFs (mouse embryonic fibroblasts) to differentiate into adipocytes is markedly increased compared with that of wild-type MEFs (Andarawewa et al., 2005). To test if MMP-11 recombinant protein can induce adipocyte dedifferentiation and which genes are involved with this phenotype change, I established MMP-11-/- MEFs from E14.5 embryos. I investigated their adipocyte differentiation and dedifferentiation after appropriate treatment, and studied gene expression pattern using microarray experiments.

2.1.1 MMP-11 genotype

I first identified MMP-11 mouse genotype with PCR analysis. I designed three primers, one sense primer (primer_A): TTC TAA CAT CCC TCT GGG CTC (locates in exon 6 of mus MMP11, NM_008606); another sense primer (primer_B): GCC GCT TTT CTG GAT TCA TCG (locates in neomycin gene); the antisense primer (primer_C): GTG GAA ACG CCA ATA GTC TCC (locates in exon 7 of mus MMP-11, NM_008606) (Figure 2.1 A).

The wild-type (primer_A+C) amplicon size is 332 bp, whereas, the MMP-11-/- (primer_B+C) amplicon size is 230 bp. Thus, the heterozygote (+/-) mouse DNA gives two bands (Figure 2.1 B). MMP-11 genotyping of embryos (E14.5 day) used to establish MEFs was done using these three primers.

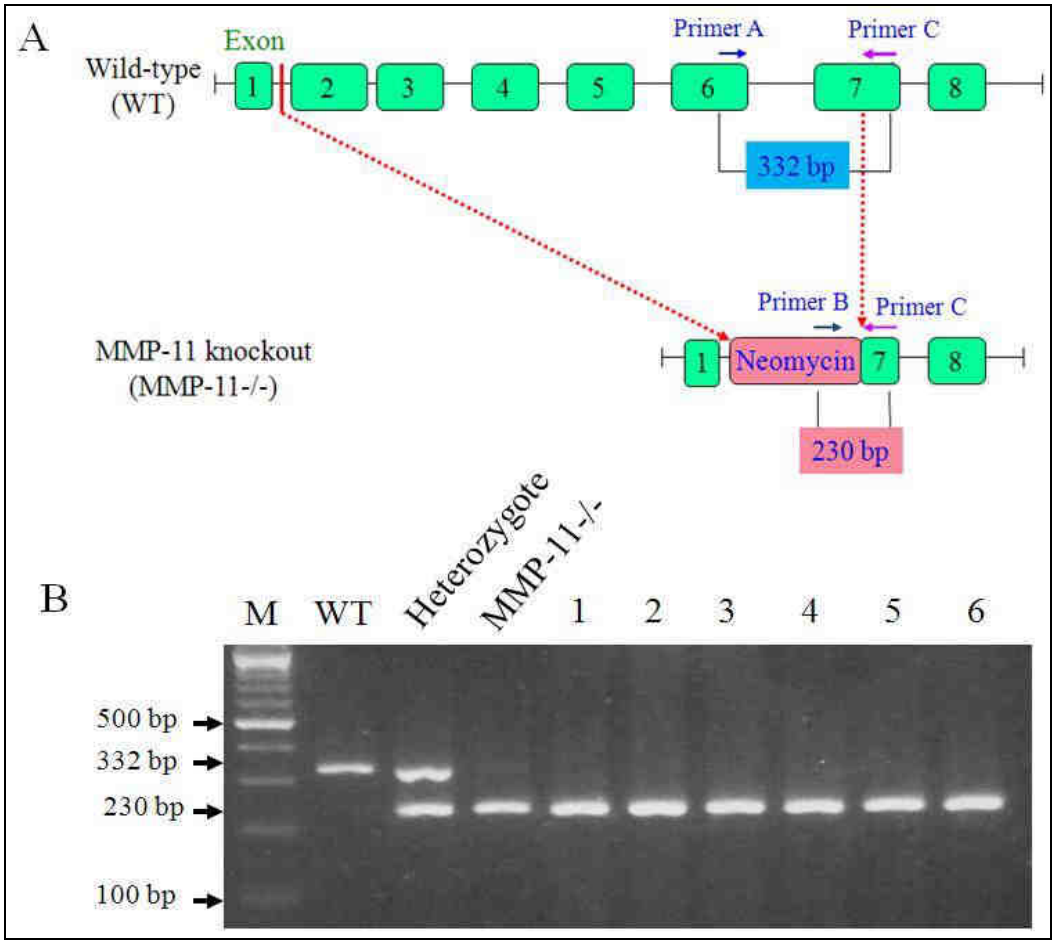

Figure 2.1 Identification of MMP-11 genotype with PCR. A: location of PCR primers. B: Six embryos coming from MMP-11-/- male and female crossing were tested. As expected, all were MMP-11-/- (lanes 1-6).

2.1.2 MMP-11 induces MEF adipocyte dedifferentiation in vitro

Primary cultures of MMP-11-/- MEFs were differentiated into adipocytes in response to the differentiation-inducing mix as described before (Andarawewa et al., 2005). Cell differentiation was phenotypically evaluated by Oil Red O staining of lipid droplets. There is only rare lipid droplet appearance at MMP-11-/- MEF confluence. Interestingly, at 13 days after differentiation-inducing mix treatment, nearly 50% of MMP-11-/- MEFs were differentiated into adipocytes, which confirms that the MMP-11-/- MEFs have potential ability to differentiate into adipocytes (Figure 2.2) (Andarawewa et al., 2005).

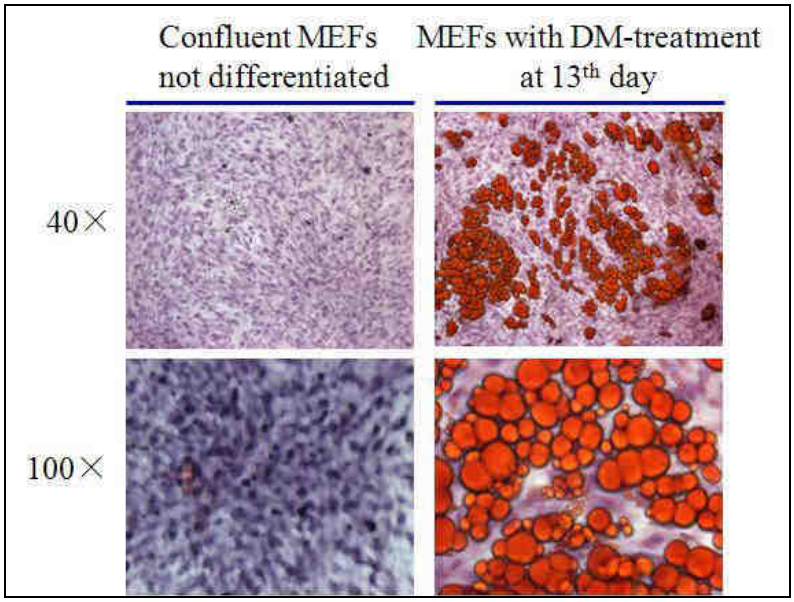

Figure 2.2 Oil Red O staining analysis for differentiation of MEFs into adipocytes. Rare lipid droplets are present when the MMP-11-/- MEFs are confluent; However, numerous lipid droplets were visualized in MMP-11-/- MEFs after 13 days of differentiation. Magnification: as indicated.

The MMP-11-/- MEFs which were differentiated into adipocytes were then treated with buffer containing active form of mouse recombinant MMP-11 (rMMP-11) protein (10 μg/ml) produced in the laboratory (Kannan et al., 1999). Medium was changed every 24 hours because MMP-11 is susceptible to autolysis. After 96 hours of active MMP-11 recombinant protein treatment, the number of adipocytes was decreased, the size of adipocytes became smaller, and cell profile no longer seemed as round as control adipocytes, but instead adopted a more fibroblast-like spindle-cell shape. This was accompanied by delipidation since we observed a decreased number and size of lipid droplets, as shown by Oil Red O staining. To test if this MMP-11 function was dependent on its enzymatic activity, similar experiments were done using an inactive recombinant MMP-11 in which the glutamic residue of the catalytic site was changed to an alanine (Glu220Ala) (Noel et al., 2000). This inactive MMP-11 was unable to induce MEF adipocyte dedifferentiation (Figure 2.3). These results indicated that MMP-11 enzymatic activity is required in adipocyte dedifferentiation.

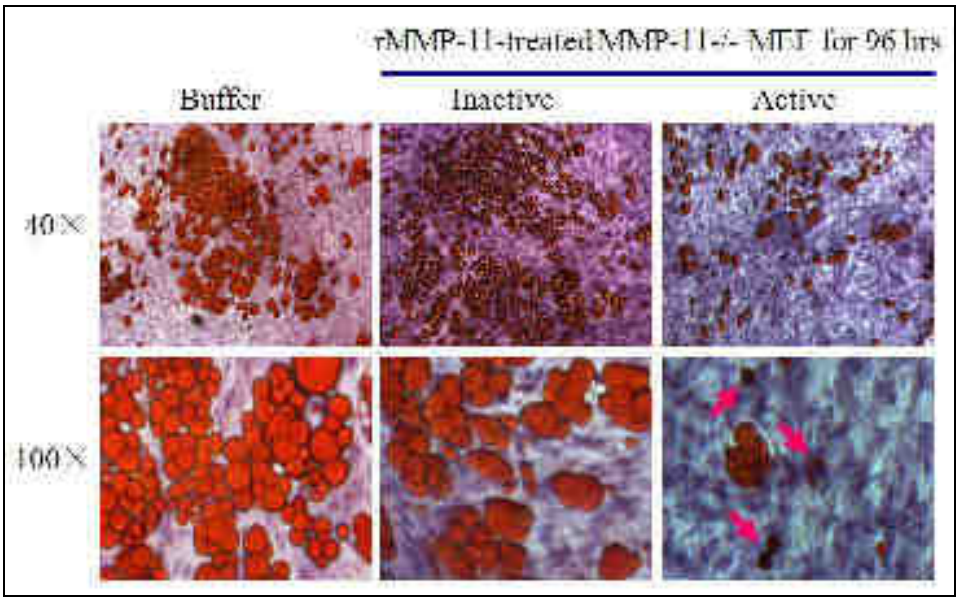

Figure 2.3 Oil Red O staining analysis of MMP-11-/- MEFs differentiated into adipocytes and treated with buffer alone or containing mouse MMP-11 recombinant proteins (rMMP-11). In active MMP-11-treated adipocytes, the number and size of lipid droplets were dramatically decreased, and cells adopted a more fibroblast-like spindle-cell shape (arrows). Compared with control buffer alone, the number and size of lipid droplets and adipocytes have no clear changes after inactive MMP-11 treatment. Magnification: as indicated.

2.1.3 Total RNA extraction and quantification

Extraction of total RNA from MEFs was performed as described in the RNeasy (mini handbook, Qiagen). Measurement of the total RNA concentration was performed with NanoDrop ND-1000 spectrophotometer (Figure 2.4).

DM-treated at 13th day

	ng/ul	260/280
NO.1	268.10	2.13
NO.2	392.67	2.12
NO.3	468.43	2.31

rMMP-11-treated (10 μg/ml) for 96 hrs

		ng/ul	260/280
NO.1	Active	235.66	2.14
	Buffer	312.25	2.14
	Inactive	340.43	2.14
NO.2	Active	297.61	2.17
	Buffer	380.73	2.12
	Inactive	242.02	2.16
NO.3	Active	282.72	2.12
	Buffer	360.83	2.14
	Inactive	473.45	2.05

Figure 2.4 RNA concentration and OD260/280 ratio. Total RNA obtained from 12 MMP-11-/- MEF samples were correct.

The requirements to perform microarray are as following:

Quantity: The concentration (Nanodrop) ≥ 0.2 µg/µl;

The minimum volume ≥ 5 µl.

Quality: Purity (Nanodrop) $OD_{260}/OD_{280} \geq 1.8$;

Integrity: capillary electrophoresis (Bioanalyser) 28S/18S ≥ 1.6;

RIN (RNA integrity number) ≥ 6.

I have checked these quality indexes. All samples were suitable with these requirements for microarray.

2.1.4 The microarray results

The corresponding RNAs have been studied by microarray analysis (Affymetrix IGBMC platform).

We used pangenomic arrays allowing to study about 30000 genes. Only 5 genes showed significant changes of their expression. Two were up-regulated and 3 down-regulated (Table 2.1).

Up-regulated	Down-regulated
Coronin, actin binding protein 1A*	Jun oncogene*
Dedicator of cytokinesis 8*	Regulator of G-protein signaling 1*
	Zinc finger CCCH type containing 12C*

Table 2.1 Gene expression changes identified by microarray. Active rMMP-11 versus inactive rMMP-11; *means $p < 0.05$.

2.1.5 Conclusion

This result is unsatisfactory. Indeed, it seems impossible to have so few genes modified whereas cell phenotype is changing from adipocyte to fibroblast. These unsuccessful experiments could probably be due to cumulative problems of ratio: adipocyte-differentiated MEFs versus fibroblastic MEFs, and dedifferentiated MEFs versus differentiated in adipocytes. Indeed, we never obtained more than 50% phenotypic change at each step. This is insufficient and led to dilution of informations into a high background and did not allow to identify genes whose expression is modified.

Part II

The impact of MMP-11 on postnatal mammary gland development

Since adipocyte is one of the more frequent stromal cell into the breast, known to be involved in adult mammary gland structure/remodeling, and since MMP-11 was shown to reduce adipogenesis and induce adipocyte dedifferentiation, it might be hypothetized that MMP-11 might play an important function in normally occuring postnatal development of the mammary gland. So, in order to further study the potential impact of MMP-11 on this event, I have studied the mammary gland postnatal development of MMP-11-/- mice at different stages with several methods, and investigated the relative impact of lack of MMP-11 on stromal and epithelial compartment function.

2.2.1 MMP-11 is expressed in WT mammary gland

To determine if MMP-11 might be involved in mammary gland development, I first examined the expression of MMP-11 in the mouse mammary gland. MMP-11 genotyping was performed as reported in paragraph 2.1.1 (Figure 3.1 A). Besides, I studied the MMP-11 expression in mammary gland with RT-PCR (Figure 3.1 B) and in situ hybridization (Figure 3.1 C), I observed MMP-11 mRNA expression in the mammary gland of WT mice. Moreover, MMP-11 was mainly localized in fibroblasts and adipocytes. As expected, no MMP-11 was detected in mammary gland from MMP-11-/- mice (Figure 3.1 B and C).

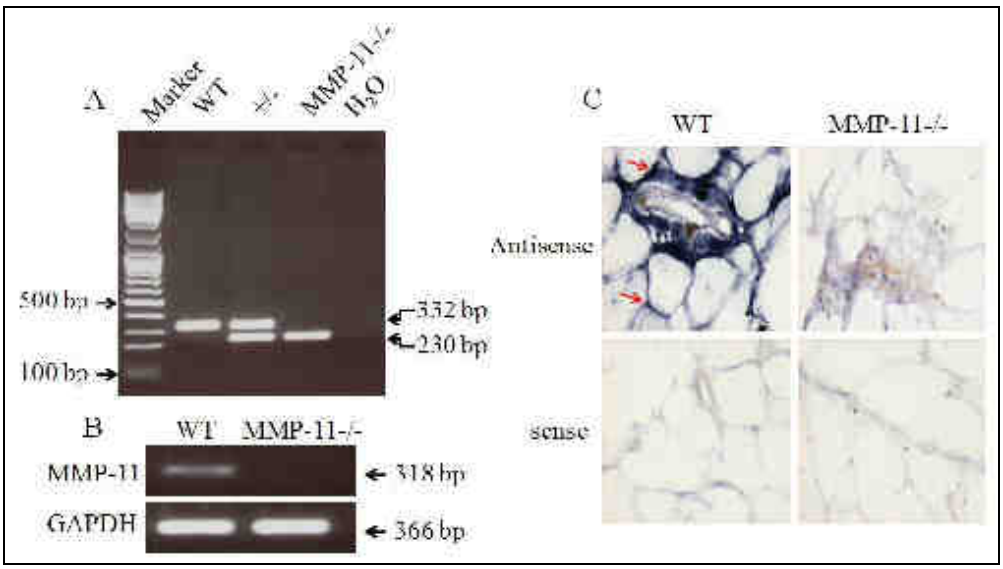

Figure 3.1 Identification of MMP-11 genotype and expression. A: identification of MMP-11 genotype with PCR (genomic DNA). B: Investigation of MMP-11 expression in mammary gland extract with RT-PCR (cDNA). C: MMP-11 localization in the mammary gland with in situ hybridization analysis; the arrows indicate that MMP-11 expression and localization in fibroblasts and adipocytes of mammary gland. +/-: heterozygote. Original magnification: X400.

2.2.2 Mammary ductal morphogenesis is impaired in MMP-11-/- mice

To investigate if loss of MMP-11 affects mammary gland postnatal development, I first examined the inguinal #4 mammary gland phenotype from five pairs of 3-, 4-, 6- and 12-week-old littermate mice by whole-mount carmine staining. The initial rudimental ductal trees appeared normal in 3-week-old pre-pubertal MMP-11-/- mice (Figure 3.2).

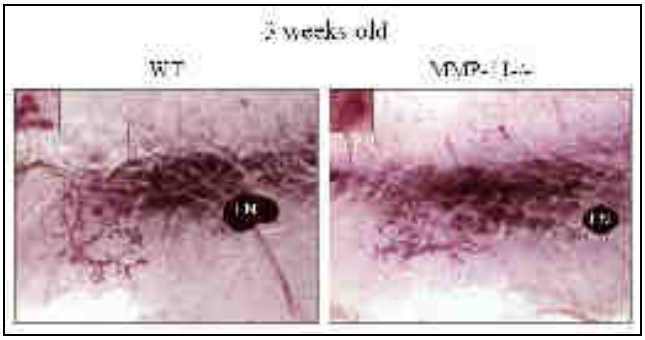

Figure 3.2 Evaluation of wild-type and MMP-11-/- mammary gland development by whole-mount carmine staining analysis at 3 weeks old. The rudimental ductal trees appeared similar in both wild-type and MMP-11-/- mice. LN: lymph node; Original magnification: X5; The insertion original magnification: X20.

Interestingly, at 4 weeks old, the wild-type mammary gland contained an extensive ductal network and many distal branches were tipped with TEBs, suggesting that active ductal morphogenesis was in progress. The number of TEBs (mean ± SD) was 32.6 ± 8.35 per gland in wild-type mice. However, there were less ductal branches, and the number of TEBs was lower in MMP-11-/- glands (22.0 ± 5.1) (per gland; p = 0.040) (Figure 3.3 A and B). Meanwhile, I have measured the mammary gland weight and volume. There were no obvious difference between wild-type and MMP-11-/- (Figure 3.3 C and D).

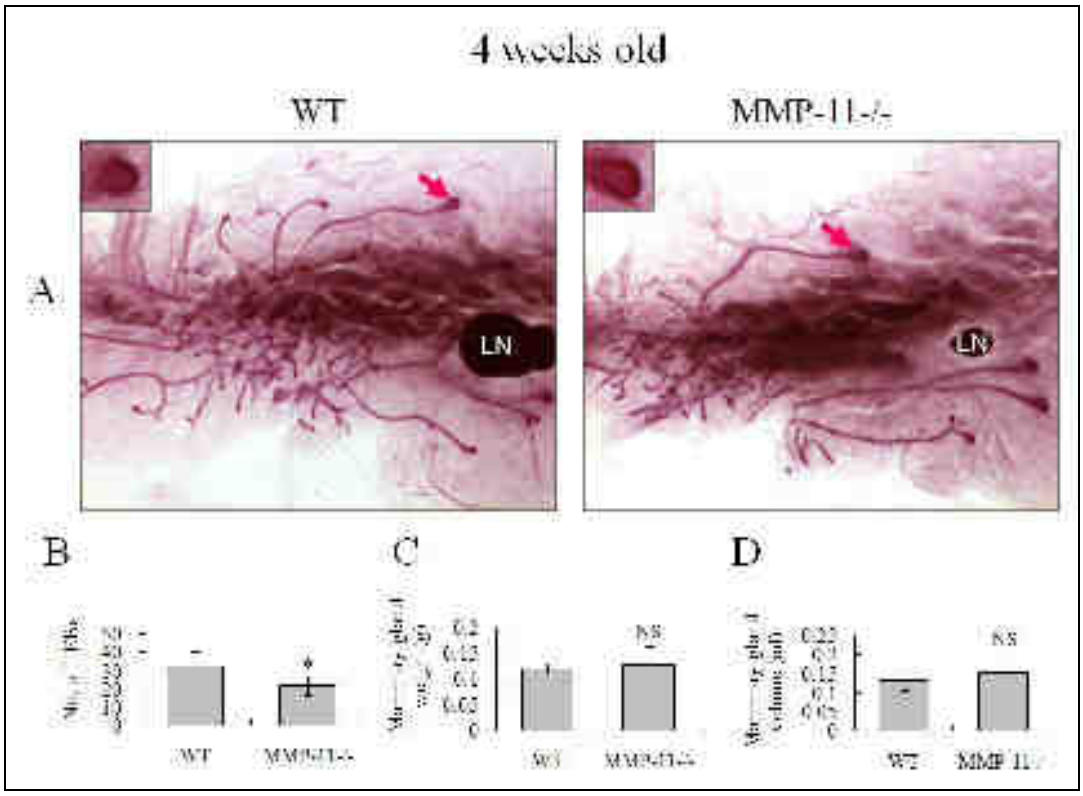

Figure 3.3 Evaluation of wild-type and MMP-11-/- mammary gland development at 4 weeks old. A: whole-mount carmine stained mammary gland; B: number of terminal end buds (TEBs); C and D: mammary gland weight and volume, respectively. The arrow shows TEB; LN: lymph node; Original magnification: X5; The insertion original magnification: X20.

This phenotype was more distinct in 6-week-old MMP-11-/- mice, compared with wild-type gland (TEBs: 13.6 ± 6.4 versus 39.6 ± 14.3; p = 0.006) (Figure 3.4 A and B). Additionally, mammary gland complexity, which represents the extent of ductal branching, was quantified by determining the number of intersecting branches with a line drawn at ahead of lymph node, perpendicularly to the long axis of the mammary gland. The wild-type mammary gland complexity was 13.6 ± 1.1. It was

decreased dramatically in MMP-11-/- gland (4.8 ± 2.0; $p < 0.001$) (Figure 3.4 A and C). As previously at 4 weeks old, there is no difference in mammary gland weight and volume between wild-type and MMP-11-/- at 6 weeks old (Figure 3.4 D and E).

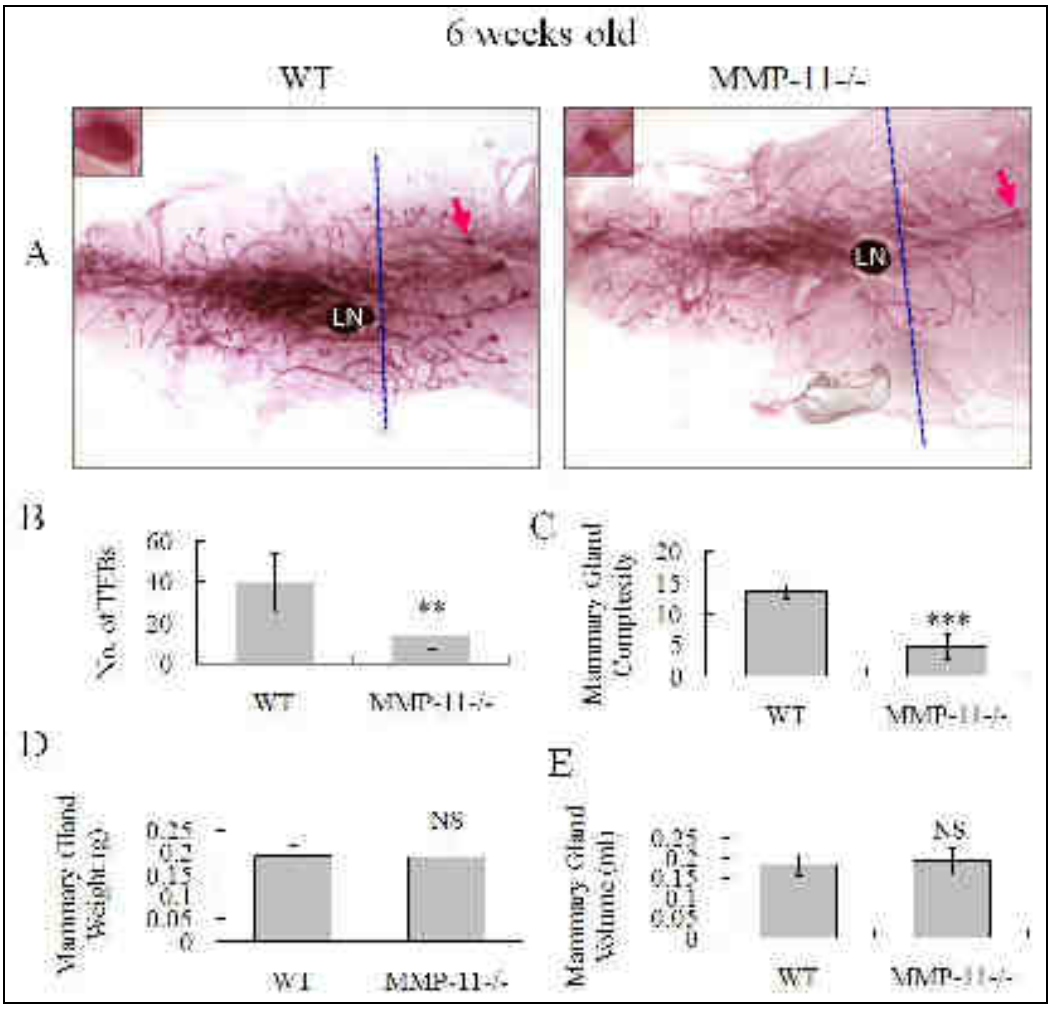

Figure 3.4 Evaluation of wild-type and MMP-11-/- mammary gland development at 6 weeks old. A: whole-mount carmine stained mammary gland; B: the number of terminal end buds (TEBs); C: mammary gland complexity as a measure of the extent of ductal branching ahead of lymph node, represented by a dotted line perpendicular to long axis of the mammary gland; D and E: mammary gland weight and volume, respectively. The arrow shows the TEB; LN: lymph node; Original magnification: X5; The insertion original magnification: X20.

Similarly, at 12 weeks old, the mammary gland complexity in wild-type mice (15.0 ± 3.3) was obviously higher than in MMP-11-/- gland (9.8 ± 1.1; $p = 0.006$) (Figure 3.5 A and B). The ductal tree in wild-type has almost reached the border of fat pad, whereas a large part of fat pad remained unoccupied in MMP-11-/- gland. Very few TEBs were present in wild-type (14.2 ± 5.3), however some were always

observed in MMP-11-/- gland (29.0 ± 12.1; p = 0.037) (Figure 3.5 A and C). Once again, there were no obvious difference between wild-type and MMP-11-/- mammary gland weight and volume (Figure 3.5 D and E).

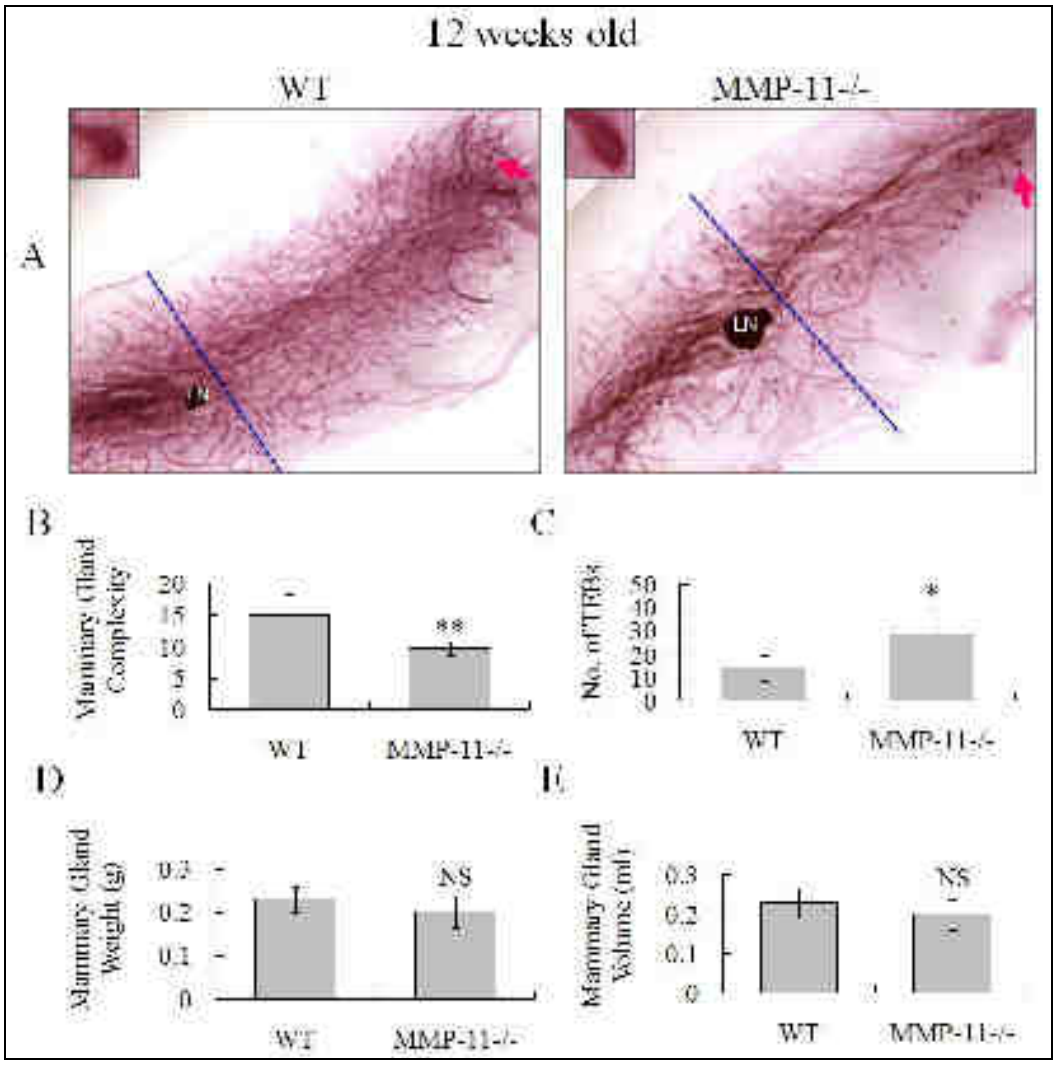

Figure 3.5 Evaluation of wild-type and MMP-11-/- mammary gland development at 12 weeks old. A: whole-mount carmine stained mammary gland; B: the mammary gland complexity given by the number of branches crossing the dotted line; C: the number of terminal end buds (TEBs); D and E: mammary gland weight and volume, respectively. The arrow shows TEBs; LN: lymph node; Original magnification: X5; The insertion original magnification: X20.

Altogether, these observations indicate that the ductal morphogenesis of MMP-11-/- mammary gland is impaired in comparison to wild-type mice. Thus, the ductal structure development is delayed and incomplete, suggesting that MMP-11 provides a non-redundant function in ductal tree development.

To determine whether MMP-11-/- also affects mammary gland functional

differentiation, I next examined their phenotype at early pregnancy (10th day after conception), late pregnancy (18th day after conception), during lactation (3rd day postpartum) and involution (7th day post-weaning) (Figure 3.6). The alveolar structures of wild-type mammary glands developed gradually during pregnancy and reach their mature forms by parturition. Similar alveolar structures also developed in MMP-11-/- glands, but their density was strongly reduced (Figure 3.6 A, B and C). Surprisingly, during mammary gland involution after weaning, there was less distinct difference between wild-type and MMP-11-/- gland (Figure 3.6 D).

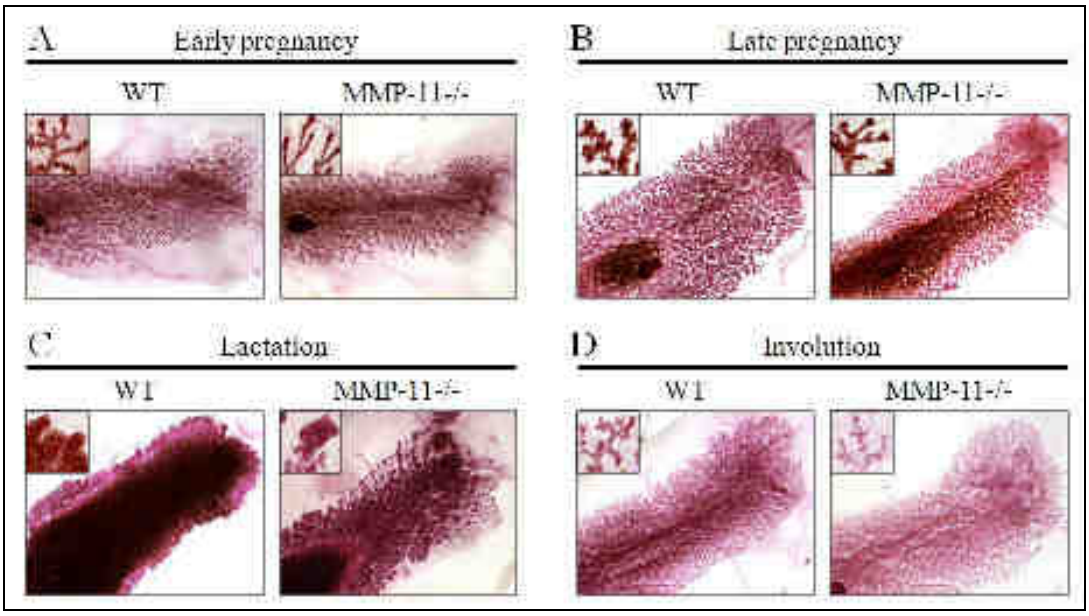

Figure 3.6 Evaluation of mammary gland functional differentiation by whole mount carmine staining analysis. A: early pregnancy (10th day after conception); B: late pregnancy (18th day after conception); C: lactation (3rd day postpartum); D: involution (7th day post-weaning). Original magnification: X5; The insertion original magnification: X80.

To assess the milk production by littermate wild-type and MMP-11-/- female mice at first pregnancy, I kept same number of pups (6 pups) per female, and measured the pup body weight from 0 to 28 days after parturition. For both wild-type and MMP-11-/- mothers, all pups were alive at the end of test. From 4th to 17th day, the body weight of pups fed by MMP-11-/- mothers was significantly lower compared with pups fed by wild-type mothers. However, after the 18th day, the pup body weight difference decreased slightly and finally arrived at similar levels (Figure 3.7). It seems reasonable to hypothesize that decreased quantity of milk production results in pup

body weight difference, as expected from the reduced density of alveoli in MMP-11-/- gland. This is further supported by the fact that at the 18th day, when pup nutrition is no more milk-dependent, the pup body weight became MMP-11 independent.

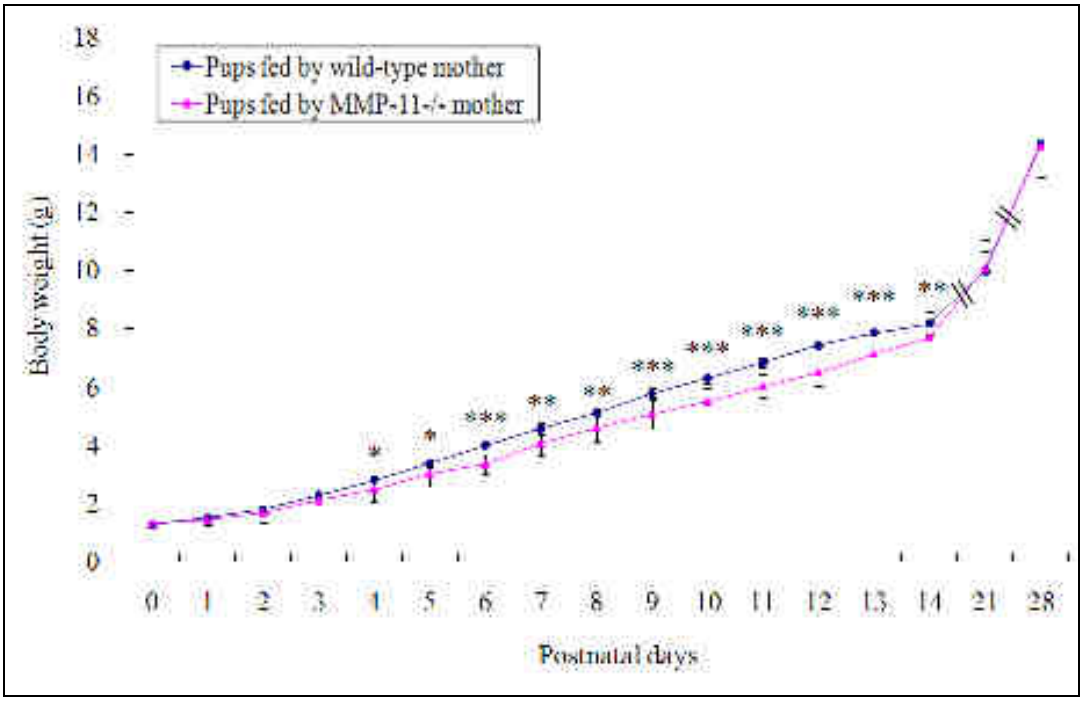

Figure 3.7 Analysis of body weight of pups fed by wild-type or MMP-11-/- females. From 4th to 17th day after parturition, pups fed by MMP-11-/- mothers have retarded growth compared with pups fed by wild-type mothers. Three litters per genotype were used for this analysis. Data are expressed as mean ± s.d.; n=18 for each group; * means $p<0.05$; ** mean $p<0.01$; *** mean $p<0.001$.

2.2.3 Mammary gland epithelium is normal in MMP-11-/- mice

The TEBs comprise a dynamic mass of luminal epithelial body cells, surrounded by a motile cap cell layer. The TEBs bifurcate repeatedly to form the ductal tree and, ultimately, develop into a mature gland. Disruption of TEBs is often associated with delayed ductal outgrowth and impaired branching morphogenesis, thus suggesting an essential function of TEBs in the overall development of mammary gland (Sternlicht et al., 2006; Kurley et al., 2012).

To determine whether there is cellular defect in MMP-11-/- epithelial ducts and TEBs, I analyzed the mammary gland histology by hematoxylin-eosin (H&E) staining.

As previously, I observed more TEB structure in wild-type glands than in MMP-11-/- glands. However, the architecture of ducts and TEBs in both gland genotypes looked normal with the inner layer of luminal epithelial cells and the outer layer of myoepithelial cells. Compared with wild-type, the ductal structure was reduced in MMP-11-/- glands (Figure 3.8). Interestingly, the size of adipocytes appeared larger in MMP-11-/- gland, in accord with previous data (Lijnen et al., 2002; Andarawewa et al., 2005; Tan et al., 2011). This could explain why, although the ductal tree and TEBs are less developed in the MMP-11-/- mammary glands, their weight and volume are similar in both wild-type and MMP-11-/- mice (Figures 3.3, 3.4 and 3.5). Both TEBs and ducts are well delineated by epithelial cell layer. Moreover, dense extracellular matrix rings were observed around both epithelial structures.

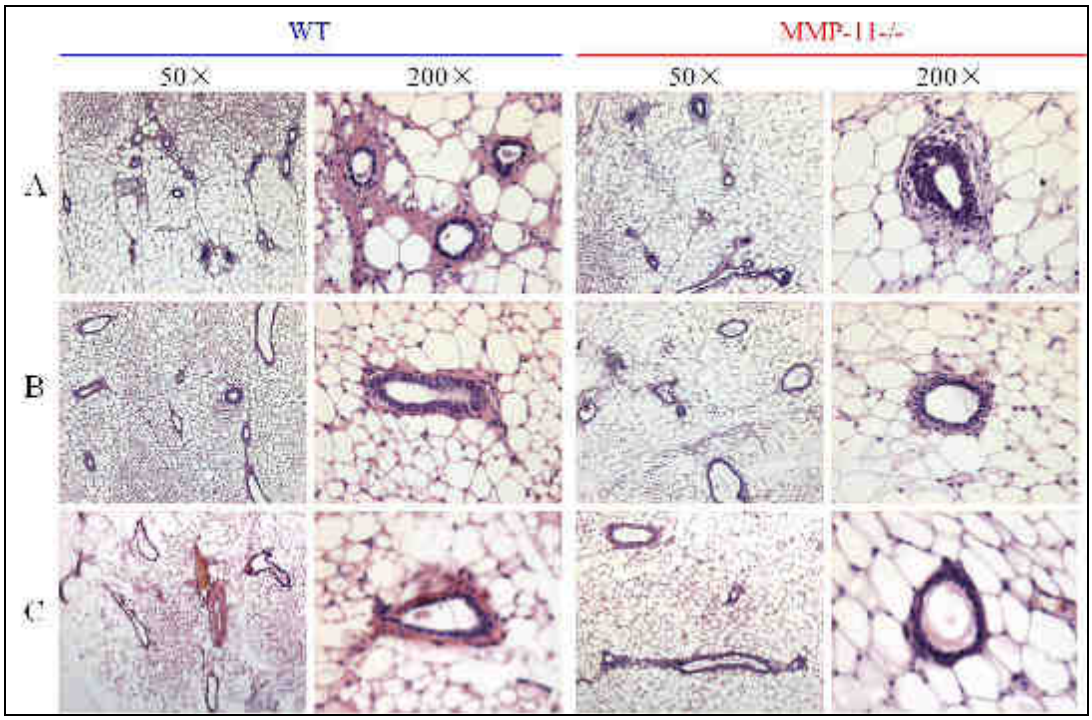

Figure 3.8 H&E staining of wild-type and MMP-11-/- mammary ducts. A: 4 weeks old; B: 6 weeks old; C: 12 weeks old. Original magnifications are as indicated.

Immunofluorescence staining for E-cadherin confirmed the identity of luminal epithelial cells in ducts (Figure 3.9 A and C) and body cells of TEBs (Figure 3.9 B and D) of 6-week-old pubertal gland.

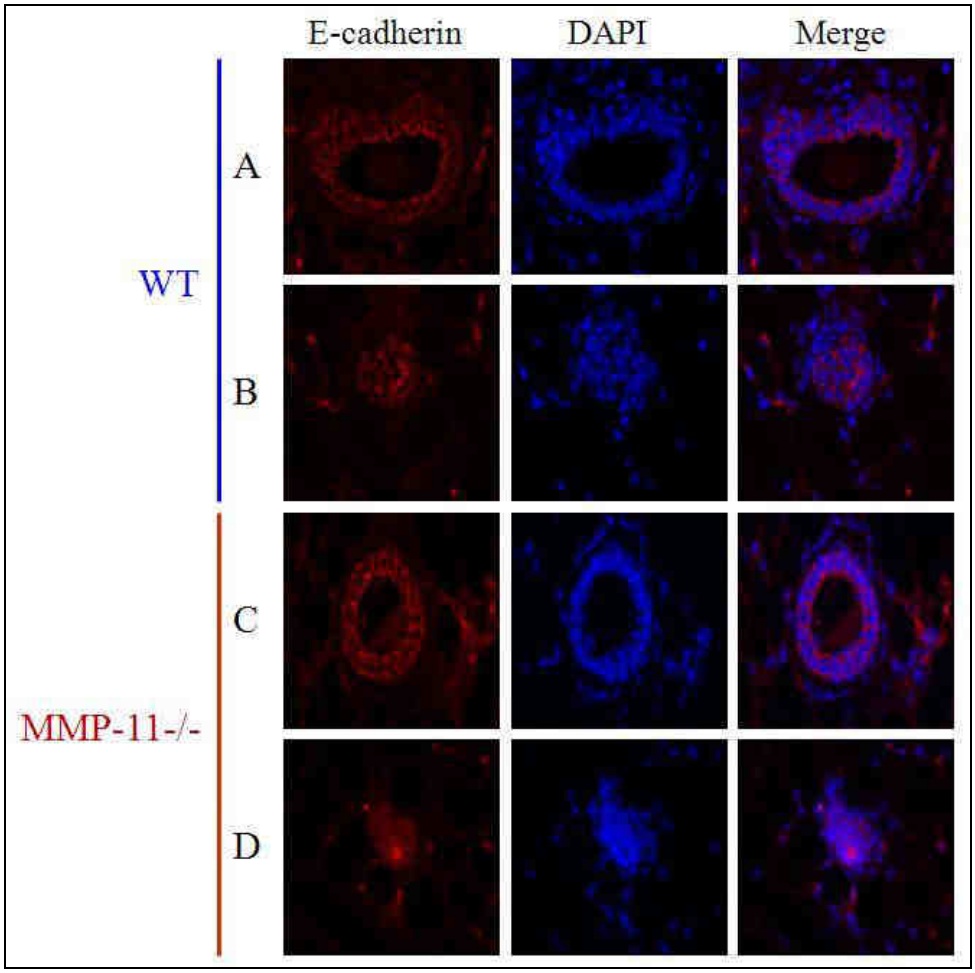

Figure 3.9 E-cadherin immunofluorescence staining of epithelial cells (red). A: Ductal luminal epithelial cells of wild-type mammary gland; B: TEB body cells of wild-type mammary gland; C: Ductal luminal epithelial cells of MMP-11-/- mammary gland; D: TEB body cells of MMP-11-/- mammary gland. DAPI: nucleus staining in blue. Original magnification: X400.

Staining for α-smooth muscle actin (α-SMA) confirmed the identity of myoepithelial cells in ducts (Figure 3.10 A and C) and cap cells of TEBs (Figure 3.10 B and D).

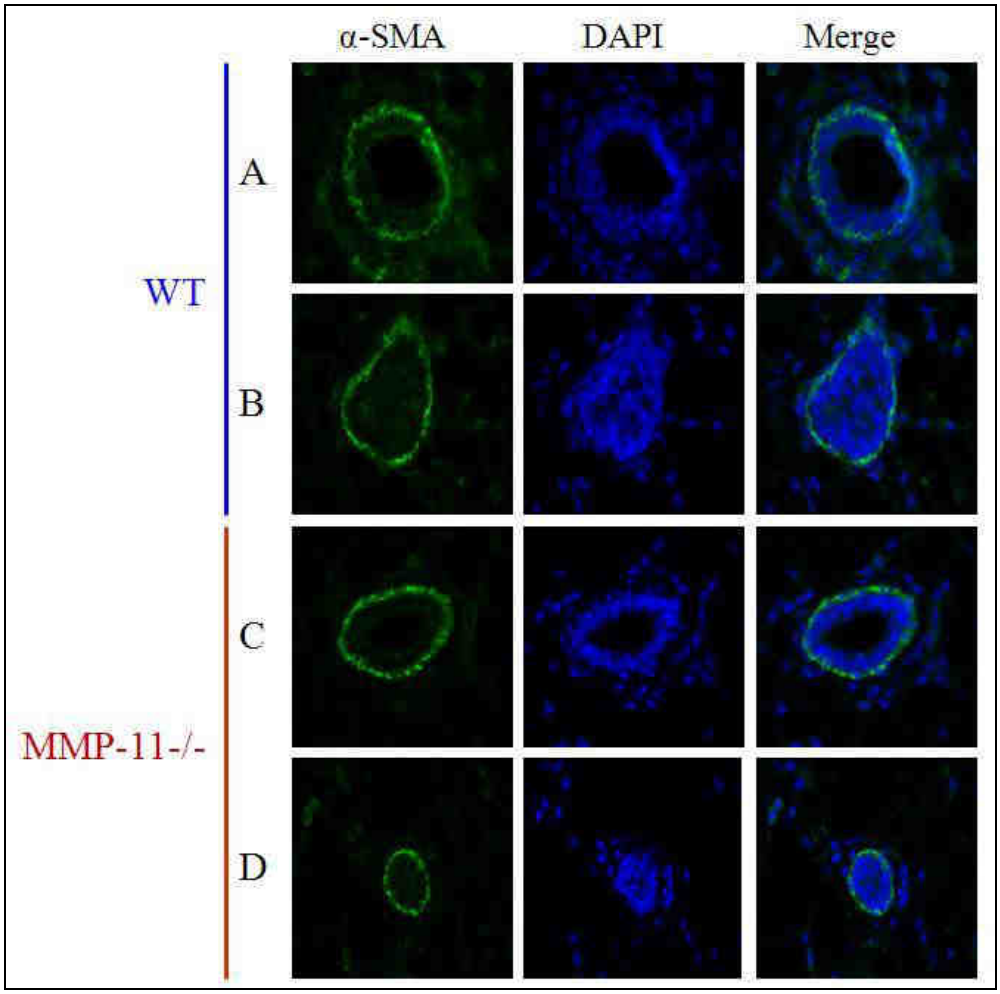

Figure 3.10 α-smooth muscle actin (α-SMA) immunofluorescence staining of myoepithelial cells (green). A: Ductal basal myoepithelial cells of wild-type mammary gland; B: TEB cap cells of wild-type mammary gland; C: Ductal basal myoepithelial cells of MMP-11-/- mammary gland; D: TEB cap cells of MMP-11-/- mammary gland. DAPI: nucleus staining in blue. Original magnification: X400.

These results indicated that there is no obvious architectural defect of mammary gland ducts and TEBs in MMP-11-/- mice, indicating that affected mammary gland postnatal development observed in MMP-11-/- mice is not due to direct alteration of the epithelial compartment of the mammary gland.

2.2.4 The mammary gland stroma is altered in MMP-11-/- mice

Then, we postulated that the MMP-11-/- phenotype could be due to alteration of the stromal compartment of the mammary gland. The periductal stroma that surrounds the epithelial ducts is mainly composed of adipocytes and collagen-rich ECM, and is

essential for the regulation of mammary gland development (Couldrey et al., 2002; Landskroner-Eiger et al., 2010; Ching et al., 2011). Thus, I studied wild-type and MMP-11-/- stroma of the mammary gland.

I checked the ECM composition using sirius red staining that allows to visualize collagens. In both wild-type and MMP-11-/- glands, there are low levels of collagen around TEBs structure (Figure 3.11 A2, A4, B2, B4, C2 and C4). The ducts are generally surrounded with a collagen-rich periductal stroma that is more developed in wild-type (Figure 3.11 A1, B1 and C1) than in MMP-11-/- glands (Figure 3.11 A3, B3 and C3).

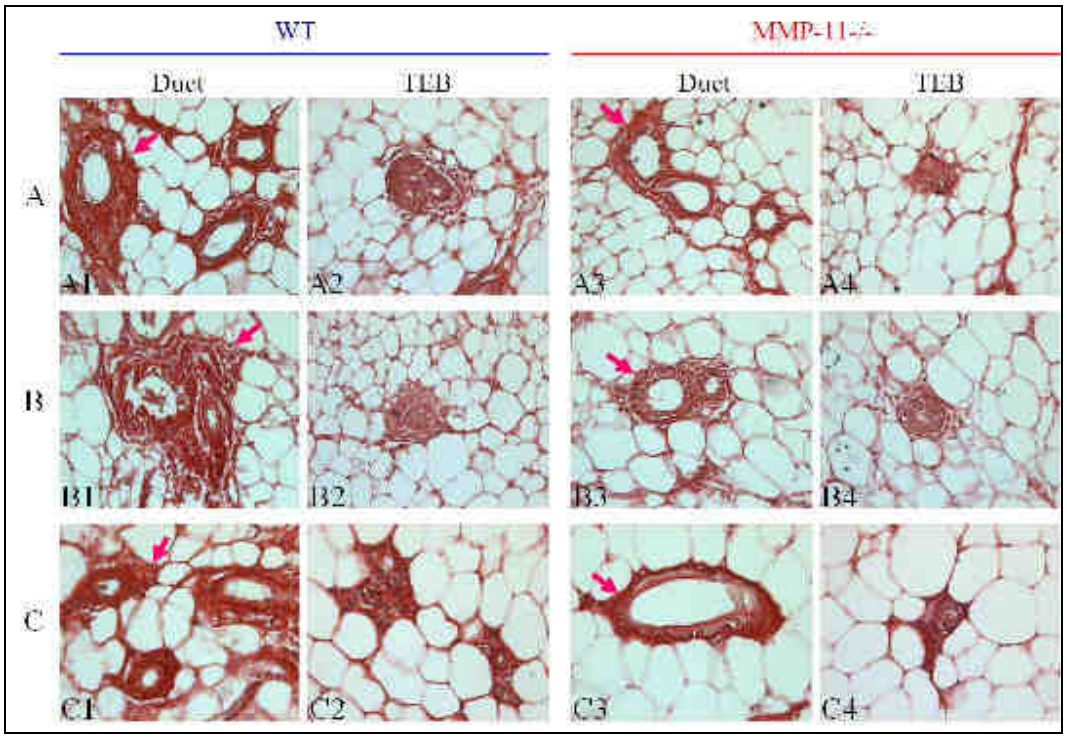

Figure 3.11 Analysis of wild-type and MMP-11-/- mammary gland collagen using Sirius red staining. Mammary gland sections from 4-week-old (A); 6-week-old (B) and 12-week-old (C) mice. Collagen was stained in red. A1, A3, B1, B3, C1 and C3 show periductal collagen; A2, A4, B2, B4, C2 and C4 show collagen located around TEBs. The arrows indicate collagen. Original magnification: X400.

To further confirm whether the MMP-11-/- glands lack of collagen in periductal stroma, I selected Masson's trichrome staining (Figure 3.12) to analyze collagen of the mammary gland. I obtained similar results.

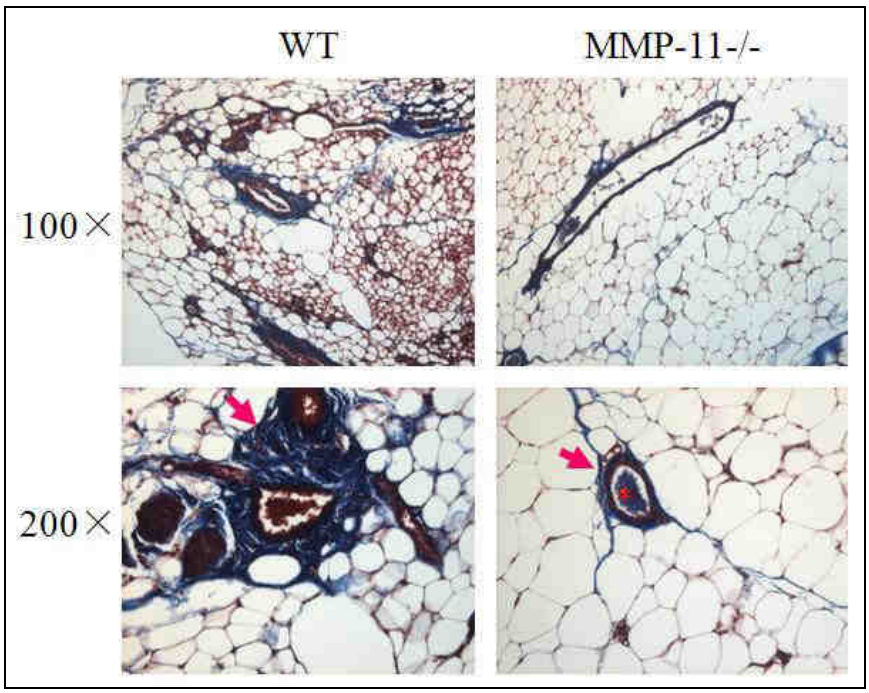

Figure 3.12 The MMP-11-/- mammary glands lack of periductal collagen. Masson's trichrome staining of mammary gland sections from 12-week-old wild-type and MMP-11-/- littermates. Collagen and mucus were stained in blue. The arrows indicate collagen, the asterisk indicates mucus. Original magnifications are as indicated.

Because MMP-11 could reduce adipogenesis (Andarawewa et al., 2005; Tan et al., 2011), and fibroblasts are important producer of collagens, this might be the reason why collagen levels were decreased in MMP-11-/- gland, since we might expect to have a lower number of fibroblasts. Thus, the lack of MMP-11 greatly affects the periductal collagen structures.

2.2.5 The lipid contents of mammary gland adipocytes is altered in MMP-11-/- mice

Previously (see chapter 2, part I), I took advantage of the MMP-11-/- MEFs to study the impact of MMP-11 on adipocytes. I showed that MEFs differentiated into adipocytes and treated with active MMP-11 recombinant protein became smaller and adopted fibroblast-like spindle-cell shape. This was accompanied by cell delipidation as shown by Oil Red O staining.

To directly test the role of MMP-11 on postnatal development of the mammary

gland, I investigated the adipocyte lipid contents in vivo. I selected the inguinal #4 mammary gland from 4-, 6- and 12-week-old littermate wild-type and MMP-11-/- mice. Interestingly, the size of lipid droplets in MMP-11-/- mammary gland were dramatically larger than in wild-type gland, as shown by Oil Red O staining (Figure 3.13). These results further confirm that MMP-11 reduces adipocyte differentiation.

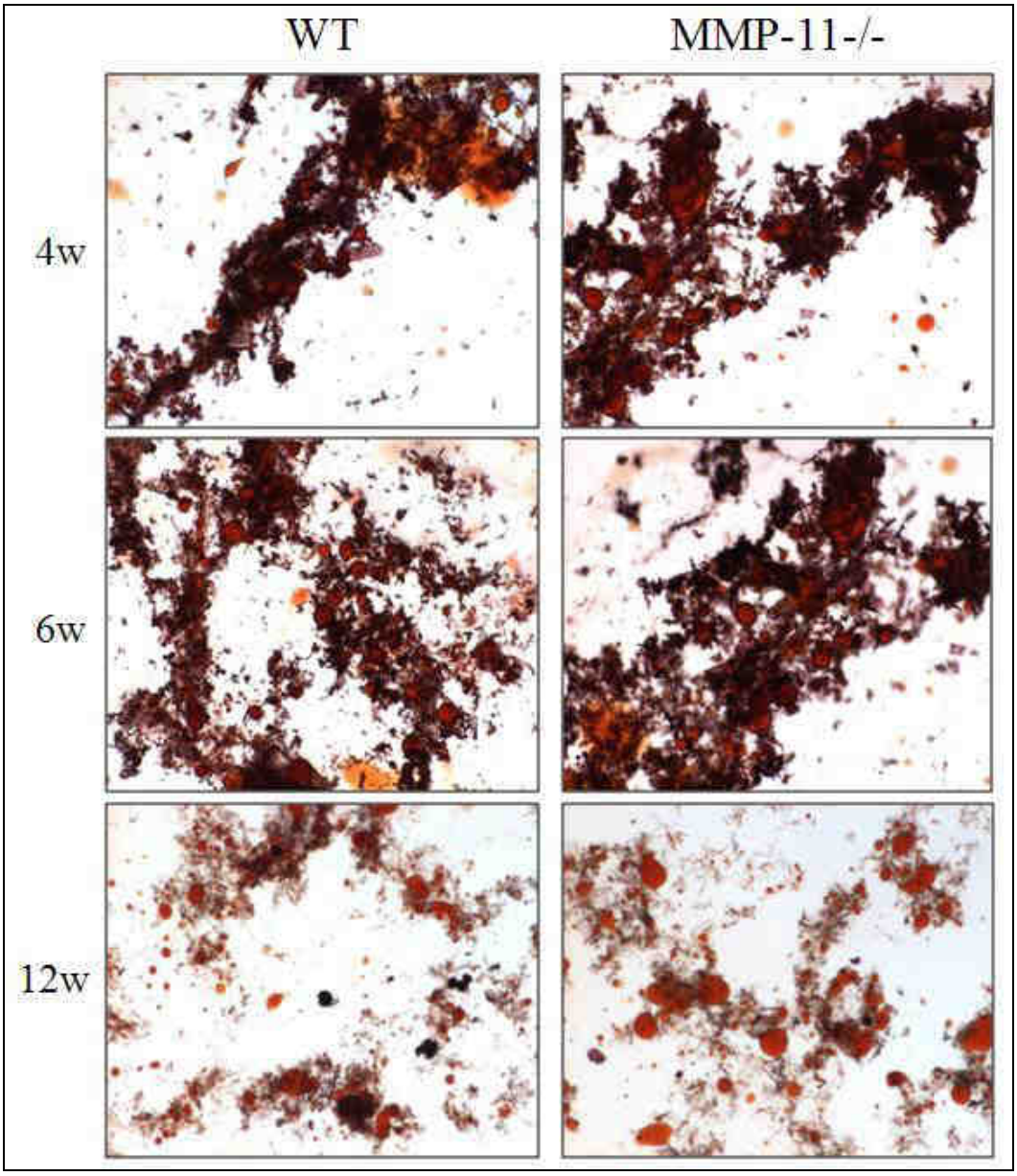

Figure 3.13 Oil Red O staining of wild-type and MMP-11-/- mammary gland. At 4, 6 and 12 weeks old, compared with wild-type, the size of lipid droplets are dramatically increased in MMP-11-/- mammary gland. Original magnification: X10.

Finally, to further study the difference between wild-type and MMP-11-/- adipocytes, I isolated adipocytes from mammary gland of 12-week-old littermate

mice, cultured them in vitro for 3 days, and then stained them with Oil Red O. Compared with wild-type, the size of lipid droplets were increased dramatically when adipocytes were isolated from MMP-11-/- gland (Figure 3.14).

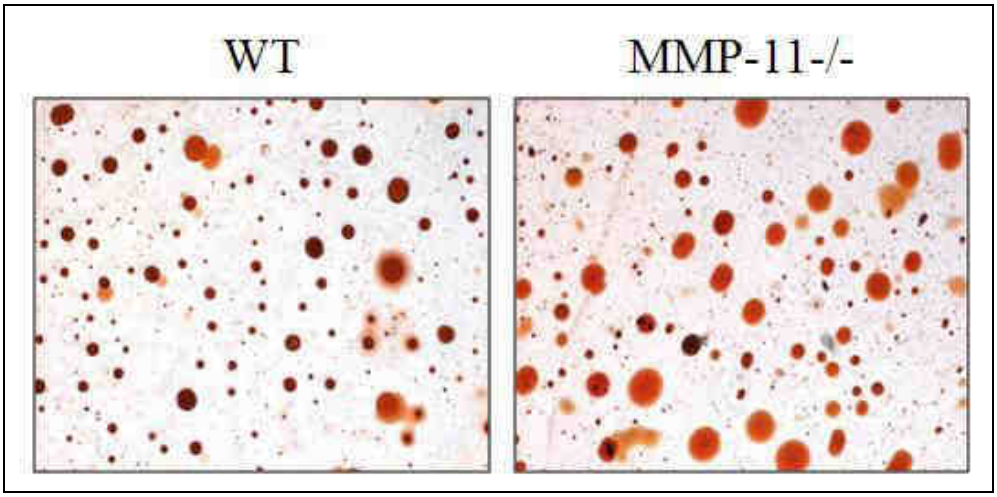

Figure 3.14 Oil Red O staining of adipocytes isolated from wild-type and MMP-11-/- mammary glands. Compared with wild-type, the number and size of lipid droplets are increased dramatically in MMP-11-/- adipocytes. Original magnification: X10.

These results indicated that the lack of MMP-11 leads to accumulation of lipids into the mammary gland, which might impair postnatal development of the epithelial structure of the mammary gland.

2.2.6 MMP-11-/- mammary gland stroma is unfavorable for ductal morphogenesis

To further study whether the MMP-11-/- epithelia have a priori defect in forming stable ductal structure, or whether MMP-11-/- stroma is unfavorable for ductal branching morphogenesis, I have performed reciprocal mammary early epithelial transplantation experiments as previously reported (Ucar et al., 2010; Khialeeva et al., 2011).

I transplanted mammary epithelial ducts from 3-week-old pre-pubertal MMP-11-/- mice into cleared fat pads of littermate wild-type mice, and vice versa (Figure 3.15). Then I analyzed the transplants for ductal outgrowth 3, 6 and 9 weeks after transplantation, and ductal structure functional differentiation at the first day of

lactation in mice mated at 9 weeks after transplantation.

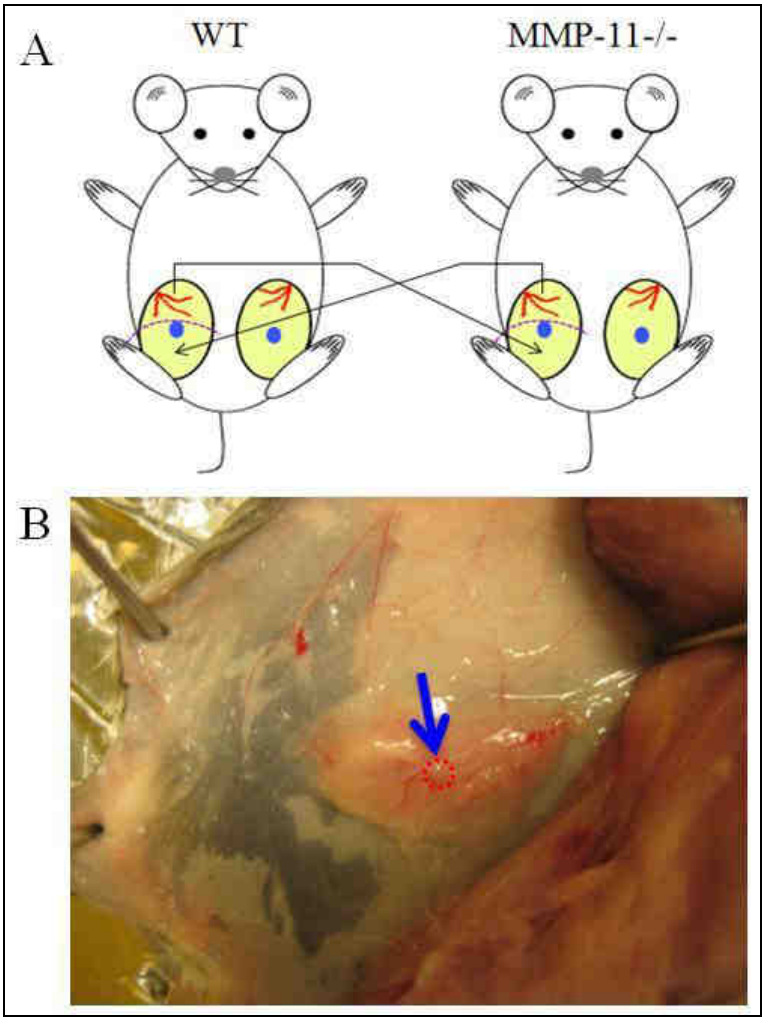

Figure 3.15 Mammary epithelial transplantation. A: The strategy of the mammary epithelial transplantation. The #4 inguinal glands of 3-week-old mice are shown together with rudimentary epithelial tree (red) in the proximal region close to the nipple area. The location of the cuts for clearing the fat pads is shown as dashed line (purple) near the lymph node (blue point). The arrows show the origin of transplants and the location to which they were transplanted. B: The transplanted mammary epithelium. The arrow and red dotted line show the location of transplant in the host cleared fat pad.

Three weeks after the transplantation, the pre-pubertal MMP-11-/- mammary epithelia transplanted into the cleared wild-type fat pad formed more TEBs and ducts than pre-pubertal wild-type mammary epithelia transplanted into MMP-11-/- cleared fat pads. Moreover, the length of ducts were also longer than wild-type mammary epithelia transplanted into cleared MMP-11-/- fat pads (Figure 3.16 A and B). Meanwhile, in the control glands (the other side non-operated #4 glands), the number of TEBs and ducts in wild-type glands were higher than in the MMP-11-/- glands

(Figure 3.16 C and D), which are in accord with previous results (Figure 3.4).

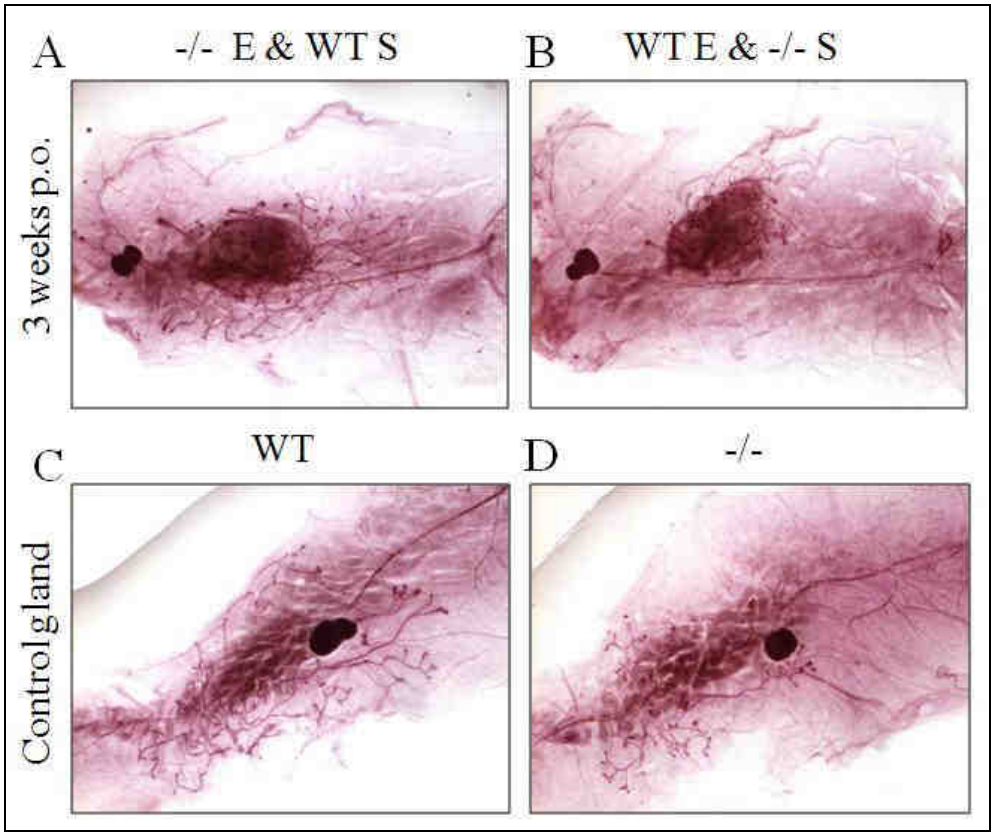

Figure 3.16 Mammary gland development three weeks after mammary epithelial transplantation using whole-mount staining. A: MMP-11-/- epithelia (−/− E) formed TEBs and underwent proper ductal outgrowth within the wild-type fat pad stroma (WT S). B: By contrast, wild-type epithelia (WT E) generated a lower number of TEBs and ducts in MMP-11-/- fat pad stroma (−/− S). The potential of duct invasion in the MMP-11-/- fat pad stroma was weaker also. C and D: In the control glands (the other side non-operated #4 glands), the number of TEBs and ducts of the wild-type glands were obviously higher than in the MMP-11-/- glands. p.o: post-transplantation. Original magnification: X5.

Six weeks after transplantation, similarly, the pre-pubertal MMP-11-/- mammary epithelia transplanted into the cleared wild-type fat pad, developed more than pre-pubertal wild-type mammary epithelia transplanted into cleared MMP-11-/- fat pads. Then, the length and the number of ducts, as well as the number of TEBs were higher (Figure 3.17 A and B). As expected, the wild-type control glands were more developed than the MMP-11-/- control glands (Figure 3.17 C and D).

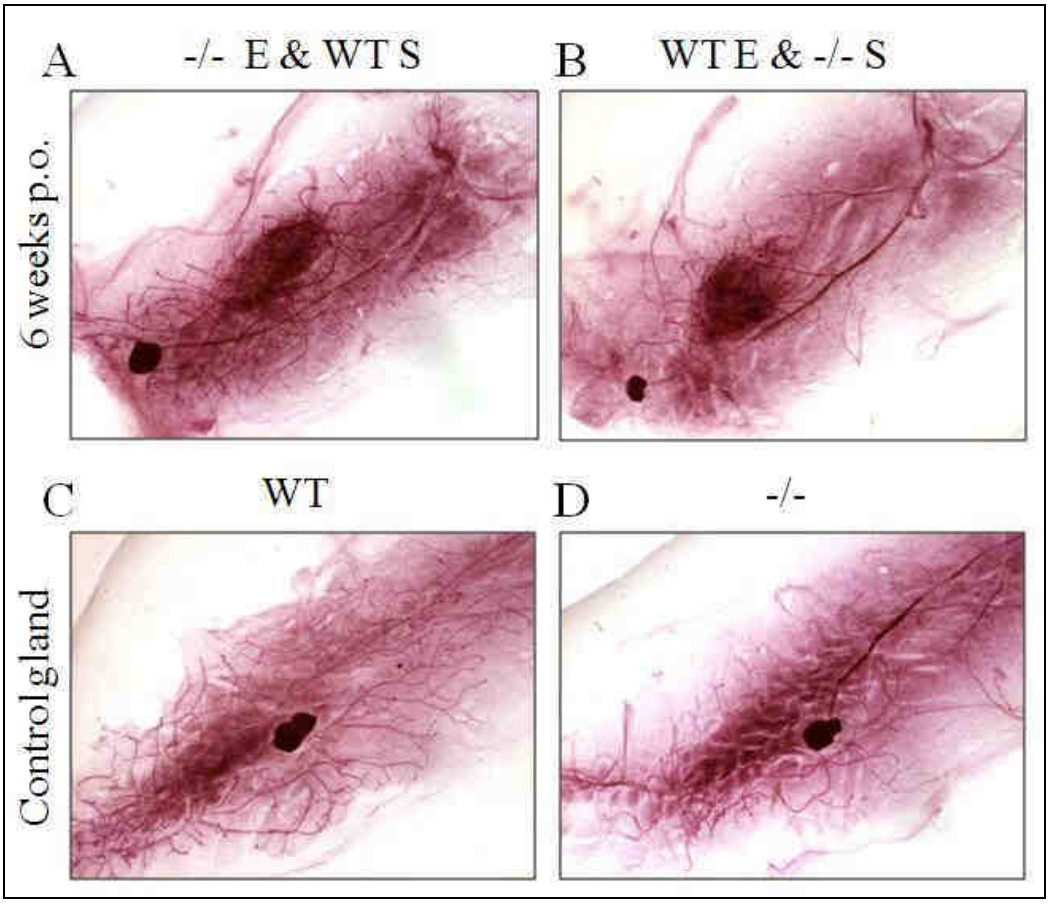

Figure 3.17 Mammary gland development six weeks after mammary epithelial transplantation using whole-mount staining. A: MMP-11-/- epithelia (−/− E) underwent proper ductal outgrowth within the wild-type fat pad stroma (WT S). B: By contrast, wild-type epithelia (WT E) generated a lower number of ducts in MMP-11-/- fat pad stroma (−/− S). The potential of duct invasion in the MMP-11-/- fat pad stroma was weaker also. C and D: In the control glands (other side non-operated of #4 glands), the wild-type glands were more developed than MMP-11-/- glands. p.o: post-transplantation. Original magnification: X5.

Nine weeks after transplantation, the pre-pubertal MMP-11-/- mammary epithelia transplanted into the cleared wild-type fat pad has formed numerous ducts, that invade the whole fat pad (Figure 3.18 A). By contrast, pre-pubertal wild-type mammary epithelia transplanted into cleared MMP-11-/- fat pads has formed sparse ducts, and did not invade the whole fat pad (Figure 3.18 B). The number of ducts in wild-type control gland are higher than in MMP-11-/- gland, and the ductal tree in wild-type almost reached the end of fat pad, whereas, the MMP11-/- ductal structure did not reach the border of fat pad.

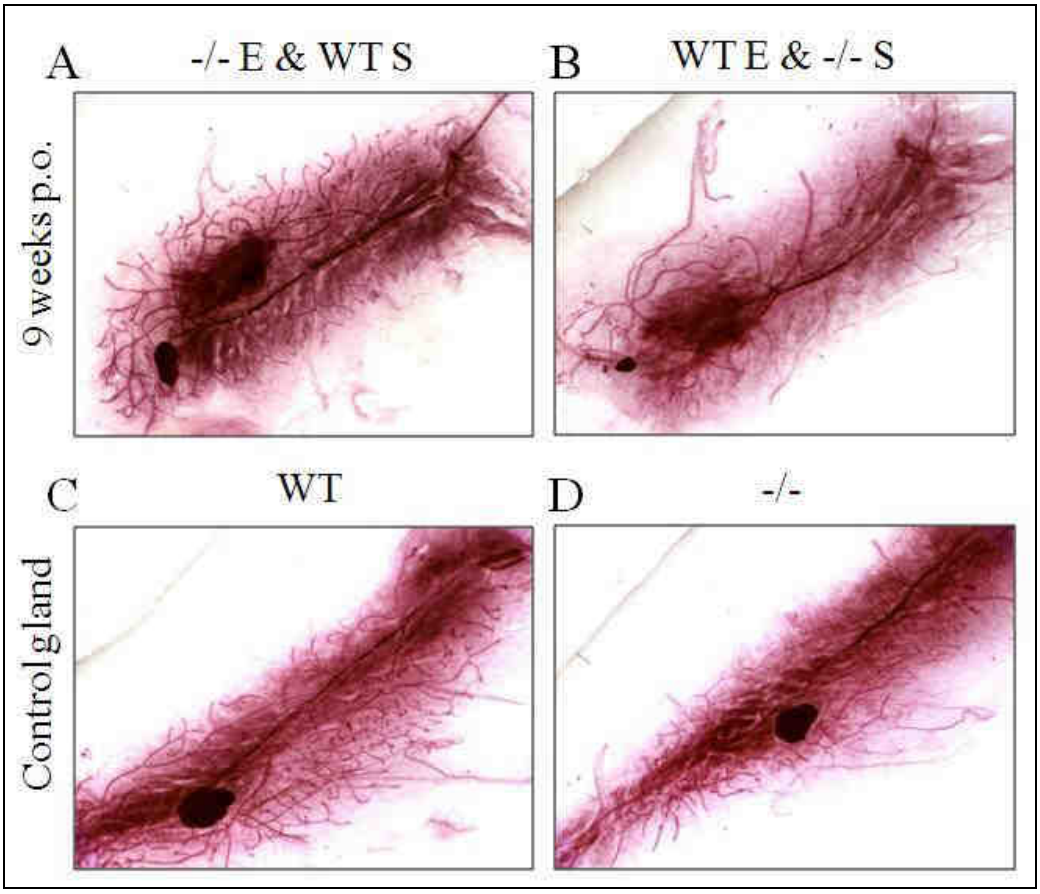

Figure 3.18 Mammary gland development nine weeks after mammary epithelial transplantation using whole-mount staining. A: MMP-11-/- epithelia (−/− E) underwent proper ductal outgrowth within the wild-type fat pad stroma (WT S), the ductal tree almost reached the fat pad border. B: By contrast, wild-type epithelia (WT E) generated a lower number of ducts when implanted in MMP-11-/- fat pad stroma (−/− S). C and D: In the control glands (other side non-operated #4 glands), the mammary glands development were higher for the wild-type glands than the MMP-11-/- glands. p.o: post-transplantation. Original magnification: X5.

Finally, we have investigated whether the fat pad of MMP-11-/- mammary gland affects ductal structure functional differentiation. Alveolar differentiation was studied using transplanted mice mated at nine weeks after operation. Euthanasia was performed within the first day lactation, and transplants and control glands were analyzed. Both the MMP-11-/- mammary epithelia transplanted into the wild-type fat pad, and wild-type mammary epithelia transplanted into MMP-11-/- fat pad developed alveolar structures (Figure 3.19 A and B). However, MMP-11-/- mammary epithelia occupied the whole wild-type fat pad, whereas wild-type mammary epithelia were restricted to a limited regions located around the transplantation site into the MMP-11-/- fat pad (Figure 3.19 A and B). Compared with wild-type control gland,

alveolar density was reduced in MMP-11-/- control gland (Figure 3.19 C and D), in accord with previous results (Figure 3.6 B).

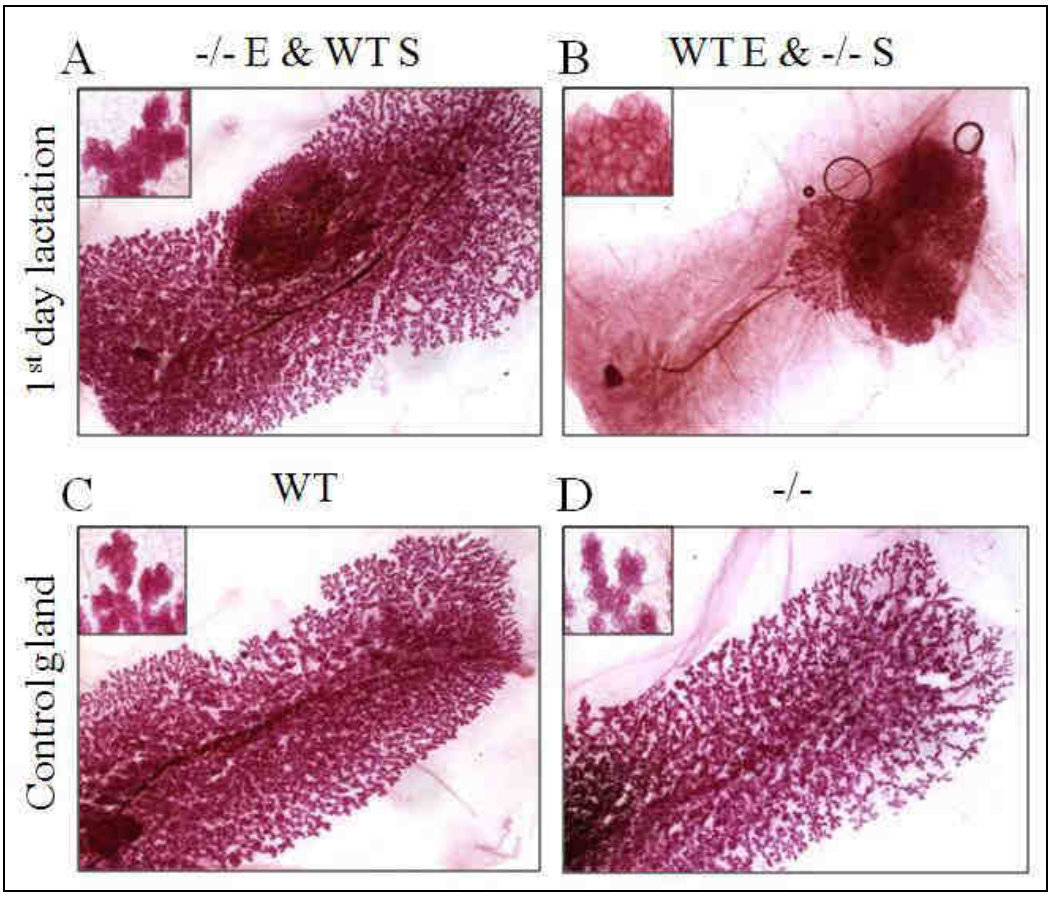

Figure 3.19 Analysis of the alveolar differentiation after mammary epithelial transplantation using whole-mount staining. A: pre-pubertal MMP-11-/- mammary epithelia (−/− E) transplanted into the cleared wild-type fat pad (WT S), exhibited a fully differentiated alveolar phenotype. B: pre-pubertal wild-type mammary epithelia (WT E) transplanted into cleared MMP-11-/- fat pad (−/− S), showed reduced alveolar differentiation. C and D: Compared with wild-type control glands, the density of alveoli was reduced in MMP-11-/- control glands. Original magnification: X5; The insertion original magnification: X80.

These results indicated that the MMP-11-/- epithelia have no obvious structural defects or inherent functional deficiencies, since they can form normal TEBs, achieve normal ductal branching morphogenesis and differentiate into functional alveoli when transplanted into wild-type fat pad. However, the wild-type epithelia transplanted into cleared MMP-11-/- fat pads showed impaired ductal outgrowth and differentiation, indicating that the lack of MMP-11 in MMP-11-/- mice, either in the mammary stroma or systemically since MMP-11 is a secreted protein, is the primary cause of these ductal defects.

Thus, to find out whether the MMP-11-dependent systemic processes are involved in ductal morphogenesis, I performed whole mammary gland transplantation experiments as previously reported (Moraes et al., 2009; Ucar et al., 2010).

From 3-week-old donor mice (wild-type or MMP-11-/-) into 3-week-old wild-type and MMP-11-/- recipient mice (Figure 3.20), and analyzed them at 3, 6, 9 weeks after transplantation for ductal outgrowth, and ductal structure functional differentiation after pregnancy 9 weeks after transplantation.

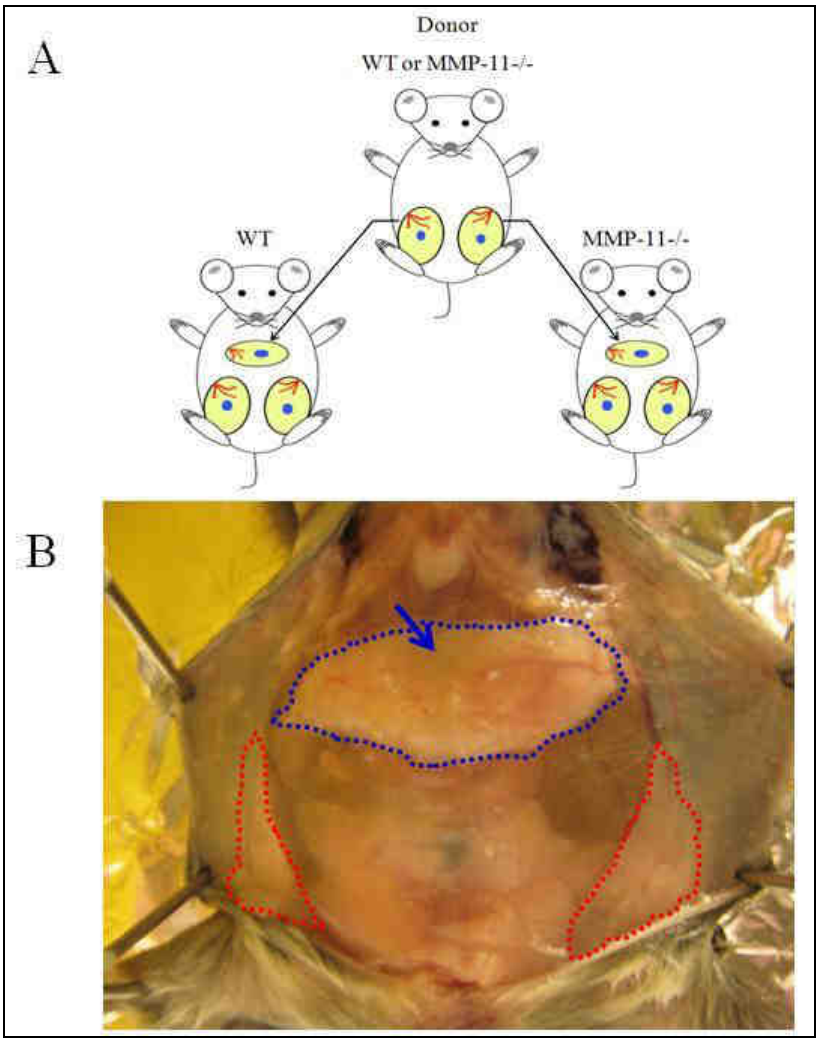

Figure 3.20 Whole mammary gland transplantation. A: The two #4 inguinal glands of donor (wild-type or MMP-11-/-) were transplanted into wild-type or MMP-11-/- recipient mice. The arrows show the origin and location of transplants. B: The transplants were placed in the upper abdomen in a perpendicular orientation to the endogenous inguinal glands. The blue arrow and dotted line show the location of transplant; the red dotted lines indicate control #4 inguinal glands.

After being transplanted into either MMP-11-/- or wild-type host mice, the

wild-type transplant contained proper TEBs and ductal outgrowth, which eventually covered the whole gland with epithelial ducts (Figure 3.21 A1, A2, B1, B2, C1 and C2), they also developed proper alveolar structures during pregnancy (Figure 3.21 D1 and D2). Thus, the development of the wild-type transplants have no distinct difference depending on their transplantation into MMP-11-/- or wild-type recipient mice. However, in the control glands, the number of TEBs and ducts in wild-type glands were higher than MMP-11-/- glands, and the density of ducts in wild-type glands are higher than in MMP-11-/- glands at 3 and 6 weeks post-operation (Figure 3.21 A3, A4, B3 and B4). At 9 weeks post-operation, the duct number/density of wild-type control glands are higher than in the MMP-11-/- control glands, the ductal tree in wild-type almost reached the end of fat pad, and most TEBs have disappeared (Figure 3.21 C3). However, the ductal structures in MMP-11-/- control glands were not arrived at the border of fat pad (Figure 3.21 C4). Interestingly, some TEBs were observed at the ends of some branches (Figure 3.21 C4). Finally, the density of alveoli was reduced in MMP-11-/- control glands (Figure 3.21 D3, D4), in accord with previous results (Figure 3.6 C).

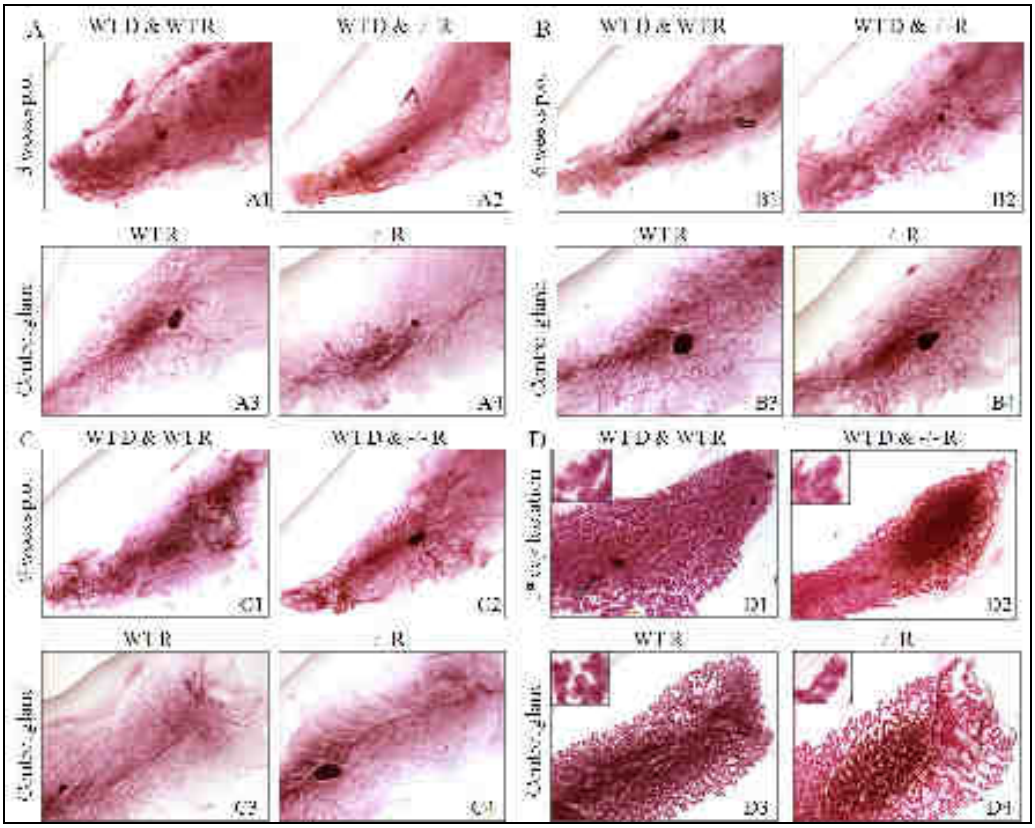

Figure 3.21 Development of whole wild-type mammary gland transplants using whole-mount staining. A-C: transplant/donor (WT D) transplanted into wild-type recipient (WT R) or MMP-11-/- recipient (-/- R) mice were analyzed at 3, 6 and 9 weeks after the operation (p.o.), respectively; D: the first day post-partum (1st day lactation). Similar TEBs and ductal outgrowth were observed after transplantion into wild-type (A1, B1 and C1) or MMP-11-/- (A2, B2 and C2) recipient mice. During pregnancy, they also developed similar alveoli structures both in WT recipient and -/- recipient mice (D1 and D2). However, in the control glands, the development of TEBs and ducts in WT recipient (A3, B3 and C3) are higher than in -/- recipient (A4, B4 and C4); Compared with wild-type, the density of alveoli was lower in -/- recipient at 1st day lactation (D3 and D4). Original magnification: X5; The insertion original magnification: X80.

These results indicate that the wild-type stroma is sufficient for correct mammary gland development, even in MMP-11-/- mice.

I therefore performed the reverse experiments using MMP-11-/- glands as transplants. I observed that ductal tree outgrowths weakly and slowly (Figure 3.22 A1, A2, B1, B2, C1 and C2), and the density of alveoli was reduced, although the epithelium could develop into alveolar structures during pregnancy (Figure 3.22 D1 and D2). The transplants have no obvious difference depending on their implantation in MMP-11-/- or in wild-type recipient mice. By contrast, as previously observed (Figure 3.3, 3.4 and 3.5), the wild-type control glands were more developed than

MMP-11-/-control glands, whatever the age of observation (Figure 3.22 A3, A4, B3, B4, C3 and C4). During pregnancy, in both wild-type and MMP-11-/- control glands, the alveolar structures developed, but alveolar density was reduced in MMP-11-/- control glands (Figure 3.22 D3 and D4).

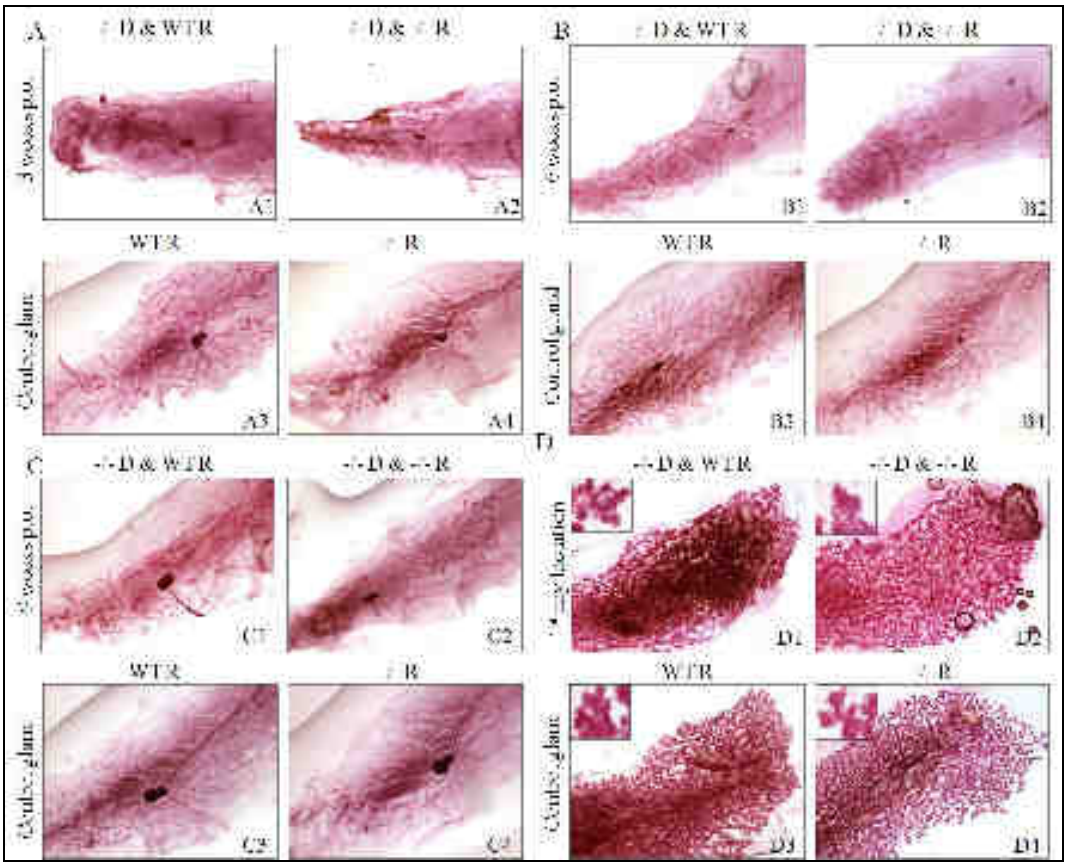

Figure 3.22 Development of whole MMP-11-/- mammary gland transplants using whole-mount staining. A-C: transplant/donor (-/- D) transplanted into wild-type recipient (WT R) or MMP-11-/- recipient (-/- R) mice, and analyzed at 3, 6 and 9 weeks after the operation (p.o.), respectively; D: the first day post-partum (1st day lactation). Transplants have some relative sparse TEBs and ductal outgrowth after being transplanted into wild-type (A1, B1 and C1) or MMP-11-/- (A2, B2 and C2) recipient mice. During pregnancy, they also developed alveolar structures both in WT recipient and -/- recipient mice (D1, D2). As expected, in the control glands, the number of TEB and duct morphogenesis are higher in wild-type than in MMP-11-/- mice (A3, A4, B3, B4, C3 and C4), as the alveoli density (D3 and D4). Original magnification: X5; The insertion original magnification: X80.

Thus, altered MMP-11-/- mammary gland development is not rescued by transplantation in wild-type mice.

Together, these results indicated that the cause of the impaired ductal branching morphogenesis phenotype observed in the MMP-11-/- mammary glands was not due

to the absence of MMP-11 at the systemic level, but at the local mammary stroma level.

2.2.7 MMP-11 promotes ductal branching morphogenesis via stromal adipocyte-related function

It has been shown in the laboratory that MMP-11 reduces adipogenesis, and induces adipocyte dedifferentiation (Andarawewa et al. 2005; Motrescu et al., 2008; Tan et al. 2011), suggesting that MMP-11 might impact ductal branching morphogenesis via adipocyte-related function. To verify this hypothesis, I performed collection of mammary gland adipocytes and cultured them in vitro (Figure 3.14). Moreover, I performed primary culture of mammary organoids isolated from mammary gland of 14-week-old virgin mice in three-dimensional gels (3D). These mammary organoids were then treated with wild-type or MMP-11-/- adipocyte-conditioned culture media without serum for 5 days, and organoids branching morphogenesis was then analyzed (Figure 3.23). In the negative controls, both wild-type and MMP-11-/- organoids were treated with basal media [DMEF/F12 with 1% ITS (insulin-transferrin-selenium) and 1% penicillin/streptomycin]. Branching was low, with only 21.7±9.2% and 19.4±4.8% of organoids developing very short branches, respectively (Figure 3.23 A and D). However, compared with negative controls, both wild-type and MMP-11-/- adipocyte culture media promoted organoid development. Wild-type adipocyte culture media induced 64.7±13.6% and 61.1±9.7% branching in wild-type and MMP-11-/- organoids, respectively. MMP-11-/- adipocyte culture media induced respectively 39.5±5.1% and 40.9±7.2% branching in wild-type and MMP-11-/- organoids (Figure 3.23 B, C and D; $p < 0.001$, $p < 0.01$; $p < 0.05$, respectively). Interestingly, although MMP-11-/- adipocyte culture medium promotes organoid branching, compared with wild-type adipocyte culture medium, its ability was weaker, not only at the quantitative level (2 fold compared to 3 fold), but also developed branches were more rare and shorter (Figure 3.23 B, C and D; $p < 0.05$).

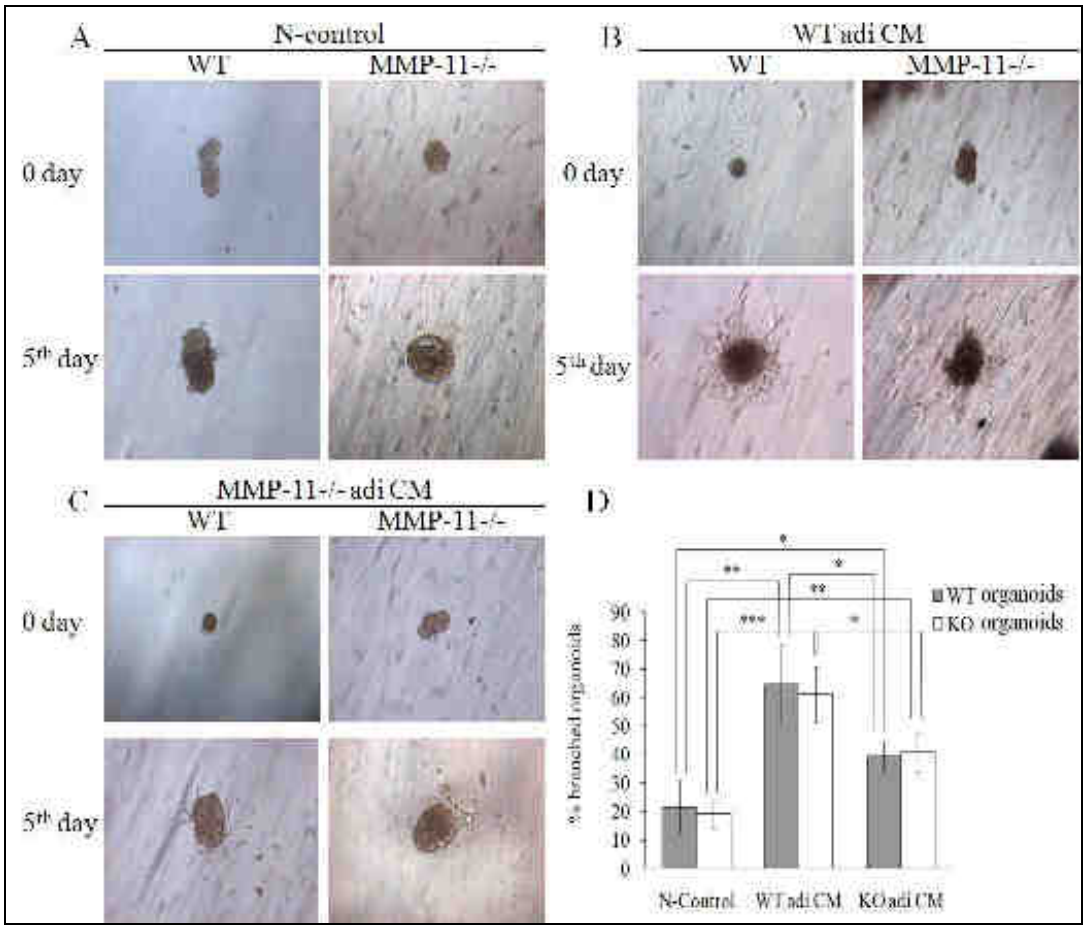

Figure 3.23 Analysis of branching morphogenesis in mammary gland organoids cultured in vitro for 5 days. A: Appearance of wild-type (WT) and MMP-11-/- primary mammary organoids (negative control). B: WT and MMP-11-/- primary mammary organoids treated with wild-type adipocyte-conditioned culture media (WT adi CM). C: WT and MMP-11-/- primary mammary organoids treated with MMP-11-/- adipocyte-conditioned culture media (MMP-11-/- adi CM). D: Quantification of the percentage of branched organoids for each treatment. The mean ± s.d. of 3 independent experiments are shown (* means $p<0.05$; ** mean $p<0.01$; *** mean $p<0.001$). Original magnification: X10.

These results showed that MMP-11-dependent adipocyte-related soluble factors promote mammary gland branching morphogenesis

Altogether, these data reveal an essential, non-redundant role for MMP-11 in mammary gland duct morphogenesis and function. It might be hypothesize that negative regulatory function of MMP-11 on adipogenesis is playing a role during postnatal mammary gland development.

Part III

The impact of MMP-11 over-expression restricted to adipocytes on mammary gland development and tumorigenesis

It has been shown that MMP-11 is a negative regulator of adipogenesis, able to reduce and even to revert mature adipocyte differentiation, which indicated that MMP-11 deficiency favors adipogenesis; The mammary gland development is impaired in MMP-11-/- mice, which indicated an essential, non-redundant role for MMP-11 in mammary ductal morphogenesis. However, one question remains open: what is the MMP-11 function strictly adipocyte-specific? So, the aim is to explore the adipogenesis and mammary gland development in transgenic mice with MMP-11 over-expression targeted in adipocytes.

I have therefore constructed JOJO-MMP-11 transgenic mouse model, allowing expression of MMP-11 specifically in adipocytes via aP2-Cre-recombinase.

2.3.1 Cleavage of JOJO vector by restriction enzyme XhoI

For conditional activation of MMP-11, I generated the constructs JOJO-MMP-11 and JOJO-MMP-11-flag (flag in C-terminus) that contain a floxed green-fluorescent-protein (GFP) stop cassette under control of the CMV/β-actin fusion promoter (Berger et al., 2007), driving ubiquitous expression of the GFP reporter gene (Figure 4.1 A).

There is only one XhoI site in the JOJO vector, and it locates between the second LoxP and IRES sequence (Figure 4.1 A). This site was used to insert the sense strand of mouse MMP-11 or MMP-11-flag.

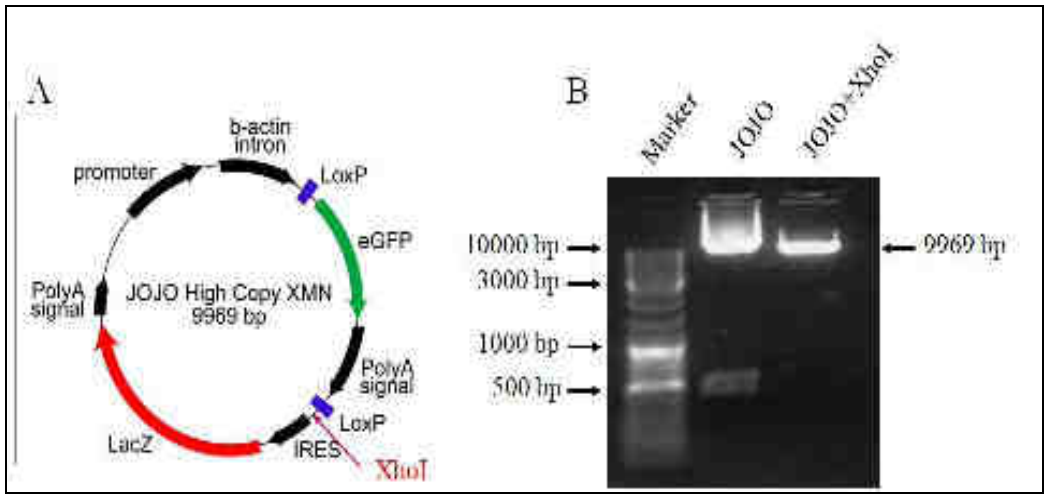

Figure 4.1 The JOJO vector architecture and cleaveage by XhoI. A: there is one XhoI site that locates between the second LoxP and IRES sequence; B: As expected, JOJO DNA is linearized by XhoI cutting.

2.3.2 The PCR products of MMP-11

The pSG5-MMP-11 plasmid (available in the laboratory) served as template DNA. It includes the full coding region of mus MMP-11 (Figure 4.2 A). Several primers containing SalI restriction site were designed: one sense primer (primer_H) was 5'-GAG GTC GAC GCC GCC ATG GCA CGG GCC GCC TGT CTC-3'; one antisense primer without flag (primer_I) was 5'-GAG GTC GAC TCA GCG GAA AGT ATT GGC AGG-3'; the another antisense primer with flag (primer_J) was 5'-CAA TTG GTC GAC TCA CTT GTC ATC GTC GTC CTT GTA ATC GCG GAA AGT ATT GGC AGG CTC-3'. As expected, the MMP-11 PCR product is 1507 bp, and the MMP-11-flag PCR product is 1528 bp (Figure 4.2 B).

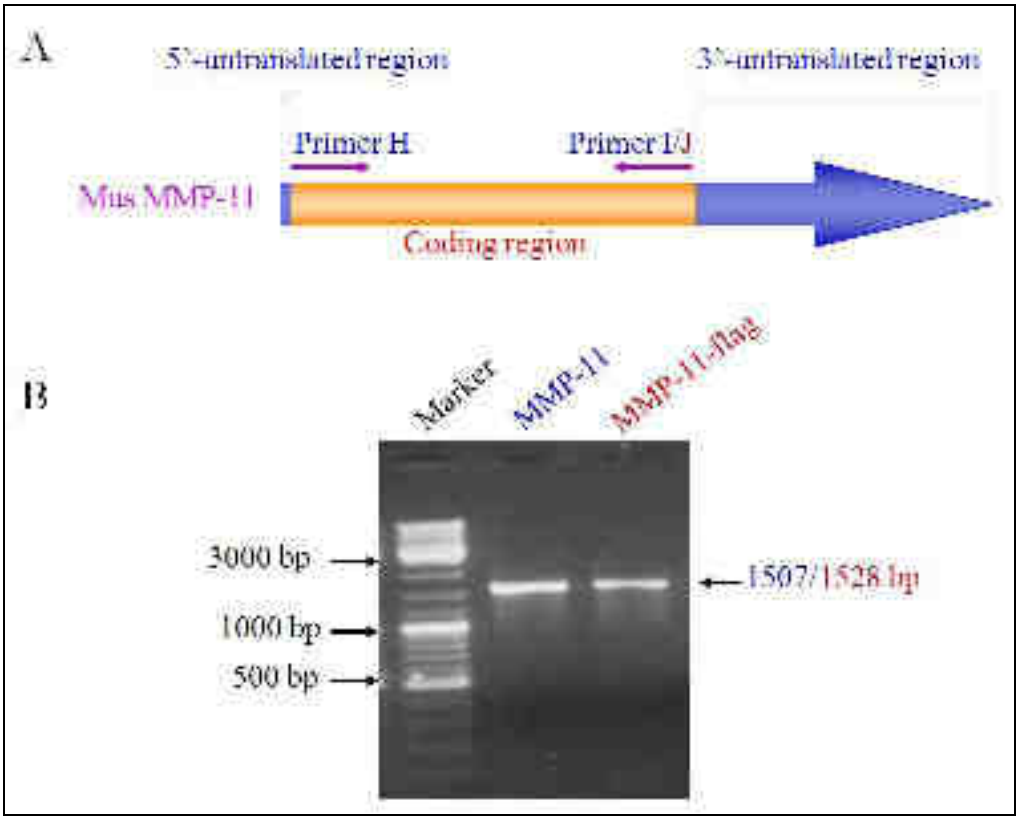

Figure 4.2 The architecture and PCR products of mouse MMP-11. A: the mus MMP-11 structure and the location of primers; B: the PCR products of MMP-11 and MMP-11-flag.

2.3.3 Semi-quantification of MMP-11 DNA and JOJO vector

The JOJO vector was cleaved by restriction enzyme XhoI, and the MMP-11 and MMP-11-flag were cleaved by SalI. Then the cleaved products were purified with « PCR clean up kit ». The standard linear GFP plasmid was used as control to semi-quantify the cleaved JOJO vector, MMP-11 and MMP-11-flag by electrophoresis (Figure 4.3). There was similar quantity among these DNA sequences (around 100 ng).

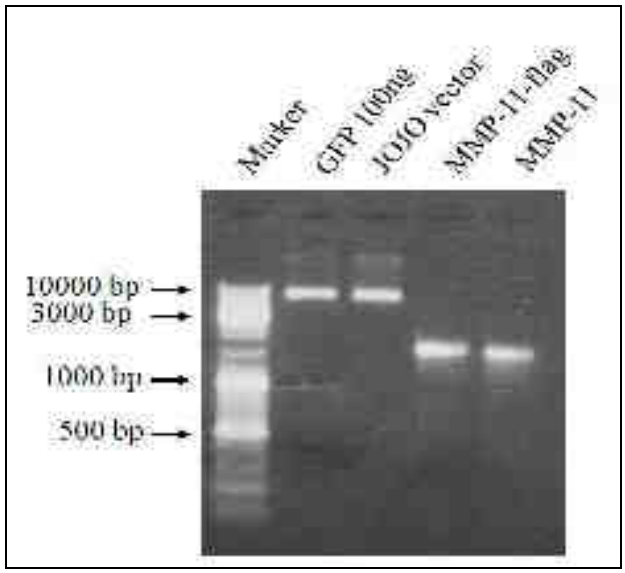

Figure 4.3 Semi-quantification of the cleaved JOJO vector, MMP-11 and MMP-11-flag by electrophoresis. The standard linear GFP plasmid served as control. Cleaved JOJO vector, MMP-11 and MMP-11-flag PCR products were in similar quantity.

2.3.4 Construction of JOJO-MMP-11 and JOJO-MMP-11-flag plasmids

Purified MMP-11 or MMP-11-flag cleavage were linked with the cleaved JOJO vector using T4 ligase (Figure 4.4 A). There were three possibilities during MMP-11/MMP-11-flag insertion into the JOJO vector : either MMP-11/ MMP-11-flag did not link with JOJO vector (Figure 4.4 B1) ; or MMP-11/ MMP-11-flag links with JOJO vector via antisense strand (Figure 4.4 B2), MMP-11/MMP-11-flag can not translate protein under this condition ; or MMP-11/MMP-11-flag links with JOJO vector by sense strand (Figure 4.4 B3), under this condition, MMP-11/MMP-11-flag can translate protein. This last form corresponds to the correct plasmid.

After insertion of MMP-11/MMP-11-flag into the JOJO vector, the JOJO-MMP-11/MMP-11-flag plasmids were cleaved by BamHI restriction enzyme (Figure 4.4 B), and different clones were analyzed by electrophoresis (Figure 4.4 C and D). Gel analysis showed that the clones loaded in lanes 8 and 9 correspond to correct plasmids since they exhibited a size of 1745 and 1769 bp (Figure 4.4 C and D).

These clones were then confirmed by sequence analysis (data not shown). I selected these clones for following experiments.

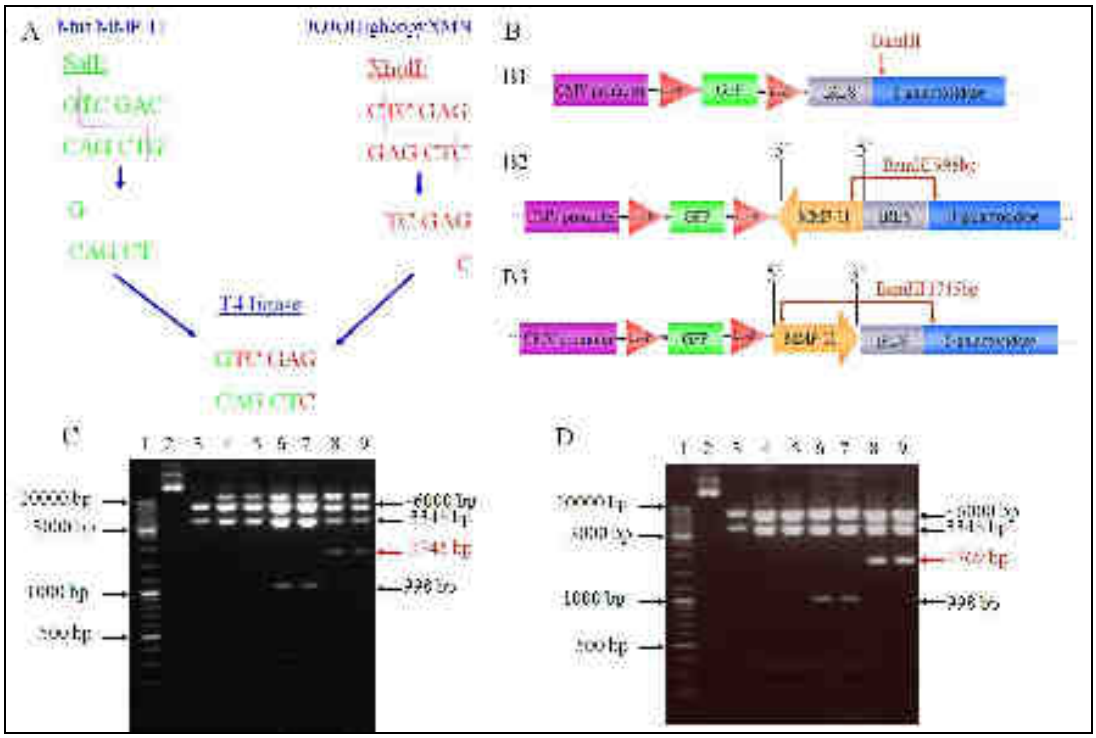

Figure 4.4 Analysis of different clones from MMP-11 and MMP-11-flag subcloning. A: cleavage of MMP-11 and MMP-11-flag was by SalI ; cleavage of JOJO vector was by XholI; linkage was with T4 ligase. B: various possibilities: B1: MMP-11/MMP-11-flag are not linked with JOJO vector; B2: MMP-11/MMP-11-flag are linked with JOJO vector, but in antisense; B3: MMP-11/MMP-11-flag are linked with JOJO vector in sense. C and D: electrophoresis analysis of different clones from JOJO-MMP-11 (C) and JOJO-MMP-11-flag (D) after BamHI digestion. 1: marker; 2: empty JOJO vector; 3: empty JOJO vector cleaved with BamHI; 4,5: clones containing no MMP-11/MMP-11-flag insert; 6,7: clones containing antisense MMP-11/MMP-11-flag; 8,9: clones containing sense MMP-11/MMP-11-flag.

2.3.5 Validation of the JOJO-MMP-11 and JOJO-MMP-11-flag plasmids

Upon Cre recombinase function, the GFP-stop cassette is excised, leading to simultaneous expression of MMP-11 or MMP-11-flag and of a second reporter, β-galactosidase/LacZ, via an IRES sequence (Figure 4.5 A).

In order to test the recombination of the integrated constructs, the plasmids were co-transfected into Hela cell with pSG5-Cre-recombinase plasmid. I checked GFP, MMP-11, MMP-11-flag, β-galactosidase and the internal control Lasp-1 expression

with western blots using appropriate antibodies (see materials and methods) (Figure 4.5 B). We can see that there are some levels of GFP expression after Hela transfection with JOJO empty vector, JOJO-MMP-11 or JOJO-MMP-11-flag alone, but no β-galactosidase, MMP-11 and MMP-11-flag expression. When JOJO empty vector was co-transfected with pSG5-Cre plasmid, the β-galactosidase was expressed accompanied with GFP decrease or disappearance, which indicates that the JOJO vector is correct. Interestingly, co-transfection of JOJO-MMP-11 with pSG5-Cre plasmid led to GFP decrease, and strong activation of MMP-11 and β-galactosidase expression. Similarly, in co-transfection of JOJO-MMP-11-flag with pSG5-Cre plasmid, MMP-11-flag visualized by MMP-11 and Flag specific antibodies, and β-galactosidase were induced. These data indicate that the JOJO-MMP-11 and JOJO-MMP-11-flag plasmids are available for conditional expression of MMP-11.

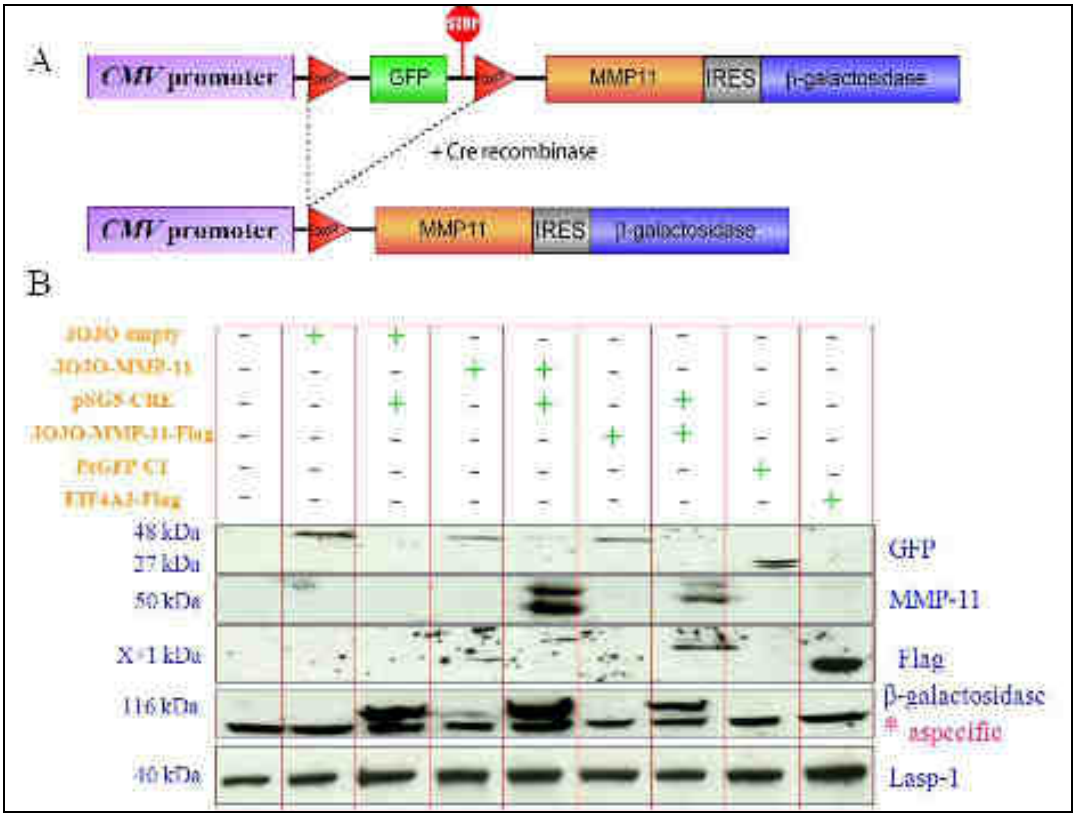

Figure 4.5 Induction of MMP-11 and MMP-11-flag expression via Cre recombinase. A: scheme of induction of MMP-11 expression, upon Cre recombination: the GFP-stop cassette is excised leading to simultaneous expression of MMP-11 and a second reporter, β-galactosidase via an IRES sequence. B: western blot analysis of GFP, β-galactosidase, MMP-11 and MMP-11-flag expression. Lasp-1 severs as loading control.

2.3.6 Linearization of JOJO-MMP-11 and JOJO-MMP-11-flag plasmids

There are two cleavage sites for restriction enzyme SalI in JOJO vector (Figure 4.6 A), which can keep all components from CMV/β-actin promoter to β-galactosidase (LacZ), without cutting MMP-11 or MMP-11-flag. So, I selected SalI to cleave and linearize JOJO-MMP-11 and JOJO-MMP-11-flag plasmids. Electrophoresis analysis (Figure 4.6 B and C) showed that the enzyme cleavage was complete since only two bands were visualized. I selected the 8970 bp (JOJO-MMP-11) and 8991 bp (JOJO-MMP-11-flag) bands for purification. Control electrophoresis is presented in Figure 4.6 D: lanes 1, 2 and 3 are linear purified JOJO-MMP-11; lanes 4, 5 and 6 lanes are linear purified JOJO-MMP-11-flag; lanes 7, 8 and 9 are linear non-purified JOJO-MMP-11; lanes 10, 11 and 12 are linear non-purified JOJO-MMP-11-flag. These results indicate that the linearization and purification of JOJO-MMP-11 and JOJO-MMP-11-flag were good.

The purified JOJO-MMP-11 DNA was sent to the animal facility for generation of transgenic mice with MMP-11 over-expression.

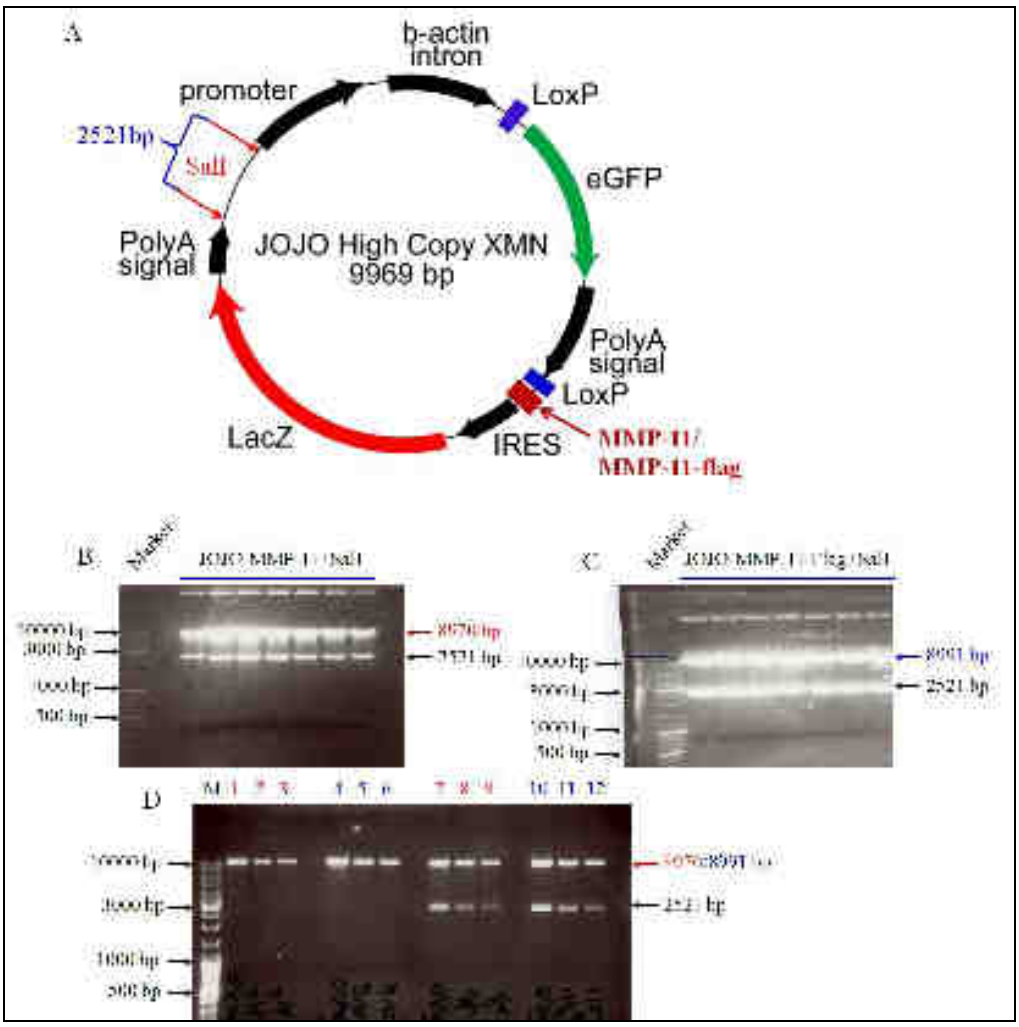

Figure 4.6 Linearization and purification of JOJO-MMP-11 and JOJO-MMP-11-flag. A: localization of the two cleavage sites for SalI restriction enzyme in JOJO vector; B and C: linearization of JOJO-MMP-11 and JOJO-MMP-11-flag by SalI, respectively. D: purification of 8970 bp (JOJO-MMP-11) and 8991 bp (JOJO-MMP-11-flag) bands. lanes 1, 2 and 3 are linear JOJO-MMP-11 purification; lanes 4, 5 and 6 are linear JOJO-MMP-11-flag purification; lanes 7, 8 and 9 are linear JOJO-MMP-11 non-purified control; lanes 10, 11 and 12 are linear JOJO-MMP-11-flag non-purified control.

2.3.7 Identification of GFP expression and genotyping of JOJO-MMP-11 transgenic mice

The JOJO-MMP-11 transgenic mouse tails were cut and checked for GFP expression under fluorescence microscope (Figure 4.7 A). There was no green fluorescence in the tail tissue of wild-type mouse (Figure 4.7 A1). As expected, the tail of JOJO-MMP-11 transgenic mice strongly expressed GFP (Figure 4.7 A2). To further identify the genotype of JOJO-MMP-11 transgenic mice, the genomic DNA

was extracted from tail tissue. I designed two primers that locate in different exons of mouse MMP-11 gene, the sense primer (primer_K: 5'-CCG AAG GGG CAT CCA GCA CC-3') located in exon 5, and the antisense primer (primer_L: 5'-GCA TCC ACA GGG CTG GGC AG-3') located in exon 6; there is an intron (120 bp) between these two exons. Because the JOJO-MMP-11 transgenic DNA sequence only contains the coding region (exons) of MMP-11, the PCR product is 288 bp. In wild-type, however, the intron (120 bp) is present and the PCR product is therefore 408 bp (Figure 4.7 B). These data indicated that the JOJO-MMP-11 transgenic mice are correct.

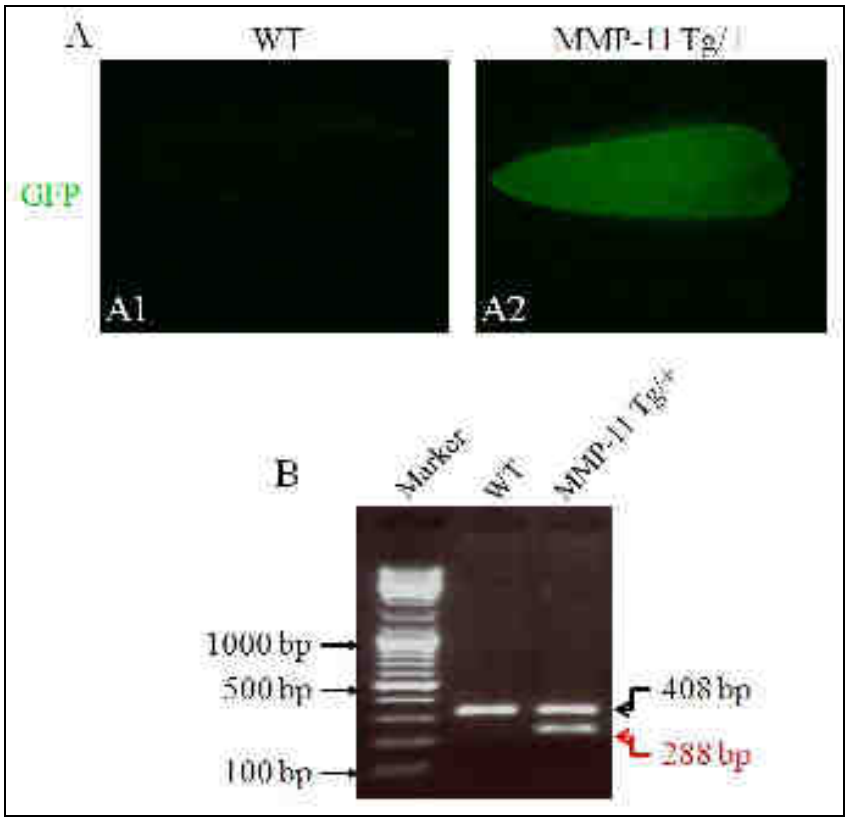

Figure 4.7 Identification of JOJO-MMP-11 transgenic mice. A: Identification of green fluorescence (GFP expression) in tail tissue under fluorescence microscope; A1: wild-type; A2: JOJO-MMP-11 transgenic mouse (MMP-11 Tg/+). B: Identification of genotype with PCR.

2.3.8 Obtention of JOJO-MMP-11-aP2-Cre-ER^{T2} co-transgenic mice

The strategy of conditional MMP-11 transgenic mice is based on the Cre/LoxP system. The transgenic mice expressing the conditional Cre-ER^{T2} recombinase

(Cre-ER^{T2}/fusion protein between the Cre recombinase and a mutated ligand-binding domain of the human estrogen receptor) selectively in adipocytes were obtained by using the aP2 promoter (Imai et al., 2001), whose activity is induced by anti-estrogens such as Tamoxifen (Tam). The aP2-Cre-ER^{T2} transcripts were found specifically in adipose tissues upon Tam treatment (Imai et al., 2001).

The aP2-Cre-ER^{T2} transgenic mice were obtained from IGBMC (*Daniel Metzger's* team), they are of same genetic background (C57Bl/6NTac) as JOJO-MMP-11 transgenic mice. I got JOJO-MMP-11-aP2-Cre-ER^{T2} co-transgenic mice via aP2-Cre-ER^{T2} crossing with JOJO-MMP-11 transgenic mice. These mice were genotyped using MMP-11 primers (see Figure 4.7) and Cre primers (see materials and methods) with PCR (Figure 4.8).

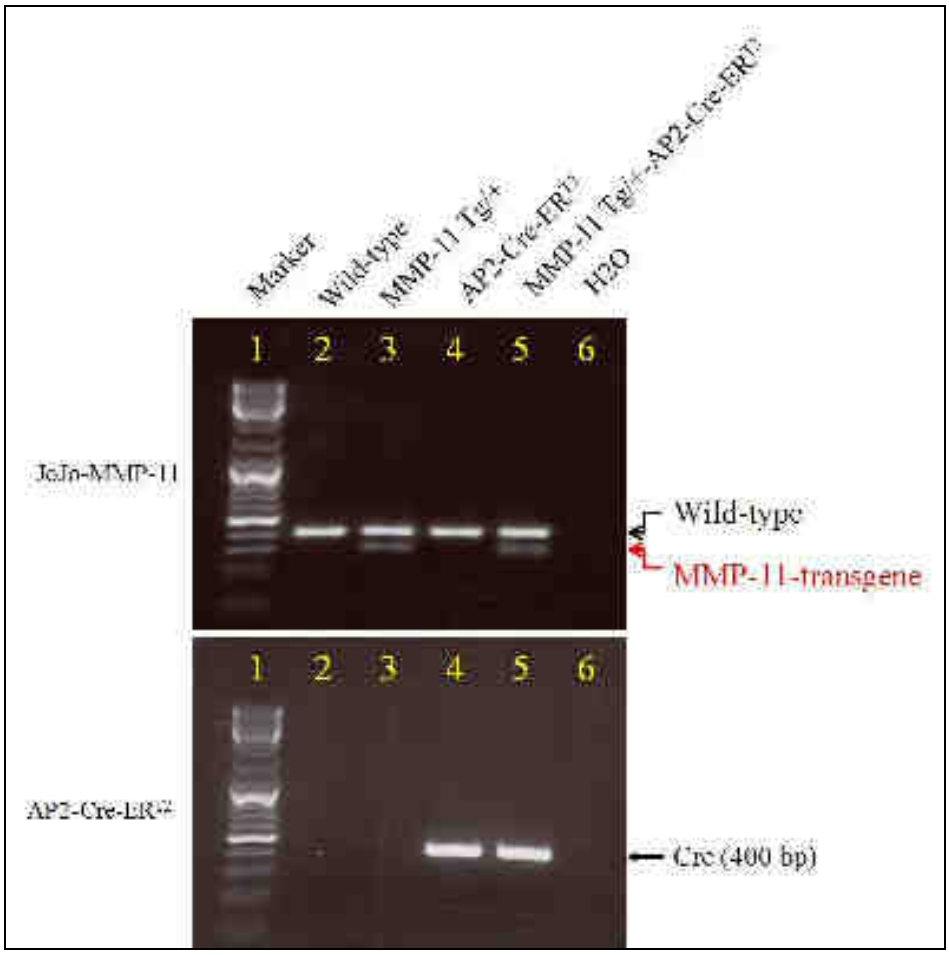

Figure 4.8 Identification of genotype for JOJO-MMP-11 crossed with aP2-Cre-ER^{T2} transgenic mice with PCR. Lane 1: maker; lane 2: wild-type; lane 3: JOJO-MMP-11 transgenic mouse (MMP-11 Tg/+); lane 4: aP2-Cre transgenic mouse (aP2-Cre-ER^{T2}); lane 5: JOJO-MMP-11 and aP2-Cre-ER^{T2} co-transgenic mouse (MMP-11 Tg/+-aP2-Cre-ER^{T2}); lane 6: control H_2O.

In the next work, the Cre recombinase will specifically be expressed in adipocytes of JOJO-MMP-11-aP2-Cre-ER^{T2} co-transgenic mice by Tam treatment, which will permit to specifically express MMP-11 in the same cell type. Then, these new mouse model should allow to study specifically the role of MMP-11 expressed by the adipocytes in both physiological and pathological conditions.

Chapter 3 Conclusion, Discussion and Perspective

My PhD data bring new insights on MMP-11 function, especially in the mammary gland development.

3.1 MMP-11 induces MEF-adipocyte dedifferentiation in vitro

Recently, more and more researches indicated that adipocytes participate in cancer progression (Andarawewa et al., 2005; Motrescu and Rio, 2008; Nieman et al., 2011; Dirat et al., 2011; Carter and Church, 2012) and mammary gland development (Couldrey et al., 2002; Landskroner-Eiger et al., 2010; Pavlorich et al., 2010; Ching et al., 2011). MMP-11 is involved in both processes. MMP-11 has been shown to be expressed by non-malignant peritumoral fibroblast-like cells and adipocytes in breast cancers (Basset et al., 1997; Andarawewa et al., 2005). Clinical trials showed that high levels of MMP-11 expression correlate with poor prognosis in patients with breast cancer (Chenard et al., 1996; Basset et al., 1997). MMP-11 is one of the factors often found in association with tumor invasion using high-throughput approaches (Peruzzi et al., 2009; Ma et al., 2009).

In this work, I first study MMP-11 function in vitro using MMP-11-/- MEFs. I found that treated with active MMP-11 recombinant protein, the number of adipocyte-differentiated MEFs was decreased, their size became smaller, and cell profile no longer seemed as round as control adipocytes, but instead adopted a more fibroblast-like spindle-cell shape. This was accompanied by delipidation since I observed decreased number and size of lipid droplets, as shown by Oil Red O staining. To test if this MMP-11 function was dependent on its enzymatic activity, similar experiments were done using an inactive recombinant MMP-11 form. This inactive MMP-11 form was unable to induce MEF adipocyte dedifferentiation. These results indicated that MMP-11 enzymatic activity is required in adipocyte dedifferentiation, in accord with previous data from the laboratory (Andarawewa et al., 2005; Motrescu et al., 2008). It has been reported that MMP-11 induces adipocyte dedifferentiation via down-regulation of peroxisome proliferator activated receptor gamma (PPARγ)

and adipocyte protein 2 (aP2) expression (Andarawewa et al., 2005). PPARγ is a crucial factor to regulate development of the adipose lineage in response to endogenous lipid activators, and serve to link the process of adipocyte differentiation to systemic lipid metabolism (Rosen et al., 1999; Zhang et al., 2012); aP2 is a carrier protein for fatty acids that is primarily expressed in adipocytes and macrophages (Maeda et al., 2005).

Several other MMP members are involved in adipogenesis. For example, it has been indicated that MMP-14 contributes to the coordination of adipocyte differentiation. Indeed, normal adipocyte maturation requires a burst in MMP-14-mediated proteolysis that modulates pericellular collagen rigidity in a fashion that controls adipogenesis, as the absence of MMP-14 aborts adipose tissue development resulting in lipodystrophic null mice (Chun et al., 2006). Moreover, MMP14-dependent collagenolysis plays a major role in regulating adipogenic histone marks by releasing the epigenetic constraints imposed by fibrillar type I collagen (Sato-Kusubata et al., 2011). MMP-3 is highly expressed during mammary gland post-weaning involution. During involution, programmed cell death of the secretory epithelium takes place concomitantly with the repopulation of the mammary fat pad with adipocytes. It has been found that during post-lactational involution, mammary glands from transgenic mice that over-express TIMP-1, or mice carrying a targeted mutation of MMP-3 showed accelerated differentiation and hypertrophy of adipocytes (Alexander et al., 2001). In the adipogenic 3T3-L1 fibroblastic cells line, transcription of a number of MMPs and TIMPs (MMP-2, MMP-3, MMP-11, MMP-14, MMP-13, TIMP-1, TIMP-2 and TIMP-3) was induced in committed preadipocytes, but only differentiated adipocytes expressed an activated MMP-2 (Alexander et al., 2001). The addition of MMP inhibitors (GM6001 and TIMP-1) dramatically accelerated the accumulation of lipid during differentiation indicating that MMPs determine the rate of adipocyte differentiation during mammary gland post-lactational remodeling (Alexander et al., 2001; Kessenbrock et al., 2010).

In this context, my results in vitro further confirm that MMP-11 plays an important function during adipogenesis as a negative autocrine regulator.

3.2 MMP-11 negatively regulates adipogenesis of mouse mammary gland-associated adipocytes in vivo

MMP-11-/- mice have a significantly higher body weight than wild-type littermates in either normal diet (Andarawewa et al., 2005) or high fat diet (Lijnen et al., 2002). Here, I analyzed whether there is any difference in the mammary gland-associated adipocytes. Compared with wild-type mammary glands, I found that the size of these adipocytes as well as the size of lipid droplets, appear larger in MMP-11-/- mice, furthermore confirming that MMP-11 limits adipogenesis (Andarawewa et al., 2005; Motrescu et al., 2008; Tan et al., 2011).

These data indicate that MMP-11 participates to adipogenesis homeostasis of the mammary fat pad in vivo.

3.3 The pubertal mammary duct morphogenesis is impaired in MMP-11-/- mice

Adipocytes, which are the main stromal cells of the mammary gland, are involved in mammary gland development (Couldrey et al., 2002; Landskroner-Eiger et al., 2010; Pavlovich et al., 2010; Ching et al., 2011). Since MMP-11 plays a role in mammary gland-associated adipocytes, in this study, I have studied the postnatal mammary gland development in the presence (wild-type) or the absence of MMP-11 (MMP-11-/-). I found that ductal morphogenesis is impaired in MMP-11-/- mice, which results in reduction of alveolus density during pregnancy, and ultimately to decreased milk production. Surprisingly, there was less clear difference between wild-type and MMP-11-/- involuting glands after weaning, suggesting that MMP-11-independent processes are involved at this step. These data shows that MMP-11 provides a non-redundant function in ductal morphogenesis. In vitro organoid culture confirms that MMP-11 favors branching process.

Several other MMPs are involved in mammary gland morphogenesis. Thus, duct branching requires transient MMP activity for invasion and branch point selection. MMP-2 facilitates TEB invasion by inhibiting epithelial cell apoptosis at the start of

puberty. MMP-2-knockout mice have deficient TEB invasion but excessive lateral branching during mid-puberty. In contrast, MMP-3 induces lateral branching of ducts since mice lacking MMP-3 show defective secondary and tertiary lateral branching of ducts during mid-puberty and early pregnancy (Wiseman et al., 2003). On the other hand, mice over-expressing MMP-3 or MMP-14 have excessive side branching, precocious alveologenesis, and eventually develop mammary tumors (Ha et al., 2001 Khokha and Werb, 2011). Introduction of exogenous TIMP-1 into pubertal mammary gland, via a pellet, resulted in repressed ductal invasion (Fata et al., 1999). However, use of slow-release TIMP-containing pellets revealed distinct effects of individual TIMPs on ductal morphogenesis: TIMP-1, TIMP-3 and TIMP-4 inhibit ductal elongation whereas TIMP-2 promotes this process (Hojilla et al., 2007).

Thus, specific MMPs refine the mammary branching pattern by distinct mechanisms during mammary ductal morphogenesis. In this context, MMP-11 favors duct branching and elongation.

3.4 Mammary duct impairment in MMP-11-/- mice is not due to epithelial compartment alteration

The architectures of TEBs and ducts are playing an essential function in the overall development of the mammary gland. Since alteration of TEBs is often associated with delayed ductal outgrowth and impaired branching morphogenesis (Sternlicht et al., 2006; Kurley et al., 2012), I analyzed the cellular architecture of the pubertal mammary glands. The structure of MMP-11-/- ducts and TEBs are similar to the wild-type with the inner layer of luminal epithelium and the outer layer of myoepithelium. These results reveal that there is no defect of ducts and TEBs in the MMP-11-/- mammary gland, indicating that the observed phenotype is not due to a defect of TEBs and ducts. This was further confirm by epithelial transplantation experiment showing that MMP-11-/- transplants develop correctly in wild-type host fat pad.

These results indicate that MMP-11 has no effect on the mammary epithelium in an autocrine manner.

3.5 Mammary duct impairment in MMP-11-/- mice is due to alteration of the stromal compartment

It has been shown that the epithelial-stromal interactions are essential for the morphogenesis and functional differentiation of most organs, including the mammary gland (Nelson and Bissell, 2006; Ucar et al., 2010). The periductal stroma is mainly composed of adipocytes and collagen-rich ECM (Couldrey et al., 2002; Landskroner-Eiger et al., 2010; Ching et al., 2011). Moreover, using in vitro model, the presence of mammary fibroblasts stimulates mammary epithelial cell growth and alveolar morphogenesis via paracrine interaction between mammary epithelial cells and fibroblasts isolated from normal rats mammary gland during puberty (Darcy et al., 2000). Fibroblast-conditioned medium induces tubulogenesis and branching morphogenesis of TAC-2 normal murine mammary epithelial cells through secretion of HGF (hepatocyte growth factor) (Soriano et al., 1995 and 1998), and co-culture with fibroblasts induces branching of primary mammary organoids (Simian et al., 2001). Both soluble factors secreted by fibroblasts and fibroblast-derived modifications of the matrix compliance contribute to the regulation of epithelial cell morphogenesis (Luehr et al., 2012).

Collagen forwards ductal epithelium proliferation, and collagen breakdown and deposition at the tip is required to create an impediment that serves as a guide for TEBs bifurcation. Additionally, collagen imposed constriction, which maintains TEB bulbous nature and promotes duct morphogenesis (Hinck and Silberstein, 2005; Khokha and Werb, 2011). It has been indicated that lack of collagen deposition around duct lead to hyper-activation of the TGF-β signaling pathway (Ucar et al., 2010). However, over-expression of TGF-β in pubertal mammary gland causes impairment of ducts outgrowth and results in simplified arborization patterns of ducts (Daniel et al., 1996; Roarty and Serra, 2007). Thereby, lack of collagen impairing ductal outgrowth via activation of TGF-β signaling pathway. The mammary epithelium does not synthesize its own basement membrane. Thus, collagen I and collagen IV are expressed by stromal cells immediately surrounding the developing ductal epithelium.

Both collagens play an important role in mammary morphogenesis. The distribution of collagen I was consistent with a role in duct formation, since collagen I was strikingly abundant around mammary ducts, but was sparse around growing TEBs (Keely et al., 1995).

Both stromal adipocytes and collagen are modified in MMP-11-/- mammary gland. MMP-11 is expressed by mammary adipocytes, and compared with wild-type, MMP-11-/- mammary gland associated-adipocytes are hypertrophied. In addition, I found that periductal collagen depots of MMP-11-/- glands are dramatically reduced. It has previously been demonstrated that MMP-11 cleaves the native α3 chain of collagen VI, which is an adipocyte-related ECM component. MMP-11 is required for correct collagen VI folding and therefore for fat tissue cohesion and adipocyte function (Motrescu et al., 2008). Whether this MMP-11 function participates to pubertal mammary gland development remains to be studied. Thus, the lack of MMP-11 leads to stromal alteration especially of adipocytes and collagen. These defects have functional consequences, since wild-type ducts transplanted into MMP-11-/- fat pad fail to develop correctly.

Thus, MMP-11 not only impacts adipogenesis, but also plays a role on collagen homeostasis, favoring constitution of important periductal collagen depots. Thus, MMP-11 might positively regulate ECM stiffness and thereby favor mammary TEB and duct postnatal development as previously showed (see chapter 1: 1.2.2).

3.6 MMP-11 promotes ductal branching morphogenesis via adipocyte-related function

Previous investigations of co-culture of mammary epithelial cells and adipocytes, have found that adipocytes profoundly influence the morphology and function of mammary epithelial cells, by affecting proliferation and enhancing alveolar morphogenesis and functional differentiation (Zangani et al., 1999; Wang et al., 2009). It has been found that mammary epithelial tubules are induced to branch when embedded in adipose stroma or treated with adipocyte-conditioned medium, suggesting that the induction of branching is mediated by paracrine signaling

(Pavlovich et al., 2010).

To further identify whether MMP-11 induces ductal morphogenesis via adipocyte-related MMP-11 function, I performed collection of adipocytes from mammary glands and cultured them in vitro. Isolated MMP-11-/- adipocytes contain more lipids as shown by Oil Red O staining. I also isolated and cultured primary mammary organoids in matrigel 3D gel culture. Organoids were treated with wild-type or MMP-11-/- adipocyte-conditioned culture media in order to recapitulate in vitro the adipocyte-epithelium cross-talk occurring in vivo. Both wild-type and MMP-11-/- adipocyte culture media promote organoid branching. However, compared with wild-type adipocyte culture medium, the inducing ability of MMP-11-/- adipocyte medium was reduced as well on wild-type than on MMP-11-/- organoids.

Thus, MMP-11 promotes mammary branching. Moreover, MMP-11 impacts mammary ductal morphogenesis via its function on adipogenesis. Interestingly, it has been shown in breast cancer that MMP-11 favors cancer cell progression via a paracrine adipocyte-related function. Collectively, these data suggest that the normal MMP-11 function during pubertal mammary gland development might be subverted in malignant condition.

3.7 Perspectives

MMP-11 promotes pubertal ductal branching morphogenesis via maintaining adipose tissue and collagen homeostasis. MMP-11 might affect expression/secretion of several soluble factors, which promote TEB and duct outgrowth via paracrine signals. The type(s) of collagen(s) involved has also to be identified.

Adipocytes release various soluble factors, including adipokines, growth factors and cytokines, free fatty acids, etc. which provide growth and survival support for surrounding epithelial and cancer cells (Andarawewa et al., 2005; Tan et al., 2011, Dirat et al., 2011; Nieman et al., 2011; Carter et al., 2012). For example, it has been shown that leptin appears to be able to control the proliferation of both normal and malignant breast epithelial cells (Hu et al., 2002). The adiponectin regulates

mammary tumor development and angiogenesis, and demonstrate that vascular T-cadherin-adiponectin association may contribute to the molecular cross-talk between tumor cells and the stromal compartment in breast cancer (Hebbard et al., 2008; Landskroner-Eiger et al., 2009). It has also been indicated that absence of cytokine IL-10 reduces mouse pubertal mammary gland development (Masso-Welch et al., 2012). The nature of adipocyte-related soluble factors regulated by MMP-11 will be investigated.

It is well known that IGF-I promotes mammary gland development via IGF-I/IGF-IR signalling pathway (Richards et al., 2004; de Ostrovich et al., 2008; Cannata et al., 2010). However, the IGF-I signalling axis is further complicated by the presence of secreted, high-affinity IGF-binding protein-1 (IGFBP-1), the IGF-I/IGFBP-1 complex lead to IGF-I inactivation. Interestingly, it has been shown that MMP-11 can cleave IGFBP-1 and release bioavailable IGF-I (Manes et al., 1997). The mechanisms by which MMP-11 exerts its function seem to involve activation of IGF-I signalling and potentially MAPK and AKT pathways. Clearly, further studies are needed to confirm and investigate the impact of MMP-11 on these pathways in the mammary gland development.

Finally, to date, we know that MMP-11 favors mammary gland development. However, the MMP-11 function strictly related to adipocytes remains to be evaluated in both mammary gland development and cancer progression. So, to address these questions, I have developed transgenic mice targeting MMP-11 expression specifically into adipocytes. These mice are under characterization. They will serve in the future to study the impact of MMP-11 expression into adipocytes on: i) pubertal mammary gland development; ii) tumor development and progression by using tumor models, especially by using DMBA gavage that give rise to mammary gland and ovary tumors (Masson et al., 1998; Brasse et al., 2010).

Chapter 4 Materials and Methods

Section I Techniques related to part I results

4.1.1 MMP-11-/- mouse embryonic fibroblasts (MEFs)

MMP-11-/- mice with 129/Svj D3 genetic background have been previously generated in the laboratory (Masson et al., 1998). After crossing with MMP-11-/- males, pregnant females were sacrificed at 14.5 days after mating. The embryos were removed into 1X PBS (phosphate buffered saline). Heads serve for genomic DNA extraction to identify the genotype using PCR. After removing the whole organs and blood, the rest of bodies were minced completely with 2 ml syringe. The resulting slurry was plated in 10-cm dishes and MEFs allowed to grow to confluence in DMEM (dulbecco's modified eagle medium) with 10% FCS (fetal calf serum).

4.1.2 Extraction of genomic DNA and PCR genotyping

4.1.2.1 Extraction of genomic DNA

(1) Add 250 µl of TNES [10 mM Tris pH 7.5, 400 mM NaCl, 100 mM EDTA (ethylene diamine tetraacetic acid), 0.6% SDS (sodium dodecyl sulfonate)] and ~200 µg/ml of proteinase K to head/tail tissue, and shake overnight (O/N) at 55^{o}C;

(2) Cool at 4^{o}C for 10~20 min (minute);

(3) Add 200 µl of 5 M NaCl, vortex 15 s (second);

(4) Spin 10,000 rpm (microfuge) for 10 min;

(5) Take the supernatant, add 600 µl of cold 100% ethanol, mix up and down 10 times;

(6) Spin 12,000 rpm for 10 min;

(7) Remove the supernatant, wash with 70% ethanol 2 times;

(8) Spin 12,000 rpm for 1 min;

(9) Remove the ethanol, air dry the pellet for > 2 hr;

(10) Add 500 µl of 10:1 TE (10 mM Tris pH 7.5, 1 mM EDTA), heat at 60^{o}C for 10 min, vortex to dissolve the DNA, then store at 4^{o}C.

4.1.2.2 PCR genotyping and electrophoresis

DNA primer sequences were designed as follows: for mouse MMP-11 gene (NM_008606), there are two sense strand primers, one is primer_A: 5'-TTC TAA CAT CCC TCT GGG CTC-3' (locates in exon 6), the other is primer_B: 5'-GCC GCT TTT CTG GAT TCA TCG-3' (locates in the inserted neomycin gene), the antisense strand primer is primer_C: 5'-GTG GAA ACG CCA ATA GTC TC-3' (locates in exon 7). The wild-type (A+C) amplicon size is 332 bp; The MMP-11-/- (B+C) amplicon size is 230 bp. Thus, the heterozygote (+/-) mouse DNA give two bands.

Each PCR tube included the following mix:

(1) 19 µl H_2O;

(2) 2.5 µl buffer (100 mM Tris HCl, 500 mM KCl, 0.1% gelatin, 15 mM $MgCl_2$);

(3) 1.25 µl DMSO (dimethylsulfoxide);

(4) 0.25 µl primer_A (1 µg/µl);

(5) 0.25 µl primer_B (1 µg/µl);

(6) 0.5 µl primer_C (1 µg/µl) ;

(7) 0.5 µl Taq polymerase;

(8) 1 µl genomic DNA.

Each PCR program involved an initial step of denaturation at 94^{o}C for 5 min, followed by 30 cycles at 94^{o}C for 15 s, 62^{o}C for 15 s and 72^{o}C for 1 min, at last 72^{o}C for 10 min.

The PCR amplified products were separated by 1.5% agarose gel electrophoresis, and the bands were visualized by staining with 0.5% Goldview and photographed.

4.1.3 Adipocyte differentiation of MEFs

To initiate adipocyte differentiation, at confluence, the differentiation-inducing mix/DIM (10 µg/ml insulin, 0.5 mol/l dexamethasone, and 0.5 mmol/l methylisobutylxanthine) was added into culture medium. After 2 days, the medium was replaced with fresh culture medium containing insulin (10 µg/ml) every 2 days. Adipocyte differentiation was estimated with Red Oil O staining. After most cells were differentiated into adipocytes, 10 µg/ml recombinant active or inactive MMP-11 protein in buffer (50 mM Tris pH 7.5, 100 mM NaCl, 5 mM $CaCl_2$, 1 µM $ZnCl_2$) was

added into the culture medium each day. Then, after 5 days, the total RNA was extracted and Oil Red O staining performed in parallel.

4.1.4 Oil Red O staining of adipocytes

Oil Red O staining was performed as described (Andarawewa et al., 2005; Motrescu et al., 2008). Briefly:

(1) Remove the culture medium, washed the cells with 1X PBS;

(2) Remove PBS, fix cells in 4% formalin (dilution with 1X PBS) for 30 min;

(3) Rinse thrice with distilled H_2O (dH_2O) and one time with 1X PBS, and then air-dry;

(4) Stain the fixed cells with 0.5% Oil Red O for 20 min;

(5) Remove the Oil Red O, washed with dH_2O one time;

(6) Counterstain with hematoxylin for 15 s;

(7) Remove the hematoxylin, wash cells with dH_2O for two times. Take photos under unverted microscope.

4.1.5 Total RNA extraction and microarray assay

4.1.5.1 Extraction of total RNA

The protocol is described in the RNeasy (mini handbook, Qiagen). Briefly:

(1) Trypsinize and wash the cells with 1X PBS for two times, then count cells;

(2) Disrupt the cells by adding 600 µl Buffer RLT;

(3) To homogenize, pass the lysate at least 5 times through a blunt 20-gauge needle (0.9 mm diameter) fitted to an RNase-free syringe;

(4) Add 1 volume of 70% ethanol, and mix well by pipetting;

(5) Transfer up to 700 µl of the sample, including any precipitate that may have formed, to an RNeasy spin column placed in a 2 ml collection tube. Centrifuge at 10,000 rpm for 15 s. Discard the flow-through. If the sample volume exceeds 700 µl, centrifuge successive aliquots in the same RNeasy spin column. Discard the flow-through after each centrifugation;

(6) Add 700 µl of Buffer RW1 to the RNeasy spin column. Centrifuge at 10,000 rpm for 15 s to wash the spin column membrane. Discard the flow-through;

(7) Add 500 µl of Buffer RPE to the RNeasy spin column. Centrifuge at 10,000

rpm for 15 s to wash the spin column membrane. Discard the flow-through;

(8) Add 500 µl of Buffer RPE to the RNeasy spin column. Centrifuge at 10,000 rpm for 2 min to wash the spin column membrane;

(9) Place the RNeasy spin column in a new 1.5 ml of collection tube. Add 30~50 µl of RNase-free H_2O directly to the spin column membrane. Centrifuge at 10,000 rpm for 1 min to elute the RNA;

(10) If the expected RNA yield > 30 µg, repeat step 9 with another 30-50 µl RNase-free H_2O, or use elute from step 9. Reuse the collection tube from step 9. The total RNA was stored at -80^{o}C.

4.1.5.2 Measurement of RNA concentration

Use the NanoDrop ND-1000 spectrophotometer to measure the total RNA concentration and OD260/OD280 ratio for microarray.

4.1.5.3 Microarray

RNA samples were then given to the person in charge of the Affymetrix platform at IGBMC, who performed microarray experiments.

Section II Techniques related to part II results

4.2.1 Total RNA extraction and RT-PCR (Reverse Transcription Polymerase Chain Reaction)

Total RNA samples from mammary gland were isolated with TriReagent (Sigma), following manufacturer's instructions.

4.2.1.1 RNA extraction from tissues using TriReagent

(1) Collect mammary gland tissue without lymph node;

(2) Add 1 ml TriReagent (TriZol) in sample and mix with the polytron machine. Rinse properly the borer with dH_2O;

(3) Incubate the mix 5 min at RT (room temperature);

(4) Add 200 µl of $CHCl_3$ (RNase-free), vortex, incubate from 2 min to 15 min at RT. Spin at 10,000 rpm for 15 min at 4°C;

(5) Collect the aqueous phase, add 500 µl isopropanol, incubate from 5 to 10 min at RT. Spin at 10,000 rpm during 10 min at 4°C;

(6) Resuspend the pellet with 100 µl of H_2O (RNase-free) + 10 µl sodium acetate 3 M pH 7.00 (RNase-free) + 250 µl absolute ethanol (RNase-free);

(7) Precipitate RNA at -20°C O/N;

(8) Spin at 10,000 rpm during 45 min at 4°C;

(9) Wash the pellet with 1 ml 70% ethanol;

(10) Spin at 10,000 rpm during 30 min at 4°C;

(11) Dry the pellet and resuspend the pellet with 100 µl H_2O (RNase-free);

(12) Determine the concentration at 260 nm.

4.2.1.2 DNase treatment

(1) 2 µg RNA;

(2) Add 0.4 U DNase (10 U/50 µg RNA);

(3) Add 3 µl 10X buffer (DNase buffer, Roche);

(4) Add dH_2O to total volume of 30 µl;

(5) Incubate 20 min at 37°C.

4.2.1.3 Phenol/Chloroforme extraction

(1) Adjust the volume to 100 µl (add 70 µl) with H_2O;

(2) Add 0.5 vol (50 µl) water-saturated phenol and 0.5 vol (50 µl) $CHCl_3$, spin 5 min at 6,500 rpm;

(3) Collect the aqueous phase, add 1 vol $CHCl_3$, vortex, spin 1 min at 6,500 rpm;

(4) Collect the aqueous phase, add 10 µl NaAc 3M pH 7.0 and 250 µl absolute ethanol;

(5) Precipitate O/N at -20°C;

(6) Centrifuge 10,000 rpm 45 min at 4°C;

(7) Wash the pellet with 100 µl 70% ethanol;

(8) Centrifuge 10,000 rpm 30 min at 4°C;

(9) Dry the pellet and re-suspend the pellet with 10.5 µl dH_2O.

4.2.1.4 Reverse transcription

(1) Warm the RNA (10.5 µl) 10 min at 50°C;

(2) Add 0.5 µl Oligo-dT (200 µg/ml);

(3) Add 1 µl 10 mM dNTP;

(4) Warm 5 min at 65°C, then cold 5 min on ice;

(5) Add 4 µl First Strand Buffer 5X, 0.5 µl DTT, 0.5 µl RTase, 1 µl RNasin and 2 µl dH_2O, mix;

(6) Incubate 50 min at 42°C;

(7) Inactivate the reaction at 70°C for 15 min;

(8) Store -20°C or -80°C for PCR.

4.2.1.5 PCR

These steps are same as before (4.1.2.2).

DNA primer sequences were designed as follows: for mouse MMP-11 gene (NM_008606), sense primer (primer_D): 5'-CCG AAG GGG CAT CCA GCA CC-3'; and antisense strand (primer_E): 5'-GCA TCC ACA GGG CTG GGC AG-3'; the amplicon size is 318 bp. For mouse GAPDH gene (NM_008084): sense primer (primer_F): 5'-ACT GGC ATG GCC TTC CGT GTT C-3'; antisense primer (primer_G), 5'-TCT TGC TCA GTG TCC TTG CTG G-3'; the amplicon size is 366

bp.

4.2.2 In situ hybridization (ISH)

ISH analysis was performed as previously described (Masson et al., 1998).

4.2.2.1 Preparation of the probe

4.2.2.1.1 Amplification of probe

(1) Cleave the pBS-SK+ plasmid with EcoRI (T7 RNA polymerase) or HindIII (T3 RNA polymerase);

(2) Use 1 μl of 1 μg/μl template DNA;

(3) Add 4 μl of 5X Buffer;

(4) Add 2 μl of 10 mM ATP, GTP and CTP;

(5) Add 1.3 μl of 10 mM UTP;

(6) Add 0.7 μl of 10 mM UTP-digoxigenin-labelled;

(7) Add 2 μl of 10 mM DTT;

(8) Add 1 μl of 20-50 units/μl RNasin;

(9) Adjust total volume to 20 μl with RNase-free H_2O;

(10) Add 1 μl of RNA polymerase (T3-T7-SP6), incubate 2 hr (hour) at 37°C.

4.2.2.1.2 Estimation of transcript quantity by agarose/TBE gel running

(1) 2 g of agarose;

(2) Add 200 ml of 0.5X TAE (Tris-Acetate-EDTA);

(3) 10% cold TBE (Tris-Borate-EDTA).

4.2.2.1.3 Purification of transcript

(1) Add 2 μl of 40 μg/μl DNase I into sample;

(2) Incubate 15 min at 37°C;

(3) Add 2 μl of 0.2 M, pH 8 EDTA;

(4) Add 2.5 μl of 4 M lithium chloride;

(5) Add 75 μl of 100% cold ethanol;

(6) Vortex;

(7) Incubate 30 min at -80°C, or 2 hr at -20°C, or O/N at 20°C;

(8) Spin 12,000 rpm 30 min at 4°C;

(9) Discard the supernatant;

(10) Wash the pellet with 50 μl of 70% cold ethanol;

(11) Spin 12,000 rpm for 15 min at 4°C;

(12) Discard the supernatant;

(13) Dry the pellet ≥ 1hr at RT;

(14) Add 50 μl of dH_2O to resuspend the pellet.

*If the plasmid ≥ 1 kb:

(1) Resuspend with 50 μl of RNase free H_2O;

(2) Add 30 μl of 0.2 M Na_2CO_3;

(3) Add 20 μl of 0.2 M $NaHCO_3$;

(4) Incubate 30 min at 60°C;

(5) Stop the hydrolysis reaction at -20°C;

(6) Add 3 μl of 3 M AcNa (sodium acetate) pH 6;

(7) Add 5 μl of 10% glacial acetic acid;

(8) Add 10 μl of yeast tRNA (10 μg);

(9) Add 250 μl of cold 100% ethanol;

(10) Incubate 30 min at -20°C;

(11) Spin 10,000 rpm 30 min at 4°C;

(12) Discard the supernatant;

(13) Add 50 μl of cold 70% ethanol;

(14) Spin 10,000 rpm 15 min at 4°C;

(15) Discard the supernatant;

(16) Air dry the pellet ≥ 1hr at RT;

(17) Add 50 μl of RNase free H_2O;

(18) Incubate 5 min at 60°C, the probe is ready.

4.2.2.2 Solutions and reagents

10X salt (1000 ml): NaCl (114 g), Tris-HCl (14.04 g), Tris-Base (1.34 g), $NaH_2PO_4.2H_2O$ (7.8 g), 0.5 M EDTA (100 ml), dilution with dH_2O.

100X Denhardt't (50 ml): BSA/bovine serum albumin (1 g), ficoll™ (1 g), PVP/poly vingl pyrolidone (1 g), dilution with dH_2O, store at -20°C.

50% Dextran sulphate (50 ml): dextran sulphate (25 g), dilution with dH_2O at 50°C for O/N.

10 mg/ml tRNA (10 ml): tRNA (100 mg), dilution with dH_2O, store at -20°C.

Hybridization Buffer (10 ml): 10X Salt (1 ml), deionised formamide (5 ml), 50% dextran sulphate (2 ml), 10 mg/ml tRNA (1 ml), 100X denhardt't (0.1 ml), dH_2O (0.9 ml).

1 M Maleic acid (1000 ml): maleic acid (116 g), dH_2O (800 ml), 10 M NaOH (160 ml) pH 7.5, dilution with dH_2O.

MABT (2000 ml): 1 M maleic acid (200 ml), 5 M NaCl (60 ml), Tween-20 (2 ml), dilution with dH_2O.

10% Blocking Reagent (BR) (20 ml): blocking reagent (2 g), MABT (20 ml), dissolve by heating in micro-oven for 10 s, store at -20°C.

Washing Solution (1000 ml prepared freahly): 2X SSC/saline sodium citrate (500 ml), formamide (500 ml), Tween-20 (1 ml), pre-warmed at 65°C one day previously.

Blocking solution (1 ml): MABT (800 µl), 10% BR (200 µl), prepared freshly on ice.

Ab-Staining Solution: dilution of goat anti-digoxigenin antibody (Roche) into 1/2500 or 1/8000 with blocking solution, 200 µl mix on one slide. Prepared freshly on ice.

NTMT-alkaline phosphatase staining buffer (500 ml): 5 M NaCl (10 ml), 1 M $MgCl_2$ (25 ml), 1 M Tris pH 9.5 (50 ml), Tween-20 (0.5 ml), dilution with dH_2O.

NBT-BCIP Solution- alkaline phosphatase staining buffer: NTMT (1 ml), levamisole (1 drop), NBT (3.5 µl), BCIP (3.5 µl), prepared freshly in dark.

4.2.2.3 Procedure for paraffin-embedded formalin-fixed specimens:

(1) 5 µm-thick sections were deparaffinized, rehydrated in decreasing concentrations of ethanol (100% ethanol 3 min X 2 times, 95% ethanol 3 min X 1 time, 75% ethanol 3 min X 1 time, 50% ethanol 2 min X 1 time, dH_2O 2 min X 1 time), and then air-dry.

(2) The slides were then washed in 1X PBS three times for 10 min each.

(3) The tissue sections were permeabilized by proteolytic digestion with proteinase K (6 µg/ml in 50 mM Tris-HCl, pH 7.6) at 50^{o}C for 10 min.

(4) The reaction was stopped by rinsing the slides twice in 1X PBS for 5 min each and heating at 92^{o}C for 2 min in a heat block.

(5) The slides were placed in 1X PBS for 5 min, 0.2 M HCl for 20 min, 1X PBS for 5 min, and subsequently dehydrated through washes in graded ethanol, for 5 min each.

(6) The slides were placed in 2X SSC at 70^{o}C for 5 min and then at 92^{o}C for another 5 min.

(7) Immediately after that, the tissue sections were covered with heat denatured digoxigenin-labelled probes diluted 1/50 in hybridization buffer. The slides were incubated at 65^{o}C overnight in a humidity chamber.

(8) The next day, the slides were washed four times for 15 min each with pre-warmed washing solution at 65^{o}C, two times 30 min each with MABT buffer at RT and covered with freshly prepared antibody blocking solution 1 hr at RT.

(9) The tissue sections were covered with goat anti-digoxigenin antibody coupled to alkaline-phosphatase (1/2000 in antibody blocking solution) and incubated 4 hr at 37^{o}C in a humidity chamber.

(10) The slides were washed two times 30 min each in MABT buffer, rinsed two times for 10 min each at RT with NTMT buffer.

(11) The slides were covered with alkaline phosphatase substrate solution (NBT, BCIP) containing levamisole and incubated for a few hours at RT or O/N at 4^{o}C humidity chamber.

(12) Reaction was stopped by washing with PBST (1X PBS, 0.1% Tween-20).

(13) Rinse slides in dH_2O.

(14) Immerse slides in vector Nuclear Fast Red counterstain or apply counterstain directly to slide, completely covering the tissue section.

(15) Incubate sections for 1 to 10 min to obtain desired stain intensity.

(16) Wash slides in H_2O for 10 min.

(17) Dehytrate and clear (70% ethanol 5 min, 95% ethanol 5 min, 100% ethanol

5 min two times, histosol 5 min two times), then mount the slides.

4.2.3 Analysis of tissue morphology with carmine-alum staining

4.2.3.1 Tissue preparation

The fourth inguinal (#4) mammary gland pair was dissected from each mouse to measure weight and volume, one gland was analyzed by whole mount and another was 10% paraformaldehyde-fixed for 24 hrs, dehydrated, and embedded in paraffin, or quick frozen in Tissue-Tec OCT for cryostat sections.

4.2.3.2 Carmine-alum staining

Whole mount carmine-alum staining of mammary glands was performed as described (Ucar et al., 2010). Briefly, the dissected #4 mammary glands were spread onto glass slides and incubated with Carnoy's fixative (60% ethanol, 30% chloroform, 10% glacial acetic acid) for O/N. The glands were then incubated with a graded series of 70%, 50% and 25% ethanol (15 min each), followed by 5 min in H_2O and stained with carmine-alum O/N. The glands were washed in 70%, 90% and 100% ethanol (15 min each), two changes of histosol (30 min each), and then mounted with permount. Take photo under microscope.

4.2.4 Hematoxylin and Eosin (H&E) staining

Paraffin-embedded or frozen in Tissue-Tec OCT mammary glands were cut into sections (5 μm or 10 μm).

4.2.4.1 Rehydration

(1) Histosol 5 min × 2 times;

(2) 100% ethanol 1 min;

(3) 70% ethanol 1 min;

(4) 50% ethanol 1 min;

(5) dH_2O 2 min.

4.2.4.2 Staining

(1) Hematoxylin 1-5 min;

(2) Rinse dH_2O;

(3) Acid alcohol 2 s (1% HCl in 50% ethanol);

(4) Rinse tap H_2O 15 min;

(5) Eosin 1min;

(6) Rinse in a few quick changes of dH_2O.

4.2.4.3 Dehydration

(1) 70% ethanol 1 min;

(2) 95% ethanol 1 min;

(3) 100% ethanol 1 min;

(4) Histosol 5 min X 2 times;

(5) Mounted with permount;

(6) cover with coverslip and take photo under microscope.

4.2.5 Immunofluorescence assay

4.2.5.1 Deparaffinization and rehydration

5 μm-thick sections were deparaffinized, rehydrated in decreasing concentrations of ethanol (histosol 15 min X 2 times, 100% ethanol 10 min X 2 times, 95% ethanol 3 min, 75% ethanol 5 min, 50% ethanol 2 min, dH_2O 3 min).

4.2.5.2 Antigen retrieval (microwave heating method)

Soak the slides in the working citrate buffer and cover with a lid. Microwave until the liquid boils about 1-5 min. Remove from microwave oven and let it stand at RT for 20 min. Wash with H_2O for 3 min, wash with 1X PBS for 3 min, wash with PBST for 5 min.

4.2.5.3 Blocking

Apply 5% NGS (normal goat serum) in 1X PBS to cover the tissues. Incubate the slides 1 hr at RT or O/N at 4°C in a humid chamber.

4.2.5.4 Primary antibody

Dilute the primary antibody to the recommended concentration in 1% NGS/PBS diluent. Remove the NGS, and incubate with primary antibody solution (anti-E-cadherin, Zymed; anti-αSMA, Sigma-Aldrich) for 1 hr at RT or O/N at 4°C in a humid chamber. Wash slides with 1X PBS for 3 times, 5 min each.

4.2.5.5 Secondary antibody

Dilute the fluorescent secondary antibody to 1:200 in 1X PBS diluent. Incubate with secondary antibody solution for 1 hr at RT in dark place. Wash slides with 1X

PBS for 3 times, 5 min each.

4.2.5.6 Cover slides

Add DAPI-mounting medium (dilution of 100X DAPI into 1/100 in mounting medium) to the middle of the tissue sections. Cover slides with coverslip and store at 4°C until ready take photo.

4.2.6 Sirius red staining for collagen

4.2.6.1 Solutions and reagents

(1) Picro-sirius red solution: sirius red (0.5 g), saturated aqueous solution of picric acid (500 ml).

(2) Acidified H_2O: add 5 ml acetic acid (glacial) to 1 liter of dH_2O.

(3) Hematoxylin (Merck)

4.2.6.2 Procedure:

(1) De-wax and hydrate paraffin sections;

(2) Stain nuclei with hematoxylin for 8 min, and then wash the slides with tap H_2O for 10 min;

(3) Stain in picro-sirius red for 1 hr;

(4) Wash in two changes of acidified H_2O;

(5) Physically remove most of the H_2O from the slides by vigorous shaking;

(6) Dehydrate in three changes of 100% ethanol;

(7) Clear in histosol and mount in a resinous medium.

4.2.7 Masson's Trichrome staining for collagen

4.2.7.1 Solutions and reagents

Bouin's solution: saturated picric acid (75 ml), 37-40% formaldehyde (25 ml), glacial acetic acid (5 ml), mix well. This solution will improve Masson Trichrome staining quality.

Weigert's Iron Hematoxylin Solution:

Stock Solution A: hematoxylin (1 g), 95% ethanol (100 ml)

Stock Solution B: 29% ferric chloride (4 ml), dH_2O (95 ml), concentrated hydrochloric acid (1 ml).

Weigert's Iron Hematoxylin Working Solution: mix equal parts of stock solution A and B.

Biebrich Scarlet-Acid Fuchsin Solution: 1% biebrich scarlet (90 ml), 1% acid fuchsin (10 ml), acetic acid glacial (1 ml).

Phosphomolybdic-Phosphotungstic Acid Solution: 5% phosphomolybdic acid (25 ml), 5% phosphotungstic acid (25 ml).

Aniline Blue Solution: aniline blue (2.5 g), acetic acid glacial (2 ml), dH_2O (100 ml).

1% Acetic Acid Solution: acetic acid glacial (1 ml), dH_2O (99 ml).

4.2.7.2 Procedure:

(1) De-paraffin and rehydrate through 100% ethanol, 95% ethanol, 70% ethanol; 50% ethanol;

(2) Wash with dH_2O;

(3) For formalin fixed tissue, re-fix in Bouin's solution for 1 hr at 56^{o}C to improve staining quality although this step is not absolutely necessary;

(4) Rinse running tap H_2O for 5-10 min to remove the yellow color;

(5) Stain in Weigert's iron hematoxylin working solution for 10 min;

(6) Rinse in running warm tap H_2O for 10 min;

(7) Wash with dH_2O;

(8) Stain in Biebrich scarlet-acid fuchsin solution for 10-15 min;

(9) Wash with dH_2O;

(10) Differentiate in phosphomolybdic-phosphotungstic acid solution for 10-15 min or until collagen is not red;

(11) Transfer sections directly (without rinse) to aniline blue solution and stain for 5-10 min. Rinse briefly in dH_2O and differentiate in 1% acetic acid solution for 2-5 min;

(12) Wash in dH_2O;

(13) Dehydrate very quickly through 95% ethanol, 100% ethanol (these step will wipe off biebrich scarlet-acid fuchsin staining) and clear in histosol;

(14) Mount with resinous mounting medium.

4.2.8 Oil Red O staining of the mammary gland

Oil Red O staining adipose tissue was performed as described (Plump et al., 1996). Briefly, the #4 mammary glands were 10% paraformaldehyde-fixed for O/N. After fixation, mammary glands were infiltrated with three changes of 30% sucrose in 1X PBS and quick frozen in Tissue-Tec OCT (Miles, Elkhart, IN). 10 μm-thick cryostat sections were placed on polyl-lysine (Sigma Chemical Co., St. Louis, MO)-coated slides, stained with Oil Red O for 20 min, and counterstained with hematoxylin for 15 s. Removed the hematoxylin, washed the cells two times with dH_2O. Sections were examined under microscope.

4.2.9 Mammary gland transplantation

Mammary gland transplantation experiments were approved by the Animal Welfare and Research Committee/AWRC at IGBMC institute.

4.2.9.1 Mammary epithelial transplantation

Mammary epithelial transplantation was performed as described (Ucar et al., 2010; Khialeeva et al., 2011). Briefly:

(1) Reciprocal mammary epithelial transplantations were done with 3-week-old female littermates (Figure 3.15);

(2) Mice were anaesthetized by intraperitoneal injection of anesthetic (the dilution contains 25 μl xylazine, 77 μl ketamine and 98 μl solution saline) and inguinal mammary glands were exposed through small incisions in the skin of the lower abdomen and along the right hind leg;

(3) For fat pad clearing, the connection between inguinal #4 and #5 glands was disrupted and the endogenous epithelia were removed by removing the region between the nipple and the line above the lymph node;

(4) Small pieces of the removed glands (~2 mm^3 close to the nipple region) were cut and transplanted into the cleared fat pads of recipient mice. The left inguinal #4 mammary glands were used as controls;

(5) For analysis of ductal outgrowth, transplanted mice were killed at 3, 6 or 9 weeks after the operation. At least three sets of transplantation were done for each experimental condition and reproducible results were obtained from all of them.

4.2.9.2 Whole mammary gland transplantation

Whole mammary gland transplantation was performed as described (Moraes et al., 2009; Ucar et al., 2010). Briefly:

(1) Both right and left inguinal #4 mammary glands were dissected from killed donor mice (3 weeks old) and kept for a short time in DMEM until transplantation;

(2) Meanwhile, recipient mice were anaesthetized by intraperitoneal injection of drug and small incisions were made in the skin of the upper abdomen. The transplants were placed on the peritoneal wall just under the sternum as shown in Figure 3.20;

(3) Transplants and endogenous inguinal glands were dissected 3, 6 or 9 weeks after the operation and analyzed by whole mount carmine-alum staining. At least three sets of transplantation were done for each experimental condition and reproducible results were obtained from all of them.

4.2.10 Culture of mouse mammary epithelial organoids and adipocytes in vitro

Isolation of primary mammary organoids and adipocytes was performed as described (Simian et al., 2001; Hsieh et al., 2009).

4.2.10.1 Isolation of primary mammary organoids and adipocytes

(1) The inguinal #4 mammary glands were removed from 14-week-old virgin mice (MMP-11-/- & wild-type) and minced with two parallel razor blades. At this age the expansion of the ductal tree within the fat pad is complete and no TEB exist in wild-type;

(2) Minced tissue (4-8 glands) was gently shaken for 1-2 hr at 37°C in a 50 ml collagenase/trypsin mixture (0.2% trypsin, 0.2% collagenase A, 5% fetal calf serum, 5 µg/ml insulin, 50 µg/ml gentamycin, diluted in 50 ml of DMEM/F12);

(3) The resulting cell suspension was centrifuged at 1,000 rpm for 10 min, the supernatant containing adipocytes, washed extensively to remove trypsin and collagenase, cultured in vitro. The pellet was re-suspended in 10 ml DMEM/F12, the suspension was pelleted again at 1,000 rpm for 10 min, re-suspended in 4 ml of DMEM/F12 + 40 µl of DNase (2 U/µl), and incubated for 5 min at RT with occasional shaking;

(4) The DNase solution was removed after centrifugation at 1,000 rpm for 10

min. The DNase solution was discarded and the epithelial pieces were separated from the single cells through differential centrifugation. The pellet was re-suspended in 10 ml of DMEM/F12 and pulsed to 1,500 rpm. The supernatant was then removed and the pellet was re-suspended in 10 ml DMEM/F12. Differential centrifugation was performed at least 4 times. The final pellet was re-suspended in the desired amount of medium or matrigel (growth factor reduced matrigel, BD Biosciences, San Jose, CA).

4.2.10.2 Morphogenesis assay

(1) Morphogenesis assays were performed in 96-well culture plates. The culture had two layers, an underlay of 50 μl of matrigel and an overlying layer of organoids suspended in matrigel. The underlay was allowed to set for 30 min at 37°C, and then a 50 μl suspension of organoids in matrigel (~100-200 organoids/100 μl of matrigel) was added to the well followed by an incubation of 30 min at 37°C;

(2) All wells were then treated with 150 μl of basal media [DMEF/F12 with 1% ITS (insulin/transferring/selenium) and 1% penicillin/streptomycin] for 24 hr;

(3) After 24 hr the basal media was replenished, treated with basal media (negative control), wild-type or MMP-11-/- adipocyte conditional culture medium (serum-free), respectively. Every other day all samples were replenished with basal media;

(4) The branching phenotype of organoids embedded in collagen gels was determined after cultivation for 0-5 days. A branching phenotype was defined as an organoid having at least one process (branch) extending from its central body. Quantification of branching was carried out by counting the percentage of branched organoids in each well. Experiments were carried out in triplicates.

Section III Techniques related to part III results

4.3.1 Construction of MMP-11 expression plasmid

4.3.1.1 Transformation of plasmid vector JOJOHighcopyXMN into E.Coli and amplification

(1) Dilute the plasmid into 1/10 with dH_2O;

(2) Take 1 µl of plasmid into a new tube, add 80 µl of dH_2O and mix;

(3) Add 20 µl of 5X KCM (0.5 M KCl, 0.15 M $CaCl_2$ and 0.25 M $MgCl_2$) buffer, keep it on ice 10 min;

(4) Add 100 µl of competent E.coli and mix, keep it on ice 20 min;

(5) Incubate at RT for 10 min;

(6) Add 1 ml of LB (lysogeny broth) medium with antibiotics-free, incubate at 37^{o}C for 1 hr;

(7) Take 100 µl mixture into LB medium plate;, uniform distribute with rod;

(8) Incubate at 37^{o}C O/N;

(9) Select a white colony of bacteria, put it in the LB medium with 1/1000 ampicillin tube, shake at 37^{o}C O/N.

4.3.1.2 Extraction of plasmid DNA

(1) Add 1 ml of bacterium suspension into a new tube, spin 10,000 rpm for 1 min;

(2) Remove supernatant, vortex for re-suspension of bacteria precipitate;

(3) Add 300 µl of TENS (10 mM Tris pH 7.5, 1 mM EDTA, 0.1 M NaOH, 0.5% SDS) buffer and mix;

(4) Add 150 µl of 3 M NaAC pH 5.0 and mix, spin 10,000 rpm for 2 min;

(5) Take the supernatant into a new tube, add 1 ml of 100% ethanol and mix, spin 10,000 rpm for 4 min;

(6) Discard the supernatant, wash with 70% ethanol, spin 10,000 rpm for 4 min;

(7) Discard the supennatant, wash with 70% ethanol again, spin 10,000 rpm for 4 min;

(8) Discard supernatant, air dry > 1 hr at RT;

(9) Add 50 µl of RB (10 mM Tris pH 7.5, 1 mM Na_2EDTA, 40 ug/ml NaAse A, 0.02% Getatine) buffer and mix, heat at 65°C H_2O for 10 min.

4.3.1.3 Cleavage of the JOJO plasmid with restriction enzyme XhoI

(1) Take 5 µl of plasmid DNA into a new tube, and 13 µl of H_2O and 2 µl of restriction buffer, mix well, then add 0.5 µl of restriction enzyme XhoI (5000 U/ml), mix well;

(2) Incubate at 37 °C for 1-2 hr;

(3) Analysis using electrophresis.

4.3.1.4 Large amplification of JOJO plasmid

Add 0.8 ml of ampicillin into 800 ml of LB liquid culture medium. Take 50 ml of culture medium, and add 0.5 ml bacteria liquid (or 10 colonnies), shake at 37 °C O/N.

4.3.1.5 Extraction of JOJO plasmid DNA (plasmid DNA purification kit, Macherey-Nagel)

(1) Harvest bacterial cells: pellet the cells by centrifugation at 6,000 rpm at 4°C for 10 min, and discard the supernatant completely;

(2) Resuspend the cell pellet completely in resuspension buffer RES-EF +RNase A by pipetting the cells up and down or vortexing the cells;

(3) Add lysis buffer LYS-EF to the suspension. Mix gently by inverting the tube 5 times. Do not vortex as this will shear and release contaminating chromosomal DNA from cellular debris into the suspension. Incubate the mixture at RT for 5 min;

(4) Equilibrate a NucleoBond Xtra Column together with the inserted column filter with equilibration buffer EQU-EF. Apply the buffer onto the rim of the column filter and make sure to wet the entire filter;

(5) Add neutralization buffer NEU-EF to the suspension and immediately mix the lysate gently by inverting the tube 10-15 times. Do not vortex;

(6) Make sure to have a homogeneous suspension of the precipitate by inverting the tube 3 times directly before applying the lysate to the equilibrated Nucleo-Bond-Xtra column filter to avoid clogging of the filter;

(7) Wash the Nucleo-Bond-Xtra column filter and Nucleo-Bond-Xtra column with 5 ml of equilibration buffer EQU;

(8) Discard column filter;

(9) Wash the Nucleo-Bond-Xtra column with 8 ml of Wash Buffer;

(10) Elute the plasmid DNA with elution buffer ELU, collect the eluate in a 15 ml centrifuge tube;

(11) Add 3.5 ml of isopropanol to precipitate the eluted plasmid DNA. Vortex well and keep the mixture for 2 min. Centrifuge at 5,000 rpm for 15 min at RT. Carefully discard the supernatant;

(12) Add 70% ethanol to the pellet and centrifuge at 5,000 rpm for 5 min at RT. Carefully remove ethanol completely from the tube with a pipette tip. Allow the pellet to air dry at RT > 1 hr;

(13) Dissolve the DNA pellet in an appropriate volume of TE buffer.

4.3.1.6 Cleavage of the JOJO plasmid DNA with restriction enzyme XhoI (see 4.3.1.3)

4.3.1.7 Clean-up of the cleaved JOJO plasmid (PCR clean up kit, Macherey-Nagel)

(1) Adjust DNA binding condition: mix 1 volume of sample with 2 volume of buffer NT;

(2) Bind DNA: place a Nucleospin Extract II column into a collection tube (2 ml) and load the sample, centrifuge at 11,000 rpm for 1 min, discard fow-through and place the Nucleospin Extract II column back into the collection tube;

(3) Wash silica membrane: add 700 µl of buffer NT3, centrifuge at 11,000 rpm for 1 min, discard flow-through and place the Nucleospin Extract II column back into the collection tube;

(4) Dry silica membrane: centrifuge at 11,000 rpm for 2 min to remove buffer NT3 quantitatively. Make sure the spin column does not come in contact with the flow-through while removing it from the centrifuge and the collection tube;

(5) Elute DNA: place the Nucleospin Extract II column into a clean 1.5 ml microcentrifuge tube, add 15-50 µl of elution buffer NE and incubate at RT for 1 min to increase the yield of eluted DNA, centrifuge at 11,000 rpm for 1 min, store at -20^{o}C;

(6) Identify by electrophoresis.

4.3.1.8 Preparation of mouse MMP-11 cDNA

4.3.1.8.1 Design of mouse MMP-11 primer

Mouse MMP-11 Primers (for construction expression vector):

Sense primer (primer_H): 5'-GAG ***GTC GAC*** GCC GCC ATG GCA CGG GCC GCC TGT CTC-3'.

Antisense primer without flag (primer_I): 5'-GAG ***GTC GAC*** TCA GCG GAA AGT ATT GGC AGG-3'.

Antisense primer contains flag (primer_J): 5'-CAA TTG ***GTC GAC*** TCA CTT GTC ATC GTC GTC CTT GTA ATC GCG GAA AGT ATT GGC AGG CTC-3'.

Blue italics is SalI site.

4.3.1.8.2 Amplification of MMP-11 cDNA with PCR, and identification of PCR products with electrophoresis

The pSG5-MMP-11 plasmid serves as mouse MMP-11 template DNA (constructed in the lab). Each PCR tube include following mix:

(1) 10.4 µl H_2O

(2) 4.0 µl PCR buffer (HF 5X)

(3) 1.0 µl primer_H (1 µg/µl)

(4) 1.0 µl primer_I /primer_J (1 µg/µl)

(5) 0.2 µl Phusion High-Fidelity DNA Polymerase

(6) 2 µl pSG5-MMP-11 plasmid (1 ng/µl)

Each PCR program involved an initial step denaturation at 98^{o}C for 15 s, followed by 22 cycles at 98 ^{o}C for 10 s, 60^{o}C for 10 s and 72 ^{o}C for 30 s. The amplicon size is about 1,500 bp.

The PCR amplified products were separated by 1.5% agarose gel electrophoresis, and the bands were visualized by staining with 0.5% Goldview and photography

4.3.1.8.3 Clean-up of the PCR products (see 4.3.1.7)

4.3.1.8.4 Cleavage of the PCR products by restriction enzyme SalI

(1) Add 42 µl of dH_2O, 10 µl of restriction buffer, 1 µl of BSA (10 mg/ml) and 2 µl of restriction enzyme SalI (20,000 U/ml) into 45 µl of PCR products tube, mix

well;

(2) Incubate at 37 ^{o}C O/N.

4.3.1.8.5 Clean-up of the cleaved PCR products by SalI (see 4.3.1.7)

4.3.1.8.6 Identification of SalI PCR products cleaved with electrophoresis

4.3.1.9 Ligation of the JOJO vector and MMP-11/MMP-11-flag

The ligation mix:

(1) Cleaved JOJO vector: 200 ng

(2) Cleaved MMP-11/MMP-11-flag cDNA: 100-400 ng

(3) T4 ligase buffer 10X: 1 µl

(4) H_2O: add to a final volume of 10 µl

(5) T4 ligase: 0.2 µl

The ligation mixture was mix well and incubated at 4^{o}C O/N.

4.3.1.10 Transformation of plasmid into E.coli and small amplification

(1) The ligation mixture was incubated at 70^{o}C for 15 min;

(2) Put on ice;

(3) Cleavage by XhoI: add 8 µl of dH_2O, 2 µl of restriction buffer and 1 µl of restriction enzyme XhoI into 10 µl of ligation mixture, mix well, incubate at 37^{o}C for 2-4 hr;

(4) Add 60 µl of dH_2O;

(5) Add 20 µl of 5X KCM buffer (0.5 M KCl, 0.15 M $CaCl_2$ and 0.25 M $MgCl_2$), keep it on ice for 10 min;

(6) Add 100 µl of competent E.coli and mix, keep it on ice for 20 min;

(7) Incubate for 10 min at RT;

(8) Add 1 ml of LB medium with antibiotics-free, incubate at 37^{o}C for 1 hr;

(9) Take 200 µl mixture into LB medium plate, uniform distribute with rod;

(10) Incubate at 37^{o}C O/N;

(11) Select 20 white colonies of bacteria with toothpick, put it in the LB medium with 1/1000 ampicillin, shake at 37^{o}C O/N.

4.3.1.11 Extraction of plasmid DNA (see 4.3.1.2)

4.3.1.12 Analysis of the different clones from JOJO-MMP11/MMP-11-flag

subcloned by BamHI digestion (see 4.3.1.3)

4.3.1.13 Large amplification of sense JOJO-MMP11/MMP11-flag plasmids (see 4.3.1.4)

4.3.1.14 Extraction of the plasmid DNA (see 4.3.1.5)

4.3.2 Identification of correct plasmids

Co-transfection of JOJO-MMP-11/MMP11-flag with pSG5-Cre plasmids into Hela cells, extraction of protein and western blot analysis.

4.3.2.1 The first day, prepare cells

Add 1.5×10^6 Hela cells into each 10-cm plate and culture.

4.3.2.2 The second day, co-transfection of JOJO-MMP-11/MMP-11-flag with pSG5-Cre plasmids into Hela cell line

(1) Dilute 10 μg of plasmid DNA into 150 mM NaCl (final volume: 200 μl per plate), vortex gently and spin down briefly;

(2) Dilute 20 μl of jetPEI^{TM} into 150 mM NaCl (final volume: 200 μl per plate), vortex gently and spin down briefly;

(3) Add the jetPEI^{TM} solution into the DNA solution at once, mix the solution in the reverse order may reduce transfection efficiency;

(4) Vortex the solution immediately and spin down briefly;

(5) Incubate at RT for 15 to 30 min;

(6) Add the jetPEI^{TM}/DNA mix to the cell plates with serum-containing medium and homogenize by gently swirling the plate;

(7) Culture in incubator for 48 hr.

4.3.2.3 The third day, change the culture medium with serum-free

4.3.2.4 The fourth day, extraction of protein from cells

(1) Wash cells twice with 4^{o}C 1X PBS;

(2) Scrape cells with 1 ml of 4^{o}C 1X PBS, collect the cell suspension into 1.5 ml collection tube;

(3) Spin 2,000 rpm at 4^{o}C for 5 min, remove PBS, keep the cell pellet;

(4) Gently suspend the cell pellet with 300 μl of RIPA lysis buffer (0.1% SDS,

0.5% NP40, 0.5% Nadeoxycholate, dilution with 1X PBS);

(5) Incubate on ice for 15 min;

(6) Spin 10,000 rpm at 4^{o}C for 10 min, take supernatant into a new tube;

(7) The protein concentration of each sample was measured with BIO-RAD protein assay reagent by spectrophotometer;

(8) Store samples at -20^{o}C.

4.3.2.5 Validation of the JOJO-MMP-11/MMP-11-flag plasmids by western blot analysis.

(1) The protein samples (~20 μg) were mixed with loading buffer 6X (0.3 M Tris-HCl, 0.6 M DTT, 10% SDS, 0.06% Bromophenol blue, 30% Glycerol). The mixture was heated at 100^{o}C for 2 min to denature the proteins;

(2) Samples were subjected to electrophoresis in 10% SDS polyacrylamide gel. After electrophoresis, the samples were transferred to nitrocellulose membrane. PBST buffer containing 5% non-fat dry milk was used to block non-specific binding for 1hr at RT;

(3) 1/20,000 diluted anti-MMP-11 (mouse anti-MMP-11 monoclonal antibody, #5ST4A9, produced in the lab), 1/5,000 diluted anti-GFP (rabbit anti-GFP polyclonal antibody, Sigma), 1/2,000 anti-flag (rabbit anti-flag polyclonal antibody, Sigma), 1/10,000 anti-β-galactosidase (mouse anti-β-galactosidase polyclonal antibody, Promega) and 1/10,000 diluted anti-lasp-1 (rabbit anti-lasp-1 polyclonal antibody, #805, produced in the lab) antibodies were added, respectively. Shake at 4^{o}C O/N;

(4) The samples were washed three times with PBST for 10 min. Then 1/10,000 diluted secondary antibody (mouse anti-rabbit or rabbit anti-mouse, Jackson Immuno Research) was added, then incubated for 1 hr at RT. The samples were washed two times with PBST for 10 min;

(5) Immunoreactive bands were visualized using an enhanced chemiluminescence detection system and Kodak BioMax MR Film. The internal control was performed using lasp-1 antibody.

4.3.3 Linearization of JOJO-MMP-11 plasmid to generate transgenic mice

There are two cleavage sites for restriction enzyme SalI in JOJO vector (Figure

4.6 A), which can keep all components from CMV/β-actin promoter to β-galactosidase completely, and no SalI cutting site in MMP-11 and MMP-11-flag. So, I selected SalI linearize the JOJO-MMP-11 and JOJO-MMP-11-flag, and checked results of SalI digestion by electrophoresis (see 4.3.1.3). I selected the 8970 bp (JOJO-MMP-11) and 8991 bp (JOJO-MMP-11-flag) bands for purification, and further identified them through electrophoresis, respectively (see 4.3.1.7).

After identification, the linearized and purified JOJO-MMP-11 DNA was given to animal facility for generation of transgenic mice over-expressing MMP-11.

4.3.4 Identification of MMP-11 transgenic mice

The JOJO-MMP-11 transgenic mouse tails were cut, and checked for GFP expression under fluorescence microscope.

To further identify the genotype of JOJO-MMP-11 transgenic mice, the genomic DNA was extracted from tail tissue. I designed two primers that locate in different exons of mouse MMP-11 gene: the sense primer (primer_K: 5'-CCG AAG GGG CAT CCA GCA CC-3') locates in exon 5, the antisense primer (primer_L: 5'-GCA TCC ACA GGG CTG GGC AG-3') locates in exon 6; there is an intron (120 bp) locates between the two exons. Because the JOJO-MMP-11 transgenic DNA sequence only contains the coding region (exons) of MMP-11, no intron, the PCR product is 288 bp. In wild-type, however, the intron (120 bp) is present, so, the PCR product is 408 bp (for PCR steps see 4.1.2).

4.3.5 Obtention and identification of double transgenic mice

The aP2-Cre-ER^{T2} transgenic mice were obtained from IGBMC (*Daniel Metzger's* team), they are of same genetic background (C57Bl/6NTac) as JOJO-MMP-11 transgenic mice. For identification of aP2-Cre-ER^{T2} transgenic mice, the sense primer (primer_M) is 5'-GCA TTA CCG GTC GAT GCA ACG AGT GAT GAG-3', the antisense primer (primer_N) is 5'-GAG TGA ACG AAC CTG GTC GAA ATC AGT GCG-3', and the PCR production is about 400 bp (for PCR steps see 4.1.2). To get JOJO-MMP-11-aP2-Cre-ER^{T2} co-transgenic mice via aP2-Cre-ER^{T2} crossing with JOJO-MMP-11 transgenic mice. These mice were genotyped using MMP-11 primers (see 4.3.4) and Cre primers (see 4.3.5) with PCR.

Chapter 5 References

Websites:

NCBI Database: http://www.ncbi.nlm.nih.gov

Biblioinserm Database: http://biblioinserm.inist.fr/

Google: http://www.google.com/

Literatures:

1. Affolter M, Bellusci S, Itoh N, Shilo B, Thiery JP, Werb Z. Tube or not tube: remodeling epithelial tissues by branching morphogenesis. ***Dev Cell.*** 2003; 4(1): 11-8.
2. Agrawal S, Anderson P, Durbeej M, van Rooijen N, Ivars F, Opdenakker G, Sorokin LM. Dystroglycan is selectively cleaved at the parenchymal basement membrane at sites of leukocyte extravasation in experimental autoimmune encephalomyelitis. ***J Exp Med.*** 2006;203(4):1007-19.
3. Ahmad A, Marshall JF, Basset P, Anglard P, Hart IR. Modulation of human stromelysin 3 promoter activity and gene expression by human breast cancer cells. ***Int J Cancer.*** 1997;73(2):290-6.
4. Ahn GO, Brown JM. Matrix metalloproteinase-9 is required for tumor vasculogenesis but not for angiogenesis: role of bone marrow-derived myelomonocytic cells. ***Cancer Cell.*** 2008;13(3):193-205.
5. Akbari A, Razzaghi Z, Homaee F, Khayamzadeh M, Movahedi M, Akbari ME. Parity and breastfeeding are preventive measures against breast cancer in Iranian women. ***Breast Cancer.*** 2011;18(1):51-5.
6. Alexander CM, Hansell EJ, Behrendtsen O, Flannery ML, Kishnani NS, Hawkes SP, Werb Z. Expression and function of matrix metalloproteinases and their inhibitors at the maternal-embryonic boundary during mouse embryo implantation. ***Development.*** 1996;122(6):1723-36.
7. Alexander CM, Reichsman F, Hinkes MT, Lincecum J, Becker KA, Cumberledge S, Bernfield M. Syndecan-1 is required for Wnt-1-induced mammary tumorigenesis in mice. ***Nat Genet.*** 2000;25(3):329-32.
8. Alexander CM, Selvarajan S, Mudgett J, Werb Z. Stromelysin-1 regulates adipogenesis during mammary gland involution. ***J Cell Biol.*** 2001; 152(4): 693-703.
9. Amano T, Fu L, Sahu S, Markey M, Shi YB. Substrate specificity of Xenopus matrix metalloproteinase stromelysin-3. ***Int J Mol Med.*** 2004;14(2):233-9.
10. Andarawewa KL, Motrescu ER, Chenard MP, Gansmuller A, Stoll I, Tomasetto C, Rio MC. Stromelysin-3 is a potent negative regulator of adipogenesis participating to cancer cell-adipocyte interaction/crosstalk at the tumor invasive front. ***Cancer Res.*** 2005;65(23):10862-71.

11. Andarawewa KL, Rio MC. New insights into MMP function in adipogenesis. In the cancer degradome (Ed DR Edwards), ***Spring Science.*** 2008; pp 353-364.
12. Andersen K, Mori H, Fata J, Bascom J, Oyjord T, Mælandsmo GM, Bissell M. The metastasis-promoting protein S100A4 regulates mammary branching morphogenesis. ***Dev Biol.*** 2011; 352(2):181-90.
13. Anderson IC, Sugarbaker DJ, Ganju RK, Tsarwhas DG, Richards WG, Sunday M, Kobzik L, Shipp MA. Stromelysin-3 is overexpressed by stromal elements in primary non-small cell lung cancers and regulated by retinoic acid in pulmonary fibroblasts. ***Cancer Res.*** 1995;55(18):4120-6.
14. Anglard P, Melot T, Guérin E, Thomas G, Basset P. Structure and promoter characterization of the human stromelysin-3 gene. ***J Biol Chem.*** 1995; 270(35): 20337-44.
15. Apte SS, Olsen BR, Murphy G. The gene structure of tissue inhibitor of metalloproteinases (TIMP)-3 and its inhibitory activities define the distinct TIMP gene family. ***J Biol Chem.*** 1995;270(24):14313-8.
16. Ardi VC, Kupriyanova TA, Deryugina EI, Quigley JP. Human neutrophils uniquely release TIMP-free MMP-9 to provide a potent catalytic stimulator of angiogenesis. ***Proc Natl Acad Sci U S A.*** 2007;104(51):20262-7.
17. Ardi VC, Van den Steen PE, Opdenakker G, Schweighofer B, Deryugina EI, Quigley JP. Neutrophil MMP-9 proenzyme, unencumbered by TIMP-1, undergoes efficient activation in vivo and catalytically induces angiogenesis via a basic fibroblast growth factor (FGF-2)/FGFR-2 pathway. ***J Biol Chem.*** 2009; 284(38): 25854-66.
18. Atabai K, Sheppard D, Werb Z. Roles of the innate immune system in mammary gland remodeling during involution. ***J Mammary Gland Biol Neoplasia.*** 2007; 12(1): 37-45.
19. Baciu PC, Suleiman EA, Deryugina EI, Strongin AY. Membrane type-1 matrix metalloproteinase (MT1-MMP) processing of pro-alphav integrin regulates cross-talk between alphavbeta3 and alpha2beta1 integrins in breast carcinoma cells. ***Exp Cell Res.*** 2003;291(1):167-75.
20. Balbín M, Fueyo A, Tester AM, Pendás AM, Pitiot AS, Astudillo A, Overall CM, Shapiro SD, López-Otín C. Loss of collagenase-2 confers increased skin tumor susceptibility to male mice. ***Nat Genet.*** 2003;35(3):252-7.
21. Ban JY, Kim SK, Kang SW, Yoon KL, Chung JH. Association between polymorphisms of matrix metalloproteinase 11 (MMP-11) and Kawasaki disease in the Korean population. ***Life Sci.*** 2010;86(19-20):756-9.
22. Barone I, Catalano S, Gelsomino L, Marsico S, Giordano C, Panza S, Bonofiglio D, Bossi G, Covington KR, Fuqua SA, Andò S. Leptin mediates tumor-stromal interactions that promote the invasive growth of breast cancercells. ***Cancer Res.*** 2012;72(6):1416-27.
23. Barrasa JI, Olmo N, Santiago-Gómez A, Lecona E, Anglard P, Turnay J, Lizarbe MA. Histone deacetylase inhibitors upregulate MMP11 gene expression through Sp1/Smad complexes in human colon adenocarcinoma cells. ***Biochim Biophys Acta.*** 2012;1823(2):570-81.

24. Basset P, Bellocq JP, Wolf C, Stoll I, Hutin P, Limacher JM, Podhajcer OL, Chenard MP, Rio MC, Chambon P. A novel metalloproteinase gene specifically expressed in stromal cells of breast carcinomas. ***Nature.*** 1990; 348(6303): 699-704.
25. Basset P, Bellocq JP, Lefebvre O, Noël A, Chenard MP, Wolf C, Anglard P, Rio MC. Stromelysin-3: a paradigm for stroma-derived factors implicated in carcinoma progression. ***Crit Rev Oncol Hematol.*** 1997;26(1):43-53.
26. Berger J, Berger S, Tuoc TC, D'Amelio M, Cecconi F, Gorski JA, Jones KR, Gruss P, Stoykova A. Conditional activation of Pax6 in the developing cortex of transgenic mice causes progenitor apoptosis. ***Development.*** 2007; 134(7): 1311-22.
27. Bergers G, Brekken R, McMahon G, Vu TH, Itoh T, Tamaki K, Tanzawa K, Thorpe P, Itohara S, Werb Z, Hanahan D. Matrix metalloproteinase-9 triggers the angiogenic switch during carcinogenesis. ***Nat Cell Biol.*** 2000;2(10):737-44.
28. Berry DL, Rose CS, Remo BF, Brown DD. The expression pattern of thyroid hormone response genes in remodeling tadpole tissues defines distinct growth and resorption gene expression programs. ***Dev Biol.*** 1998;203(1):24-35.
29. Bochet L, Meulle A, Imbert S, Salles B, Valet P, Muller C. Cancer-associated adipocytes promotes breast tumor radioresistance. ***Biochem Biophys Res Commun.*** 2011; 411(1):102-6.
30. Boire A, Covic L, Agarwal A, Jacques S, Sherifi S, Kuliopulos A. PAR1 is a matrix metalloprotease-1 receptor that promotes invasion and tumorigenesis of breast cancer cells. ***Cell.*** 2005;120(3):303-13.
31. Bonacci G, Schopfer FJ, Batthyany CI, Rudolph TK, Rudolph V, Khoo NK, Kelley EE, Freeman BA. Electrophilic fatty acids regulate matrix metalloproteinase activity and expression. ***J Biol Chem.*** 2011; 286(18):16074-81.
32. Boulanger CA, Mack DL, Booth BW, Smith GH. Interaction with the mammary microenvironment redirects spermatogenic cell fate in vivo. ***Proc Natl Acad Sci U S A.*** 2007;104(10):3871-6.
33. Boulay A, Masson R, Chenard MP, El Fahime M, Cassard L, Bellocq JP, Sautès-Fridman C, Basset P, Rio MC. High cancer cell death in syngeneic tumors developed in host mice deficient for the stromelysin-3 matrix metalloproteinase. ***Cancer Res.*** 2001;61(5):2189-93.
34. Bourboulia D, Stetler-Stevenson WG. Matrix metalloproteinases (MMPs) and tissue inhibitors of metalloproteinases (TIMPs): Positive and negative regulators in tumor cell adhesion. ***Semin Cancer Biol.*** 2010;20(3):161-8.
35. Boyd NF, Martin LJ, Yaffe M, Minkin S. Mammographic density. ***Breast Cancer Res.*** 2009;11 Suppl 3:S4.
36. Brasse D, Mathelin C, Leroux K, Chenard MP, Blaise S, Stoll I, Tomasetto C, Rio MC. Matrix metalloproteinase 11/stromelysin-3 exerts both activator and repressor functions during the hematogenous metastatic process in mice. ***Int J Cancer.*** 2010;127(6):1347-55.
37. Brew K, Nagase H. The tissue inhibitors of metalloproteinases (TIMPs): an ancient family with structural and functional diversity. ***Biochim Biophys Acta.***

2010;1803(1):55-71.
38. Brinkmann V, Reichard U, Goosmann C, Fauler B, Uhlemann Y, Weiss DS, Weinrauch Y, Zychlinsky A. Neutrophil extracellular traps kill bacteria. ***Science.*** 2004;303(5663):1532-5.
39. Brisken C, Kaur S, Chavarria TE, Binart N, Sutherland RL, Weinberg RA, Kelly PA, Ormandy CJ. Prolactin controls mammary gland development via direct and indirect mechanisms. ***Dev Biol.*** 1999;210(1):96-106.
40. Brisken C, Duss S. Stem cells and the stem cell niche in the breast: an integrated hormonal and developmental perspective. ***Stem Cell Rev.*** 2007;3(2):147-56.
41. Brooks PC, Strömblad S, Sanders LC, von Schalscha TL, Aimes RT, Stetler-Stevenson WG, Quigley JP, Cheresh DA. Localization of matrix metalloproteinase MMP-2 to the surface of invasive cells by interaction with integrin alpha v beta 3. ***Cell.*** 1996;85(5):683-93.
42. Brown E, McKee T, diTomaso E, Pluen A, Seed B, Boucher Y, Jain RK. Dynamic imaging of collagen and its modulation in tumors in vivo using second-harmonic generation. ***Nat Med.*** 2003;9(6):796-800.
43. Bruyère F, Melen-Lamalle L, Blacher S, Roland G, Thiry M, Moons L, Frankenne F, Carmeliet P, Alitalo K, Libert C,. et al. Modeling lymphangiogenesis in a three-dimensional culture system. ***Nat Methods.*** 2008;5(5):431-7.
44. Burns JM, Summers BC, Wang Y, Melikian A, Berahovich R, Miao Z, Penfold ME, Sunshine MJ, Littman DR, Kuo CJ., et al. A novel chemokine receptor for SDF-1 and I-TAC involved in cell survival, cell adhesion, and tumor development. ***J Exp Med.*** 2006;203(9):2201-13.
45. Butcher DT, Alliston T, Weaver VM. A tense situation: forcing tumour progression. ***Nat Rev Cancer.*** 2009;9(2):108-22.
46. Cannata D, Lann D, Wu Y, Elis S, Sun H, Yakar S, Lazzarino DA, Wood TL, Leroith D. Elevated circulating IGF-I promotes mammary gland development and proliferation. ***Endocrinology.*** 2010;151(12):5751-61.
47. Capobianco E, White V, Sosa M, Di Marco I, Basualdo MN, Faingold MC, Jawerbaum A. Regulation of Matrix Metalloproteinases 2 and 9 Activities by Peroxynitrites in Term Placentas From Type 2 Diabetic Patients. ***Reprod Sci.*** 2012 Feb 16. [Epub ahead of print].
48. Carter JC, Church FC. Mature breast adipocytes promote breast cancer cell motility. ***Exp Mol Pathol.*** 2012;92(3):312-317.
49. Caterina NC, Windsor LJ, Bodden MK, Yermovsky AE, Taylor KB, Birkedal-Hansen H, Engler JA. Glycosylation and NH2-terminal domain mutants of the tissue inhibitor of metalloproteinases-1 (TIMP-1). ***Biochim Biophys Acta.*** 1998;1388(1):21-34.
50. Chepko G, Dickson RB. Ultrastructure of the putative stem cell niche in rat mammary epithelium. ***Tissue Cell.*** 2003;35(2):83-93.
51. Chin JR, Werb Z. Matrix metalloproteinases regulate morphogenesis, migration and remodeling of epithelium, tongue skeletal muscle and cartilage in the mandibular arch. ***Development.*** 1997;124(8):1519-30.
52. Ching S, Kashinkunti S, Niehaus MD, Zinser GM. Mammary adipocytes

bioactivate 25-hydroxyvitamin D_3 and signal via vitamin D3 receptor, modulating mammary epithelial cell growth. ***J Cell Biochem.*** 2011; 112(11): 3393-405.
53. Chu EY, Hens J, Andl T, Kairo A, Yamaguchi TP, Brisken C, Glick A, Wysolmerski JJ, Millar SE. Canonical WNT signaling promotes mammary placode development and is essential for initiation of mammary gland morphogenesis. ***Development.*** 2004;131(19):4819-29.
54. Chun TH, Hotary KB, Sabeh F, Saltiel AR, Allen ED, Weiss SJ. A pericellular collagenase directs the 3-dimensional development of white adipose tissue. ***Cell.*** 2006;125(3):577-91.
55. Codony-Servat J, Albanell J, Lopez-Talavera JC, Arribas J, Baselga J. Cleavage of the HER2 ectodomain is a pervanadate-activable process that is inhibited by the tissue inhibitor of metalloproteases-1 in breast cancer cells. ***Cancer Res.*** 1999; 59(6): 1196-201.
56. Cole SE, Wiltshire T, Reeves RH. Physical mapping of the evolutionary boundary between human chromosomes 21 and 22 on mouse chromosome 10. ***Genomics.*** 1998;50(1):109-11.
57. Conant K, St Hillaire C, Nagase H, Visse R, Gary D, Haughey N, Anderson C, Turchan J, Nath A. Matrix metalloproteinase 1 interacts with neuronal integrins and stimulates dephosphorylation of Akt. ***J Biol Chem.*** 2004;279(9):8056-62.
58. Cornelius LA, Nehring LC, Harding E, Bolanowski M, Welgus HG, Kobayashi DK, Pierce RA, Shapiro SD. Matrix metalloproteinases generate angiostatin: effects on neovascularization. ***J Immunol.*** 1998;161(12):6845-52.
59. Couldrey C, Moitra J, Vinson C, Anver M, Nagashima K, Green J. Adipose tissue: a vital in vivo role in mammary gland development but not differentiation. ***Dev Dyn.*** 2002;223(4):459-68.
60. Cowden Dahl KD, Symowicz J, Ning Y, Gutierrez E, Fishman DA, Adley BP, Stack MS, Hudson LG. Matrix metalloproteinase 9 is a mediator of epidermal growth factor-dependent e-cadherin loss in ovarian carcinoma cells. ***Cancer Res.*** 2008;68(12):4606-13.
61. Cowin P, Wysolmerski J. Molecular mechanisms guiding embryonic mammary gland development. ***Cold Spring Harb Perspect Biol.*** 2010;2(6):a003251.
62. Cox JH, Dean RA, Roberts CR, Overall CM. Matrix metalloproteinase processing of CXCL11/I-TAC results in loss of chemoattractant activity and altered glycosaminoglycan binding. ***J Biol Chem.*** 2008;283(28):19389-99.
63. Crawford HC, Scoggins CR, Washington MK, Matrisian LM, Leach SD. Matrix metalloproteinase-7 is expressed by pancreatic cancer precursors and regulates acinar-to-ductal metaplasia in exocrine pancreas. ***J Clin Invest.*** 2002; 109(11): 1437-44.
64. Cribier B, Noacco G, Peltre B, Grosshans E. Stromelysin 3 expression: a useful marker for the differential diagnosis dermatofibroma versus dermatofibrosarcoma protuberans. ***J Am Acad Dermatol.*** 2002;46(3):408-13.
65. Crocker SJ, Pagenstecher A, Campbell IL. The TIMPs tango with MMPs and

more in the central nervous system. ***J Neurosci Res.*** 2004;75(1):1-11.
66. Cruz-Munoz W, Khokha R. The role of tissue inhibitors of metalloproteinases in tumorigenesis and metastasis. ***Crit Rev Clin Lab Sci.*** 2008;45(3):291-338.
67. Dallas SL, Rosser JL, Mundy GR, Bonewald LF. Proteolysis of latent transforming growth factor-beta (TGF-beta)-binding protein-1 by osteoclasts. A cellular mechanism for release of TGF-beta from bone matrix. ***J Biol Chem.*** 2002; 277(24): 21352-60.
68. Damjanovski S, Ishizuya-Oka A, Shi YB. Spatial and temporal regulation of collagenases-3, -4, and stromelysin -3 implicates distinct functions in apoptosis and tissue remodeling during frog metamorphosis. ***Cell Res.*** 1999;9(2):91-105.
69. Dao Thi MU, Trocmé C, Montmasson MP, Fanchon E, Toussaint B, Tracqui P. Investigating Metalloproteinases MMP-2 and MMP-9 Mechanosensitivity to Feedback Loops Involved in the Regulation of In Vitro Angiogenesis by Endogenous Mechanical Stresses. ***Acta Biotheor.*** 2012 Jan 24. [Epub ahead of print].
70. Darcy KM, Zangani D, Shea-Eaton W, Shoemaker SF, Lee PP, Mead LH, Mudipalli A, Megan R, Ip MM. Mammary fibroblasts stimulate growth, alveolar morphogenesis, and functional differentiation of normal rat mammary epithelial cells. ***In Vitro Cell Dev Biol Anim.*** 2000;36(9):578-92.
71. de Ostrovich KK, Lambertz I, Colby JK, Tian J, Rundhaug JE, Johnston D, Conti CJ, DiGiovanni J, Fuchs-Young R. Paracrine overexpression of insulin-like growth factor-1 enhances mammary tumorigenesis in vivo. ***Am J Pathol.*** 2008; 173(3): 824-34.
72. de Visser KE, Eichten A, Coussens LM. Paradoxical roles of the immune system during cancer development. ***Nat Rev Cancer.*** 2006;6(1):24-37.
73. del Mar Barbacid M, Fernández-Resa P, Buesa JM, Márquez G, Aracil M, Quesadaand AR, Mira E. Expression and purification of human stromelysin 1 and 3 from baculovirus-infected insect cells. ***Protein Expr Purif.*** 1998; 13(2): 243-50.
74. Delany AM, Canalis E. Dual regulation of stromelysin-3 by fibroblast growth factor-2 in murine osteoblasts. ***J Biol Chem.*** 1998;273(26):16595-600.
75. Dennis JW, Granovsky M, Warren CE. Protein glycosylation in development and disease. ***Bioessays.*** 1999;21(5):412-21.
76. Deryugina EI, Ratnikov BI, Postnova TI, Rozanov DV, Strongin AY. Processing of integrin alpha(v) subunit by membrane type 1 matrix metalloproteinase stimulates migration of breast carcinoma cells on vitronectin and enhances tyrosine phosphorylation of focal adhesion kinase. ***J Biol Chem.*** 2002;277(12):9749-56.
77. Detry B, Erpicum C, Paupert J, Blacher S, Maillard C, Bruyère F, Pendeville H, Remacle T, Lambert V, Balsat C, et al. Matrix metalloproteinase-2 governs lymphatic vessel formation as an interstitial collagenase. ***Blood.*** 2012 Apr 6. [Epub ahead of print]
78. Dirat B, Bochet L, Dabek M, Daviaud D, Dauvillier S, Majed B, Wang YY, Meulle A, Salles B, Le Gonidec S., et al. Cancer-associated adipocytes exhibit an activated phenotype and contribute to breast cancer invasion. ***Cancer Res.*** 2011;

71(7): 2455-65.
79. Dive V, Andarawewa KL, Boulay A, Matziari M, Beau F, Guerin E, Rousseau B, Yiotakis A, Rio MC. Dosing and scheduling influence the antitumor efficacy of a phosphinic peptide inhibitor of matrix metalloproteinases. ***Int J Cancer.*** 2005; 113(5):775-81.
80. Dong W, Li H, Zhang Y, Yang H, Guo M, Li L, Liu T. Matrix metalloproteinase 2 promotes cell growth and invasion in colorectal cancer. ***Acta Biochim Biophys Sin (Shanghai).*** 2011;43(11):840-8.
81. Dontu G, Abdallah WM, Foley JM, Jackson KW, Clarke MF, Kawamura MJ, Wicha MS. In vitro propagation and transcriptional profiling of human mammary stem/progenitor cells. ***Genes Dev.*** 2003;17(10):1253-70.
82. Du R, Lu KV, Petritsch C, Liu P, Ganss R, Passegué E, Song H, Vandenberg S, Johnson RS, Werb Z, Bergers G. HIF1alpha induces the recruitment of bone marrow-derived vascular modulatory cells to regulate tumor angiogenesis and invasion. ***Cancer Cell.*** 2008;13(3):206-20.
83. Dufour A, Sampson NS, Zucker S, Cao J. Role of the hemopexin domain of matrix metalloproteinases in cell migration. ***J Cell Physiol.*** 2008;217(3):643-51.
84. Dufour A, Sampson NS, Li J, Kuscu C, Rizzo RC, Deleon JL, Zhi J, Jaber N, Liu E, Zucker S, Cao J. Small-molecule anticancer compounds selectively target the hemopexin domain of matrix metalloproteinase-9. ***Cancer Res.*** 2011; 71(14): 4977-88.
85. Dunbar ME, Dann PR, Robinson GW, Hennighausen L, Zhang JP, Wysolmerski JJ. Parathyroid hormone-related protein signaling is necessary for sexual dimorphism during embryonic mammary development. ***Development.*** 1999;126(16):3485-93.
86. Dupé V, Ghyselinck NB, Thomazy V, Nagy L, Davies PJ, Chambon P, Mark M. Essential roles of retinoic acid signaling in interdigital apoptosis and control of BMP-7 expression in mouse autopods. ***Dev Biol.*** 1999;208(1):30-43.
87. Edwards PA. The use of transplanted mammary gland to study cancer signalling pathways. ***Adv Exp Med Biol***. 2000;480:163-7.
88. Egeblad M, Werb Z. New functions for the matrix metalloproteinases in cancer progression. ***Nat Rev Cancer.*** 2002;2(3):161-74.
89. Ellerbroek SM, Stack MS. Membrane associated matrix metalloproteinases in metastasis. ***Bioessays.*** 1999;21(11):940-9.
90. Elliott BE, Tam SP, Dexter D, Chen ZQ. Capacity of adipose tissue to promote growth and metastasis of a murine mammary carcinoma: effect of estrogen and progesterone. ***Int J Cancer.*** 1992;51(3):416-24.
91. Engel G, Heselmeyer K, Auer G, Bäckdahl M, Eriksson E, Linder S. Correlation between stromelysin-3 mRNA level and outcome of human breast cancer. ***Int J Cancer.*** 1994;58(6):830-5.
92. English JL, Kassiri Z, Koskivirta I, Atkinson SJ, Di Grappa M, Soloway PD, Nagase H, Vuorio E, Murphy G, Khokha R. Individual Timp deficiencies differentially impact pro-MMP-2 activation. ***J Biol Chem.*** 2006;281(15): 10337-46.
93. Fanelli MF, Chinen LT, Begnami MD, Costa WL Jr, Fregnami JH, Soares

FA, Montagnini AL. The influence of transforming growth factor-α, cyclooxygenase-2, matrix metalloproteinase (MMP)-7, MMP-9 and CXCR4 proteins involved in epithelial-mesenchymal transition on overall survival of patients with gastric cancer. ***Histopathology.*** 2012 May 14. [Epub ahead of print].

94. Fata JE, Leco KJ, Moorehead RA, Martin DC, Khokha R. Timp-1 is important for epithelial proliferation and branching morphogenesis during mouse mammary development. ***Dev Biol.*** 1999;211(2):238-54.
95. Fata JE, Chaudhary V, Khokha R. Cellular turnover in the mammary gland is correlated with systemic levels of progesterone and not 17beta-estradiol during the estrous cycle. ***Biol Reprod.*** 2001a;65(3):680-8.
96. Fata JE, Leco KJ, Voura EB, Yu HY, Waterhouse P, Murphy G, Moorehead RA, Khokha R. Accelerated apoptosis in the Timp-3-deficient mammary gland. ***J Clin Invest.*** 2001b;108(6):831-41.
97. Fata JE, Werb Z, Bissell MJ. Regulation of mammary gland branching morphogenesis by the extracellular matrix and its remodeling enzymes. ***Breast Cancer Res.*** 2004;6(1):1-11.
98. Fata JE, Mori H, Ewald AJ, Zhang H, Yao E, Werb Z, Bissell MJ. The MAPK(ERK-1,2) pathway integrates distinct and antagonistic signals from TGFalpha and FGF7 in morphogenesis of mouse mammary epithelium. ***Dev Biol.*** 2007;306(1):193-207
99. Fiorentino M, Fu L, Shi YB. Mutational analysis of the cleavage of the cancer-associated laminin receptor by stromelysin-3 reveals the contribution of flanking sequences to site recognition and cleavage efficiency. ***Int J Mol Med.*** 2009;23(3):389-97.
100. Fitzgerald ML, Wang Z, Park PW, Murphy G, Bernfield M. Shedding of syndecan-1 and -4 ectodomains is regulated by multiple signaling pathways and mediated by a TIMP-3-sensitive metalloproteinase. ***J Cell Biol.*** 2000;148(4): 811-24.
101. Foley J, Dann P, Hong J, Cosgrove J, Dreyer B, Rimm D, Dunbar M, Philbrick W, Wysolmerski J. Parathyroid hormone-related protein maintains mammary epithelial fate and triggers nipple skin differentiation during embryonic breast development. ***Development.*** 2001;128(4):513-25.
102. Friedl P, Wolf K. Tube travel: the role of proteases in individual and collective cancer cell invasion. ***Cancer Res.*** 2008;68(18):7247-9.
103. Fu X, Kassim SY, Parks WC, Heinecke JW. Hypochlorous acid generated by myeloperoxidase modifies adjacent tryptophan and glycine residues in the catalytic domain of matrix metalloproteinase-7 (matrilysin): an oxidative mechanism for restraining proteolytic activity during inflammation. ***J Biol Chem.*** 2003; 278(31):28403-9.
104. Gall AL, Ruff M, Kannan R, Cuniasse P, Yiotakis A, Dive V, Rio MC, Basset P, Moras D. Crystal structure of the stromelysin-3 (MMP-11) catalytic domain complexed with a phosphinic inhibitor mimicking the transition-state. ***J Mol Biol.*** 2001;307(2):577-86.
105. Giannelli G, Falk-Marzillier J, Schiraldi O, Stetler-Stevenson WG, Quaranta V.

Induction of cell migration by matrix metalloprotease-2 cleavage of laminin-5. ***Science.*** 1997;277(5323):225-8.
106. Glasheen BM, Kabra AT, Page-McCaw A. Distinct functions for the catalytic and hemopexin domains of a Drosophila matrix metalloproteinase. ***Proc Natl Acad Sci U S A.*** 2009;106(8):2659-64.
107. Gomez DE, Alonso DF, Yoshiji H, Thorgeirsson UP. Tissue inhibitors of metalloproteinases: structure, regulation and biological functions. ***Eur J Cell Biol.*** 1997;74(2):111-22.
108. Gouon-Evans V, Rothenberg ME, Pollard JW. Postnatal mammary gland development requires macrophages and eosinophils. ***Development.*** 2000; 127(11): 2269-82.
109. Gouon-Evans V, Pollard JW. Unexpected deposition of brown fat in mammary gland during postnatal development. ***Mol Endocrinol.*** 2002; 16(11): 2618-27.
110. Green KA, Lund LR. ECM degrading proteases and tissue remodelling in the mammary gland. ***Bioessays.*** 2005;27(9):894-903.
111. Gregoire FM. dipocyte differentiation: from fibroblast to endocrine cell. ***Exp Biol Med (Maywood).*** 2001;226(11):997-1002.
112. Gu Y, Zheng G, Xu M, Li Y, Chen X, Zhu W, Tong Y, Chung SK, Liu KJ, Shen J. Caveolin-1 regulates nitric oxide-mediated matrix metalloproteinases activity and blood-brain barrier permeability in focal cerebral ischemia and reperfusion injury. ***J Neurochem.*** 2012;120(1):147-56.
113. Guérin E, Ludwig MG, Basset P, Anglard P. Stromelysin-3 induction and interstitial collagenase repression by retinoic acid. Therapeutical implication of receptor-selective retinoids dissociating transactivation and AP-1-mediated transrepression. ***J Biol Chem.*** 1997 ;272(17):11088-95.
114. Gutiérrez-Fernández A, Inada M, Balbín M, Fueyo A, Pitiot AS, Astudillo A, Hirose K, Hirata M, Shapiro SD, Noël A., et al. Increased inflammation delays wound healing in mice deficient in collagenase-2 (MMP-8). ***FASEB J.*** 2007; 21(10): 2580-91.
115. Gutiérrez-Fernández A, Fueyo A, Folgueras AR, Garabaya C, Pennington CJ, Pilgrim S, Edwards DR, Holliday DL, Jones JL, Span PN., et al. Matrix metalloproteinase-8 functions as a metastasis suppressor through modulation of tumor cell adhesion and invasion. ***Cancer Res.*** 2008;68(8):2755-63.
116. Ha HY, Moon HB, Nam MS, Lee JW, Ryoo ZY, Lee TH, Lee KK, So BJ, Sato H, Seiki M, Yu DY. Overexpression of membrane-type matrix metalloproteinase-1 gene induces mammary gland abnormalities and adenocarcinoma in transgenic mice. ***Cancer Res.*** 2001;61(3):984-90.
117. Haines P, Samuel GH, Cohen H, Trojanowska M, Bujor AM. Caveolin-1 is a negative regulator of MMP-1 gene expression in human dermal fibroblasts via inhibition of Erk1/2/Ets1 signaling pathway. ***J Dermatol Sci.*** 2011;64(3):210-6.
118. Halberg N, Wernstedt-Asterholm I, Scherer PE. The adipocyte as an endocrine cell. ***Endocrinol Metab Clin North Am.*** 2008;37(3):753-68.
119. Hamano Y, Zeisberg M, Sugimoto H, Lively JC, Maeshima Y, Yang C, Hynes RO, Werb Z, Sudhakar A, Kalluri R. Physiological levels of tumstatin, a fragment

of collagen IV alpha3 chain, are generated by MMP-9 proteolysis and suppress angiogenesis via alphaV beta3 integrin. ***Cancer Cell.*** 2003;3(6):589-601.
120. Hannemann J, Velds A, Halfwerk JB, Kreike B, Peterse JL, van de Vijver MJ. Classification of ductal carcinoma in situ by gene expression profiling. ***Breast Cancer Res.*** 2006;8(5):R61.
121. Haro H, Crawford HC, Fingleton B, Shinomiya K, Spengler DM, Matrisian LM. Matrix metalloproteinase-7-dependent release of tumor necrosis factor-alpha in a model of herniated disc resorption. ***J Clin Invest.*** 2000;105(2):143-50.
122. Harvell DM, Strecker TE, Tochacek M, Xie B, Pennington KL, McComb RD, Roy SK, Shull JD. Rat strain-specific actions of 17beta-estradiol in the mammary gland: correlation betweenestrogen-induced lobuloalveolar hyperplasia and susceptibility to estrogen-induced mammarycancers. ***Proc Natl Acad Sci U S A.*** 2000;97(6):2779-84.
123. Hebbard LW, Garlatti M, Young LJ, Cardiff RD, Oshima RG, Ranscht B. T-cadherin supports angiogenesis and adiponectin association with the vasculature in a mouse mammary tumor model. ***Cancer Res.*** 2008;68(5):1407-16.
124. Heldin CH, Landström M, Moustakas A. Mechanism of TGF-beta signaling to growth arrest, apoptosis, and epithelial-mesenchymal transition. ***Curr Opin Cell Biol.*** 2009;21(2):166-76.
125. Heljasvaara R, Nyberg P, Luostarinen J, Parikka M, Heikkilä P, Rehn M, Sorsa T, Salo T, Pihlajaniemi T. Generation of biologically active endostatin fragments from human collagen XVIII by distinct matrix metalloproteases. ***Exp Cell Res.*** 2005;307(2):292-304.
126. Hens JR, Wysolmerski JJ. Key stages of mammary gland development: molecular mechanisms involved in the formation of the embryonic mammary gland. ***Breast Cancer Res.*** 2005;7(5):220-4.
127. Hernandez-Barrantes S, Toth M, Bernardo MM, Yurkova M, Gervasi DC, Raz Y, Sang QA, Fridman R. Binding of active (57 kDa) membrane type 1-matrix metalloproteinase (MT1-MMP) to tissue inhibitor of metalloproteinase (TIMP)-2 regulates MT1-MMP processing and pro-MMP-2 activation. ***J Biol Chem.*** 2000; 275(16):12080-9.
128. Heuberger B, Fitzka I, Wasner G, Kratochwil K. Induction of androgen receptor formation by epithelium-mesenchyme interaction in embryonic mouse mammary gland. ***Proc Natl Acad Sci U S A.*** 1982;79(9):2957-61.
129. Hinck L, Silberstein GB. Key stages in mammary gland development: the mammary end bud as a motile organ. ***Breast Cancer Res.*** 2005;7(6):245-51.
130. Hojilla CV, Mohammed FF, Khokha R. Matrix metalloproteinases and their tissue inhibitors direct cell fate during cancer development. ***Br J Cancer.*** 2003;89(10): 1817-21.
131. Hojilla CV, Kim I, Kassiri Z, Fata JE, Fang H, Khokha R. Metalloproteinase axes increase beta-catenin signaling in primary mouse mammary epithelial cells lacking TIMP3. ***J Cell Sci.*** 2007;120(Pt 6):1050-60.
132. Holtz B, Cuniasse P, Boulay A, Kannan R, Mucha A, Beau F, Basset P, Dive V. Role of the S1' subsite glutamine 215 in activity and specificity of stromelysin-3

by site-directed mutagenesis. ***Biochemistry.*** 1999;38(37):12174-9.
133. Horiuchi K, Kimura T, Miyamoto T, Takaishi H, Okada Y, Toyama Y, Blobel CP. Cutting edge: TNF-alpha-converting enzyme (TACE/ADAM17) inactivation in mouse myeloid cells prevents lethality from endotoxin shock. ***J Immunol.*** 2007; 179(5):2686-9.
134. Houghton AM, Grisolano JL, Baumann ML, Kobayashi DK, Hautamaki RD, Nehring LC, Cornelius LA, Shapiro SD. Macrophage elastase (matrix metalloproteinase-12) suppresses growth of lung metastases. ***Cancer Res.*** 2006; 66(12):6149-55.
135. Houghton AM, Hartzell WO, Robbins CS, Gomis-Rüth FX, Shapiro SD. Macrophage elastase kills bacteria within murine macrophages. ***Nature.*** 2009; 460(7255): 637-41.
136. Hovey RC, Aimo L. Diverse and active roles for adipocytes during mammary gland growth and function. ***J Mammary Gland Biol Neoplasia.*** 2010; 15(3): 279-90.
137. Howlett AR, Bissell MJ. The influence of tissue microenvironment (stroma and extracellular matrix) on the development and function of mammary epithelium. ***Epithelial Cell Biol.*** 1993;2(2):79-89.
138. Hsieh CW, Millward CA, DeSantis D, Pisano S, Machova J, Perales JC, Croniger CM. Reduced milk triglycerides in mice lacking phosphoenolpyruvate carboxykinase in mammary gland adipocytes and white adipose tissue contribute to the development of insulin resistance in pups. ***J Nutr.*** 2009;139(12): 2257-65.
139. Hu X, Juneja SC, Maihle NJ, Cleary MP. Leptin--a growth factor in normal and malignant breast cells and for normal mammary gland development. ***J Natl Cancer Inst.*** 2002;94(22):1704-11.
140. Hynes NE, Lane HA. ERBB receptors and cancer: the complexity of targeted inhibitors. ***Nat Rev Cancer.*** 2005;5(5):341-54.
141. Illman SA, Lehti K, Keski-Oja J, Lohi J. Epilysin (MMP-28) induces TGF-beta mediated epithelial to mesenchymal transition in lung carcinoma cells. ***J Cell Sci.*** 2006;119(Pt 18):3856-65.
142. Imai T, Jiang M, Chambon P, Metzger D. Impaired adipogenesis and lipolysis in the mouse upon selective ablation of the retinoid X receptor alpha mediated by a tamoxifen-inducible chimeric Cre recombinase (Cre-ERT2) in adipocytes. ***Proc Natl Acad Sci U S A.*** 2001;98(1):224-8.
143. Ingman WV, Wyckoff J, Gouon-Evans V, Condeelis J, Pollard JW. Macrophages promote collagen fibrillogenesis around terminal end buds of the developing mammary gland. ***Dev Dyn.*** 2006;235(12):3222-9.
144. Ishizuya-Oka A, Ueda S, Shi YB. Transient expression of stromelysin-3 mRNA in the amphibian small intestine during metamorphosis. ***Cell Tissue Res.*** 1996;283(2):325-9.
145. Ishizuya-Oka A, Li Q, Amano T, Damjanovski S, Ueda S, Shi YB. Requirement for matrix metalloproteinase stromelysin-3 in cell migration and apoptosis during tissue remodeling in Xenopus laevis. ***J Cell Biol.*** 2000; 150(5): 1177-88.
146. Işlekel H, Oktay G, Terzi C, Canda AE, Füzün M, Küpelioğlu A. Matrix

metalloproteinase-9,-3 and tissue inhibitor of matrix metalloproteinase-1 in colorectal cancer: relationship to clinicopathological variables. ***Cell Biochem Funct.*** 2007;25(4):433-41.

147. Iyengar P, Combs TP, Shah SJ, Gouon-Evans V, Pollard JW, Albanese C, Flanagan L, Tenniswood MP, Guha C, Lisanti MP., et al. Adipocyte-secreted factors synergistically promote mammary tumorigenesis through induction of anti-apoptotic transcriptional programs and proto-oncogene stabilization. ***Oncogene.*** 2003;22(41):6408-23.
148. Iyengar P, Espina V, Williams TW, Lin Y, Berry D, Jelicks LA, Lee H, Temple K, Graves R, Pollard J,. et al. Adipocyte-derived collagen VI affects early mammary tumor progression in vivo, demonstrating a critical interaction in the tumor/stroma microenvironment. ***J Clin Invest.*** 2005;115(5):1163-76.
149. Jenkins G. The role of proteases in transforming growth factor-beta activation. ***Int J Biochem Cell Biol.*** 2008;40(6-7):1068-78.
150. Jodele S, Blavier L, Yoon JM, DeClerck YA. Modifying the soil to affect the seed: role of stromal-derived matrix metalloproteinases in cancer progression. ***Cancer Metastasis Rev.*** 2006;25(1):35-43.
151. Kajita M, Itoh Y, Chiba T, Mori H, Okada A, Kinoh H, Seiki M. Membrane-type 1 matrix metalloproteinase cleaves CD44 and promotes cell migration. ***J Cell Biol.*** 2001;153(5):893-904.
152. Kang Y, Siegel PM, Shu W, Drobnjak M, Kakonen SM, Cordón-Cardo C, Guise TA, Massagué J. A multigenic program mediating breast cancer metastasis to bone. ***Cancer Cell.*** 2003;3(6):537-49.
153. Kannan R, Ruff M, Kochins JG, Manly SP, Stoll I, El Fahime M, Noël A, Foidart JM, Rio MC, Dive V, Basset P. Purification of active matrix metalloproteinase catalytic domains and its use for screening of specific stromelysin-3 inhibitors. ***Protein Expr Purif.*** 1999;16(1):76-83.
154. Kaplan RN, Riba RD, Zacharoulis S, Bramley AH, Vincent L, Costa C, MacDonald DD, Jin DK, Shido K, Kerns SA,. Et al. VEGFR1-positive haematopoietic bone marrow progenitors initiate the pre-metastatic niche. ***Nature.*** 2005;438(7069):820-7.
155. Kassiri Z, Defamie V, Hariri M, Oudit GY, Anthwal S, Dawood F, Liu P, Khokha R. Simultaneous transforming growth factor beta-tumor necrosis factor activation and cross-talk cause aberrant remodeling response and myocardial fibrosis in Timp3-deficient heart. ***J Biol Chem.*** 2009;284(43):29893-904.
156. Keely PJ, Wu JE, Santoro SA. The spatial and temporal expression of the alpha 2 beta 1 integrin and its ligands, collagen I,collagen IV, and laminin, suggest important roles in mouse mammary morphogenesis. ***Differentiation.*** 1995; 59(1): 1-13.
157. Kelsey JL, Gammon MD, John EM. Reproductive factors and breast cancer. ***Epidemiol Rev.*** 1993;15(1):36-47.
158. Kesanakurti D, Chetty C, Dinh DH, Gujrati M, Rao JS. Role of MMP-2 in the regulation of IL-6/Stat3 survival signaling via interaction with α5β1 integrin in glioma. Oncogene. 2012 Feb 20. [Epub ahead of print].

159. Kessenbrock K, Krumbholz M, Schönermarck U, Back W, Gross WL, Werb Z, Gröne HJ, Brinkmann V, Jenne DE. Netting neutrophils in autoimmune small-vessel vasculitis. ***Nat Med.*** 2009;15(6):623-5.
160. Kessenbrock K, Plaks V, Werb Z. Matrix metalloproteinases: regulators of the tumor microenvironment. ***Cell.*** 2010;141(1):52-67.
161. Khan KM, Kothari P, Du B, Dannenberg AJ, Falcone DJ. Matrix metalloproteinase-dependent microsomal prostaglandin E synthase-1 expression in macrophages: role of TNF-α and the EP4 prostanoid receptor. ***J Immunol.*** 2012; 188(4):1970-80.
162. Khialeeva E, Lane TF, Carpenter EM. Disruption of reelin signaling alters mammary gland morphogenesis. ***Development.*** 2011;138(4):767-76.
163. Khokha R, Werb Z. Mammary gland reprogramming: metalloproteinases couple form with function. ***Cold Spring Harb Perspect Biol.*** 2011;3(4). pii: a004333.
164. Kim HJ, Lee JY, Kim SH, Seo YJ, Lee JH, Park JK, Kim MH, Cinn YW, Cho KH, Yoon TY. Stromelysin-3 expression in the differential diagnosis of dermatofibroma and dermatofibrosarcoma protuberans: comparison with factor XIIIa and CD34. ***Br J Dermatol.*** 2007;157(2):319-24.
165. Kim JH, Kim KY, Jeon JH, Lee SH, Hwang JE, Lee JH, Kim KK, Lim JS, Kim KI, Moon EY., Adipocyte culture medium stimulates production of macrophage inhibitory cytokine 1 in MDA-MB-231 cells. ***Cancer Lett.*** 2008; 261(2): 253-62.
166. Kimijima I, Ohtake T, Sagara H, Watanabe T, Takenoshita S. Scattered fat invasion: an indicator for poor prognosis in premenopausal, and for positive estrogen receptor in postmenopausal breast cancer patients. ***Oncology.*** 2000;59 Suppl 1:25-30.
167. Kirmse R, Otto H, Ludwig T. The extracellular matrix remodeled: Interdependency of matrix proteolysis, cell adhesion, and force sensing. ***Commun Integr Biol.*** 2012;5(1):71-3.
168. Konttinen YT, Ainola M, Valleala H, Ma J, Ida H, Mandelin J, Kinne RW, Santavirta S, Sorsa T, López-Otín C, Takagi M. Analysis of 16 different matrix metalloproteinases (MMP-1 to MMP-20) in the synovial membrane: different profiles in trauma and rheumatoid arthritis. ***Ann Rheum Dis.*** 1999; 58(11):691-7.
169. Koo BH, Kim YH, Han JH, Kim DS. Dimerization of matrix metalloproteinase-2(MMP-2): functional implication in MMP-2 activation. ***J Biol Chem.*** 2012 May 10. [Epub ahead of print].
170. Koshikawa N, Giannelli G, Cirulli V, Miyazaki K, Quaranta V. Role of cell surface metalloprotease MT1-MMP in epithelial cell migration over laminin-5. ***J Cell Biol.*** 2000;148(3):615-24.
171. Kurley SJ, Bierie B, Carnahan RH, Lobdell NA, Davis MA, Hofmann I, Moses HL, Muller WJ, Reynolds AB. p120-catenin is essential for terminal end bud function and mammary morphogenesis. ***Development.*** 2012;139(10):1754-64.
172. Landskroner-Eiger S, Qian B, Muise ES, Nawrocki AR, Berger JP, Fine EJ, Koba W, Deng Y, Pollard JW, Scherer PE. Proangiogenic contribution of

adiponectin toward mammary tumor growth in vivo. ***Clin Cancer Res.*** 2009;15(10):3265-76.
173. Landskroner-Eiger S, Park J, Israel D, Pollard JW, Scherer PE. Morphogenesis of the developing mammary gland: stage-dependent impact of adipocytes. ***Dev Biol.*** 2010;344(2):968-78.
174. Langenskiöld M, Holmdahl L, Falk P, Ivarsson ML. Increased plasma MMP-2 protein expression in lymph node-positive patients with colorectal cancer. ***Int J Colorectal Dis.*** 2005;20(3):245-52.
175. Langton KP, Barker MD, McKie N. Localization of the functional domains of human tissue inhibitor of metalloproteinases-3 and the effects of a Sorsby's fundus dystrophy mutation. ***J Biol Chem.*** 1998;273(27):16778-81.
176. Le Maux Chansac B, Missé D, Richon C, Vergnon I, Kubin M, Soria JC, Moretta A, Chouaib S, Mami-Chouaib F. Potentiation of NK cell-mediated cytotoxicity in human lung adenocarcinoma: role of NKG2D-dependent pathway. ***Int Immunol.*** 2008;20(7):801-10.
177. Lee EY, Parry G, Bissell MJ. Modulation of secreted proteins of mouse mammary epithelial cells by the collagenous substrata. ***J Cell Biol.*** 1984; 98(1): 146-55.
178. Lee PP, Hwang JJ, Murphy G, Ip MM. Functional significance of MMP-9 in tumor necrosis factor-induced proliferation and branching morphogenesis of mammary epithelial cells. ***Endocrinology.*** 2000;141(10):3764-73.
179. Lee S, Jilani SM, Nikolova GV, Carpizo D, Iruela-Arispe ML. Processing of VEGF-A by matrix metalloproteinases regulates bioavailability and vascular patterning in tumors. ***J Cell Biol.*** 2005;169(4):681-91.
180. Lefebvre O, Wolf C, Limacher JM, Hutin P, Wendling C, LeMeur M, Basset P, Rio MC. The breast cancer-associated stromelysin-3 gene is expressed during mouse mammary gland apoptosis. ***J Cell Biol.*** 1992;119(4):997-1002.
181. Lefebvre O, Régnier C, Chenard MP, Wendling C, Chambon P, Basset P, Rio MC. Developmental expression of mouse stromelysin-3 mRNA. ***Development.*** 1995;121(4):947-55.
182. Levi E, Fridman R, Miao HQ, Ma YS, Yayon A, Vlodavsky I. Matrix metalloproteinase 2 releases active soluble ectodomain of fibroblast growth factor receptor 1. ***Proc Natl Acad Sci U S A.*** 1996;93(14):7069-74.
183. Levy A, Zucman J, Delattre O, Mattei MG, Rio MC, Basset P. Assignment of the human stromelysin 3 (STMY3) gene to the q11.2 region of chromosome 22. ***Genomics.*** 1992;13(3):881-3.
184. Li J, Liang VC, Sedgwick T, Wong J, Shi YB. Unique organization and involvement of GAGA factors in transcriptional regulation of the Xenopus stromelysin-3 gene. ***Nucleic Acids Res.*** 1998;26(12):3018-25.
185. Li J, Lau GK, Chen L, Dong SS, Lan HY, Huang XR, Li Y, Luk JM, Yuan YF, Guan XY. Interleukin 17A promotes hepatocellular carcinoma metastasis via NF-kB induced matrix metalloproteinases 2 and 9 expression. ***PLoS One.*** 2011; 6(7):e21816.
186. Li M, Li Q, Gao X. Expression and function of leptin and its receptor in dairy

goat mammary gland. ***J Dairy Res.*** 2010;77(2):213-9.
187. Li Q, Park PW, Wilson CL, Parks WC. Matrilysin shedding of syndecan-1 regulates chemokine mobilization and transepithelial efflux of neutrophils in acute lung injury. ***Cell.*** 2002;111(5):635-46.
188. Lijnen HR, Van Hoef B, Vanlinthout I, Verstreken M, Rio MC, Collen D. Accelerated neointima formation after vascular injury in mice with stromelysin-3 (MMP-11) gene inactivation. ***Arterioscler Thromb Vasc Biol.*** 1999; 19(12): 2863-70.
189. Lijnen HR, Van Hoef B, Collen D. Inactivation of the serpin alpha(2)-antiplasmin by stromelysin-1. ***Biochim Biophys Acta.*** 2001;1547(2): 206-13.
190. Lijnen HR, Van HB, Frederix L, Rio MC, Collen D. Adipocyte hypertrophy in stromelysin-3 deficient mice with nutritionally induced obesity. ***Thromb Haemost.*** 2002;87(3):530-5.
191. Lin CY, Tsai PH, Kandaswami CC, Lee PP, Huang CJ, Hwang JJ, Lee MT. Matrix metalloproteinase-9 cooperates with transcription factor Snail to induce epithelial-mesenchymal transition. ***Cancer Sci.*** 2011;102(4):815-27.
192. Lin WW, Karin M. A cytokine-mediated link between innate immunity, inflammation, and cancer. ***J Clin Invest.*** 2007;117(5):1175-83.
193. Littlepage LE, Sternlicht MD, Rougier N, Phillips J, Gallo E, Yu Y, Williams K, Brenot A, Gordon JI, Werb Z. Matrix metalloproteinases contribute distinct roles in neuroendocrine prostate carcinogenesis, metastasis, and angiogenesis progression. ***Cancer Res.*** 2010;70(6):2224-34.
194. Liu Z, Zhou X, Shapiro SD, Shipley JM, Twining SS, Diaz LA, Senior RM, Werb Z. The serpin alpha1-proteinase inhibitor is a critical substrate for gelatinase B/MMP-9 in vivo. ***Cell.*** 2000;102(5):647-55.
195. Liu Z, Ivanoff A, Klominek J. Expression and activity of matrix metalloproteases in human malignant mesothelioma cell lines. Int J Cancer. 2001; 91(5):638-43.
196. Lochter A, Galosy S, Muschler J, Freedman N, Werb Z, Bissell MJ. Matrix metalloproteinase stromelysin-1 triggers a cascade of molecular alterations that leads to stable epithelial-to-mesenchymal conversion and a premalignant phenotype in mammary epithelial cells. ***J Cell Biol.*** 1997;139(7):1861-72.
197. Lohi J, Wilson CL, Roby JD, Parks WC. Epilysin, a novel human matrix metalloproteinase (MMP-28) expressed in testis and keratinocytes and in response to injury. J Biol Chem. 2001; 276(13):10134-44.
198. Lu P, Sternlicht MD, Werb Z. Comparative mechanisms of branching morphogenesis in diverse systems. ***J Mammary Gland Biol Neoplasia.*** 2006; 11(3-4):213-28.
199. Lu P, Werb Z. Patterning mechanisms of branched organs. ***Science.*** 2008; 322 (5907):1506-9.
200. Lu X, Wang Q, Hu G, Van Poznak C, Fleisher M, Reiss M, Massagué J, Kang Y. ADAMTS1 and MMP1 proteolytically engage EGF-like ligands in an osteolytic signaling cascade for bone metastasis. ***Genes Dev.*** 2009; 23(16): 1882-94.

201. Ludwig MG, Basset P, Anglard P. Multiple regulatory elements in the murine stromelysin-3 promoter. Evidence for direct control by CCAAT/enhancer-binding protein beta and thyroid and retinoid receptors. ***J Biol Chem.*** 2000; 275(51): 39981-90.
202. Luehr I, Friedl A, Overath T, Tholey A, Kunze T, Hilpert F, Sebens S, Arnold N, Roesel F, Oberg HH, et al. Mammary fibroblasts regulate morphogenesis of normal and tumorigenic breast epithelial cells bymechanical and paracrine signals. ***Cancer Lett.*** 2012 Jul 6. [Epub ahead of print]
203. Lund LR, Rømer J, Thomasset N, Solberg H, Pyke C, Bissell MJ, Danø K, Werb Z. Two distinct phases of apoptosis in mammary gland involution: proteinase-independent and -dependent pathways. ***Development.*** 1996;122(1): 181-93.
204. Lund LR, Bjørn SF, Sternlicht MD, Nielsen BS, Solberg H, Usher PA, Osterby R, Christensen IJ, Stephens RW, Bugge TH., et al. Lactational competence and involution of the mouse mammary gland require plasminogen. ***Development.*** 2000;127(20):4481-92.
205. Luo D, Guérin E, Ludwig MG, Stoll I, Basset P, Anglard P. Transcriptional induction of stromelysin-3 in mesodermal cells is mediated by an upstream CCAAT/enhancer-binding protein element associated with a DNase I-hypersensitive site. ***J Biol Chem.*** 1999;274(52):37177-85.
206. Luo D, Mari B, Stoll I, Anglard P. Alternative splicing and promoter usage generates an intracellular stromelysin 3 isoform directly translated as an active matrix metalloproteinase. ***J Biol Chem.*** 2002;277(28):25527-36.
207. Luo JL, Maeda S, Hsu LC, Yagita H, Karin M. Inhibition of NF-kappaB in cancer cells converts inflammation- induced tumor growth mediated by TNFalpha to TRAIL-mediated tumor regression. ***Cancer Cell.*** 2004;6(3):297-305.
208. Lynch CC, Hikosaka A, Acuff HB, Martin MD, Kawai N, Singh RK, Vargo-Gogola TC, Begtrup JL, Peterson TE, Fingleton B,, et al. MMP-7 promotes prostate cancer-induced osteolysis via the solubilization of RANKL. ***Cancer Cell.*** 2005;7(5):485-96.
209. Ma XJ, Dahiya S, Richardson E, Erlander M, Sgroi DC Gene expression profiling of the tumor microenvironment during breast cancer progression. ***Breast Cancer Res.*** 2009;11(1):R7.
210. Maeda K, Okubo K, Shimomura I, Mizuno K, Matsuzawa Y, Matsubara K. Analysis of an expression profile of genes in the human adipose tissue. ***Gene.*** 1997;190(2):227-35.
211. Maeda K, Cao H, Kono K, Gorgun CZ, Furuhashi M, Uysal KT, Cao Q, Atsumi G, Malone H, Krishnan B, Adipocyte/macrophage fatty acid binding proteins control integrated metabolic responses inobesity and diabetes. ***Cell Metab.*** 2005; 1(2):107-19.
212. Manabe Y, Toda S, Miyazaki K, Sugihara H. Mature adipocytes, but not preadipocytes, promote the growth of breast carcinoma cells in collagen gel matrix culture through cancer-stromal cell interactions. ***J Pathol.*** 2003; 201(2): 221-8.

213. Mañes S, Mira E, Barbacid MM, Ciprés A, Fernández-Resa P, Buesa JM, Mérida I, Aracil M, Márquez G, Martínez-A C. Identification of insulin-like growth factor-binding protein-1 as a potential physiological substrate for human stromelysin-3. ***J Biol Chem.*** 1997;272(41):25706-12.
214. Mañes S, Llorente M, Lacalle RA, Gómez-Moutón C, Kremer L, Mira E, Martínez-A C. The matrix metalloproteinase-9 regulates the insulin-like growth factor-triggered autocrine response in DU-145 carcinoma cells. ***J Biol Chem.*** 1999;274(11):6935-45.
215. Manicone AM, McGuire JK. Matrix metalloproteinases as modulators of inflammation. ***Semin Cell Dev Biol.*** 2008;19(1):34-41.
216. Maquoi E, Assent D, Detilleux J, Pequeux C, Foidart JM, Noël A. MT1-MMP protects breast carcinoma cells against type I collagen-induced apoptosis. ***Oncogene.*** 2012;31(4):480-93.
217. Maquoi E, Polette M, Nawrocki B, Bischof P, Noël A, Pintiaux A, Santavicca M, Schaaps JP, Pijnenborg R, Birembaut P, Foidart JM. Expression of stromelysin-3 in the human placenta and placental bed. ***Placenta.*** 1997; 18(4): 277-85.
218. Mari BP, Anderson IC, Mari SE, Ning Y, Lutz Y, Kobzik L, Shipp MA. Stromelysin-3 is induced in tumor/stroma cocultures and inactivated via a tumor-specific and basic fibroblast growth factor-dependent mechanism. ***J Biol Chem.*** 1998;273(1):618-26.
219. Martin DC, Fowlkes JL, Babic B, Khokha R. Insulin-like growth factor II signaling in neoplastic proliferation is blocked by transgenic expression of the metalloproteinase inhibitor TIMP-1. ***J Cell Biol.*** 1999;146(4):881-92.
220. Massagué J. TGFbeta in Cancer. ***Cell.*** 2008;134(2):215-30.
221. Masson R, Lefebvre O, Noël A, Fahime ME, Chenard MP, Wendling C, Kebers F, LeMeur M, Dierich A, Foidart JM, et al., In vivo evidence that the stromelysin-3 metalloproteinase contributes in a paracrine manner to epithelial cell malignancy. ***J Cell Biol.*** 1998;140(6):1535-41.
222. Masso-Welch PA, Merhige PM, Veeranki OL, Kuo SM. Loss of IL-10 decreases mouse postpubertal mammary gland development in the absence of inflammation. ***Immunol Invest.*** 2012;41(5):521-37.
223. Matziari M, Dive V, Yiotakis A. Matrix metalloproteinase 11 (MMP-11; stromelysin-3) and synthetic inhibitors. ***Med Res Rev.*** 2007;27(4):528-52.
224. McCave EJ, Cass CA, Burg KJ, Booth BW. The normal microenvironment directs mammary gland development. ***J Mammary Gland Biol Neoplasia.*** 2010; 15(3):291-9.
225. McQuibban GA, Gong JH, Wong JP, Wallace JL, Clark-Lewis I, Overall CM. Matrix metalloproteinase processing of monocyte chemoattractant proteins generates CC chemokine receptor antagonists with anti-inflammatory properties in vivo. ***Blood.*** 2002;100(4):1160-7.
226. Mentzel T, Brown LF, Dvorak HF, Kuhnen C, Stiller KJ, Katenkamp D, Fletcher CD. The association between tumour progression and vascularity in myxofibrosarcoma and myxoid/round cell liposarcoma. ***Virchows Arch.*** 2001;

438(1): 13-22.
227. Mitsiades N, Yu WH, Poulaki V, Tsokos M, Stamenkovic I. Matrix metalloproteinase-7-mediated cleavage of Fas ligand protects tumor cells from chemotherapeutic drug cytotoxicity. ***Cancer Res.*** 2001;61(2):577-81.
228. Miyamoto S, Yano K, Sugimoto S, Ishii G, Hasebe T, Endoh Y, Kodama K, Goya M, Chiba T, Ochiai A. Matrix metalloproteinase-7 facilitates insulin-like growth factor bioavailability through its proteinase activity on insulin-like growth factor binding protein 3. ***Cancer Res.*** 2004;64(2):665-71.
229. Miyoshi Y, Funahashi T, Tanaka S, Taguchi T, Tamaki Y, Shimomura I, Noguchi S. High expression of leptin receptor mRNA in breast cancer tissue predicts poor prognosis for patients with high, but not low, serum leptin levels. ***Int J Cancer.*** 2006;118(6):1414-9.
230. Mohammed FF, Smookler DS, Taylor SE, Fingleton B, Kassiri Z, Sanchez OH, English JL, Matrisian LM, Au B, Yeh WC, Khokha R. Abnormal TNF activity in Timp3-/- mice leads to chronic hepatic inflammation and failure of liver regeneration. ***Nat Genet.*** 2004;36(9):969-77.
231. Mohammed FF, Khokha R. Thinking outside the cell: proteases regulate hepatocyte division. ***Trends Cell Biol.*** 2005;15(10):555-63.
232. Mohammed FF, Pennington CJ, Kassiri Z, Rubin JS, Soloway PD, Ruther U, Edwards DR, Khokha R. Metalloproteinase inhibitor TIMP-1 affects hepatocyte cell cycle via HGF activation in murine liver regeneration. ***Hepatology.*** 2005;41(4):857-67.
233. Moitra J, Mason MM, Olive M, Krylov D, Gavrilova O, Marcus-Samuels B, Feigenbaum L, Lee E, Aoyama T, Eckhaus M., et al. Life without white fat: a transgenic mouse. ***Genes Dev.*** 1998;12(20):3168-81.
234. Monks J, Smith-Steinhart C, Kruk ER, Fadok VA, Henson PM. Epithelial cells remove apoptotic epithelial cells during post-lactation involution of the mouse mammary gland. ***Biol Reprod.*** 2008;78(4):586-94.
235. Moore CS, Crocker SJ. An alternate perspective on the roles of TIMPs and MMPs in pathology. ***Am J Pathol.*** 2012;180(1):12-6.
236. Moore L, Fan D, Basu R, Kandalam V, Kassiri Z. Tissue inhibitor of metalloproteinases (TIMPs) in heart failure. ***Heart Fail Rev.*** 2011 Jun 30. [Epub ahead of print].
237. Moraes RC, Chang H, Harrington N, Landua JD, Prigge JT, Lane TF, Wainwright BJ, Hamel PA, Lewis MT. Ptch1 is required locally for mammary gland morphogenesis and systemically for ductal elongation. ***Development.*** 2009; 136(9):1423-32.
238. Mori H, Gjorevski N, Inman JL, Bissell MJ, Nelson CM. Self-organization of engineered epithelial tubules by differential cellular motility. ***Proc Natl Acad Sci U S A.*** 2009;106(35):14890-5.
239. Motrescu ER, Blaise S, Etique N, Messaddeq N, Chenard MP, Stoll I, Tomasetto C, Rio MC. Matrix metalloproteinase-11/stromelysin-3 exhibits collagenolytic function against collagen VI under normal and malignant conditions. ***Oncogene.*** 2008;27(49):6347-55.

240. Motrescu ER, Rio MC. Cancer cells, adipocytes and matrix metalloproteinase 11: a vicious tumor progression cycle. ***Biol Chem.*** 2008; 389(8): 1037-41.
241. Mu D, Cambier S, Fjellbirkeland L, Baron JL, Munger JS, Kawakatsu H, Sheppard D, Broaddus VC, Nishimura SL. The integrin alpha(v)beta8 mediates epithelial homeostasis through MT1-MMP-dependent activation of TGF-beta1. ***J Cell Biol.*** 2002;157(3):493-507.
242. Mucha A, Cuniasse P, Kannan R, Beau F, Yiotakis A, Basset P, Dive V. Membrane type-1 matrix metalloprotease and stromelysin-3 cleave more efficiently synthetic substrates containing unusual amino acids in their P1' positions. ***J Biol Chem.*** 1998;273(5):2763-8.
243. Mueller MM, Fusenig NE. Tumor-stroma interactions directing phenotype and progression of epithelial skin tumor cells. ***Differentiation.*** 2002; 70(9-10): 486-97.
244. Murphy G, Segain JP, O'Shea M, Cockett M, Ioannou C, Lefebvre O, Chambon P, Basset P. The 28-kDa N-terminal domain of mouse stromelysin-3 has the general properties of a weak metalloproteinase. ***J Biol Chem.*** 1993; 268(21): 15435-41.
245. Murphy G. The ADAMs: signalling scissors in the tumour microenvironment. ***Nat Rev Cancer.*** 2008;8(12):929-41.
246. Murphy G, Murthy A, Khokha R. Clipping, shedding and RIPping keep immunity on cue. ***Trends Immunol.*** 2008;29(2):75-82.
247. Murphy G, Nagase H. Progress in matrix metalloproteinase research. ***Mol Aspects Med.*** 2008;29(5):290-308.
248. Murphy GJ, Murphy G, Reynolds JJ. The origin of matrix metalloproteinases and their familial relationships. ***FEBS Lett.*** 1991;289(1):4-7.
249. Nagase H, Visse R, Murphy G. Structure and function of matrix metalloproteinases and TIMPs. ***Cardiovasc Res.*** 2006;69(3):562-73.
250. Nakajima I, Muroya S, Tanabe R, Chikuni K. Positive effect of collagen V and VI on triglyceride accumulation during differentiation in cultures of bovine intramuscular adipocytes. ***Differentiation.*** 2002;70(2-3):84-91.
251. Nakamura ES, Koizumi K, Kobayashi M, Saiki I. Inhibition of lymphangiogenesis-related properties of murine lymphatic endothelial cells and lymph node metastasis of lung cancer by the matrix metalloproteinase inhibitor MMI270. ***Cancer Sci.*** 2004;95(1):25-31.
252. Nath D, Williamson NJ, Jarvis R, Murphy G. Shedding of c-Met is regulated by crosstalk between a G-protein coupled receptor and the EGF receptor and is mediated by a TIMP-3 sensitive metalloproteinase. ***J Cell Sci.*** 2001;114(Pt 6):1213-20.
253. Neville MC, Medina D, Monks J, Hovey RC. The mammary fat pad. ***J Mammary Gland Biol Neoplasia.*** 1998;3(2):109-16.
254. Neville MC, McFadden TB, Forsyth I. Hormonal regulation of mammary differentiation and milk secretion. ***J Mammary Gland Biol Neoplasia.*** 2002; 7(1): 49-66.
255. Ng ST, Zhou J, Adesanya OO, Wang J, LeRoith D, Bondy CA. Growth

hormone treatment induces mammary gland hyperplasia in aging primates. ***Nat Med.*** 1997;3(10):1141-4.

256. Nieman KM, Kenny HA, Penicka CV, Ladanyi A, Buell-Gutbrod R, Zillhardt MR, Romero IL, Carey MS, Mills GB, Hotamisligil GS, et al. Adipocytes promote ovarian cancer metastasis and provide energy for rapid tumor growth. ***Nat Med.*** 2011;17(11):1498-503.
257. Noë V, Fingleton B, Jacobs K, Crawford HC, Vermeulen S, Steelant W, Bruyneel E, Matrisian LM, Mareel M. Release of an invasion promoter E-cadherin fragment by matrilysin and stromelysin-1. ***J Cell Sci.*** 2001;114(Pt 1):111-118.
258. Noël A, Santavicca M, Stoll I, L'Hoir C, Staub A, Murphy G, Rio MC, Basset P. Identification of structural determinants controlling human and mouse stromelysin-3 proteolytic activities. ***J Biol Chem.*** 1995;270(39):22866-72.
259. Noël A, Boulay A, Kebers F, Kannan R, Hajitou A, Calberg-Bacq CM, Basset P, Rio MC, Foidart JM. Demonstration in vivo that stromelysin-3 functions through its proteolytic activity. ***Oncogene.*** 2000;19(12):1605-12.
260. Nozawa H, Chiu C, Hanahan D. Infiltrating neutrophils mediate the initial angiogenic switch in a mouse model of multistage carcinogenesis. ***Proc Natl Acad Sci U S A.*** 2006;103(33):12493-8.
261. Oakes SR, Rogers RL, Naylor MJ, Ormandy CJ. Prolactin regulation of mammary gland development. ***J Mammary Gland Biol Neoplasia.*** 2008; 13(1): 13-28.
262. O'Brien J, Schedin P. Macrophages in breast cancer: do involution macrophages account for the poor prognosis of pregnancy-associated breast cancer? ***J Mammary Gland Biol Neoplasia.*** 2009;14(2):145-57.
263. O'Brien J, Martinson H, Durand-Rougely C, Schedin P. Macrophages are crucial for epithelial cell death and adipocyte repopulation during mammary gland involution. ***Development.*** 2012;139(2):269-75.
264. Okada A, Tomasetto C, Lutz Y, Bellocq JP, Rio MC, Basset P. Expression of matrix metalloproteinases during rat skin wound healing: evidence that membrane type-1 matrix metalloproteinase is a stromal activator of pro-gelatinase A. ***J Cell Biol.*** 1997;137(1):67-77.
265. Padera TP, Kadambi A, di Tomaso E, Carreira CM, Brown EB, Boucher Y, Choi NC, Mathisen D, Wain J, Mark EJ, Munn LL, Jain RK. Lymphatic metastasis in the absence of functional intratumor lymphatics. ***Science.*** 2002; 296(5574): 1883-6.
266. Page-McCaw A, Ewald AJ, Werb Z. Matrix metalloproteinases and the regulation of tissue remodelling. ***Nat Rev Mol Cell Biol.*** 2007;8(3):221-33.
267. Pajvani UB, Trujillo ME, Combs TP, Iyengar P, Jelicks L, Roth KA, Kitsis RN, Scherer PE. Fat apoptosis through targeted activation of caspase 8: a new mouse model of inducible and reversible lipoatrophy. ***Nat Med.*** 2005; 11(7): 797-803.
268. Palavalli LH, Prickett TD, Wunderlich JR, Wei X, Burrell AS, Porter-Gill P, Davis S, Wang C, Cronin JC, Agrawal NS., et al. Analysis of the matrix

metalloproteinase family reveals that MMP8 is often mutated in melanoma. ***Nat Genet.*** 2009;41(5):518-20.
269. Pang WW, Hartmann PE. Initiation of human lactation: secretory differentiation and secretory activation. ***J Mammary Gland Biol Neoplasia.*** 2007; 12(4): 211-21.
270. Park JH, Park SM, Park KH, Cho KH, Lee ST. Analysis of apolipoprotein A-I as a substrate for matrix metalloproteinase-14. ***Biochem Biophys Res Commun.*** 2011;409(1):58-63.
271. Park JY, Park JH, Jang W, Hwang IK, Kim IJ, Kim HJ, Cho KH, Lee ST. Apolipoprotein A-IV is a novel substrate for matrix metalloproteinases. ***J Biochem.*** 2012; 151(3):291-8.
272. Parks WC, Wilson CL, López-Boado YS. Matrix metalloproteinases as modulators of inflammation and innate immunity. ***Nat Rev Immunol.*** 2004; 4(8): 617-29.
273. Patterson BC, Sang QA. Angiostatin-converting enzyme activities of human matrilysin (MMP-7) and gelatinase B/type IV collagenase (MMP-9). ***J Biol Chem.*** 1997; 272(46):28823-5.
274. Patterton D, Hayes WP, Shi YB. Transcriptional activation of the matrix metalloproteinase gene stromelysin-3 coincides with thyroid hormone-induced cell death during frog metamorphosis. ***Dev Biol.*** 1995;167(1):252-62.
275. Pavlovich AL, Manivannan S, Nelson CM. Adipose stroma induces branching morphogenesis of engineered epithelial tubules. ***Tissue Eng Part A.*** 2010; 16(12):3719-26.
276. Pei D, Majmudar G, Weiss SJ. Hydrolytic inactivation of a breast carcinoma cell-derived serpin by human stromelysin-3. J Biol Chem. 1994; 269(41): 25849-55.
277. Pei D, Weiss SJ. Furin-dependent intracellular activation of the human stromelysin-3 zymogen. ***Nature.*** 1995;375(6528):244-7.
278. Peruzzi D, Mori F, Conforti A, Lazzaro D, De Rinaldis E, Ciliberto G, La Monica N, Aurisicchio L. MMP11: a novel target antigen for cancer immunotherapy. ***Clin Cancer Res.*** 2009;15(12):4104-13.
279. Peschon JJ, Slack JL, Reddy P, Stocking KL, Sunnarborg SW, Lee DC, Russell WE, Castner BJ, Johnson RS, Fitzner JN, Boyce RW, Nelson N, Kozlosky CJ,Wolfson MF, Rauch CT, Cerretti DP, Paxton RJ, March CJ, Black RA. An essential role for ectodomain shedding in mammalian development. ***Science.*** 1998;282(5392):1281-4.
280. Pinilla S, Alt E, Abdul Khalek FJ, Jotzu C, Muehlberg F, Beckmann C, Song YH. Tissue resident stem cells produce CCL5 under the influence of cancer cells and thereby promote breast cancer cell invasion. ***Cancer Lett.*** 2009;284(1):80-5.
281. Pivetta E, Scapolan M, Pecolo M, Wassermann B, Abu-Rumeileh I, Balestreri L, Borsatti E, Tripodo C, Colombatti A, Spessotto P. MMP-13 stimulates osteoclast differentiation and activation in tumour breast bone metastases. ***Breast Cancer Res.*** 2011;13(5):R105.
282. Plump AS, Erickson SK, Weng W, Partin JS, Breslow JL, Williams DL. Apolipoprotein A-I is required for cholesteryl ester accumulation in steroidogenic

cells and for normal adrenal steroid production. ***J Clin Invest.*** 1996; 97(11): 2660-71.
283. Polyak K, Weinberg RA. Transitions between epithelial and mesenchymal states: acquisition of malignant and stem cell traits. ***Nat Rev Cancer.*** 2009; 9(4): 265-73.
284. Propper AY. Wandering epithelial cells in the rabbit embryo milk line. A preliminary scanning electron microscope study. ***Dev Biol.*** 1978;67(1):225-31.
285. Puzianowska-Kuznicka M, Damjanovski S, Shi YB. Both thyroid hormone and 9-cis retinoic acid receptors are required to efficiently mediate the effects of thyroid hormone on embryonic development and specific gene regulation in Xenopus laevis. ***Mol Cell Biol.*** 1997;17(8):4738-49.
286. Radisky DC, Levy DD, Littlepage LE, Liu H, Nelson CM, Fata JE, Leake D, Godden EL, Albertson DG, Nieto MA, Werb Z, Bissell MJ. Rac1b and reactive oxygen species mediate MMP-3-induced EMT and genomic instability. ***Nature.*** 2005; 436(7047):123-7.
287. Radisky DC, Hartmann LC. Mammary involution and breast cancer risk: transgenic models and clinical studies. ***J Mammary Gland Biol Neoplasia.*** 2009; 14(2): 181-91.
288. Radisky ES, Radisky DC. Matrix metalloproteinase- induced epithelial-mesenchymal transition in breast cancer. ***J Mammary Gland Biol Neoplasia.*** 2010; 15(2):201-12.
289. Redondo-Muñoz J, Ugarte-Berzal E, Terol MJ, Van den Steen PE, Hernández del Cerro M, Roderfeld M, Roeb E, Opdenakker G, García-Marco JA, García-Pardo A. Matrix metalloproteinase-9 promotes chronic lymphocytic leukemia b cell survival through its hemopexin domain. ***Cancer Cell.*** 2010; 17(2): 160-72.
290. Remacle AG, Golubkov VS, Shiryaev SA, Dahl R, Stebbins JL, Chernov AV, Cheltsov AV, Pellecchia M, Strongin AY. Novel MT1-MMP Small-Molecule Inhibitors Based on Insights into Hemopexin Domain Function in Tumor Growth. ***Cancer Res.*** 2012;72(9):2339-49.
291. Ribatti D. Endogenous inhibitors of angiogenesis: a historical review. ***Leuk Res.*** 2009;33(5):638-44.
292. Richards RG, Klotz DM, Walker MP, Diaugustine RP. Mammary gland branching morphogenesis is diminished in mice with a deficiency of insulin-like growth factor-I (IGF-I), but not in mice with a liver-specific deletion of IGF-I. ***Endocrinology.*** 2004;145(7):3106-10.
293. Rio MC, Lefebvre O, Santavicca M, Noël A, Chenard MP, Anglard P, Byrne JA, Okada A, Régnier CH, Masson R, Stromelysin-3 in the biology of the normal and neoplastic mammary gland. ***J Mammary Gland Biol Neoplasia.*** 1996;1(2): 231-40.
294. Rio MC. Strmelysin-3, a particular member of the matrix metalloproteinase family . ***Kluwer academic ed.,*** 2002; Vol.4, Dordrecht:Kluwer Acadimic Publisher, pp. 81-107.
295. Rio MC. From a unique cell to metastasis is a long way to go: clues to stromelysin-3 participation. ***Biochimie.*** 2005;87(3-4):299-306.

296. Rio MC. The Role of Cancer-Associated Adipocytes (CAA) in the Dynamic Interaction Between the Tumor and the Host: 2011; ***Springer SBM.***
297. Rio MC. Matrix metalloproteinase-11/stromelysin 3. Handbook of proteolytic enzymes 3rd Edition. ***Elsevier Editor.*** 2012 Chapter 160: pp 780-786.
298. Roarty K, Serra R. Wnt5a is required for proper mammary gland development and TGF-beta-mediated inhibition of ductal growth. ***Development.*** 2007; 134(21): 3929-39.
299. Robichaud TK, Steffensen B, Fields GB. Exosite interactions impact matrix metalloproteinase collagen specificities. ***J Biol Chem.*** 2011;286(43):37535-42.
300. Robinson GW, McKnight RA, Smith GH, Hennighausen L. Mammary epithelial cells undergo secretory differentiation in cycling virgins but require pregnancy for the establishment of terminal differentiation. ***Development.*** 1995; 121(7): 2079-90.
301. Robinson GW. Cooperation of signalling pathways in embryonic mammary gland development. ***Nat Rev Genet.*** 2007;8(12):963-72.
302. Robinson SD, Silberstein GB, Roberts AB, Flanders KC, Daniel CW. Regulated expression and growth inhibitory effects of transforming growth factor-beta isoforms in mouse mammary gland development. ***Development.*** 1991; 113(3):867-78.
303. Rocks N, Paulissen G, Quesada-Calvo F, Munaut C, Gonzalez ML, Gueders M, Hacha J, Gilles C, Foidart JM, Noel A, Cataldo DD. ADAMTS-1 metalloproteinase promotes tumor development through the induction of a stromal reaction in vivo. ***Cancer Res.*** 2008;68(22):9541-50.
304. Rodgers WH, Matrisian LM, Giudice LC, Dsupin B, Cannon P, Svitek C, Gorstein F, Osteen KG. Patterns of matrix metalloproteinase expression in cycling endometrium imply differential functions and regulation by steroid hormones. ***J Clin Invest.*** 1994;94(3):946-53.
305. Rønnov-Jessen L, Petersen OW, Koteliansky VE, Bissell MJ. The origin of the myofibroblasts in breast cancer. Recapitulation of tumor environment in culture unravels diversity and implicates converted fibroblasts and recruited smooth muscle cells. ***J Clin Invest.*** 1995;95(2):859-73.
306. Rosen ED, Sarraf P, Troy AE, Bradwin G, Moore K, Milstone DS, Spiegelman BM, Mortensen RM. PPAR gamma is required for the differentiation of adipose tissue in vivo and in vitro. ***Mol Cell.*** 1999;4(4):611-7.
307. Rossiter H, Barresi C, Ghannadan M, Gruber F, Mildner M, Födinger D, Tschachler E. Inactivation of VEGF in mammary gland epithelium severely compromises mammary gland development and function. ***FASEB J.*** 2007; 21(14): 3994-4004.
308. Rouyer N, Wolf C, Chenard MP, Rio MC, Chambon P, Bellocq JP, Basset P. Stromelysin-3 gene expression in human cancer: an overview. Invasion Metastasis. 1994-1995; 14(1-6):269-75.
309. Rozanov DV, Sikora S, Godzik A, Postnova TI, Golubkov V, Savinov A, Tomlinson S, Strongin AY. Non-proteolytic, receptor/ligand interactions associate cellular membrane type-1 matrix metalloproteinase with the complement

component C1q. ***J Biol Chem.*** 2004;279(48):50321-8.
310. Rupp PA, Visconti RP, Czirók A, Cheresh DA, Little CD. Matrix metalloproteinase 2-integrin alpha(v)beta3 binding is required for mesenchymal cell invasive activity but not epithelial locomotion: a computational time-lapse study. ***Mol Biol Cell.*** 2008;19(12):5529-40.
311. Rutkowski JM, Davis KE, Scherer PE. Mechanisms of obesity and related pathologies: the macro- and microcirculation of adipose tissue. ***FEBS J.*** 2009; 276(20):5738-46.
312. Sabeh F, Ota I, Holmbeck K, Birkedal-Hansen H, Soloway P, Balbin M, Lopez-Otin C, Shapiro S, Inada M, Krane S, Allen E, Chung D, Weiss SJ. Tumor cell traffic through the extracellular matrix is controlled by the membrane-anchored collagenase MT1-MMP. ***J Cell Biol.*** 2004;167(4):769-81.
313. Sabeh F, Shimizu-Hirota R, Weiss SJ. Protease-dependent versus -independent cancer cell invasion programs: three-dimensional amoeboid movement revisited. ***J Cell Biol.*** 2009;185(1):11-9.
314. Sakakura T, Nishizuka Y, Dawe CJ. Mesenchyme-dependent morphogenesis and epithelium-specific cytodifferentiation in mouse mammary gland. ***Science.*** 1976;194(4272):1439-41.
315. Sakakura T, Sakagami Y, Nishizuka Y. Dual origin of mesenchymal tissues participating in mouse mammary gland embryogenesis. ***Dev Biol.*** 1982; 91(1): 202-7.
316. Sakakura T. Embryogenesis. In: Neville M.C., Daniel C.W., editors. Development, Regulation and Function. ***New York: Plenum.*** 1987; pp 37-65.
317. Sakamoto T, Seiki M. Cytoplasmic tail of MT1-MMP regulates macrophage motility independently from its protease activity. ***Genes Cells.*** 2009; 14(5): 617-26.
318. Santavicca M, Noel A, Angliker H, Stoll I, Segain JP, Anglard P, Chretien M, Seidah N, Basset P. Characterization of structural determinants and molecular mechanisms involved in pro-stromelysin-3 activation by 4-aminophenylmercuric acetate and furin-type convertases. ***Biochem J.*** 1996;315 (Pt 3):953-8.
319. Sato-Kusubata K, Jiang Y, Ueno Y, Chun TH. Adipogenic histone mark regulation by matrix metalloproteinase 14 in collagen-rich microenvironments. ***Mol Endocrinol.*** 2011;25(5):745-53.
320. Schäffler A, Schölmerich J, Buechler C. Mechanisms of disease: adipokines and breast cancer - endocrine and paracrine mechanisms that connect adiposity and breast cancer. ***Nat Clin Pract Endocrinol Metab.*** 2007;3(4):345-54.
321. Schenk S, Hintermann E, Bilban M, Koshikawa N, Hojilla C, Khokha R, Quaranta V. Binding to EGF receptor of a laminin-5 EGF-like fragment liberated during MMP-dependent mammary gland involution. ***J Cell Biol.*** 2003; 161(1): 197-209.
322. Schönbeck U, Mach F, Sukhova GK, Atkinson E, Levesque E, Herman M, Graber P, Basset P, Libby P. Expression of stromelysin-3 in atherosclerotic lesions: regulation via CD40-CD40 ligand signaling in vitro and in vivo. ***J Exp Med.*** 1999;189(5):843-53.

323. Shi H, Seeley RJ, Clegg DJ. Sexual differences in the control of energy homeostasis. ***Front Neuroendocrinol.*** 2009;30(3):396-404.
324. Shi YB. Cell-cell and cell-ECM interactions in epithelial apoptosis and cell renewal during frog intestinal development. ***Cell Biochem Biophys.*** 1995; 27(3): 179-202.
325. Shi YB, Fu L, Hasebe T, Ishizuya-Oka A. Regulation of extracellular matrix remodeling and cell fate determination by matrix metalloproteinase stromelysin-3 during thyroid hormone-dependent post-embryonic development. ***Pharmacol Ther.*** 2007;116(3):391-400.
326. Shim KN, Jung SA, Joo YH, Yoo K. Clinical significance of tissue levels of matrix metalloproteinases and tissue inhibitors of metalloproteinases in gastric cancer. ***J Gastroenterol.*** 2007; 42(2):120-8.
327. Shimizu-Hirota R, Xiong W, Baxter BT, Kunkel SL, Maillard I, Chen XW, Sabeh F, Liu R, Li XY, Weiss SJ. MT1-MMP regulates the PI3Kδ.Mi-2/ NuRD-dependent control of macrophage immune function. ***Genes Dev.*** 2012; 26(4):395-413.
328. Shin YJ, Kim JH. The role of EZH2 in the regulation of the activity of matrix metalloproteinases in prostate cancer cells. ***PLoS One.*** 2012;7(1):e30393.
329. Simian M, Hirai Y, Navre M, Werb Z, Lochter A, Bissell MJ. The interplay of matrix metalloproteinases, morphogens and growth factors is necessary for branching of mammary epithelial cells. ***Development.*** 2001;128(16):3117-31.
330. Simian M, Bissell MJ, Barcellos-Hoff MH, Shyamala G. Estrogen and progesterone receptors have distinct roles in the establishment of the hyperplastic phenotype in PR-A transgenic mice. ***Breast Cancer Res.*** 2009;11(5):R72.
331. Singer CF, Marbaix E, Lemoine P, Courtoy PJ, Eeckhout Y. Local cytokines induce differential expression of matrix metalloproteinases but not their tissue inhibitors in human endometrial fibroblasts. ***Eur J Biochem.*** 1999;259(1-2):40-5.
332. Smith ML, Gourdon D, Little WC, Kubow KE, Eguiluz RA, Luna-Morris S, Vogel V. Force-induced unfolding of fibronectin in the extracellular matrix of living cells. ***PLoS Biol.*** 2007;5(10):e268.
333. Smookler DS, Mohammed FF, Kassiri Z, Duncan GS, Mak TW, Khokha R. Tissue inhibitor of metalloproteinase 3 regulates TNF-dependent systemic inflammation. ***J Immunol.*** 2006;176(2):721-5.
334. Soriano JV, Pepper MS, Nakamura T, Orci L, Montesano R. Hepatocyte growth factor stimulates extensive development of branching duct-like structures by cloned mammary gland epithelial cells. ***J Cell Sci.*** 1995;108 (Pt 2):413-30.
335. Soriano JV, Pepper MS, Orci L, Montesano R. Roles of hepatocyte growth factor/scatter factor and transforming growth factor-beta1 in mammary gland ductal morphogenesis. ***J Mammary Gland Biol Neoplasia.*** 1998;3(2):133-50.
336. Sounni NE, Dehne K, van Kempen L, Egeblad M, Affara NI, Cuevas I, Wiesen J, Junankar S, Korets L, Lee J, et al. Stromal regulation of vessel stability by MMP14 and TGFbeta. ***Dis Model Mech.*** 2010;3(5-6):317-32.
337. Sternlicht MD, Lochter A, Sympson CJ, Huey B, Rougier JP, Gray JW, Pinkel D, Bissell MJ, Werb Z. The stromal proteinase MMP3/stromelysin-1 promotes

mammary carcinogenesis. ***Cell.*** 1999;98(2):137-46.
338. Sternlicht MD, Werb Z. How matrix metalloproteinases regulate cell behavior. ***Annu Rev Cell Dev Biol.*** 2001;17:463-516.
339. Sternlicht MD. Key stages in mammary gland development: the cues that regulate ductal branching morphogenesis. ***Breast Cancer Res.*** 2006;8(1):201.
340. Sternlicht MD, Kouros-Mehr H, Lu P, Werb Z. Hormonal and local control of mammary branching morphogenesis. ***Differentiation.*** 2006;74(7):365-81.
341. Streuli C. Extracellular matrix remodelling and cellular differentiation. ***Curr Opin Cell Biol.*** 1999;11(5):634-40.
342. Strongin AY, Collier I, Bannikov G, Marmer BL, Grant GA, Goldberg GI. Mechanism of cell surface activation of 72-kDa type IV collagenase. Isolation of the activated form of the membrane metalloprotease. ***J Biol Chem.*** 1995; 270(10): 5331-8.
343. Stroud RE, Deschamps AM, Lowry AS, Hardin AE, Mukherjee R, Lindsey ML, Ramamoorthy S, Zile MR, Spencer WH, Spinale FG. Plasma monitoring of the myocardial specific tissue inhibitor of metalloproteinase-4 after alcohol septal ablation in hypertrophic obstructive cardiomyopathy. ***J Card Fail.*** 2005; 11(2): 124-30.
344. Struyf S, Proost P, Vandercappellen J, Dempe S, Noyens B, Nelissen S, Gouwy M, Locati M, Opdenakker G, Dinsart C, Van Damme J. Synergistic up-regulation of MCP-2/CCL8 activity is counteracted by chemokine cleavage, limiting its inflammatory and anti-tumoral effects. ***Eur J Immunol.*** 2009; 39(3): 843-57.
345. Talhouk RS, Chin JR, Unemori EN, Werb Z, Bissell MJ. Proteinases of the mammary gland: developmental regulation in vivo and vectorial secretion in culture. ***Development.*** 1991;112(2):439-49.
346. Talhouk RS, Bissell MJ, Werb Z. Coordinated expression of extracellular matrix-degrading proteinases and their inhibitors regulates mammary epithelial function during involution. ***J Cell Biol.*** 1992;118(5):1271-82.
347. Tan J, Buache E, Chenard MP, Dali-Youcef N, Rio MC. Adipocyte is a non-trivial, dynamic partner of breast cancer cells. ***Int J Dev Biol.*** 2011; 55(7-9): 851-9.
348. Tatti O, Vehviläinen P, Lehti K, Keski-Oja J. MT1-MMP releases latent TGF-beta1 from endothelial cell extracellular matrix via proteolytic processing of LTBP-1. ***Exp Cell Res.*** 2008;314(13):2501-14.
349. Thewes M, Worret WI, Engst R, Ring J. Stromelysin-3 (ST-3): immunohistochemical characterization of the matrix metalloproteinase (MMP)-11 in benign and malignant skin tumours and other skin disorders. ***Clin Exp Dermatol.*** 1999;24(2):122-6.
350. Trujillo ME, Scherer PE. Adipose tissue-derived factors: impact on health and disease. ***Endocr Rev.*** 2006;27(7):762-78.
351. Tuuttila A, Morgunova E, Bergmann U, Lindqvist Y, Maskos K, Fernandez-Catalan C, Bode W, Tryggvason K, Schneider G. Three-dimensional structure of human tissue inhibitor of metalloproteinases-2 at 2.1 A resolution. ***J Mol Biol.*** 1998;284(4):1133-40.

352. Tyan SW, Kuo WH, Huang CK, Pan CC, Shew JY, Chang KJ, Lee EY, Lee WH. Breast cancer cells induce cancer-associated fibroblasts to secrete hepatocyte growth factor to enhance breast tumorigenesis. ***PLoS One.*** 2011;6(1):e15313.
353. Ucar A, Vafaizadeh V, Jarry H, Fiedler J, Klemmt PA, Thum T, Groner B, Chowdhury K. miR-212 and miR-132 are required for epithelial stromal interactions necessary for mouse mammary gland development. ***Nat Genet.*** 2010; 42(12):1101-8.
354. Undén AB, Sandstedt B, Bruce K, Hedblad M, Stahle-Bäckdahl M. Stromelysin-3 mRNA associated with myofibroblasts is overexpressed in aggressive basal cell carcinoma and in dermatofibroma but not in dermatofibrosarcoma. ***J Invest Dermatol.*** 1996;107(2):147-53.
355. Ursin G, Parisky YR, Pike MC, Spicer DV. Mammographic density changes during the menstrual cycle. ***Cancer Epidemiol Biomarkers Prev.*** 2001; 10(2): 141-2.
356. Van den Steen PE, Proost P, Wuyts A, Van Damme J, Opdenakker G. Neutrophil gelatinase B potentiates interleukin-8 tenfold by aminoterminal processing, whereas it degrades CTAP-III, PF-4, and GRO-alpha and leaves RANTES and MCP-2 intact. ***Blood.*** 2000;96(8):2673-81.
357. Van Nguyen A, Pollard JW. Colony stimulating factor-1 is required to recruit macrophages into the mammary gland to facilitate mammary ductal outgrowth. ***Dev Biol.*** 2002;247(1):11-25.
358. Vassiliou S, Mucha A, Cuniasse P, Georgiadis D, Lucet-Levannier K, Beau F, Kannan R, Murphy G, Knäuper V, Rio MC, et al., Phosphinic pseudo-tripeptides as potent inhibitors of matrix metalloproteinases: a structure-activity study. ***J Med Chem.*** 1999;42(14):2610-20.
359. Vecchi M, Rudolph-Owen LA, Brown CL, Dempsey PJ, Carpenter G. Tyrosine phosphorylation and proteolysis. Pervanadate-induced, metalloprotease-dependent cleavage of the ErbB-4 receptor and amphiregulin. ***J Biol Chem.*** 1998; 273(32):20589-95.
360. Veltmaat JM, Mailleux AA, Thiery JP, Bellusci S. Mouse embryonic mammogenesis as a model for the molecular regulation of pattern formation. ***Differentiation.*** 2003;71(1):1-17.
361. Veltmaat JM, Van Veelen W, Thiery JP, Bellusci S. Identification of the mammary line in mouse by Wnt10b expression. ***Dev Dyn.*** 2004;229(2):349-56.
362. Veltmaat JM, Relaix F, Le LT, Kratochwil K, Sala FG, van Veelen W, Rice R, Spencer-Dene B, Mailleux AA, Rice DP., et al. Gli3-mediated somitic Fgf10 expression gradients are required for the induction and patterning of mammary epithelium along the embryonic axes. ***Development.*** 2006;133(12):2325-35.
363. Veronesi U, Boyle P, Goldhirsch A, Orecchia R, Viale G. Breast cancer. ***Lancet.*** 2005;365(9472):1727-41.
364. Vona-Davis L, Rose DP. Adipokines as endocrine, paracrine, and autocrine factors in breast cancer risk and progression. ***Endocr Relat Cancer.*** 2007; 14(2): 189-206.
365. Walker NI, Bennett RE, Kerr JF. Cell death by apoptosis during involution of

the lactating breast in mice and rats. ***Am J Anat.*** 1989;185(1):19-32.
366. Wang CS, Têtu B. Stromelysin-3 expression by mammary tumor-associated fibroblasts under in vitro breast cancer cell induction. ***Int J Cancer.*** 2002; 99(6): 792-9.
367. Wang X, Zhang X, Sun L, Subramanian B, Maffini MV, Soto A, Sonnenschein C, Kaplan DL. Preadipocytes stimulate ductal morphogenesis and functional differentiation of human mammary epithelial cells on 3D silk scaffolds. ***Tissue Eng Part A.*** 2009;15(10):3087-98.
368. Watson CJ. Involution: apoptosis and tissue remodelling that convert the mammary gland from milk factory to a quiescent organ. ***Breast Cancer Res.*** 2006; 8(2):203.
369. Watson CJ, Khaled WT. Mammary development in the embryo and adult: a journey of morphogenesis and commitment. ***Development.*** 2008; 135(6): 995-1003.
370. Weathington NM, van Houwelingen AH, Noerager BD, Jackson PL, Kraneveld AD, Galin FS, Folkerts G, Nijkamp FP, Blalock JE. A novel peptide CXCR ligand derived from extracellular matrix degradation during airway inflammation. ***Nat Med.*** 2006;12(3):317-23.
371. Weiss SJ, Peppin G, Ortiz X, Ragsdale C, Test ST. Oxidative autoactivation of latent collagenase by human neutrophils. ***Science.*** 1985;227(4688):747-9.
372. Werb Z. ECM and cell surface proteolysis: regulating cellular ecology. ***Cell.*** 1997;91(4):439-42.
373. Weskamp G, Ford JW, Sturgill J, Martin S, Docherty AJ, Swendeman S, Broadway N, Hartmann D, Saftig P, Umland S., et al. ADAM10 is a principal 'sheddase' of the low-affinity immunoglobulin E receptor CD23. ***Nat Immunol.*** 2006; 7(12):1293-8.
374. Whitelock JM, Murdoch AD, Iozzo RV, Underwood PA. The degradation of human endothelial cell-derived perlecan and release of bound basic fibroblast growth factor by stromelysin, collagenase, plasmin, and heparanases. ***J Biol Chem.*** 1996; 271(17):10079-86.
375. Wiseman BS, Werb Z. Stromal effects on mammary gland development and breast cancer. ***Science.*** 2002;296(5570):1046-9.
376. Wiseman BS, Sternlicht MD, Lund LR, Alexander CM, Mott J, Bissell MJ, Soloway P, Itohara S, Werb Z. Site-specific inductive and inhibitory activities of MMP-2 and MMP-3 orchestrate mammary gland branching morphogenesis. ***J Cell Biol.*** 2003;162(6):1123-33.
377. Witters L, Scherle P, Friedman S, Fridman J, Caulder E, Newton R, Lipton A. Synergistic inhibition with a dual epidermal growth factor receptor/HER-2/neu tyrosine kinase inhibitor and a disintegrin and metalloprotease inhibitor. ***Cancer Res.*** 2008;68(17):7083-9.
378. Witty JP, Wright JH, Matrisian LM. Matrix metalloproteinases are expressed during ductal and alveolar mammary morphogenesis, and misregulation of stromelysin-1 in transgenic mice induces unscheduled alveolar development. ***Mol Biol Cell.*** 1995;6(10):1287-303.

379. Wolf C, Chenard MP, Durand de Grossouvre P, Bellocq JP, Chambon P, Basset P. Breast-cancer-associated stromelysin-3 gene is expressed in basal cell carcinoma and during cutaneous wound healing. ***J Invest Dermatol.*** 1992; 99(6): 870-2.
380. Wolf K, Wu YI, Liu Y, Geiger J, Tam E, Overall C, Stack MS, Friedl P. Multi-step pericellular proteolysis controls the transition from individual to collective cancer cell invasion. ***Nat Cell Biol.*** 2007;9(8):893-904.
381. Wu E, Mari BP, Wang F, Anderson IC, Sunday ME, Shipp MA. Stromelysin-3 suppresses tumor cell apoptosis in a murine model. ***J Cell Biochem.*** 2001;82(4):549-55.
382. Wu Y, Smas CM. Wdnm1-like, a new adipokine with a role in MMP-2 activation. ***Am J Physiol Endocrinol Metab.*** 2008;295(1):E205-15.
383. Wyckoff J, Wang W, Lin EY, Wang Y, Pixley F, Stanley ER, Graf T, Pollard JW, Segall J, Condeelis J. A paracrine loop between tumor cells and macrophages is required for tumor cell migration in mammary tumors. ***Cancer Res.*** 2004; 64(19): 7022-9.
384. Xu J, Rodriguez D, Petitclerc E, Kim JJ, Hangai M, Moon YS, Davis GE, Brooks PC. Proteolytic exposure of a cryptic site within collagen type IV is required for angiogenesis and tumor growth in vivo. ***J Cell Biol.*** 2001; 154(5): 1069-79.
385. Xu R, Boudreau A, Bissell MJ. Tissue architecture and function: dynamic reciprocity via extra- and intra-cellular matrices. ***Cancer Metastasis Rev.*** 2009; 28(1-2):167-76.
386. Yamaguchi J, Ohtani H, Nakamura K, Shimokawa I, Kanematsu T. Prognostic impact of marginal adipose tissue invasion in ductal carcinoma of the breast. ***Am J Clin Pathol.*** 2008;130(3):382-8.
387. Yeh WL, Lu DY, Lee MJ, Fu WM. Leptin induces migration and invasion of glioma cells through MMP-13 production. ***Glia.*** 2009;57(4):454-64.
388. Yoo YA, Kang MH, Lee HJ, Kim BH, Park JK, Kim HK, Kim JS, Oh SC. Sonic hedgehog pathway promotes metastasis and lymphangiogenesis via activation of Akt, EMT, and MMP-9 pathway in gastric cancer. ***Cancer Res.*** 2011; 71(22): 7061-70.
389. Yu Q, Stamenkovic I. Localization of matrix metalloproteinase 9 to the cell surface provides a mechanism for CD44-mediated tumor invasion. ***Genes Dev.*** 1999; 13(1):35-48.
390. Yu Q, Stamenkovic I. Cell surface-localized matrix metalloproteinase-9 proteolytically activates TGF-beta and promotes tumor invasion and angiogenesis. ***Genes Dev.*** 2000;14(2):163-76.
391. Yu WH, Woessner JF Jr, McNeish JD, Stamenkovic I. CD44 anchors the assembly of matrilysin/MMP-7 with heparin-binding epidermal growth factor precursor and ErbB4 and regulates female reproductive organ remodeling. ***Genes Dev.*** 2002;16(3):307-23.
392. Zangani D, Darcy KM, Shoemaker S, Ip MM. Adipocyte-epithelial interactions regulate the in vitro development of normal mammary epithelial cells. ***Exp Cell Res.*** 1999;247(2):399-409.

393. Zarrabi K, Dufour A, Li J, Kuscu C, Pulkoski-Gross A, Zhi J, Hu Y, Sampson NS, Zucker S, Cao J. Inhibition of matrix metalloproteinase 14 (MMP-14)-mediated cancer cell migration. ***J Biol Chem.*** 2011; 286(38): 33167-77.
394. Zarzynska J, Motyl T. Apoptosis and autophagy in involuting bovine mammary gland. ***J Physiol Pharmacol.*** 2008;59 Suppl 9:275-88.
395. Zhang H, Qi M, Li S, Qi T, Mei H, Huang K, Zheng L, Tong Q. microRNA-9 targets matrix metalloproteinase 14 to inhibit invasion, metastasis and angiogenesisof neuroblastoma cells. ***Mol Cancer Ther.*** 2012 May 7. [Epub ahead of print].
396. Zhang P, Takeuchi K, Csaki LS, Reue K. Lipin-1 phosphatidic phosphatase activity modulates phosphatidate levels to promote peroxisome proliferator-activated receptor γ (PPARγ) gene expression during adipogenesis. ***J Biol Chem.*** 2012;287(5):3485-94.
397. Zhang X, Halvorsen K, Zhang CZ, Wong WP, Springer TA. Mechanoenzymatic cleavage of the ultralarge vascular protein von Willebrand factor. ***Science.*** 2009; 324(5932):1330-4.

Chapter 6 Publications and Oral Communication

Publications:

1. Tan J, Buache E, Chenard MP, Dali-Youcef N and Rio MC. Adipocyte is a non-trivial, dynamic partner of breast cancer cells. Int J Dev Biol. 2011; 55(7-9):851-9.
2. Tan J, Buache E, Daguenet E, Alpy F, Tomasetto C, Ren G and Rio MC. Environmental matrix metalloproteinase 11 is required for correct mammary gland post-natal morphogenesis and function (In preparation).

Oral Communication:

Tan J, Buache E, Alpy F, Tomasetto C and Rio MC: The technic of transgenic mouse model construction-MMP11 transgenic mouse as example. The 5th Chinese-French International Breast Cancer Conference. April 22nd, 2012. Chongqing. China.

Int. J. Dev. Biol. 55: 851-858
doi: 10.1387/ijdb.113392jt

INTERNATIONAL JOURNAL OF DEVELOPMENTAL BIOLOGY
www.intjdevbiol.com

Adipocyte is a non-trivial, dynamic partner of breast cancer cells

JINXIANG TAN[1*], EMILIE BUACHE[1*], MARIE-PIERRE CHENARD[2], NASSIM DALI-YOUCEF[1*], MARIE-CHRISTINE RIO[1*]

[1]Institut de Génétique et de Biologie Moléculaire et Cellulaire (IGBMC), Functional Genomics and Cancer Department, Centre National de la Recherche Scientifique UMR 7104, Institut National de la Santé et de la Recherche Médicale U964, Université de Strasbourg, France, [2]Centre Hospitalier Universitaire de Hautepierre, Département de Pathologie and [3]Université de Strasbourg et de Génétique Médicale, Hôpitaux Universitaires de Strasbourg, Strasbourg, France

ABSTRACT While the participation of adipocytes is well known in tissue architecture, energy supply and endocrine processes, their implication during natural cancer history is just beginning to unfold. An extensive review of the literature concerning the impact of resident adipocytes on breast cancer development/progression was performed. This review provides *in vitro* and *in vivo* evidence that adipocytes located close to invasive cancer cells, referred to as cancer-associated adipocytes (CAAs), are essential for breast tumor development/progression. Their deleterious function is dependent, at least partly, on their crosstalk with invasive cancer cells. Indeed, this event leads to dramatic phenotypic and/or functional modifications of both cell types. Adipocytes exhibit delipidation and acquire a fibroblast-like shape. In parallel, cancer cell aggressiveness is exacerbated through increased migratory and invasive properties. Moreover, obesity is currently a sign of poor prognosis in human carcinomas. In this context, a high number of "obese" resident adipocytes might be predicted to be detrimental. Accordingly, there are some similarities between the molecular alterations observed in hypertrophied adipocytes and in CAAs. How adipocytes function to favor tumorigenesis at the molecular level remains largely unknown. Nevertheless, progress has been made recently and molecular clues are starting to emerge. Deciphering the cellular and molecular mechanisms behind the adipocyte-cancer cell heterotypic crosstalk is of great interest since it might provide new targets for improving diagnosis/prognosis and for the design of innovative therapeutic strategies. They might also improve our understanding of the relationship between obesity/metabolic disorders and cancer risk and/or poor patient outcome.

KEY WORDS: *adipocyte, breast cancer, metabolism, obesity, diabetes*

Introduction

It is now well established that the tumor microenvironment actively participates in breast cancer progression (Hanahan *et al.*, 1996; Joyce, 2005; Kessenbrock *et al.*, 2010). The connective tissue, also named stroma, is a complex structure composed of an extracellular matrix (ECM), and a variety of cell types including endothelial cells, inflammatory cells, fibroblasts, fibroblast-like cells and adipocytes. The present review is restricted to the latter cell type, and more precisely to the impact of mammary gland resident adipocytes on breast cancers. The first part focuses on cancer-associated adipocytes (CAAs) as key regulators of tumor-stroma cell growth, local invasion and/or metastases in carcinogenesis. Although the nature of interplay between adipocytes and cancer cells remains at present largely unknown, investigations in the last few years indeed show that the adipocyte occupies a central place in this disease. The morphological and functional alterations

Abbreviations used in this paper: Ad-adipocyte, cultured alone; Ad_{BCC}-adipocyte cultured in the presence of breast cancer cells; BCC, breast cancer cells cultured alone; BCC_{Ad}, breast cancer cells cultured in the presence of adipocytes; CAAs, cancer-associated adipocytes; CAF, cancer-associated fibroblasts; ECM, extracellular matrix; ER, estrogen receptor; MMP, matrix metalloproteinase.

*Address correspondence to: Marie-Christine Rio, IGBMC, 1 rue L Fries, B.P. 10142, 67404 Illkirch cedex, France. Tel: +44 388 65 3424. Fax: +44 388 65 3201. e-mail: mcr@igbmc.fr - web: http://www.igbmc.fr. #Note: these authors contributed equally to this work.

Final, author-corrected PDF published online: 2 September 2011.

ISSN: Online 1696-3547, Print: 0214-6282

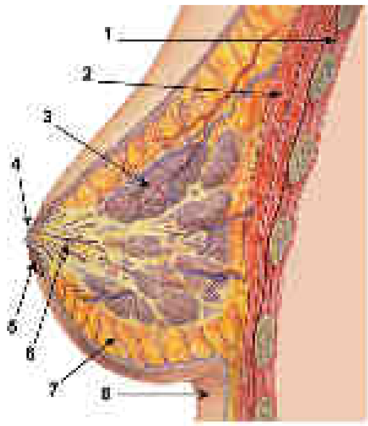

Fig. 1. Schematic diagram of normal breast (adult female human cross-section, *Wikipedia). 1, chest wall; 2, pectoralis muscles; 3, lobules; 4, nipple; 5, areola; 6, duct; 7, fatty tissue; 8, skin. Resident adipocytes represent one of the predominant cell types of the mammary gland.*

in both adipocytes and cancer cells induced by the CAA-cancer cell heterotypic crosstalk, are discussed, as well as the emerging molecular basis that underlies the deleterious effect of CAAs on the behavior of cancer cells. The second part focuses on how adipocyte alterations due to metabolic diseases (e.g. obesity, diabetes) might impact the development and progression of breast cancers. A thorough understanding of the role of adipocytes in mammary gland tumorigenesis could present numerous opportunities to improve tumor prognosis, to design innovative therapies and/or to modify breast cancer risk.

Cancer-associated adipocyte (CAA)-cancer cell cross-talk favors breast tumor progression

The role of adipocytes in the normal breast

The mammary gland is a dynamic organ that continually changes its architecture and function. Reciprocal interactions between the epithelium and the connective tissues exert profound effects on mammary gland morphogenesis, development and homeostasis, even though the details of these events are not fully understood. The normal development and function of the mammary gland are reviewed elsewhere in the present issue. Here only a brief overview of the anatomy of the human adult mammary gland is given in order to better understand the particular place of the adipocyte in breast tissues. The fully differentiated breast (after the first gestation lactation cycle) is composed of two cell compartments (Fig. 1). The epithelial compartment is constituted by the gland (strictly speaking) composed of branched ducts and lobuloalveolar differentiated units able to produce milk proteins when necessary. This gland is embedded in the connective tissue compartment commonly referred to as the mammary fat pad (Hovey and Aimo, 2010) since it mainly contains adipose tissues. In man, the mammary adipose depot is composed of fat lobules involving 100-1000 mature white adipocytes and stromal-vascular cells, blood vessels, lymph nodes and nerves.

In a general manner, each adipocyte is itself encapsulated by a basement membrane. Once cells are committed pre-adipocytes, the original ECM is remodeled. Indeed, adipogenesis is characterized by the conversion of a fibronectin-rich matrix to a basement membrane (Gregoire, 2001). During adipocyte differentiation, there is an increase in the secretion of basement membrane components such as type IV and VI collagens (Nakajima *et al.*, 2002; Iyengar *et al.*, 2003). Thus, in a general fashion, normal mature adipocytes are separated from epithelial cells by basement membranes, limiting therefore the possibilities of heterotypic cross-talk between the 2 cell types. In the normal breast, this equilibrium is dramatically disrupted during the post-weaning mammary gland involution. At this time, there is an intense restructuration of the gland and cells of the 2 compartments are mixed together within the ECM, as observed in invasive mammary tumors (Lochter *et al.*, 1997).

Thus, fat tissue represents an important component of the normal breast. This obvious proximity of adipocytes and epithelial cells in the breast allows one to hypothesize that adipocytes might play a role during tumor progression.

Histological evidence that adipocytes participate in breast cancer

The role of adipocytes during cancer invasive processes has until recently been neglected. This lapse was mainly due to the fact that adipocytes disappear rapidly via the desmoplastic response of connective tissues during the early invasive steps. Thus, histological images of breast tumor biopsies contain very few adipocytes, or most often are totally devoid of adipocytes. However, from the breast anatomy (see above and Fig. 1), it might be expected that early local tumor invasion occurs in the immediate proximity of pre-adipocytes and/or adipocytes, allowing heterotypic cross-talk between invasive cancer cells and adipocytes, even if this event is ephemeral. In this context, histological sections of human breast carcinomas show that dynamic desmoplastic events involving adipocytes occur at the tumor invasive front located at the periphery of primary tumors (Fig. 2) (Andarawewa *et al.*, 2005) (Dirat *et al.*, 2011). Indeed, this area is devoid of fully constituted stroma and exhibits a high ratio

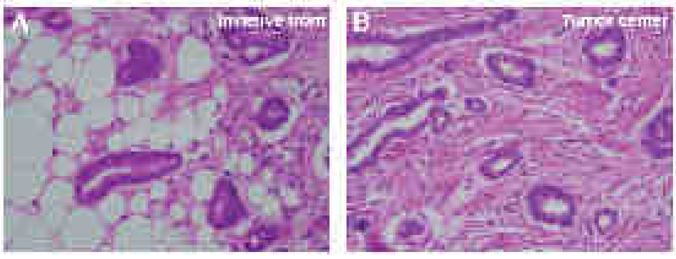

Fig. 2. Histology of the invasive front and the center of a human breast carcinoma. *Hematoxylin-eosin, histological examination. (A) The invasive front of a primary tumor. Components of connective tissues are dramatically modified in response to cancer cell local invasion. Most importantly, CAAs (spots in white color) located at the interface of invading cancer cells exhibit reduced size in comparison with normal adipocytes located in adult tissue.* **(B)** *The center of the same tumor shows a predominance of fibroblasts/fibroblast-like cells (CAFs), and adipocytes are no longer present.*

of adipocytes to fibroblasts. Interestingly, a reduction in adipocyte size compared with those observed at a distance is observed. This also results in reduction of adipocytes in cell lipolysis, modification of lipid droplets and modification of adipocyte-related basement membrane and the ECM. By contrast, at the tumor center, an extremely high fibroblast like cell adipocyte ratio is observed in the stroma surrounding cancer cells. Thus, one of the most obvious morphological changes that occur consecutively to cancer cell invasion concerns adipocytes, pointing out the notion of CAAs. It is therefore clear that CAA-cancer cell heterotypic crosstalk occurs at least in invasive primary tumors, when both cell types are physically close during the dynamic tumor progression processes. This event leads to a kind of 'adipocyte dedifferentiation' and ultimately to an accumulation of fibroblast like cells. Tumor progression may thus depend on the CAA "activation" induced by invading cancer cell stroma. Moreover, these data strongly support the concept that cancer-associated fibroblasts (CAFs) might at least partly derive from CAAs (Andarawewa *et al.* 2005; Mohsen and Ho, 2008). Interestingly, numerous studies have shown that peritumor fibroblasts provide structural and biochemical support for cancer development (Hanahan Jessen *et al.*, 1995)(Kessenbrock *et al.*, 2010).

Thus, the adipocyte is an excellent candidate to play a key role in influencing tumor behavior through heterotypic crosstalk with invasive cancer cells. In turn, signaling pathways critical for cancer cell survival, tumor growth and/or metastasis development may be inadvertently activated.

In vivo evidence that adipocytes favor tumor progression

Does CAA-cancer cell cross-talk have a deleterious impact on tumor progression? Numerous recent clinical studies have evaluated the prognostic value of local adipocytes invasion by cancer cells at the tumor margin. Most of the data report a positive correlation with poor patient outcome. This is the case not only for breast cancers (Kinjima et al., 2000, Yamaguchi et al., 2006), but also for prostate, pancreas, kidney and colon cancers (Tan, 2011). Experimental data report a similar pejorative impact of adipocytes on cancer progression. It was shown that an adipocyte rich environment facilitates B16 murine mammary carcinoma cell growth after subcutaneous injection in mice, and it was proposed that the adipose tissue exerts an estrogen-dependent positive regulatory effect on B16 (Elliott et al., 1992). The impact of the mammary fat pad in tumor development has also been extensively studied (Edwards 2008). Moreover, adipose stromal cells have been shown to stimulate the migration and invasion of estrogen receptor (ER) negative breast cancer cells *in vitro* and *in vivo* in a co-transplant xenograft mouse model. However, it should be noted that both the mammary fat pad and adipose stromal cells include both pre-adipocytes and/or adipocytes, as well as other cells like endothelial cells, that may interfere. An *in vivo* competition system using 3T3-L1 murine adipocytes and BLM1d3GFP human breast cancer cells to recapitulate heterotypic crosstalk occurring in primary breast tumors has demonstrated that adipocytes favor tumorigenesis (Iyengar et al., 2003). Using a similar model, it has recently been shown that adipocytes also favor metastasis development. Indeed, tail vein injection of breast cancer cells previously co-cultured in the presence of adipocytes gives more lung metastases than breast cancer cells grown without adipocytes (Dirat et al., 2011).

Thus, clinical observations and *in vivo* experimental data strongly support a major function for mammary gland resident adipocytes in tumor progression.

In vitro evidence that adipocytes favor cancer cell aggressiveness

Because *in vivo*, several other local or systemic factors might interfere, *in vitro* cell models have been designed to uncover the intrinsic properties and functions of adipocytes in breast cancer. The cellular influence of pre-adipocytes and mature adipocytes on various cancer cell lines have been studied by several laboratories. Mature adipocytes, but not pre-adipocytes, have been shown to promote the growth of breast cancer cells in collagen gel matrix cultures through cancer stromal cell interactions (Manabe *et al.*, 2008). More recently, a co-culture system in which adipocytes and breast cancer cells were separated by an insert to allow the diffusion of soluble factors, but not direct, heterotypic cell-cell contact, was used to mimic the CAA-cancer cell crosstalk. The impact of this co-culture on both adipocytes and cancer cells was evaluated. As expected from previous histological studies (see above), dramatic morphological changes were observed in adipocytes co-cultured in the presence of breast cancer cells (Ad_{BCC}) compared with those cultured alone (Ad). As observed at the invasive front of breast primary tumors, adipocytes became more elongated and exhibited a fibroblast-like phenotype with delipidation (Fig. 3). There was no obvious alteration in cancer cell morphology. However, adipocyte-primed cancer cells ($HBC)_{Ad}$ adopted new phenotypes, notably an increased migration and invasive phenotype compared with cancer cells that had not "seen" adipocytes (BCC) (Fig. 4) (Dirat et al., 2011) (our unpublished results). Thus, this model satisfactorily recapitulates the invasive front of human breast tumors. These data indicate that soluble factors resulting from the adipocyte-cancer cell crosstalk impact both cell types. Indeed, adipocyte derived secreted factors have been shown to promote breast cancer cell proliferation and

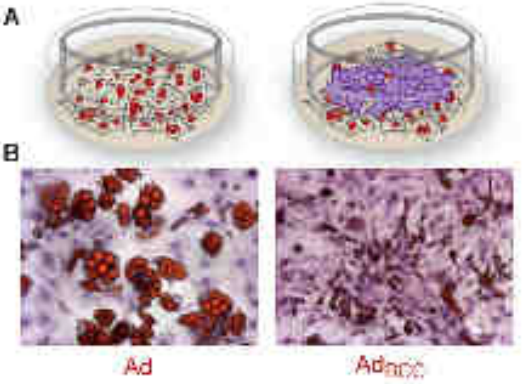

Fig. 3. *In vitro* adipocyte-cancer cell crosstalk leads to adipocyte "dedifferentiation". **(A)** *Schemes of the co-culture model which allows the passage of soluble factors but denies of heterotypic cell-cell contact.* **(B)** *Adipocytes cultured for six days alone (Ad) or with breast cancer cells (Ad_{BCC}). Note delipidation and morphological fibroblast-like phenotype acquired by adipocytes cultured along cells. The alterations observed in Ad_{BCC} are similar to those observed *in vivo* in CAAs at the invasive front of breast tumors (see Figure 2). Cytokeratin 8/18 staining (brown).*

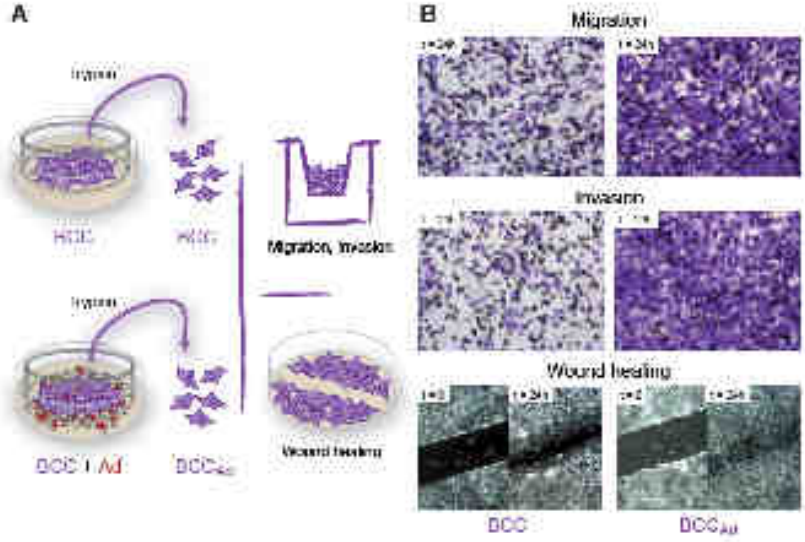

Fig. 4. *In vitro* adipocyte-cancer cell crosstalk increases cancer cell aggressiveness. (A) *Schematic of the co-culture experiments.* Breast cancer cells cultured in the presence (BCC$_{Ad}$) or in the absence (BCC) of adipocytes were further used to study their aggressive properties (migration, invasion, wound healing). (B) *Histographs show cells conversion through the membrane and pores of the lower surface.* BCC$_{Ad}$ *also increased cancer cell migration and invasion compared with* BCC; *wound closure is also higher for* BCC$_{Ad}$ *than* BCC (= *open wound healing*) *at 24 h.*

invasion (Iyengar et al., 2003).

Interestingly, similar effects have been reported using other types of cancer cells. Adipocytes have been shown to promote the proliferation of colon and prostate cancer cells, indicating that this pro-carcinoma is not limited to breast cancers but is a general event (Tan, 2011).

Collectively these data indicate that *in vitro* adipocyte-cancer cell crosstalk leads to the production of soluble factors that increase cancer cell aggressiveness.

Molecular characterization of the adipocyte-cancer cell crosstalk

To date, the molecular mechanisms responsible for the pro-invasive impact between *in vivo*/*in vitro* CAAs/adipocyte-cancer cell heterotypic crosstalk have remained largely unknown. However, it might be hypothesized that they include paracrine pathways acting in both directions: from invasive cancer cells to adipocytes/CAAs and from adipocytes/CAAs to cancer cells. Moreover, adipocyte- or cancer cell-specific autocrine pathways might also be activated. The few results to date indicate that various biological processes are affected, including tissue remodeling, adipogenesis/energy metabolism, angiogenesis, inflammation and immune response.

ECM remodeling related factors

There is some evidence that adipocyte ECM and ECM-related enzymes are modified, which is consistent with the dynamic modification in CAA morphology. Matrix metalloproteinase (MMP)s are enzymes specialized in ECM remodeling. They have been shown to be involved at several steps of cancer development and represent markers of poor prognosis in breast cancer (Basset et al., 1990; Jodele et al., 2006; Kessenbrock et al., 2010). MMPs are mainly paracrine factors which are expressed and secreted by connective tissue cells. Immunohistochemical analysis of the breast cancer invasive front shows that MMP11 (also named stromelysin-3) is expressed by CAAs at the proximity of invading cancer cells. In contrast, normal resting mature adipocytes are devoid of MMP11. Thus, cancer cells induce MMP11 expression in CAAs (Fig. 1g). Interestingly, MMP11 has been shown to play a role in adipogenesis since it decreases preadipocyte differentiation. Moreover, *in vitro* addition of active MMP11 recombinant protein to the culture medium of mature adipocytes induces their "de-differentiation" (Andarawewa et al., 2005). Collectively, these data indicate that the positive regulatory function on adipogenesis of MMP11 is aberrantly restored during the early steps of local tumor invasion. MMP11 therefore participates in the accumulation of fibroblast-like cells that might in reality be pre-adipocytes or de-differentiated adipocytes, since these cells are morphologically indistinguishable from fibroblasts. Accordingly, at later points of invasive carcinoma development when the constituted stroma no longer contains adipocytes, MMP11 is restricted to a particular subpopulation of fibroblast-like cells that are not myofibroblasts (Fig. 1i) (Andarawewa et al., 2005). Interestingly, the concept of "cancer cell imprinted" fibroblasts which express MMP11 has been proposed in studies using CAFs and cancer cells isolated from human breast tumors (Wang and Lotz, 2005). Consistently, in the *in vitro* model described above, adipocytes co-cultured with cancer cells (Ad$_{BCC}$) exhibit an activated phenotype marked by MMP11 overexpression (Tiwari et al., 2011) (our unpublished results). In addition to MMP11, MMP1 and MMP10 expression are also upregulated but by cancer cells (BCC$_{Ad}$) (Iyengar et al., 2003; Kim et al., 2008). It cannot be excluded that some other MMPs might similarly be involved in adipocyte-cancer cell crosstalk as several MMPs contribute to adipogenesis as either positive or negative regulators (Andarawewa and Hin, 2008). Finally, the enzymatic plasminogen system is also involved since the inhibitor of plasminogen activator (PAI1) is overexpressed in adipocytes (Ad$_{BCC}$).

One of the ECM components that is altered is type VI collagen, a specific member of the extracellular collagen family with predominant expression in the adipose tissue. Type VI collagen was shown to be up-regulated in adipocytes during tumorigenesis and to be critical for tumor progression due to effects of a alpha 3 chain C-terminal

fragment (Iyengar et al., 2005). Interestingly, it has recently been shown that MMP11 cleaves the native alpha 3 chain of collagen VI. The MMP11 ascribed collagenolytic activity is functional during fat tissue compaction as well as during the cancer invasive steps (Maquoi et al., 2008). Laminin and alpha 2 integrin have also been shown to be overexpressed by cancer cells following adipocyte-cancer cell crosstalk (Iyengar et al., 2005).

Angiogenesis related factors

Adipocytes might locally provide growth/survival support to cancer cells via the secretion of various adipokines, growth factors and cytokines (Maeda et al., 1997). The sequential morphological modification of CAAs from mature adipocytes to fibroblast-like cells implies fibroblasts and a defect in canonical adipocyte-differentiating factors. Consistently, adipocytes co-cultured with cancer cells exhibit decreased mRNA levels for PPARγ, aP2, LPL-HPs, resistin and perilipin, sensitive lipase (HSL) (Dirat et al., 2011). Moreover, the *in vitro* reconstituted MMP11-induced adipocyte 'de-differentiation' is also associated with the downregulation at the transcriptional level of PPARγ and aP2 (Andarawewa et al., 2005). Moreover, CAAs have been shown to express abnormal levels of growth factors (IGF1, IGFBPs) and adipokines (leptin and adiponectin). There is increasing evidence that adiponectin and leptin, secreted by peritumor adipose tissues in several cancers including breast, are important (Miyoshi et al., 2006; Schaffler et al., 2007). Leptin appears to be a positive factor for tumor development and aggressiveness, while adiponectin protects against cancers.

Immune response and inflammation related factors

A study profiling gene expression of breast cancer cells treated with adipocyte culture medium showed induction of several immune system related genes (Kim et al., 2009). *In vitro* activated adipocytes or cultures with cancer cells (Ad_{bcc}) also overexpress pro-inflammatory cytokines (IL-6, IL-1β) (Dirat et al., 2011). Interestingly, it has been reported that the process of migration and invasion of estrogen receptor (ER)-negative breast cancer cells is dependent on adipocyte-secreted IL-6 (Walter et al., 2009).

Oncogenesis related factors

Analysis of adipocyte stained cancer cells (eCC_{Ad}) showed several modifications in gene expression patterns. The affected genes have been shown to be involved in various cellular functions but all are known to contribute to tumor development/progression. Thus, cyclin D1, NFκB, cFos, ATF3, SOX9, A20 and IGF2 are overexpressed while E-cadherin is down-regulated (Iyengar et al., 2005) (Dirat et al., 2011).

Thus, resident mammary gland adipocytes play an essential role during the first steps of the tumor stromagenic response. Adipocyte/CAA-cancer cell crosstalk induces dramatic changes in the production of molecules able to potentially impact on cancer cell survival, proliferation and differentiation as well as invasive properties (Fig. 4).

Conclusion

Collectively, these data support the concept that crosstalk with adipocytes confers a selective advantage to invasive cancer cells. Adipocytes therefore participate in a kind of vicious tumor progression cycle, initiated by the invasive cancer cells (Fig. 5) (Montague and Hay, 2008). Although some clues have started to emerge, most of the molecular mechanisms involved remain to be determined.

Do adipocyte/metabolic disorders impact on breast cancer development/progression?

Epidemiological evidence that obesity and insulin resistance/diabetes are detrimental for breast cancer patients

From the studies described above, an obvious concern is whether modifications in mammary resident adipocytes influence breast health. Normal adipocyte size heterogeneity (cell size) often precedes hyperplastic processes (cell number). Adipocyte hypertrophy in vivo results from excess triglyceride accumulation in existing adipocytes. Hyperplasia, referred to adipogenesis, results from the recruitment of new adipocytes from precursor cells in the adipose tissue, and involves the proliferation and differentiation of these pre-adipocytes (Gregoire, 2001). Several epidemiological studies have provided that large amounts of adipose tissue are closely associated with poor prognosis for breast cancer in obese post menopausal women. It was proposed that elevated numbers of hypertrophied adipocytes might promote aggressive hormone-dependent breast cancers by increasing hormone synthesis (Manolio et al., 2003). Indeed, it is established that breast adipose tissue is an important site of estrogen production in post menopausal women, and elevated estrogen biosynthesis from peritumoral adipose tissue has been demonstrated (Kamal et al., 2002). This is dependent on aromatase, a key enzyme that is involved in peripheral estrogen aromatisation in the adipose tissue (Macedo et al., 2006). Moreover, several findings have indicated that mature human adipocytes possess estrogen receptors (ER), and that adipose tissue might itself be an estrogen responsive tissue (Cooke and Naaz, 2004). However, more recent studies show that the poor prognosis for obese people with breast cancer is independent of menopause status, tumor stage, and tumor hormone status (Majed et al., 2009). Interestingly, emerging evidence suggest that host factors contribute to the occurrence of aggressive tumors in obese women as connoting advanced stage, high grade and propensity to metastasize (Hess and Vona-Davis, 2009). In addition, it has been shown that hyperinsulinemia and type 2 diabetes are independent risk factors for poor prognosis in women with breast cancers (Duggan et al., 2011) (Goodwin et al., 2011).

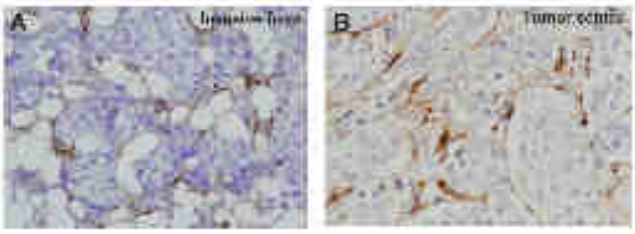

Fig. 5: Matrix metalloproteinase 11 (MMP11) immunohistochemistry of a breast carcinoma. (A) At the invasive front, MMP11 immunostaining stains the cancer associated adipocytes (CAAs) expressing MMP11 (brown staining). (B) At the tumor center, numerous unstained cancer cells (CCs) also express MMP11.

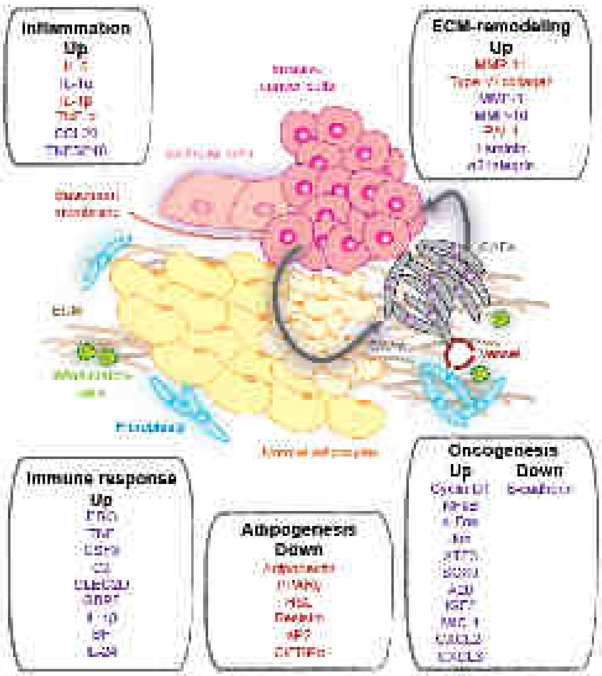

Fig. 6. Cancer-associated adipocyte (CAA)-cancer cell crosstalk orchestrates a vicious cycle promoting cancer progression. *In a bi-directional way, the initial crosstalk between invading cancer cells and resident adipocytes and/or pre-adipocytes induces the dedifferentiation of CAAs and/or prevents pre-adipocyte differentiation, leading to the acquisition/maintenance of CAFs. In turn, CAFs promote tumor progression. These events are sustained by expression/secretion of various factors by both cell types, most of which remain unidentified. Molecules whose expression have been shown to be modified at the transcriptional level following adipocyte/CAA-cancer cell crosstalk either in vitro or in vivo are mentioned in colors (red, expressed by Ad_{mat}/CAAs; violet, expressed by BCC/cancer cells; up, overexpression; down, lower expression). Their biological functions have been arbitrarily subdivided into 5 sets related to inflammation, immune response, ECM remodeling, oncogenesis and adipogenesis. aP2: Adipocyte fatty acid binding protein; ATF3: activating transcription factor; BF: B factor; C/EBPα: CCAAT/enhancer-binding protein α; C2: complement component 2; CCL20: chemokine (C-C motif) ligand 20; CLEC2D: C-type lectin domain family 2, member D; CSF3: colony stimulating factor 3; CXCL: chemokine (C-X-C motif) ligand; CYR: Cysteine-rich angiogenic inducer; GBP1: guanylate binding protein 1; HSL: hormone sensitive lipase; IGF2: insulin-like growth factor 2; IL: interleukin; MIC-1: macrophage inhibitory cytokine-1; MMP: matrix metalloproteinase; NFκB: nuclear factor-kappa B; PAI-1: plasminogen activator inhibitor-1; PPARγ: Peroxisome proliferator activated receptor γ; SOX9: SRY related HMG box 9; TNF: tumor necrosis factor; TNFSF18: tumor necrosis factor superfamily, member 18.*

Finally, weight gain in breast cancer survivors has been shown to be associated with adverse health consequences (Duggan et al., 2010).

The pejorative effects of obesity are not restricted to breast cancer. Solid epidemiological data support the role of fat mass/distribution in the development of risk factors, morbidity and mortality in several types of cancers (Schaffler et al., 2007; Fair and Montgomery, 2009; Rio, 2011). A large american prospective analysis of the weight-cancer relationship has shown that excess body mass index (BMI) is the cause of approximately 14% of all cancer deaths in men and 20% in women aged 50 years or older (Calle et al., 2003). The International Agency for Research on Cancer (IARC) has concluded that there is sufficient evidence of a cancer-preventive effect for avoiding weight gain in several cancers (Vainio et al., 2002). A similar conclusion was drawn from a Shanghai Breast Cancer Study for breast cancer (Malin et al., 2005).

The main conclusions from epidemiological studies are that obesity as well as insulin resistance/diabetes influence cancer risk, tumor behavior and clinical outcome. Excess of fat tissues is detrimental for cancer patients regardless organ. There is therefore great interest in understanding the mechanisms by which adipocytes contribute to carcinogenesis, since obesity/metabolic disorders are worldwide epidemic diseases.

"Obese" adipocytes and cancer cell-primed cancer-associated adipocytes (CAAs) show similar molecular modifications

The clinical data call into question the potential molecular impact of excess of hypertrophied resident adipocytes on breast cancer development/progression. This topic is extremely difficult to explore, and very few data are available. Most concern circulating molecules. Indeed, in addition to their local function, it cannot be excluded that adipocytes/CAAs may also act systemically. In this context, it has been shown in vitro that several molecules expressed by CAAs following crosstalk with invasive cancer cells are secreted factors that might reach the circulation (see Fig. 6). Accordingly, breast cancer patients devoid of adipocyte/metabolic disorders exhibit molecular modifications in the blood, indicating that CAAs act via systemic route. In obese patients with breast cancer, we might expect obesity-dependent local and systemic effects to synergize with CAA effects. Indeed, the cellular homeostasis and the secretory profiles of hypertrophied adipocytes from cancer-free obese people are altered and increasingly dysregulated compared with normal adipocytes. Further, excess of adipose tissues located elsewhere in the body might also impact on tumor behavior via a systemic route. For example, obesity is associated with an altered cytokine profile, characterized by a reduction in the release of anti-inflammatory factors and an increase in the secretion of pro-inflammatory factors. Consequently, obesity is considered an important source of chronic inflammation (Lorenz and Weigel, 2006). Moreover, in obesity, the adipose tissue is infiltrated with increased numbers of TNFα- and IL6-secreting macrophages (Weisberg et al., 2003). Leptin is also activated by obesity related stimuli in adipocytes while adiponectin is decreased (Schaffler et al., 2007)(Kaur and Zhang, 2005). It is known that expanding adipose tissues require local active angiogenesis and neovascularization (Hausman and Richardson, 2004). Moreover, there are adipocyte dysfunctions linking obesity to insulin resistance and type 2 diabetes (Guilherme et al., 2008)(Tabe et al., 2008). In addition, hyperinsulinemia promotes the synthesis and biological activity of

insulin-like growth factor (IGF-I) which regulates cell proliferation (Pollak, 2008). Finally, adipose tissue also impacts the hormonal status since insulin affects the synthesis and the bioavailability of male and female sex steroids (Fischer-Posovszky *et al.*, 2007). Interestingly, there are some molecular similarities between the block alterations observed in breast cancer patients devoid of adipocyte/metabolic disorders and those observed in cancer-free obese people. Several of these factors have been shown to be modified in CAAs (see above Fig. 6).

Thus, several molecular alterations commonly found in adipocytes of people suffering obesity/metabolic disorders are similar to those detected in CAAs of invasive tumors. It is therefore tempting to speculate that whereas in people devoid of any adipocyte/metabolic disorders, factors that favor tumor progression are provided subsequently to stimuli initiated by CAA-cancer cell crosstalk, in obese people, this permissive microenvironment for invasive cancer cells is permanent due to stimuli coming from the plethora of hypertrophied resident adipocytes. These optimal conditions might then more boost cancer cell aggressiveness.

Adipocytes as "fuel" for cancer cells

Although metabolic changes do not cause malignancies, they are necessary for tumor progression. Indeed, cancer cells need to proliferate rapidly and therefore use a high rate of energy-consuming processes to drive increased protein and DNA synthesis (Menendez and Lupu, 2007). There is also a need to maintain a constant supply of lipids and lipid precursors to fuel membrane production in the highly proliferating cancer cell population. The data reported above question the possible direct involvement of CAAs in these events. Interestingly, it has been reported that epithelial cells within the mouse mammary gland are able to utilize fatty acids sequestered from fat pad adipocytes (Hovey and Aimo, 2010). In this case, epithelial cells clearly induce lipolysis in adjacent adipocytes during lactation, presumably through the action of epithelium-derived lipoprotein lipase. In turn, these adipocyte-derived fatty acids can be utilized for de novo fatty acid synthesis by lactating mammary epithelial cells. It might therefore be hypothesized that this crosstalk could be aberrantly restored between invasive cancer cells and resident adipocytes. Delipidation in CAAs supports such a process. Moreover, in a mouse model, Raman microscopy revealed intracellular lipid accumulation in cancer cells. Lipid-rich cancer cells are linked to cancer metastasis (Le *et al.*, 2009). Free fatty acids (FFAs) might be used for the production of signaling lipids, converted to specific lipid species for incorporation into membranes, or used for mitochondrial β-oxidation to produce ATP. Although it is thought that the bioenergetic needs of cancer are predominantly met through glycolysis, the oxidation of FFAs offers an interesting alternative. Indeed, it has been shown that an increase in intracellular FFAs enhances tumor progression potentially through β-oxidation (Nomura *et al.*, 2010).

There is a clear link between deregulated energy processing and increased cancer aggressiveness. Emerging evidence suggest that the "transfer" of lipids between adipocytes and cancer cells might represent a key energetic source for cancer cells and as such stimulate cancer progression. In this context, having an excess of "obese" adipocytes could obviously provide more triglycerides and more available FFAs to the developing tumor than normal adipocytes.

Conclusion

Improving knowledge of adipocyte/CAA functions might help to decipher the relationship between high BMI, or type 2 diabetes, and increased cancer risk and poor clinical outcome. In this context, modulating the plasticity of adipocytes and elucidating their extracellular and intracellular signaling pathways are major challenges for future research in this field. Molecules linked to adipocyte biology might offer new therapeutic opportunities for treating cancer. These data justify work aimed at exploring the feasibility of current metabolic syndrome and associated disorder treatments for anti-cancer therapy (Gouveri *et al.*, 2011). For example, recent studies provide clues that metformin, a drug usually given for the treatment of type 2 diabetes, is associated with reduced incidence and improved prognosis of various cancers including breast cancers (Ben Sahra *et al.*, 2010).

General conclusion

The present review provides new insights into the function of resident adipocytes in tumors. As outlined above, adipocytes within mammary gland carcinomas are clearly dynamic cells that contribute to human breast cancer progression. Its deleterious function is initiated through crosstalk with cancer cells. This review strongly supports the more general concept that the loss of adipose tissue homeostasis favors tumor aggressive behavior. In this context, it provides insights into the relationship between obesity/diabetes and cancer. This is of particular interest since recent epidemiological studies have identified obesity as one of the major risk factors for cancer. Moreover, several important considerations arise from such data, notably concerning the possibility of promoting cancer recurrence by "activating" residual cancer cells in post mastectomy reconstruction with autologous fat transfer, or dormant malignant cells or microtumors in breast augmentation.

The cellular and molecular processes underlying adipocyte function in cancer is just beginning to unfold. Many questions remain unanswered, and it is important to further study mechanisms and signaling pathways involved to understand how adipocytes promote tumor progression. One of the most important questions to be addressed concerns the possible role of resident adipocytes in the distant tissues colonized by metastatic cells. Indeed, phenomenons similar to those observed at the primary tumor sites might be expected to exist at the secondary tumor sites. In this context, it should be noted that the microenvironment of preferential organs for metastasis development often contains adipocytes/lipids (Sidoni *et al.*, 2008).

This research might lead in fine to the identification of adipocyte-related targets to improve diagnosis and prognosis, and/or to design innovative anticancer strategies.

Acknowledgements

We thank Susan Chan for helpful discussion. This work was supported by funds from the Institut National de la Santé et de la Recherche Médicale, the Centre National de la Recherche Scientifique, the Hôpital Universitaire de Strasbourg, the Association pour la Recherche sur le Cancer, the Ligue Nationale Française Contre le Cancer and the Comités du Haut-Rhin, du Bas-Rhin et de la Haute-Savoie (Equipe labellisée LIGUE 2010) and the Institut National du Cancer (Contrat PL-BIO/ADIPOK 2011-2013). J.T. was a recipient of a Chinese fellowship (Department of Endocrine and Breast Surgery, the first Affiliated Hospital of Chongqing Medical University, Chongq

[illegible]

References

ANDARAWEWA KL, RIO MC (2008) New insights into MMP function in adipogenesis. In: The cancer degradome [illegible]. Springer Science [illegible]

ANDARAWEWA KL, MOTRESCU ER, CHENARD MP, GANSMULLER A, STOLL I, TOMASETTO C, RIO MC (2005) Stromelysin-3 is a potent negative regulator of adipogenesis participating in cancer cell-adipocyte interaction/crosstalk at the tumor invasive front. *Cancer Res* 65: 10862-10871.

BASSET P, BELLOCQ JP, WOLF C, STOLL I, HUTIN P, LIMACHER JM, PODHAJCER OL, CHENARD MP, RIO MC, CHAMBON P (1990) A novel metalloproteinase gene specifically expressed in stromal cells of breast carcinomas. *Nature* 348: 699-704.

BEN SAHRA I, LE MARCHAND-BRUSTEL Y, TANTI JF, BOST F (2010) Metformin in cancer therapy: a new perspective for an old antidiabetic drug? *Mol Cancer Ther* 9: 1092-1099.

CALLE EE, RODRIGUEZ C, WALKER-THURMOND K, THUN MJ (2003) Overweight, obesity, and mortality from cancer in a prospectively studied cohort of U.S. adults. *N Engl J Med* 348: 1625-1638.

COOKE PS, NAAZ A (2004) Role of estrogens in adipose tissue development and function. *Exp Biol Med (Maywood)* 229: 1127-1135.

DIRAT B, BOCHET L, DABEK M, DAVIAUD D, DAUVILLIER S, MAJED B, WANG YY, MEULLE A, SALLES B, LE GONIDEC S, GARRIDO I, ESCOURROU G, VALET P, MULLER C (2011) Cancer-associated adipocytes exhibit an activated phenotype and contribute to breast cancer invasion. *Cancer Res* 71: 2455-2465.

DUGGAN C, IRWIN ML, XIAO L, HENDERSON KD, SMITH AW, BAUMGARTNER RN, BAUMGARTNER KB, BERNSTEIN L, BALLARD-BARBASH R, MCTIERNAN A (2011) Associations of insulin resistance and adiponectin with mortality in women with breast cancer. *J Clin Oncol* 29: 32-39.

[illegible] (2000) The role of [illegible] signaling pathways. *Adv Exp Med Biol* 480: 109-117.

ELLIOTT BE, TAM SP, DEXTER D, CHEN ZQ (1992) Capacity of adipose tissue to promote growth and metastasis of a murine mammary carcinoma: effect of estrogen and progesterone. *Int J Cancer* 51: 416-424.

FAIR AM, MONTGOMERY K (2009) Energy balance, physical activity, and cancer risk. *Methods Mol Biol* 472: 57-88.

FISCHER-POSOVSZKY P, WABITSCH M, HOCHBERG Z (2007) Endocrinology of adipose tissue - an update. *Horm Metab Res* 39: 314-321.

[illegible] (2011) The female breast and diabetes. *The Breast* 20: 205-211.

GREGOIRE FM (2001) Adipocyte differentiation: from fibroblast to endocrine cell. *Exp Biol Med (Maywood)* 226: 997-1002.

GUILHERME A, VIRBASIUS JV, PURI V, CZECH MP (2008) Adipocyte dysfunctions linking obesity to insulin resistance and type 2 diabetes. *Nat Rev Mol Cell Biol* 9: 367-377.

HOENE M, WEIGERT C (2008) The role of interleukin-6 in insulin resistance, body fat distribution and energy balance. *Obes Rev* 9: 20-29.

HOVEY RC, AIMO L (2010) Diverse and active roles for adipocytes during mammary gland growth and function. *J Mammary Gland Biol Neoplasia* 15: 279-290.

IYENGAR P, COMBS TP, SHAH SJ, GOUON-EVANS V, POLLARD JW, ALBANESE C, FLANAGAN L, TENNISWOOD MP, GUHA C, LISANTI MP, PESTELL RG, SCHERER PE (2003) Adipocyte-secreted factors synergistically promote mammary tumorigenesis through induction of anti-apoptotic transcriptional programs and proto-oncogene stabilization. *Oncogene* 22: 6408-6423.

IYENGAR P, ESPINA V, WILLIAMS TW, LIN Y, BERRY D, JELICKS LA, LEE H, TEMPLE K, GRAVES R, POLLARD J, CHOPRA N, RUSSELL RG, SASISEKHARAN R, TROCK BJ, LIPPMAN M, CALVERT VS, PETRICOIN EF, 3RD, LIOTTA L, DADACHOVA E, PESTELL RG, LISANTI MP, BONALDO P, SCHERER PE (2005) Adipocyte-derived collagen VI affects early mammary tumor progression in vivo, demonstrating a critical interaction in the tumor/stroma microenvironment. *J Clin Invest* 115: 1163-1176.

JODELE S, BLAVIER L, YOON JM, DECLERCK YA (2006) Modifying the soil to affect the seed: role of stromal-derived matrix metalloproteinases in cancer progression. *Cancer Metastasis Rev* 25: 35-43.

KAMAT A, HINSHELWOOD MM, MURRY BA, MENDELSON CR (2002) Mechanisms in tissue-specific regulation of estrogen biosynthesis in humans. *Trends Endocrinol Metab* 13: 122-128.

[illegible] (2005) Obesity, breast cancer and the role of adipocytokines. *Asian Pac J Cancer Prev* 6: 547-552.

KESSENBROCK K, PLAKS V, WERB Z (2010) Matrix metalloproteinases: regulators of the tumor microenvironment. *Cell* 141: 52-67.

KIM JH, KIM KY, JEON JH, LEE SH, HWANG JE, LEE JH, KIM KK, LEE HJ, KIM KI, MOON EY, LEE HG, RYU JH, YANG Y (2008) Adipocyte culture medium stimulates production of macrophage inhibitory cytokine 1 in MDA-MB-231 cells. *Cancer Lett* 261: 253-262.

KIMIJIMA I, OHTAKE T, SAGARA H, WATANABE T, TAKENOSHITA S (2000) Scattered fat invasion: an indicator for poor prognosis in premenopausal, and for positive estrogen receptor in postmenopausal breast cancer patients. *Oncology* 59 Suppl 1: 25-30.

LE TT, HUFF TB, CHENG JX (2009) Coherent anti-Stokes Raman scattering imaging of lipids in cancer metastasis. *BMC Cancer* 9: 42.

LEFEBVRE O, WOLF C, LIMACHER JM, HUTIN P, WENDLING C, LEMEUR M, BASSET P, RIO MC (1992) The breast cancer-associated stromelysin-3 gene is expressed during mouse mammary gland apoptosis. *J Cell Biol* 119: 997-1002.

MACEDO LF, SABNIS G, BRODIE A (2009) Aromatase inhibitors and breast cancer. *Ann N Y Acad Sci* 1155: 162-173.

MAEDA K, OKUBO K, SHIMOMURA I, MIZUNO K, MATSUZAWA Y, MATSUBARA K (1997) Analysis of an expression profile of genes in the human adipose tissue. *Gene* 190: 227-235.

MAJED B, MOREAU T, SENOUCI K, SALMON RJ, FOURQUET A, ASSELAIN B (2008) Is obesity an independent prognosis factor in woman breast cancer? *Breast Cancer Res Treat* 111: 329-342.

MALIN A, MATTHEWS CE, SHU XO, CAI H, DAI Q, JIN F, GAO YT, ZHENG W (2005) Energy balance and breast cancer risk. *Cancer Epidemiol Biomarkers Prev* 14: 1496-1501.

MANABE Y, TODA S, MIYAZAKI K, SUGIHARA H (2003) Mature adipocytes, but not preadipocytes, promote the growth of breast carcinoma cells in collagen gel matrix culture through cancer-stromal cell interactions. *J Pathol* 201: 221-228.

MENENDEZ JA, LUPU R (2007) Fatty acid synthase and the lipogenic phenotype in cancer pathogenesis. *Nat Rev Cancer* 7: 763-777.

MIYOSHI Y, FUNAHASHI T, TANAKA S, TAGUCHI T, TAMAKI Y, SHIMOMURA I, NOGUCHI S (2006) High expression of leptin receptor mRNA in breast cancer tissue predicts poor prognosis for patients with high, but not low, serum leptin levels. *Int J Cancer* 118: 1414-1419.

MOTRESCU ER, RIO MC (2008) Cancer cells, adipocytes and matrix metalloproteinase 11: a vicious tumor progression cycle. *Biol Chem* 389: 1037-1041.

MOTRESCU ER, BLAISE S, ETIQUE N, MESSADDEQ N, CHENARD MP, STOLL I, TOMASETTO C, RIO MC (2008) Matrix metalloproteinase-11/stromelysin-3 exhibits collagenolytic function against collagen VI under normal and malignant conditions. *Oncogene* 27: 6347-6355.

NAKAJIMA I, MUROYA S, TANABE R, CHIKUNI K (2002) Positive effect of collagen V and VI on triglyceride accumulation during differentiation in cultures of bovine intramuscular adipocytes. *Differentiation* 70: 84-91.

NOMURA DK, LONG JZ, NIESSEN S, HOOVER HS, NG SW, CRAVATT BF (2010) Monoacylglycerol lipase regulates a fatty acid network that promotes cancer pathogenesis. *Cell* 140: 49-61.

POLLAK M (2008) Insulin and insulin-like growth factor signalling in neoplasia. *Nat Rev Cancer* 8: 915-928.

RABE K, LEHRKE M, PARHOFER KG, BROEDL UC (2008) Adipokines and insulin resistance. *Mol Med* 14: 741-751.

RIO MC (2011) The role of Cancer-Associated Adipocytes (CAA) in the dynamic interaction between the tumor and the host. Springer SBM.

RONNOV-JESSEN L, PETERSEN OW, KOTELIANSKY VE, BISSELL MJ (1995) The origin of the myofibroblasts in breast cancer. Recapitulation of tumor environment in culture unravels diversity and implicates converted fibroblasts and recruited smooth muscle cells. *J Clin Invest* 95: 859-873.

ROSE DP, VONA-DAVIS L (2009) Influence of obesity on breast cancer receptor status and prognosis. *Expert Rev Anticancer Ther* 9: 1091-1101.

SCHAFFLER A, SCHOLMERICH J, BUECHLER C (2007) Mechanisms of disease:

adipokines and breast cancer - endocrine and paracrine mechanisms that connect adiposity and breast cancer. *Nat Clin Pract Endocrinol Metab* 3: [illegible]

SCLAFANI [illegible], GUISE TA, CHIRGWIN JM (2002) Molecular interactions between breast cancer cells and the bone microenvironment [illegible]. *Cancer Metastasis Rev* 20: 321-339.

VAINIO H, KAAKS R, BIANCHINI F (2002) Weight control and physical activity in cancer prevention: international evaluation of the evidence. *Eur J Cancer Prev* 11 Suppl 2: S94-100.

WALTER M, LIANG S, GHOSH S, HORNSBY PJ, LI R (2009) Interleukin 6 secreted from adipose stromal cells promotes migration and invasion of breast cancer cells. *Oncogene* 28: 2745-2755.

WANG [illegible] (1997) [illegible] fibroblasts under *in vivo* breast cancer cell induction. [illegible] 39: 792-793.

WEISBERG SP, MCCANN D, DESAI M, ROSENBAUM M, LEIBEL RL, FERRANTE AW, JR (2003) Obesity is associated with macrophage accumulation in adipose tissue. *J Clin Invest* 112: 1796-1808.

YAMAGUCHI J, OHTANI H, NAKAMURA K, SHIMOKAWA I, KANEMATSU T (2008) Prognostic impact of marginal adipose tissue invasion in ductal carcinoma of the breast. *Am J Clin Pathol* 130: 382-388.

Further Related Reading, published previously in the *Int. J. Dev. Biol.*

Growth factor-defined culture medium for human mesenchymal stem cells
Satoru Mimura, Naoshi Kimura, Masumi Hirata, Daiki Tateyama, Midori Hayashida, Akihiro Umezawa, Akiko Kohara, Hiroki Nikawa, Tetsuji Okamoto and Miho K. Furue
Int. J. Dev. Biol. (2011) 55: 181-187

Pdx1-transfected adipose tissue-derived stem cells differentiate into insulin-producing cells in vivo and reduce hyperglycemia in diabetic mice
Hiromitsu Kajiyama, Tatsuo S. Hamazaki, Makoto Tokuhara, Shinji Masui, Ken Okabayashi, Kiyoshi Ohnuma, Shigeharu Yabe, Kazuhiro Yasuda, Shoichi Ishiura, Hitoshi Okochi and Makoto Asashima
Int. J. Dev. Biol. (2010) 54: 699-705

Epithelial-Mesenchymal Transitions in development and disease: old views and new perspectives
M. Angela Nieto
Int. J. Dev. Biol. (2009) 53: 1541-1547

Analysis of tenascin mRNA expression in the murine mammary gland from embryogenesis to carcinogenesis: an in situ hybridization study
I Kalembey, T Yoshida, K Iriyama and T Sakakura
Int. J. Dev. Biol. (1997) 41: 569-573

Expression of c-ets-1 and uPA genes is associated with mammary epithelial cell tubulogenesis or neoplastic scattering
A Delannoy-Courdent, W Fauquette, X F Dong-Le Bourhis, B Boilly, B Vandenbunder and X Desbiens
Int. J. Dev. Biol. (1996) 40: 1097-1108

5 yr ISI Impact Factor (2010) = 2.961

The technique of transgenic mouse model construction--MMP11 transgenic mouse as example

Jinxiang TAN, Emilie BUACHE, Fabien ALPY, Catherine-Laure TOMASETTO, Marie-Christine RIO

Molecular and cellular biology of breast cancer, IGBMC, University of Strasbourg, France

It has been shown that MMP11 is a negative regulator of adipogenesis, able to reduce and even to revert mature adipocyte differentiation. The MMP11 deficient mice have a significantly higher mean body weight and adipose tissue deposits than control littermates, which indicated that MMP11 deficiency favors adipogenesis. Once again, several questions remain open: how about the adipose tissue in transgenic mice with MMP11 over-expression in adipocytes specifically? So, the aims are to explore the adipogenesis and tumorigenesis in transgenic mice with MMP11 over-expression in adipocytes.

In order to answer these questions, I have constructed JOJO-MMP11 expression plasmids, allowing the expression of MMP11 coding sequence with or without a flag at its C-terminal end. The plasmids permit to express MMP11 protein by co-transfection into Hela cell line of these vectors and Cre-recombinase. We have checked the MMP11 expession with western blot. Then we sent the plasmid to animal facility for generation of transgenic mice with MMP11 over-expression in the adipocytes. The constructs contain Lox P sites, which will permit to specifically express MMP11 into adipocyte after crossing the mice with transgenic mice expressing the Cre-recombinase under the control of an adipocyte-specific promoter.

Chapter 7 Résumé en Français

Etude de la fonction de la métalloprotéase matricielle 11 dans l'interaction/dialogue adipocyte-cellule épithéliale dans la glande mammaire

Etat de la question

Il est bien établi que le microenvironnement tumoral joue un rôle dans la progression tumorale. L'invasion tumorale conduit à un interaction/dialogue entre cellules épithéliales cancéreuses et cellules normales mésenchymateuses. À ce jour, la plupart des études portant sur ces interactions hétérotypiques mettent l'accent sur les fibroblastes, les cellules endothéliales ou encore inflammatoires. Très peu d'attention est accordée aux adipocytes bien que dans de nombreux cancers tels que ceux touchant la glande mammaire ces cellules entrent en contact direct avec les cellules cancéreuses invasives. D'autre part, plusieurs études épidémiologiques ont mis l'accent sur l'effet du métabolisme sur le développement tumoral et sur le devenir des patients. Les mécanismes biologiques et moléculaires impliqués restent à ce jour peu connus. Dans ce contexte, les adipocytes qui sont non seulement capables d'exercer localement des fonctions autocrines et/ou paracrines mais également des fonctions endocrines via la synthèse d'hormones peptidiques (adipokines) représentent donc un terrain d'étude privilégié. L'obèsité, l'insuline résistance et le diabète de type 2 étant en augmentation constante (Doria et al 2008 Cell Metab 8 :186), il apparait fondamental d'étudier l'impact du tissu adipeux sur la progression tumorale aussi bien au niveau local qu'à distance.

Mon sujet de thèse s'inscrit dans cette problèmatique et vise à définir le rôle de la métalloprotéase matricielle 11 (MMP-11 ; aussi appellée stromélysine-3) sur l'adipocyte d'une part et sur les cellules épithéliales d'autre part. La MMP-11 a été

clonée au laboratoire dans une biopsie de tumeur mammaire (Basset et al 1990 Nature 348 :699). Il s'agit d'une molécule exprimée par les cellules d'origine mésenchymateuse. Ainsi, dans les cancers du sein, la MMP-11 n'est pas exprimée par les cellules cancéreuses mais par des cellules du microenvironnement péritumoral. Il a été montré par de nombreux laboratoires dont le nôtre que sa surexpression représente un facteur de mauvais pronostic quelque soit le type de carcinomes. De plus, dans plusieurs modèles murins de tumorigenèse la MMP-11 joue un rôle clé dans la progression tumorale. Plus récemment, il a été montré au laboratoire qu'au niveau du front d'invasion des tumeurs mammaires les cellules cancéreuses invasives induisent l'expression de la MMP-11 dans les adipocytes localisés à leur proximité (cancer-associated adipocytes, CAA). Cette expression entraine un changement phénotypique de ces adipocytes qui acquièrent alors une morphologie de type fibroblastique (Andarawewa et al 2005 Cancer Res 65:10862). Des expériences in vitro et in vivo ont également montré que la MMP-11 est un régulateur négatif de l'adipogénèse (Andarawewa et al 2005 Cancer Res 65:10862), et que la MMP-11 clive la chaine alpha 3 du collagène de type VI, un composant majeur de la matrice adipocytaire (Motrescu et al 2008 Oncogene 27:6347).

L'adipocyte participe donc, via la MMP-11, à une sorte de cercle vicieux initié par les cellules cancéreuses invasives et favorisant la progression tumorale (Motrescu et Rio 2008 Biol Chem 389:1037 ; Buache et Rio 2012 Matrix proteases in health and disease. Chapter 15 p373).

Questions posées

Ces données soutiennent le concept selon lequel : i) les adipocytes jouent un rôle dans la progression tumorale ; ii) la MMP-11 participe à cette action. Cependant, les processus cellulaires et moléculaires impliqués restent à découvrir. Dans ce contexte, ma thèse porte sur trois questions primordiales :

Question 1: Quels sont les processus moléculaires impliqués dans la « dédifférenciation » des CAAs induite par la MMP-11?

Question 2: Quel est l'impact de la MMP-11 sur le développement post-natal normal de la glande mammaire ?

Question 3: Quel est l'impact de la MMP-11 adipocytaire sur le développement post-natal de la glande mammaire et sur la progression tumorale ?

Approches expérimentales

A mon arrivée au laboratoire, le matériel suivant été déjà disponible: lignées celulaires mammaires normales immortalisées ou cancéreuses; modèles murins notamment des souris transgéniques surexprimant la MMP-11 ou au contraire déficientes pour son expression (MMP-11-/-) ; J'ai également bénéficié de l'aide de différentes plateformes de l'IGBMC et plus particulièrement la Clinique de la Souris (ICS) et l'animalerie conventionnelle, et la plateforme de transcriptome (Affymetrix). Afin d'essayer de répondre à ces questions, j'ai entrepris les approches expérimentales suivantes :

Question 1: J'ai étudié la « dédifférenciation » adipocytaire à partir de fibroblastes embryonnaires de souris MMP-11-/- préalablement différenciés en adipocytes. Ils ont été ensuite traités ou non par de la MMP-11 recombinante produite au laboratoire. Les modifications phénotypiques ont été observés et les gènes exprimés différentiellement en fonction du traitement ont été recherchés par analyse transcriptomique.

Question 2: L'effet de la MMP-11 sur le développement de la glande mammaire a été étudié par comparaison morphologique des glandes mammaires de souris sauvages et de souris MMP-11-/- à différents ages de leur différenciation post-natale (pré-puberté, puberté, gestation, lactation, involution). Des expériences de greffes croisées de glandes mammaires entre souris sauvages et souris MMP-11-/- ont également été réalisées pour définir l'impact relatif de la composante stromale et de la composante épithéliale. Des analyses histologiques et immunohistochimiques ont été réalisées.

Question 3: Les modèles murins dont nous disposons au laboratoire ne permettent pas d'étudier les effets dus à la seule production adipocytaire de la MMP-11. Afin de disposer d'un tel modèle permettant de mimer ce qui se passe au front d'invasion des tumeurs où la MMP-11 est surexprimée par les adipocytes, j'ai développé des souris transgéniques conditionnelles qui, après croisement avec des

souris transgéniques appropriées, permettent d'obtenir une surexpression de MMP11 ciblée dans les adipocytes.

Résultats obtenus

J'ai obtenu les résultats suivants :

Question 1: Des MEFs ont été isolés et cultivés à partir d'embryons de 14.5 jours MMP-11-/- et mis en culture jusqu'à confluence. La différenciation adipocytaire a alors été initiée par traitement avec un tampon spécifique. Après 2 jours, les cellules étaient passées en milieu de culture frais et la différenciation suivie par marquage des goutelettes lipidiques à l'huile rouge (Oil Red O). Une fois que la majorité des MEFs étaient différenciés, l'effet sur le phénotype cellulaire d'un ajout journalier de MMP-11 recombinante active ou inactive (produite au laboratoire) était étudié. D'autre part l'ARN des cellules était extrait. Douze couples de MEF traités avec de la MMP-11 active ou inactive ont été obtenus. Les ARNs correspondants ont été analysés par microarray (platforme Affymetrix). *Conclusion:* Malheureusement l'analyse des résultats obtenus n'a pas permis de mettre clairement en évidence un panel de gènes impliqués dans la "dédifférenciation" adipocytaire induite par la MMP-11. Cela semble du à la grande variation existant entre les différents MEFs (chacun étant issu d'un embryon différent). D'autre part, chaque culture de MEFs analysée par Affymétrix comprenaient trois populations en proportion variable d'un MEF à l'autre, c'est-à-dire des MEFs à l'état fibroblastique, des MEFs différenciés en adipocytes et des MEFs dédifférenciés. Ce modèle qui avait été choisi parce qu'il faisait intervenir des cellules n'ayant aucune possibilité d'exprimer de la MMP-11 endogène puisqu'issus de souris MMP-11-/- s'est donc révélé trop complexe pour être efficace. D'autres approches impliquant des lignées
cellulaires ont été suivies en parallèle au laboratoire avec plus de succès.

Question 2: La comparaison des glandes mammaires des souris MMP-11-/- avec celles de souris sauvages montre une altération de leur développement. Cela se traduit par une diminution des branchements des canaux galactophoriques et du nombre de bourgeons terminaux dès la 4ième semaine post-natale. Les anomalies sont accentuées avec l'âge et pendant la gestation et la lactation. Les analyses

histologiques des glandes mammaires greffées montrent que: i) la structure épithéliale mammaire (la glande proprement dite) des souris MMP-11-/- n'est pas affectée par l'absence de MMP-11 puisqu'une greffe de cette dernière dans un environnement conjonctif sauvage permet une différenciation correcte; ii) par contre, le tissus conjonctif dépourvu de MMP-11 est incapable d'assurer le développement correcte de la structure épithéliale issue de souris sauvages, indiquant ainsi que la composante stromale est impliquée dans la différenciation post-natale de la glande mammaire et que la MMP-11 est un acteur de cette dernière. Les altérations phénotypiques observées en absence de MMP-11 s'accompagnent de modifications moléculaires notamment en ce qui concerne les collagènes. *Conclusion*: la MMP-11 exerce un effet paracrine sur la composante épithéliale de la glande mammaire et est requise pour sa différenciation post-natale.

Question 3: Afin d'exprimer spécifiquement la MMP-11 dans les adipocytes, j'ai entrepris de réaliser des souris transgéniques conditionnelles. J'ai réalisé une construction présentant un ADN GFP suivi d'un codon STOP et encadré par des sites Lox suivi de la séquence codante de la MMP-11 couplé ou non à un flag à son extrémité C-terminale. Les plasmides obtenus (JOJO-MMP-11 et JOJO-MMP-11-flag) permettent d'une part de suivre l'expression de la construction dans les différents tissus grâce à l'expression constitutive de la GFP. D'autre part, d'exprimer la MMP-11 après excision de la GFP par la Cre-recombinase. Ces plasmides ont permis de générer des souris transgéniques exprimant MMP-11 dans les adipocytes après croisement avec des souris transgéniques exprimant la Cre sous le contrôle du promoteur spécifique des adipocytes aP2 (aP2-Cre ; inductible par le tamoxifen ; D Metzger IGBMC). *Conclusion* : j'ai obtenu une lignée de souris transgéniques conditionnelles ayant une expression ciblée de la MMP-11 dans les adipocytes.

Conclusions et perspectives

De nombreuses études épidémiologiques montrent que l'excès de tissu adipeux et les pathologies associées telles que l'obésité, l'insuline résistance, voire le diabète représentent un facteur de risque et de mauvais pronostic dans de nombreux cancers (International Agency for Research on Cancer (IACR Handbooks of cancer

prevention, Lyon, 2002). Cent-soixante-dix millions d'individus dans le monde souffrent de telles altérations et la prévalence de ces maladies devrait doubler d'ici 2025. Les données cellulaires et moléculaires pouvant expliquer ceci restent à ce jour très limitées. Cependant, un faisceau de données indique qu'effectivement un lien étroit pourrait exister entre adipocytes et cancers. Il y a donc une nécessité de définir et d'étudier les processus biologiques et moléculaires liant adipocytes et cancers. Actuellement, alors que le rôle des MMPs ne fait aucun doute dans le développement tumoral, peu de données existent quand à la relation entre MMPs et adipocytes (Andarawewa et Rio, 2008 The cancer degradome. Chapter 19 p353).

Dans ce contexte, mon travail de thèse apporte des données originales quand au rôle de la MMP-11 à l'interface tissu adipeux/cellules épithéliales. Cela devrait aider à comprendre les processus moléculaires impliquant les adipocytes dans la survie des cellules cancéreuses, la croissance tumorale et/ou le développement de métastases (Tan et al Int J Dev Biol. 2011 55 :851 ; Tan et al, manuscrit en préparation)

D'autre part, j'ai développé de nouveaux outils, notamment les souris MMP-11 transgéniques conditionnelles qui seront très utiles pour entreprendre l'étude des événements moléculaires impliqués dans la progression tumorale. Des essais de tumorigenèse seront développés chez ces souris pour étudier l'impact d'une surexpression de MMP-11 dans les adipocytes de l'hôte sur le développement tumoral ; les tumeurs et les métastases obtenues seront analysées: incidence, délais d'apparition, taille, nombre, histologie, transcriptome, protéome… Les altérations moléculaires d'intérêt identifiées seront recherchées dans des biopsies de cancers du sein, notamment au front d'invasion des tumeurs, dans le but in fine de trouver des marqueurs diagnostiques et pronostiques originaux, voire de nouvelles cibles thérapeutiques.

Jinxiang TAN

Etude de la fonction de la métalloprotéase matricielle 11 dans l'interaction/dialogue adipocyte-cellule épithéliale dans la glande mammaire

Résumé

Dans les tumeurs, les cellules cancéreuses invasives induisent l'expression de la métalloprotéase matricielle 11 (MMP-11) dans les adipocytes adjacents (cancer-associated adipocytes) entrainant leur « dédifférenciation » en fibroblastes, la MMP-11 régulant négativement l'adipogénèse. Au cours de ma thèse, j'ai étudié la fonction de la MMP-11 sur le développement mammaire postnatal. La structure de la glande ainsi que la production de lait sont altérées dans les souris déficientes pour la MMP-11. De plus, la MMP-11 régule l'homéostase du collagène. In vivo, des transplantations montrent une fonction locale paracrine de la MMP-11 essentielle à la morphogenèse mammaire. In vitro, la MMP-11 adipocytaire favorise le branchement d'organoïdes primaires. Ainsi, la MMP-11 est un facteur paracrine majeur pour le développement de la glande mammaire. Enfin, pour poursuivre ces travaux, j'ai établi des souris transgéniques conditionnelles ciblant l'expression de la MMP-11 dans les adipocytes.

Mots-clés : MMP-11 ; glande mammaire ; développement ; adipocyte ; cellule épithéliale ; collagène ; stroma ; galactophore ; bourgeons terminaux ; branchement.

Résumé en anglais

In tumors, invasive cancer cells induce matrix metalloproteinase 11 (MMP-11) expression in adjacent adipocytes (cancer-associated adipocytes), leading to their « dedifferentiation » into fibroblast-like cells. Indeed, MMP-11 is a negative regulator of adipogenesis. During my PhD, I have investigated MMP-11 function during postnatal mammary gland development. The ductal tree and alveolar structures, and milk production are reduced in MMP-11-deficient mice. Moreover, MMP-11 plays a role in collagen homeostasis. Transplantation experiments show that MMP-11 exerts an essential local paracrine function for ductal morphogenesis. Using primary mammary organoids, I show that adipocyte-related MMP-11 is a pro-branching factor in vitro. Thus, MMP-11 is a master paracrine factor during mammary gland development. Finally, to further investigate the adipocyte-related MMP-11 function, I have developed conditional transgenic mice targeting MMP-11 expression specifically into adipocytes.

Keywords: MMP-11; mammary gland development; adipocyte; epithelial cell; collagen; stroma; ducts; terminal end bud ; branching.